Université de Montréal

ADDRESSING THE ROLES OF THE RETINOIC ACID RECEPTORS DURING MAMMALIAN DEVELOPMENT

Par
Angelo Iulianella

Programme de biologie moléculaire
Faculté des études supérieures

Thèse présentée à la Faculté des études supérieures
en vue de l'obtention du grade de
Philosophiæ Doctor (Ph.D.)
en biologie moléculaire

Décembre, 2001

Université de Montréal
Faculté des études supérieures

Cette thèse intitulée

ADDRESSING THE ROLES OF THE RETINOIC ACID RECEPTORS DURING MAMMALIAN DEVELOPMENT

présentée par

Angelo Iulianella

a été évaluée par un jury composé des personnes suivantes:

Dr Jean Vacher	Président-Rapporteur Université de Montréal
Dr Mark Featherstone	Examinateur Externe Université McGill
Dr Muriel Aubry	Membre du Jury Université de Montréal
Dr Francois Dubé	Membre du Jury C.H.U.M. Pavillion Saint-Luc

Thèse acceptée le: .....

SUMMARY

The formation of the embryonic axes are highly sensitive to the effects of retinoids. Signaling by these dietary factors are mediated by a group of transcription factors called the retinoic acid receptors (RARs). The objective of this thesis was to investigate the roles of retinoid signaling in the patterning of the antero-posterior and left-right axes by using mice harboring mutations for the RARs. This work demonstrated that retinoids influence vertebral identities through a previously unsuspected role for the RARs late in the formation of the vertebrae. Exogenous RA can also truncate the axis, however, previous studies were unsuccessful in defining the cellular and molecular basis for this caudal regression phenotype. This was addressed by examining the effects of retinoid excess on several tissue specific markers in the posterior embryo. I documented a specific down-regulation of mesodermal markers, such as *brachyury* and *wnt3a*, in response to retinoids, and therefore concluded that newly forming mesoderm is the primary site of the lesion leading to the axial truncations. Furthermore, this work generated novel insights into the regulation of retinoid signaling in the caudal embryo by documenting a feedback mechanism of retinoid degradation involving the catabolic enzyme Cyp26A1. Finally, in an effort to define new roles for the RARs, a gene replacement approach using a dominant negative RAR was developed to circumvent redundancy among the RAR genes. Indeed, this strategy demonstrated, for the first time, a role for retinoid signaling in late heart looping morphogenesis involving the left side-specific determinant, *pitx2*. Collectively, these results identify key effectors of RAR function during development and significantly further our knowledge of the roles of retinoid signaling in the patterning of the embryonic axes.

KEY WORDS : *Brachyury,* cardiac looping, caudal regression, dominant negative, *pitx2*, retinoic acid, retinoic acid receptor γ, myocardium, vertebral patterning.

SOMMAIRE

La formation des axes embryonnaires est hautement sensible aux effets des rétinoïdes dont les médiateurs sont les récepteurs de l'acide rétinoïque (RARs). L'objectif premier de cette thèse fut d'étudier les rôles des rétinoïdes dans l'établissement des axes antéro-postérieur et gauche-droite, par l'utilisation de souris présentant des mutations pour les RARs. Les résultats de cette étude ont démontré l'existence d'une nouvelle fonction pour les RARs dans la formation tardive des vertèbres. L'excès d'AR peut également résulter en une troncation axiale. Néanmoins, les études antérieures n'ont pu définir les bases cellulaire et moléculaire associées au phénotype de régression caudale. Cette question fut donc adressée en examinant les effets causés par l'excès de rétinoïdes sur l'expression de plusieurs marqueurs spécifiques dans la région postérieure de l'embryon. Une diminution de l'expression de certains marqueurs du mésoderme, tels que *brachyury* et *wnt3a*, fut observée indiquant que le mésoderme en formation est le site primaire affecté menant aux troncations axiales. De plus, les résultats obtenus ont permis de révéler de nouveaux aspects de la régulation par les rétinoïdes en démontrant la présence d'un mécanisme de rétro-action impliquant l'enzyme catabolique Cyp26A1. Finalement, dans le but de définir de nouveaux rôles pour les RARs, une approche de remplacement de gène, utilisant un RAR dominant négatif, fut développée afin de contourner la redondance parmi les RARs. Cette stratégie permis de démontrer, pour la première fois, un rôle pour les rétinoïdes dans le processus de morphogenèse tardive du cœur. En conclusion, l'ensemble de ces résultats a mené à l'approfondissement de nos connaissances des rôles des rétinoïdes, et de leurs effecteurs, dans l'établissement des axes embryonnaires.

MOTS CLÉS: Acide retinoïque, *brachyury*, dominant négatif, identité vertébrale, morphogenèse du cœur, myocarde, récepteurs de l'acide rétinoïque, régression caudale, *pitx2*.

TABLE OF CONTENTS

LIST OF FIGURES

CHAPTER 1

CHAPTER 2

CHAPTER 3

CHAPTER 4

CHAPTER 5

LIST OF TABLES

CHAPTER 1

CHAPTER 2

ABBREVIATIONS

ACTR:	Activator of the TR and RAR
ActRIIA/B:	Activin receptor type II A or B
AIB1:	Amplified in breast cancer 1
A-P:	Anterior-Posterior
AP-1:	Activator protein 1
AVE:	Anterior visceral endoderm
β-gal:	β-galactosidase
BMP:	Bone morphogenetic protein
CBP:	Creb-binding protein
cDNA:	Complimentary DNA
CNS:	Central nervous system
Cyp26A1:	Cytochrome P450 member 26A1; used interchangeably with P450RAI
DBD:	DNA-binding domain
DNA:	Deoxyribonucleic acid
DR:	Direct repeat
DRIP:	Vitamin D_3 receptor-interacting protein
dpc:	Days post-coitum; used interchangeably with E
DR:	Direct repeat
D-V:	Dorso-Ventral
E:	Embryonic day
EGF-CFC:	Epidermal growth factor-like-cryptic-FRL-crypto cystein-rich domain
FGF:	Fibroblast growth factor
FGFR1:	Fibroblast growth factor receptor 1
GRIP1:	Glucocorticoid receptor-interacting protein 1
HAT:	Histone acetyl transferase
HDAC:	Histone deacetylase
Hox:	Homeobox gene

HPLC:	High performance liquid chromatography
inv:	*inversion of embryonic turning*
iv:	*inversus viscerum*
JNK:	c-jun N-terminal kinase
Kb:	Kilobase
LBD:	Ligand binding domain
LPM:	Lateral plate mesoderm
L-R:	Left-Right
mSIN3:	Mouse homolog of the yeast transcriptional repressor Sin3
NCC:	Neural crest cell
N-CoA:	Nuclear receptor coactivator
N-CoR:	Nuclear receptor corepressor
NR:	Nuclear hormone receptor
P/CAF:	p300/CBP-associated factor
P/CIP:	p300/CBP co-integrator-associated protein
PBX:	Polycomb/bithorax group gene
Pitx2:	Pituitary homeobox gene 2
RA:	Retinoic acid
Raldh2:	Retinal dehydrogenase type 2
RAR:	Retinoic acid receptor
RARγE:	RAR dominant negative harboring a glycine to glutamic acid change at amino acid position 305
RARE:	Retinoic acid response element
RXR:	Retinoid x receptor
SAP30:	mSin3-associated protein 30
Shh:	Sonic hedgehog
Smad:	Sma/Mad homolog
SMRT:	Silencing mediator for RAR and TR
SRC-1:	Steroid hormone receptor coactivator-1
TAF:	TBP-associated factor
TBP:	TATA-binding protein

TGFβ:	Transforming growth factor β
TR:	Thyroid hormone receptor
TRAP:	Thyroid hormone receptor-associated protein
TIF2:	Transcriptional intermediary factor 2
Wnt:	Wingless/int-related
VAD:	Vitamin A deficiency
VDR:	Vitamin D_3 receptor

DEDICATION

To my family

ACKNOWLEDGEMENTS

I wish to thank my thesis supervisor, Dr David Lohnes, for welcoming me in his laboratory and giving me the opportunity to develop skills in experimental science. He has never negated on his duties to teach me a strict adherence to the burden of proof, and for this I am enormously grateful.

I would like to express my appreciation for the members of the laboratory for their comradeship. Their wit and humor provided for many memorable times that made laboratory life both enjoyable and stimulating. During the course of my studies I have befriended many past and present laboratory members, and wish to single them out for their support: Debbie Allan, Martin Houle, and Marie-Claude Marchand. In particular, I wish to acknowledge the assistance of Melanie Beland for her expert translation of my summary. They have made my stay at the IRCM an unforgettable experience.

I am especially indebted to my loving family for their exuberant support of my studies during past several years. Their resolve and faith has never wavered from my initial explorations into the world of science to the completion of my doctorate. They have been a source of enduring strength for me. In particular, this work would never have been possible without the support of my mother and father. It is to their credit if any value is accrued from this work.

This thesis is, in a way, a continuation of a journey began by my grandparents so long ago. I am in their debt for ultimately providing me with opportunities denied to themselves, and am eternally grateful for their boundless affection and sagacity.

Finally, I am grateful to the Medical Research Council of Canada/ Canadian Institutes of Health Research, the Institute de Recherches Cliniques de Montréal, and the Université de Montréal for their financial support during the course of my studies.

Every animal an end in itself springs forth perfect
From the womb of nature and produces perfect children.
All the limbs form themselves according to eternal laws,
And the rarest forms preserve in secret the original pattern.
So each foot, long or short, moves in complete harmony,
With the essence of the animal and its requirements,
For all the animate limbs never contradict themselves,
Rather all are directed toward life.
The form of the animal determines its way of life,
While its ways powerfully react on every form,
And so the ordered formation holds fast,
Though inclining to change through the action of External conditions.

Johanne Wolfgang von Goethe

As quoted in *The Meaning of Evolution*, by Robert J. Richards

I decided to appear openly in the theater of the world as a witness of the sober truth.

Galileo Galilei in *Dialogue*

As quoted in *Galileo's Daughter*, by Dava Sobel

Important lessons: look carefully; record what you see. Find a way to make beauty necessary; find a way to make necessity beautiful.

Anne Michaels in *Fugitive Pieces*

CHAPTER 1

INTRODUCTION

1.1 Vitamin A Signaling

A fundamental question of modern biological sciences is the identity of the genetic and environmental factors that influence vertebrate development. The generation of animal form is accomplished by highly inventive and adaptive iterative cellular processes that are driven by conservative signaling pathways. The intrinsic aspects of development are only now beginning to be understood genetically. Yet, animal morphogenesis is also dependent upon extrinsic factors. The retinoids (vitamin A and its derivatives) are such external agents that have dramatic capacity to modify and regulate vertebrate embryogenesis. They interact with an organism's genome by specifically activating the retinoic acid receptors (RARs), transcription factors that influence diverse embryological processes such as cranio-facial, heart and nervous system development, among others.

1.1.1. Retinoid Biosynthesis And Binding Proteins

Retinoids are acquired in the diet from either animal sources in the form of retinal esters or vegetal sources as provitamin carotenoids. Although these compounds exhibit remarkably diverse functions, they are relatively simple, consisting of a β-ionone ring, an isoprenoid tail and a polar end group that varies in its oxidation state. The parental compound is vitamin A or retinol and is characterized by a hydroxyl group attached at its end. The metabolism of vitamin A produces increasing polar molecules such as retinal, which contains an aldehyde, and retinoic acid (RA), which harbors a carboxyl group at its extremity (Fig. 1-1).

Dietary retinoids are absorbed from the enterocytes in the lumen or the mucosa of the small intestine where its processing depends on its source. Retinyl esters are hydrolyzed to retinol, whereas provitamin β-carotenoids are oxidized to retinal and subsequently reduced to retinol (Gottesman *et al.*, 2001; Napoli, 1999; Noy, 2000). The retinol is then re-esterfied within the enterocytes and is packaged into chylomicrons. These lipoproteins are secreted into the lymphatic system and the majority is taken up and stored by the liver and other tissues. Bioactive retinoids, such as retinoic acid (RA), are synthesized from retinyl ester stores in serial oxidation reactions catalyzed by various enzymes.

Figure 1-1. Simplified depiction of the metabolism of vitamin A (retinol) and the role of the various enzymes in each step.

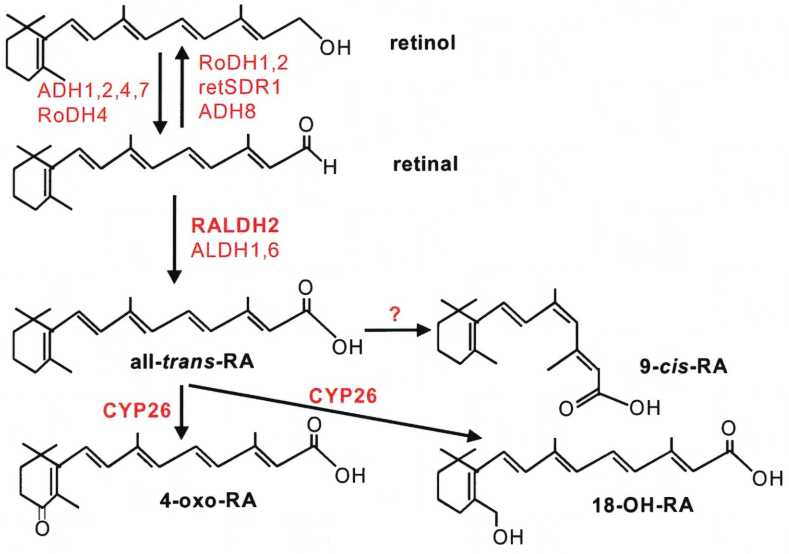

The major site of storage of retinoids is the liver. It expresses a large diversity of enzymes involved in the synthesis and metabolism of these compounds. The first step in the synthesis of RA, the active form of vitamin A, involves the hydrolysis of retinyl esters to produce retinol. The hydrolase activity that cleaves retinyl esters, such as retinyl palmitate, in the liver have yet to be fully characterized but involve bile-salt dependent and independent pathways (Gottesman *et al.*, 2001; Napoli, 1999). Mobilized retinol travels throughout the bloodstream complexed to retinol binding protein (RBP). This protein is involved in secretion of retinol from hepatocytes but is not critically required for the delivery of retinol to cells, as $RBP^{-/-}$ mice are viable and fertile (Quandro *et al.*, 1999). Gottesman and colleagues (2001) have speculated that there exists several RBP-independent pathways that deliver retinoids to target tissues. These include the circulation of free RA circulating in the serum (estimated at 0.2-0.7% the concentration of retinol-RBP), retinyl esters in chylomicrons and chylomicron remnants, soluble glucoronides of retinol and RA, and provitamin A carotenoids that can be metabolized within diverse tissues. However, as the retinoids are highly lipophilic, they can conceivably pass through the cell membrane and enter cells passively.

Once inside the cell, retinol or retinal associate with cytosolic binding proteins called cellular retinol binding proteins (CRBPI and CRBPII). These conserved proteins may be involved in the metabolism and storage of retinol. Both CRBPI and CRBPII bound to retinol direct its esterification by lecithin retinol acyltransferases (LRAT), while the absence of retinol bound to CRBPI stimulates the hydrolysis of retinyl esters (Ong *et al.,* 1988; reviewed in Gottesman *et al.*, 2001; Noy, 2000). Another proposed function for CRBPI to present retinol and retinal to specific dehydrogenases via direct protein-protein interactions (Napoli, 2000; Noy, 20002). Thus, CRBPI acts as an intracellular transporter of retinol and retinal, facilitates the uptake of retinol from the blood, and enhances retinoid metabolism and storage. These seemingly important roles are, however, not required for viability as CRBPI null mutant mice are largely normal (Ghyselinck *et al.*, 1999). CRBPI$^{-/-}$ mice do have reduced retinyl ester stores and retinoid uptake in their livers, supporting a modest requirement for this gene in retinoid storage and mobilization. As mammals have an additional CRBP gene (CRBPII), it may compensate for the lack of CRBPI. The difficulty in this hypothesis is that CRBPII is only transiently expressed in the liver during embryogenesis, and is restricted to the small intestine of the adult. CRBPI, on the other hand, is expressed in multiple tissues of the fetus and adult, being particularly abundant in the liver (Gustafson *et al.,* 1993). Additionally, CRBPII seems to have a distinct function in the initial processing of vitamin A from food and may also play a role in the targeting of retinal to microsomal enzymes for its reduction to RA. As CRBP double null mutants have yet to be described, functional redundancy remains a possible explanation for the lack of an obvious phenotype associated with CRBPI$^{-/-}$ mice.

RA binds to another class of retinoid binding proteins, the cellular retinoic acid binding proteins (CRABPI and CRABPII). These proteins are highly similar and are widely expressed during embryogenesis, while in the adult the near ubiquitous expression of CRABPI contrasts with the more restricted domain of CRABPII (i.e. skin, uterus, ovary, brain; Dollé *et al.*, 1990; Fiorella *et al.*, 1993; Perez-Castro *et al.,* 1989; Ruberte *et al.*, 1991). These proteins are thought to render RA soluble in the cytosol and shuttle the bioactive retinoid between different cellular compartments. CRABPI also seems to stimulate the formation of polar metabolites from RA by serving as substrate (when complexed with RA) for microsomal enzymes such as CYP26 (Fiorella and Napoli,

1991; Fujii *et al.*, 1997; White *et al.*, 1996). CRABPII associates with retinoid receptors (RARα and RXRα) in a ligand-dependent fashion, raising the intriguing possibility that CRABPII functions as a chaperone for RA by transporting it from the cytosol to the nucleus where it is presented to RXR:RAR heterodimers (Delva *et al.*, 1999). Whether these observations have any physiological relevance was placed in doubt by the generation of null mutations for these genes. CRABPI null mice are viable and fertile (Gorry *et al.,* 1994), and with the exception of a mild limb phenotype, CRABPII$^{-/-}$ and CRABPI/CRABPII double null mutants are completely normal (Fawcett *et al.,* 1995; Lampron *et al.*, 1995). Thus, in a vitamin A sufficient diet, there may be enough retinoids within the cytoplasm to drive RA synthesis at levels competent for normal development without the aid of these putative chaperones.

1.1.2. Biosynthesis Of Retinal

The oxidation of vitamin A to retinal is accomplished by at least two different families of alcohol dehydrogenases that are grouped according to their size. Furthermore, the synthesis of retinal from retinol is reversible (Fig. 1-1). In the presence of NAD, retinol is oxidized by alcohol dehyrogenases, whereas NADPH favors the reverse reaction, (i.e. the reduction of retinal to retinol), via the activities of members of the same family of enzymes (Duester, 2000). Hence, they are often referred to as alcohol dehydrogenases/ reductases, whose activity depends on the availability of protonated cofactors.

Medium-chain alcohol dehydrogenases. These are cytosolic zinc metalloenzymes represented by four classes in mouse (Adh1-4) and additional members in the chick (ADH7) and frog (ADH8; Duester, 2000; Ross *et al.*, 2000). ADH1, ADH2 and ADH4 have been reported catalyze the oxidation of retinol to retinal in a NAD-dependent manner, with ADH4 being the most efficient (Duester, 2000). However, their specificity is not limited to retinol as ethanol can also serve as a substrate (Ross *et al.*, 2000). Adh1 is expressed in a variety of embryonic and adult tissues consistent with RA production and is particularly abundant in the liver (Ang and Duester, 1999; Deuster, 2000; Vonesch *et al.*, 1994). ADH4 is also expressed in retinoid-target tissues but is absent from the liver. Expression begins in the primitive streak coinciding with the onset of RA in the embryo, and is subsequently detected in the trunk, forelimb bud, cranial neural crest and

cranio-facial mesenchyme (Ang *et al.*, 1996). Disruption of ADH1 or ADH4 function in the mouse did not result in any defects, however, when challenged with a dose of retinol, *adh1*$^{-/-}$ and *adh4*$^{-/-}$ mice were compromised in their ability to synthesize RA (Deltour *et al.*, 1999a, 1999b). The lack of any severe phenotypes in ADH null mice demonstrates the robustness of the retinoid biosynthetic pathway and is consistent with the relatively large number of enzymes capable of oxidizing retinol (Fig. 1-1).

Short-chain dehydrogenases/reductases (SDRs). These enzymes are smaller than ADHs and do not require a catalytic metal ion (Deuster, 2000). This group includes RoDH1-4, RDH5, and ret SDR1, among others, which share extensive sequence homology to one another. They associate with the microsomal fraction of cells and are collectively widely expressed (Duester, 2000). In particular, RoDH1 and RoDH2 are abundant in the liver and kidneys and prefer NADP as a cofactor over NAD, and are thus likely involved in the reduction of retinal to retinol. The physiological role of these proteins in retinoid biosynthesis remains preliminary as the mouse mutations for SDRs have not yet been reported.

1.1.3. Biosynthesis Of Retinoic Acid

The synthesis of RA from retinal is irreversible and requires its own set of specific enzymes (Fig. 1-1; Deuster, 2000; Ross *et al.*, 1999). They are cytosolic NAD-dependent dehydrogenases such as ALDH1 (AHD2/RALDHI), ALDH6 and Raldh2 (ALDH1A7). The earliest expression of *ALDH1* and *raldh2* occurs in the primitive streak during mouse gastrulation (Ang and Duester, 1997; Niederrether *et al.*, 1997). For both of these genes, and particularly for *raldh2*, transcripts are excluded from the node, but are enriched in the surrounding mesoderm layer being generated by the primitive streak. Shortly after gastrulation, *raldh2* is expressed throughout the posterior embryo with an anterior limit at the base of the headfolds. At subsequent stages (E8.5 and onwards), *raldh2* transcripts are restricted to the mesoderm along the trunk of the embryo, the hindbrain, developing eye, and in the somites (Fig. 1-2; Niederreither *et al.*, 1997). Furthermore, its expression seems to accompany the cranio-caudal formation of the somites, being initially detected within the newly condensing somites in the posterior region, with expression increasing substantially in more mature somites rostrally (Fig. 1-2). *Raldh2* expression in the spinal

cord begins at day 10 to 11 of gestation in the mouse, in the anterior (cervical) and posterior (lumbar) regions adjacent to the developing fore- and hind limb buds, respectively (Niederreither *et al.*, 1997). The anterior limit of expression never surpassed the posterior-most hindbrain, while the posterior boundary remained fixed at the level of the most recently formed somite throughout mouse development, and did not extend into the caudal embryo (Fig. 1-2C; Niederreither *et al.*, 1997). Expression in the limb buds is restricted to the interdigital mesenchyme that eventually undergoes apoptosis.

Raldh2 activity seems to be highly specific for RA synthesis from retinal precursors in the embryo (Haselback *et al.,* 1999; Zhao *et al.*, 1996). In a rare example of the lack of functional redundancy in the retinoid biosynthetic pathway, the null mutation of *raldh2* results in embryo lethality and a syndrome of abnormalities that are consistent with a role for this enzyme in RA synthesis during development (Niederreither *et al.*, 1999). Particularly, *raldh2*$^{-/-}$ embryos display severe heart, neural tube, hindbrain and neural crest cell defects, and caudal axial truncations (Niederreither *et al.*, 1999, 2000, 2001). Importantly, these tissues are often targeted by aberrant retinoid signaling in both avians and mammals (Means and Gudas, 1995; Zile, 1998, 2001). Niederreither and colleagues (1999) also demonstrated that the *raldh2*$^{-/-}$ lacked RA, as the expression of a RA responsive transgene was lost in the mutants. These studies therefore suggest that Raldh2 is the principal RA synthesizing enzyme during mammalian embryogenesis.

1.1.4. Cyp26A1 And RA Catabolism

Developmental processes are highly sensitive to the effects of bioactive retinoids (Collins and Mao, 1999; Means and Gudas, 1995). Controlling the availability of RA during development is accomplished by the regulated expression of RA biosynthetic enzymes, as briefly outlined above. In addition, vertebrates have also evolved RA degradative pathways to counteract the teratogenic effects of this molecule and strictly regulate RA levels during embryogenesis. Within the last few years, a novel family of cytochrome RA hydroxylases represented by P450RAI/Cyp26A1, has been identified (Fujii *et al.*, 1997; Ray *et al.*, 1997; White *et al.*, 1996). This enzyme is highly conserved between mice and humans (93% identity) and is believed to play a major role in inactivating retinoids by catabolizing RA into more polar compounds (Abu-Abed *et al.*, 1998). Over-expression of

Cyp26 in several different cell lines leads to the production of 4-oxo-RA, 4-OH-RA, and 18-OH-RA from all-*trans*-RA (Fig. 1-1; Fujii *et al.*, 1997; White *et al.*, 1996, 1997). Furthermore, the oxidation of RA generating more polar metabolites reduces its biological activity and likely initiates its ultimate destruction (Fiorella and Napoli, 1994; Fujii *et al.*, 1997; White at al., 1996, 1997). Interestingly, this enzyme is involved in a positive feedback loop with RA directly regulating its expression in cells and in the embryo (Abu-Abed *et al.*, 1998; Fujii *et al.*, 1997; Ray *et al.*, 1997; White *et al.*, 1996). Indeed, White and colleagues (1996) isolated Cyp26A1 based on a differential screen for RA-induced transcripts. Moreover, the proximal promoter region of this gene has been found to harbor a conserved retinoic acid response element (RARE) that binds RXRα/ RARγ heterodimers *in vitro* and is required for efficient induction of reporter gene expression in response to RA (Loudig *et al.*, 2000). This suggests that it serves to protect the embryo from retinoid toxicity, as increased levels of RA lead to increased expression of Cyp26A1 and subsequently enhanced degradation of the retinoid. Consistent with this, the over expression of *cyp26A1* in *Xenopus* embryos inhibits the teratogenic effects of RA on neurectodermal development (Hollermann *et al.*, 1998).

The earliest expression of *cyp26A1* is in the primitive streak of the gastrulating mouse embryo as a posterior-high gradient (Fig. 1-2; deRoos *et al.,* 1999; Fujii *et al.*, 1997). Transcripts are also transiently detected in the neuroepithelium and mesoderm anterior to the node during head fold formation stages (E7.5-8), where the future CNS forms (deRoos *et al.,* 1999; Fujii *et al.*, 1997; MacLean *et al.*, 2001; Swindell *et al.*, 1999). The node and its derivative, the notochord, do not express this gene during these stages in both the chick and mouse. At later stages (E8.5 and onwards), abundant *cyp26A1* transcripts are found in the neuroepithelium, mesoderm and hindgut in the open caudal neuropore of the embryo (Fig. 1-2C). This expression is maintained in the posterior region as it develops into the tail bud. Other sites of *cyp26A1* expression include the condensing mesenchyme of the limb buds, medial aspect of the developing eye, endocardium of the rostral and caudal heart, prospective second rhombomere, first pharyngeal arch ectoderm, migrating rhombomeric neural crest cells, and the cranial ganglia (deRoos *et al.,* 1999; Fujii *et al.*, 1997; MacClean *et al.*, 2001). These populations are highly sensitive to the effects of excess RA, and agree with a role for this enzyme in

limiting retinoid signaling to permit normal development (Means and Gudas, 1995). In the adult, *cyp26A1* transcripts are detected primarily in the liver, consistent with a role in retinoid metabolism (Ray *et al.*, 1997).

Recently, the importance of Cyp26A1 during mammalian development was confirmed by the targeted mutagenesis of this gene (Abu-Abed *et al.*, 2001; Sakai *et al.*, 2001). These mutants display malformations striking similar to those evoked by excess RA. For instance, *cyp26A1*$^{-/-}$ embryos exhibit a severe truncation of the caudal embryo and posterior transformations of the cervical vertebrae. However, the rostral hindbrain is largely normal in these mutants. This is puzzling in light of the fact that excess RA has been shown to perturb this region (Galvalas and Krumlauf, 2000). A possible explanation may be a partial functional redundancy with a second Cyp26 member (P450RAI-2/Cyp26B1), which is highly expressed in the developing hindbrain throughout its development from E8.5 to E11.5 (MacLean *et al.*, 2001; White *et al.*, 2000a). Indeed, *cyp26B1* expression in the hindbrain is much greater and more extensive than that of *cyp26A1*, supporting the possibility for functional redundancy between the two genes in the posterior CNS. *Cyp26B1* is also highly expressed in the ectoderm and endoderm of the caudal pharyngeal arches, which nicely complements the mesenchymal expression of *cyp26A1* in this region. (Fujii *et al.*, 1997; MacClean *et al.*, 2001). Additional regions of *cyp26B1* expression include the developing limb bud during its outgrowth phase. Despite possibly redundancies between the Cyp26 family members, these results generally support a role for Cyp26A1 in the generation of RA deficiencies within particular embryonic regions and at specific times during development.

1.2. Embryonic RA Distribution

Determining the tissues that contain vitamin A derivatives is of primary interest to retinoid biology. Initial studies have identified the posterior region of the limb bud (the zone of polarizing activity or ZPA) as a source of RA that was believed to assign posterior pattering information to the developing autopod (reviewed in Hofmann and Eichele, 1994). In the same vein, others have noted that presumed RA production in the organizer tissue, such as the mouse node (see below), and midline tissues (floorplate and

notochord) are able to induce mirror-image duplications of digits when grafted onto anterior regions of the chick wing bud (Chen *et al.*, 1992; Chen and Solursh, 1992; Hogan *et al.*, 1992). Importantly, it was noted that organizer tissues from avians and amphibians also contain high levels of endogenous retinoids (Chen *et al.*, 1992, 1994). These interesting observations led to the hypothesis that RA functions as a conserved posteriorizing signal in the vertebrate embryo. Subsequent work in the mouse and chick embryo has revealed that the node and midline tissues themselves do not contain retinoids, but that the mesoderm surrounding these tissues do (Horton and Maden, 1995; Maden *et al.*, 1998). Furthermore, the polarizing activities of the notochord and floorplate detected in these assays were likely due the abundant expression of Sonic Hedgehog (Shh) protein in these tissues (Echelard *et al.*, 1993; Riddle *et al.*, 1993). Shh is also expressed in the posterior margin of the early limb bud and in itself can mediate the effects of the ZPA (Echelard *et al.*, 1993; Riddle *et al.*, 1993). In support of this, organizer tissue from vitamin A deficient (VAD) quail embryos is still able to induce limb duplication in heterotopic grafts in chick wing buds (Chen *et al.*, 1996). Shh expression was found to be unaffected in VAD tissues, likely accounting for their observed limb-inducing abilities in grafting experiments. These initial claims of organizer-like properties of retinoids have therefore been tempered with a more limited role for these molecules in the antero-posterior patterning of the various axial and apendicular structures, principally by regulating *Homeobox* (*Hox*) gene expression (see below; Conlon, 1995; Gavalas and Krumlauf, 2000; Means and Gudas, 1995).

1.2.1. Retinoid Distribution Reflects The Expression Of Biosynthetic And Degradative Enzymes

As one might expect, the level and distribution of bioactive retinoids closely parallel the distribution of RA biosynthetic and degredative enzymes, such as Raldh2 and Cyp26A1, respectively (Fig. 1-2; Fujii *et al.*, 1997; McCaffery and Drager, 1994; McCaffery *et al.*, 1999; Niederreither *et al.*, 1997). This becomes obvious by early somitogenesis stages, with the lack of RA from the posterior embryo occurring concomitantly with the up-regulation of Cyp26A1. As a result, a very sharp boundary of RA-containing and RA-deficient regions is created at the interface between the nascent posterior mesoderm and

developing somites. This has been strikingly demonstrated by the expression of an RA-responsive transgene in the mouse embryo (Balkan *et al.*, 1992; Mendelsohn *et al.*, 1991; Rossant *et al.*, 1991). These transgenic mice harbor a β-gal reporter gene driven by a tandem repeat of the RARβ2 RARE, which is activated in a manner that closely reflects the distribution of endogenous retinoids determined by HPLC and F9 reporter explant assays (Horton and Maden, 1995; Maden *et al.*, 1998; Wagner *et al.*, 1992). Particularly, the transgenic embryos show abundant β-gal activity throughout the trunk and developing spinal cord with a clear posterior boundary at the caudal-most (i.e. most recently formed) somite, and an anterior boundary at the level of the posterior hindbrain.

HPLC studies in the chick embryo also reveal a sharp transition between retinoid-rich and retinoid deficient regions in the equivalent anterior and posterior regions (Maden *et al.*, 1998). However, in the gastrulating chick embryo, *raldh2* and *cyp26A1* expression are highly complementary (Swindell *et al.*, 1999). In contrast to the mouse, the authors found little or no *cyp26A1* expression in the posterior chick embryo, but abundant expression was seen anterior to the node in the ectoderm surrounding the notochord. Interestingly, they also observed a gradient of *raldh2* expression in the mesoderm surrounding the primitive streak and Hensen's node, with the higher levels in anterior mesoderm. Indeed, unlike mammalian embryos, the posterior-most mesoderm in the chick gastrula does not express *raldh2*. In both cases, however, bioactive retinoids are expected to be low or lacking in the posterior region of the embryo. Thus, the two species have evolved different ways to keep the caudal-most mesoderm relatively free of RA, elegantly demonstrating the mechanistic conservatism of vertebrate development.

Further differences between avians and mammals include the type of retinoids found in embryonic tissues. In the chick embryo, for example, didehydro RA is the most abundant bioactive retinoid and seems as effective as all-*trans*-RA in inducing retinoid-responsive reporter gene expression in cells (Maden *et al.*, 1998). In the mouse embryo, all-*trans*-RA was the only RA detected (Horton and Maden, 1995). Although 9-*cis*-RA isomer can be generated from retinoid precursors in cells (Fig. 1-1), and is able to bind and activate retinoid receptors, it has not been detected in embryonic tissues in the mouse nor chick (Chambon, 1996; Horton and Maden, 1995; Maden *et al.*, 1998). This remains a matter of contention as a dehydrogenase specific for the 9-*cis* retinol isomer was

identified in the mouse embryo (Romert *et al.*, 1998). Furthermore, this enzyme displays restricted embryonic expression in regions that require retinoid signaling, such as the developing spinal cord, eye, somites and the heart. However, due to the lack of detection of 9-*cis*-RA during mouse development, its physiological role remains uncertain.

1.2.2. Dorso-Ventral Distribution Of Retinoids In The Embryonic Axis

Retinoid levels in the developing vertebrate axis are distributed as an increasing concentration along the ventral-dorsal axis, with the highest levels detected in spinal cord throughout embryogenesis (Fig. 1-2C; Horton and Maden, 1995; Maden *et al.*, 1998; McCaffery and Drager, 1994; Wagner *et al.*, 1992). This contrasts with an earlier more uniform retinoid distribution in the primitive streak, which includes all tissues posterior to, but excluding, the node (Fig. 1-2A). At later stages, regions containing moderate to high levels of retinoids include the mesenchyme surrounding the hindbrain, somites, eyes and limb bud mesoderm. Sites containing relatively low retinoids are the pharyngeal arches and frontonasal mass, lateral plate mesoderm, and the heart (Maden *et al.*, 1998). Importantly, the node and anterior CNS neuroepthelium have no or barely detectable levels of retinoids, respectively. This is in accordance with the recent analyses of *raldh2* and *cyp26A1* expression, confirming that RA is produced in mesoderm surrounding the node and not within the organizer itself (Fig. 1-2).

1.2.3. Implications For Developmental Mechanisms

Perhaps the most interesting observation derived from these studies is that regions rich in bioactive retinoids seem to be distributed adjacent to retinoid-deficient ones, creating sharp boundaries, instead of gradients, of retinoids across embryonic tissues, as was initially assumed (Chen et al., 1992; Hofmann and Eichele, 1994). The implications for developmental mechanisms are profound as it suggests that retinoids do not behave as morphogens. To be a morphogen, a molecule must spread out from a localized source to form a concentration gradient along an embryonic axis and directly influence the types of cells formed along that gradient (Lawrence, 2001). Morphogens presumably pattern tissues by virtue of the generation of different cell types depending on the graded

Figure 1-2. RA distribution and *cyp26A1* and *raldh2* expression in the mouse embryo.

(**A**) RA distribution and (**B**) expression of *cyp26A1* and *raldh2* in the late primitive streak stage. (**C**) RA distribution and (**D**) expression of *cyp26A1* and *raldh2* in 9 day old mouse embryos [Please refer to text for references].

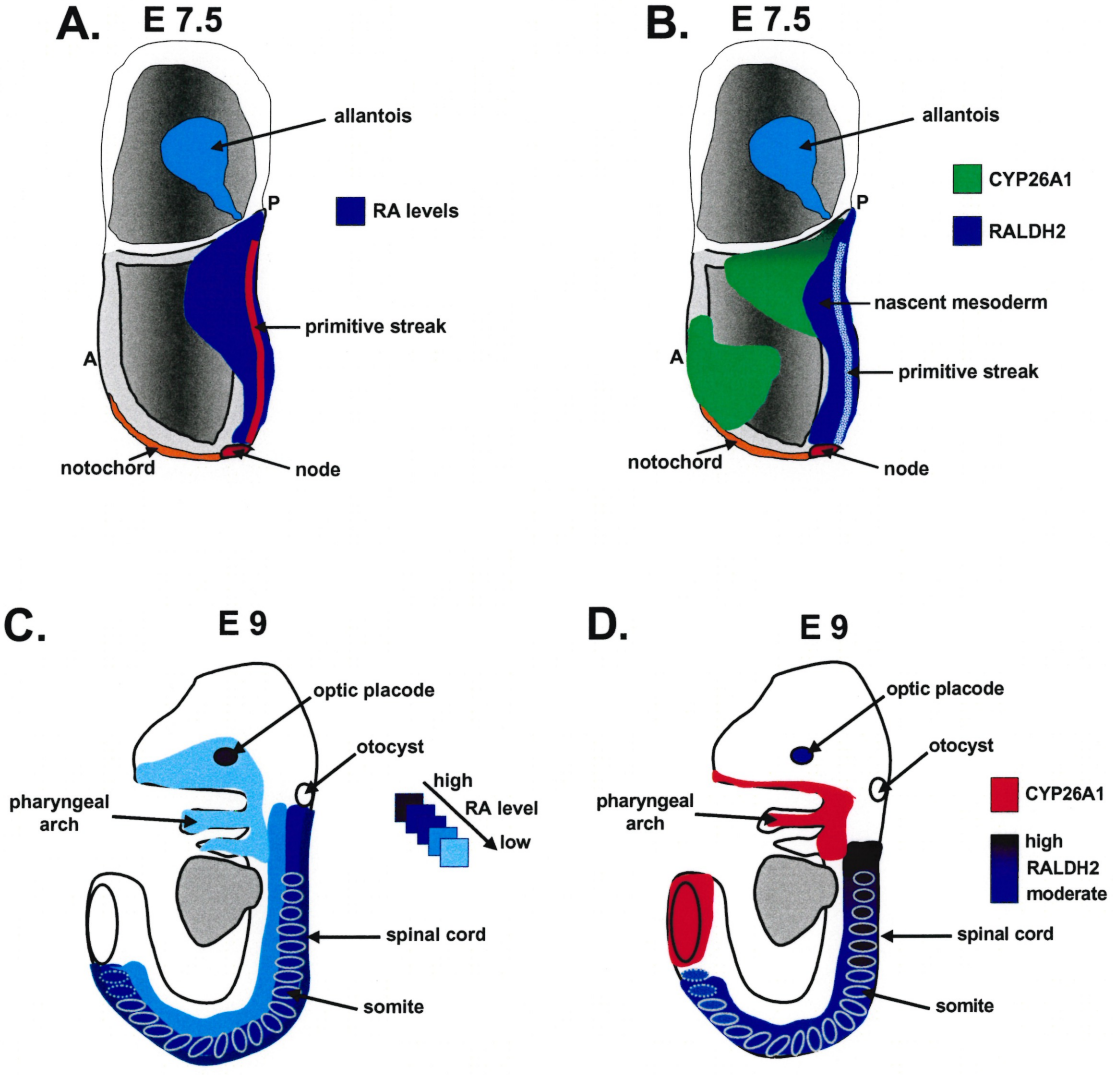

concentration of the molecule. The idea that molecular gradients pattern tissues is a powerful and unifying one in developmental biology and has been given much support within the last few years (Tabata, 2001). Shh is an example of a morphogen that influences the development of diverse neuronal cell types along the dorso-ventral axis in response to a ventral-high gradient of the protein (Ericson *et al.,* 1997; McMahon, 2000; Tabata, 2001). Yet, retinoids do not appear to influence cell fate decisions simply based on concentration as they are distributed in an almost uniform manner along the antero-posterior axis. The information supplied by RA may involve an all or none decision making process at the boundaries of retinoid-enriched and deficient areas at particular times of development. During gastrulation, when retinoids are abundant in the primitive streak, they likely instruct ingressing presumptive paraxial mesoderm to adopt progressively more posterior fates (see section 1.6). At later stages, when somitogenesis is well underway, RA diffusing from the trunk may influence the condensation of newly forming paraxial mesoderm in the caudal embryo.

It remains possible, however, the cells at the on/off retinoid boundaries at the extremities of the spinal cord experience a steep gradient of RA, and that this gradient can pattern the intervening tissues. For instance, at the anterior end of the spinal neural tube near the hindbrain (or rhombencephalon), RA can presumably bias rhombomeric identity to more posterior fates in a gradient-dependent manner by inducing a cohort of *hox* gene expression (see below; Gavalas and Krumlauf, 2000). This phenomenon provides the most compelling evidence yet for the existence of a retinoid gradient, however steep, that is able to pattern tissues, and is discussed at length in section 1.6.3.

1.3. Retinoic Receptors: Transducing The RA Signal

1.3.1. The Retinoic Acid Receptors

The discovery that RA exerts its function by binding to a group of transcription factors, referred to as the retinoic acid receptors (RARs), revolutionized our understanding of retinoid biology (Giguère *et al.*, 1987; Petkovich *et al.*, 1987). The principal ligands that are able to bind to activate the RARs are both all-*trans*- and 9-*cis*-RA (Allanby *et al.*, 1993). The RARs belong to the nuclear receptor (NR) superfamily of ligand-induced

transcription factors that includes steroid hormone receptors, thyroid hormones, and vitamin D_3 receptors, among others (Mangelsdorf *et al.*, 1995). In mammals, the RARs are represented by three members (α,β, and γ), which share a modular structure characteristic of the nuclear receptors that includes six regions (A-F; Fig. 1-3; Chambon, 1996). These regions encode a DNA binding domain (DBD), ligand-binding domain (LBD), and both ligand-dependent and independent transcriptional activation functions. With the exception of the carboxy-terminal F region, these receptors show remarkable species conservation, with amino acid identities reaching as high as 97% in the LBD region (Chambon, 1996; Lohnes *et al.*, 1992; Mangelsdorf *et al.*, 1995). Moreover, the conservation of a given receptor type across species is greater than the degree of conservation of the three RAR types within a given species. This implies that each RAR type performs unique functions.

Amino-terminal (A/B) domain. Additional complexity in RAR signaling results from the generation of isoforms that differ in their amino-terminal A region (Lohnes *et al.*, 1992). This is achieved by alternative splicing and the use of two separate promoters, P1 and P2 (Chambon, 1996). For RARα and RARγ, alternate promoter usage produces two isoforms (RARα1, α2, and RARγ1, γ2), while for RARβ, the combination of alternate promoter usage, differential splicing, and an isoform-specific start codon creates four isoforms (RARβ1-β4; Lohnes *et al.*, 1992; Nagpal *et al.*, 1992; Zelent *et al.*, 1991).

The amino-terminus harbors a transcription activation function, called AF-1, that is required for the full transcriptional activity of the RARs (Folkers *et al.* 1993; Nagpal *et al.*, 1993). This transcription activation domain functions independently of ligand binding, however it synergizes with a ligand-dependent transcription activation function, referred to as AF-2, located in the carboxy-terminus of the RARs (see below; Nagpal *et al.*, 1993; Taneja *et al.*, 1997). Amino-terminal RAR isoforms have been conserved during evolution, suggesting a possible mechanism for generating tissue-specific differences in RAR function by modulating the availability of the AF-1 domain. Interestingly, AF-1 region undergoes regulatory phosphorylations at conserved serine residues from cyclic-dependent kinases, among others, that enhance both the ligand-dependent and independent transcriptional activities of the RARs (Bastein *et al.*, 2000; Delmotte *et al.*, 1999; Rochette-Egly *et al.*, 1997, Taneja *et al.*, 1997). As this kinase

activity seems to be mediated by a complex containing TFIIH holoenzyme and CDK7, it raises the intriguing possibility that RARs may activate transcription in part by stimulating the formation of the initiation complex. Thus, several different signaling pathways can affect the transcriptional activity of the RARs through the phosphorylation of their amino-terminal region.

DNA-binding (C) domain. RARs, like all transcription factors, contain a sequence-specific DBD that recognizes a core consensus half-site of the retinoic acid response element (RARE; see below). It is composed of two alpha helices, the first of which, the recognition helix, makes direct contacts with the bases of target DNA sequences located in the major groove (Perlmann *et al.,* 1993; Schwabe *et al.,* 1993; reviewed in Aranda and Pascula, 2001; Mangelsdorf and Evans, 1995). The recognition helix contains one of two zinc finger motifs that are unique to the NRs. The second alpha helix encompasses the carboxyl terminus of the second zinc finger which projects away from the recognition helix at a right angle and is involved in receptor dimerization with another class of retinoid receptors, called the retinoid x receptors or RXRs (see below; Froman *et al.,* 1989; Gampe *et al.,* 2000; Kurokawa *et al.,* 1993; Perlmann *et al.,* 1993; Rosen *et al.,* 1993; Zechel *et al.,* 1994a, 1994b).

Ligand binding (E) domain. The LBD is a complex multifunctional region that is involved in ligand binding, receptor dimerization, ligand-dependent transcriptional activation, and co-factor interactions (Aranda and Pascual, 2001; Chambon, 1996; Mangelsdorf and Evans, 1995; Rosen *et al.,* 1993). It is composed of 12 conserved helices (H1-H12) and a β-turn between helices 5 and 6 (Renaud *et al.,* 1995; Wurtz *et al.,* 1996). These motifs are folded into an intricate triple-layered anti-parallel helical sandwich, with a central core of several helices squeezed between two layers of protein structure to create the ligand binding pocket. This cavity is predominantly hydrophobic and forms extensive contacts with RA deep within the ligand binding domain.

Perhaps the most important function of the retinoid receptors is encoded by the ligand-dependent transcription activation function, AF-2, located at the carboxyl extremity of the LBD. This highly conserved motif mediates the induction of target promoters by various NRs in response to ligand (Barettino *et al.,* 1994; Danielian *et al.,* 1992; Durand *et al.,* 1994; Webster *et al.,* 1988). In the absence of ligand, the AF-2

module extends an amphipathic α-helix (helix 12) at a 45° angle from the core structure (Bourguet *et al.*, 1995; Renaud *et al.,* 1995; Wurtz *et al.,* 1996). The addition of RA dramatically alters this structure, resulting in a significantly more compact LBD. Crystallographic analysis of a ligand-bound RARα carboxyl-terminal region demonstrates that the AF-2 core, which is contained in helix 12, bends towards the main body of the LBD to cover the RA bound within its pocket (Renaud *et al.*, 1995). The folding over of helix 12 has been compared to a mouse-trap, that acts to capture RA buried deep within the core of the LBD (Wurtz *et al.*, 1996). This, in addition with other less dramatic structural movements, generates a binding surface for co-activator proteins on the exterior of the molecule, while maintaining a highly hydrophobic interior that is intimately interacting with the ligand (Feng *et al.,* 1998). Herein lies the key to retinoid function: these small lipophilic molecules act as a switch that is able to transform the retinoid receptors into potent transcriptional activators.

Hinge (D) region. Between the DBD and LBD lies the hinge region. It confers a certain degree of rotational flexibility to the DBD, which is important for efficient dimerization of NRs on consensus DNA binding elements (Mader *et al.*, 1993a). This domain is also involved in the binding of co-repressors, and cooperates with the primary sites of co-repressor binding in the LBD (reviewed in Aranda and Pascual, 2001; Chambon,1996).

Figure 1-3. Modular structure of the retinoic acid receptors.

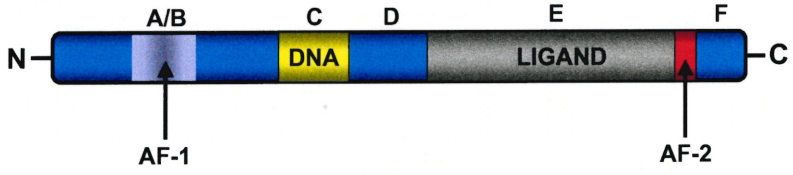

1.3.2. The Retinoid X Receptors: The Heterodimer Partner Of The RARs

Following the isolation of the RARs, several laboratories discovered that their effect on transcription can be potentiated by another group of retinoic acid receptors, the retinoid x receptors (RXRs; Leid *et al.*, 1992; Mangelsdorf *et al.*, 1990; Yu *et al.*, 1991). The RXRs

are also members of the nuclear hormone receptor superfamily and thus display a modular structure highly similar to the RARs (Fig.1-3). As with the RARs, multiple isoforms also exist for the three RXR genes (RXRα1, α2, β1, β2, γ1, and γ2; Chambon *et al.*, 1996). The homology between the RARs and RXRs is quite low, and suggests that they have diverged relatively early in vertebrate evolution (Chambon, 1996). Indeed, a RXR homolog exists in invertebrates, whereas the RARs have no counterpart outside the vertebrate phylum (Oro *et al.*, 1990). Another difference between the two retinoid receptor types is that RXRs can only bind the 9-*cis*-RA isomer, whereas RARs can associate with both all-*trans* and 9-*cis*-RA (Allenby *et al.*, 1993; Heyman *et al.*, 1992; Levin *et al.*, 1992; Zhang *et al.*, 1992; reviewed in Mangelsdorf *et al.*, 1994; Mangelsdorf and Evans, 1995). RXRs act as rather promiscuous heterodimer partners for a number of nuclear hormones receptors, including retinoic acid, thyroid hormone and vitamin D_3 receptors, among several others (Mangelsdorf and Evans, 1995). They can also function as homodimers depending on the RARE type, whereas they are obligatory heterodimers with the RARs (Kurokawa *et al.*, 1993, 1994; Mader *et al.*, 1993a; Perlmann *et al.*, 1993; Zechel *et al.*, 1994a; Zhang *et al.*, 1992). Within the RXR/RAR heterodimer, an RXR-selective ligand alone is unable to activate transcription of a reporter gene, while the addition of a RAR-specific ligand, such as all-*trans*-RA is able to induce transcription (Minucci *et al.*, 1997). This suggests that ligand binding to the RAR partner is an obligatory initial step in the activation of retinoid target genes.

1.3.3. Retinoic Acid Response Elements (RAREs)

The retinoid receptors bind to direct repeats of a conserved hexameric motif with the following consensus: PuG(G/T)TCA (Aranda and Pascual, 2001; Chambon, 1996; Mangelsdorf *et al.*, 1994). These response elements, referred to as retinoic acid response elements (RAREs), have been identified in the promoter regions of several genes, including the RARs themselves, some *hox* genes, and CRBPI and CRABPI, among others (Mangelsdorf *et al.*, 1991; Mangelsdorf *et al.*, 1994; Means and Gudas, 1995; Sucov *et al.*, 1990). The spacing between the repeats of the core RARE consensus is variable, but a separation of the hexameric motifs by five (DR5) or two (DR2) nucleotides seems to be optimal for RXR/RAR binding (Mader *et al.*, 1993b).

Furthermore, the sequences flanking the RAREs greatly influence receptor binding. Interestingly, RXR/RAR heterodimers bind to response elements more efficiently than do RXR homodimers, suggesting that the former constitutes the functional receptor complex *in vivo* (Mader *et al.*, 1993a). Additionally, several groups have shown that the heterodimer partner of RXR occupies the 3' consensus half-site and that this orientation is conferred by the dimerization interface contained within carboxyl terminal portion of the DNA-binding domain (Kurokawa *et al.*, 1993; Mader *et al.*, 1993a; Perlmann *et al.*, 1993; Zechel *et al.*, 1994a, 1994b). Indeed, cooperative binding of RXR/RAR and RXR/TR heterodimers were only observed when the RXR partner occupied the 5' half site. In support of these binding studies, crystallographic analyses of the RXR/TR pair has revealed that the RXR partner binds to the upstream hexameric DNA repeat (Rastinejad *et al.*, 1995). These observations therefore strengthen the hypothesis that the RXR/RAR heterodimer is the functional receptor complex that is involved in binding to and activating the promoters of target genes.

1.4. Retinoid Receptors And Transcriptional Activation

1.4.1. RARs And Transcriptional Co-Repressors

The transcriptional prowess of the RARs is modulated different groups of co-factors that can either suppress or activate transcription in a ligand-dependent fashion. Several important developments within the last few years have shed light on the regulatory machinery that mediates transcriptional repression conferred by unliganded nuclear receptors (Aranda and Pascual, 2001; Glass and Rosenfeld, 2000). Particularly, two large highly related proteins, termed N-CoR (nuclear receptor co-repressor) and SMRT (silencing mediator for RARs and TRs), have been independently isolated as RAR and TR interacting factors that mediate transcriptional repression by the NRs (Chen and Evans, 1995; Hörlein *et al.*, 1995). They define a novel class of co-repressor proteins that interact strongly with unliganded NRs. Moreover, expression of N-CoR or SMRT in tissue culture experiments led to a potent repression of both a TR and RAR responsive reporters in a ligand-independent manner (Chen and Evans, 1995; Hörlein *et al.*, 1995). Hörlein *et al.* (1995) also determined that NRs interact with these proteins largely

through their hinge region and LBDs. Importantly, the addition of ligand results in a dissociation of the co-repressors from the NRs concomitant with the induction of reporter gene expression (Chen and Evans, 1995; Hörlein *et al.*, 1995). This ligand-dependent release of co-repressors likely results from the loss of co-repressor binding surfaces due to the dramatic conformational changes that occur within the LBD of NRs (Glass and Rosenfeld, 2000; Wurst *et al.,* 1996).

1.4.2. Co-Repressors And Histone Deacetylation

The primary amino acid sequence of N-CoR and SMRT initially offered little insight into the nature of how they mediate transcriptional repression. They contain three unrelated repression domains (RD1, RD2, and RD3) and a carboxyl terminal NR interaction domain consisting of a bipartite motif (Hörlein *et al.*, 1995; Hu and Lazar, 1999; Perissi *et al.*, 1999; reviewed in Glass and Rosenfeld, 2000). Subsequent studies linked the co-repressors to a conserved histone deacetylase machinery which is thought to inactivate transcription by rendering chromatin more compact and relatively inaccessible to the basal transcription machinery (Alland *et al.*, 1997; Heinzel *et al.*, 1997; Nagy *et al.*, 1997). This is accomplished by the deacetylation of lysine residues within the amino-terminal tails of core histones (Ayer, 1999; Glass and Rosenfeld, 2000). Moreover, the acetylation state of the core histones is an important determinant of transcriptional activity (Marmorstein, 2001). A simple model of acetylation and transcription holds that in the absence of acetyl groups, histone tails are predominately basic and associate tightly with the acidic DNA backbone. As a consequence of this, the DNA becomes inaccessible to transcriptional activators leading to repression.

The principal enzymes involved in the deacetylation of chromatin are the HDACs (histone deacetylases). There are at least 7 members identified to date that are related to the yeast global transcriptional repressor, Rpd3p (Ayer, 1999). They form the enzymatic core of large multiprotein complex that are conserved in all eukaryotes. In mammalian cells, there are two distinct repressor complexes, both containing HDAC1 and HDAC2, but differing primarily by the presence of a scaffolding protein, mSin3A (Huang *et al.,* 2000). It is through mSin3A that NRs are able to recruit HDACs. Several groups have demonstrated that SMRT and N-CoR exert their repressive function by forming a ternary

complex with HDACs via mSin3A or mSin3B (Alland *et al.*, 1997; Heinzel *et al.*, 1997; Nagy *et al.*, 1997). N-CoR/SMRT recruits mSin3A through their amino terminal repressor domain (RD1), and also directly interacts with HDACs via RD2 and RD3. Thus, in the absence of ligand, RARs associate with N-CoR/SMRT which recruit histone deacetylases principally by associating with the molecular scaffolding proteins mSin3A and mSin3B (Fig. 1-4). Furthermore, the ternary complex formed by RAR (or TR) bound to N-CoR/SMRT, and HDACs via mSin3A is sufficient to confer active repression on RARE (or TRE) reporters *in vitro* (Nagy *et al.*, 1997). These observations suggest that unliganded RARs function to target histone deacetylases to RARE-containing promoters and specifically repress the transcription of retinoid-responsive genes by localized increases in histone-DNA interactions.

1.4.3. RARs, Transcriptional Co-Activators, and Histone Acetylation

The simple addition of RA converts RARs from transcriptional repressors to activators. Clues as to the nature of this interesting behavior occurred with the isolation of several proteins that are able to mediate the activational properties of the NRs (Glass *et al.*, 1997; Freedman, 1999). Among the first in a series of discoveries is the identification of a new family of transcriptional co-activators called CREB-binding protein (CBP) and p300 (Chakravarti *et al.*, 1996; Kamei *et al.*, 1996). These large highly similar proteins contain multiple zinc-finger domains that interact with a variety of transcription factors including RARs (Glass *et al.*, 1997). Moreover, CBP/p300 specifically associate with the LBD of the RARs in a ligand-dependent manner, and this interaction leads to increased activation of RA reporters in cell culture (Chakravarti *et al.*, 1996; Kamei *et al.*, 1996). Interestingly, CBP/p300 contain histone acetyltransferase (HAT) activity that can acetylate both free and nucleosomal histones (Bannister and Kouzarides, 1996; Ogryzko *et al.*, 1996). The acetylation of histones in their amino terminal tails results in a decreased affinity between core histone subunits and therefore relaxes the compaction of DNA in chromatin (Fry and Peterson, 2001; Marmorstein, 2001). As this is associated with increased transcriptional activation, CBP/p300 likely confers transcriptional activation by the RARs via the co-activator HAT domains (Fig. 1-4). In support of this, Dilworth *et al.* (1999) have shown that CBP enhanced transcription mediated by RA

binding to RXR/RAR heterodimers on a chromatinized reporter. Furthermore, the addition of RA leads to a rapid but transient increase in the acetylation of histones, and is associated with the activation of retinoid target genes (Chen *et al.*, 1999). This study thus suggests a link between retinoid receptor function and histone acetylation, consistent with the involvement of HAT-containing co-factors in transcriptional activation by the RARs.

The identification of an additional family of co-activators able to interact with liganded NRs, termed the p160 proteins (due to their molecular weight), further indicates the importance of co-regulation in hormonal and retinoid signaling (Chen *et al.,* 1997; Torchia *et al.*, 1997; Voegel *et al.*, 1998; Yao *et al.*, 1996; reviewed in Freedman, 1999; Glass *et al.*, 1997; Glass and Rosenfeld, 2000). The are currently three related members of the p160 co-activators including SRC-1/N-CoA-1 (steroid receptor co-activator-1/ nuclear receptor co-activator-1), TIF2/GRIP1/N-CoA-2 (transcriptional intermediary factor 2/glucocorticoid receptor interacting protein/nuclear receptor co-activator 2), and p/CIP/ACTR/AIB1 (p300/CBP interacting protein/activator of the thyroid and RA receptor/amplified in breast cancer 1). Like CBP/p300, p160 proteins associate with RARs in a RA-dependent manner (Chen *et al.,* 1997; Torchia *et al.*, 1997; Voegel *et al.*, 1998; Yao *et al.*, 1996). They also possess intrinsic HAT activity which is essential for mediating the transcriptional activation of the RARs and other NRs (Korzus *et al.*, 1998; Spencer *et al.* 1997). Importantly, not only do p160 proteins bind RARs, but they directly associate with CBP/p300, thereby forming co-activator complexes with NRs that mediate transcriptional activation via their HAT activities (Chen *et al.,* 1997; Torchia *et al.*, 1997; Yao *et al.*, 1996). These HAT-containing co-activator complexes are believed to be preformed and are recruited to RARs in the promoters of target genes in response to ligand binding. Furthermore, the targeting of several HAT proteins to promoters via the RARs illustrates the primacy of histone acetylation in gene activation. An interesting possibility for a scaffolding role for the p160 co-activators is suggested by the presence of a highly conserved bHLH-PAS domain in their amino terminus. As these domains mediate protein-protein interactions, the p160 members may catalyze the formation of a transcription-competent complex.

The role of histone acetylation in RAR-mediated transcriptional activation was strengthened by the identification of a multi-subunit complex containing a homolog of

the prototypical yeast histone acetyltansferase GCN5, termed p/CAF (p300/CBP associated factor; Blanco *et al.*, 1998). P/CAF is able to acetylate both free and nucleosomal core histones in response to RA in cell culture. It is therefore a HAT protein that is distinct from the p160 co-activators but that nonetheless is able to associate with RXR/RAR heterodimers in a RA-dependent fashion *via* the LBD of the RAR partner (Blanco *et al.*, 1998; Korzus *et al.*, 1998). Moreover, it also interacts with CBP/p300, and its overexpression leads to an increased activation of retinoid reporter genes.

Interestingly, biochemical analysis of the p/CAF complex reveals that it contains several TAFs that were previously shown to be part of the TFIID complex (Ogryzko *et al.*, 1998). Another resemblance to TFIID is the presence of histone-like subunits within the p/CAF complex. These surprising findings suggest that P/CAF bridges the gap between RXR/RAR heterodimers, co-activator complexes containing p160 and CBP/p300, and the basal transcription apparatus. Thus, in response to RA, RXR/RAR recruits a vast HAT machinery that transduces the retinoid signal to the basal apparatus by locally unraveling chromatin and enabling transcriptional activation.

1.4.4. Bridging To The Basal Transcription Machinery: TRAP/DRIP Complexes

Recent developments have identified protein complexes that can bridge the gap between the NRs, their co-activators and the basal transcription machinery. In addition to the p/CAF complex described above, another unrelated NR-associating complex has been isolated. This includes the TRAP/DRIP (thyroid receptor associated protein/vitamin D_3 receptor interacting protein) complexes that contain at least 10 subunits and associates with NRs in a ligand-dependent manner primarily through a single component, TRAP220/DRIP205 (Fondell *et al.*, 1996; Lee *et al.*, 1995; Rachez *et al.*, 1998; Yuan *et al.*, 1998). Interestingly, TRAP/DRIP complexes do not possess intrinsic HAT activity, but are able to enhance transcription on chromatinized templates, raising the possibility that they activate transcription independently of the HAT machinery. In support of this, several subunits of the TRAP/DRIP complexes are homologous to those found in the yeast Mediator complex, which associates with the carboxyl terminal tail of RNA polymerase II to form the holoenzyme (Gu *et al.*, 1999). This suggests that the function of TRAP/DRIP complex is to indirectly link ligand-activated NRs to the basal

transcription apparatus, and possibly, to recruit RNA polymerase II to RXR/RAR-bound promoters. However, the functional significance of this complex is just beginning to be understood. There is presently little evidence that links the TRAP/DRIP complexes to the co-activators. Indeed, as both complexes bind to the same region of the NRs (i.e. the AF-2 core of the LBD), it has been suggested that they may act independently or sequentially in the activation of target genes (Glass and Rosenfeld, 2000). For instance, the p160 and CBP/p300 co-activators may first be recruited to promoters containing NRs in response to ligand-binding, where they render local chromatin accessible to transcription factors via histone acetylation. Subsequently, according to this model, the TRAP/DRIP complex displaces the HAT proteins from the NR AF-2 core and recruits the RNA polymerase II machinery to allow transcription. Thus, the first step involves a de-repression of gene expression, while the following events prime the target promoter for transcription initiation. Collectively, these findings demonstrate the hierarchical and dynamic nature of eucaryotic transcription, and have shattered all previous allusions to simplicity in the retinoid signal transduction pathway.

1.4.5. Co-Factor NR Interaction Motifs And Co-Regulator Exchange Model

A common feature both the CBP/p300 and p160 families of co-activators is the presence of a LXXLL motif (where L is leucine and X any amino acid), which is often repeated in the NR interaction domains of these factors, and interacts directly with helix 12 containing the core AF-2 domain of NRs (Glass and Rosenfeld, 2000). This motif, referred to as the NR box, is found in the central region of p160 proteins and amino terminus of CBP/p300, and is predicted to form a short α-helix (Heery *et al.*, 1997; Torchia *et al.*, 1997). Interestingly, the NR co-repressors SMRT/N-CoR have remarkably similar leucine-rich motifs, called the CoRNR box (Hu and Lazar, 1999; Perissi *et al.*, 1999). The consensus for this motif is LXXXIXXXI/L (I is isoleucine), and represents an extended α-helix compared to the NR box. Indeed, molecular modeling of co-repressor and co-activator binding sites on NRs indicates that they both associate to the same general region formed by helices 3, 5, and 6 of the LBD (Perissi *et al.,* 1999). The differential affinity of the co-repressors and co-activators to the LBD of RARs is modulated simply by the binding of RA. The basis for this interesting property lies in the

dramatic structural changes that occur in the carboxyl terminus of RARs upon the binding of ligand. Particularly, ligand binding results in a major shift of helix 12, which contains the AF-2 core, to cover the hydrophobic binding pocket created by helices 3, 4 and 5 (Wurtz *et al.*, 1996). This results in the formation of a charged interface on helix 12 running along the length of the hydrophobic groove created by the ligand binding pocket associated with the ligand. This is known as the 'charged clamp' and associates strongly with helix formed by the LXXLL motifs in co-activators (Glass and Rosenfeld, 2000). Thus, in the absence of ligand, the helices of the CoRNR box extend within the hydrophobic pocket of the LBD of NRs. This interaction is effectively competed out by the ligand, which also alters the shape of the LBD and creates an additional binding surface for the LXXLL helix of the co-activators through the juxtapositioning of helix 12 with the ligand-binding pocket.

A highly simplified representation of transcriptional activation by the RARs, termed the co-regulatory factor exchange model, is presented in Figure 1-4 below. Briefly, in summarizing the above discussion, RARs act as nucleating agents that bring histone modifying enzymes and scaffolding proteins onto the promoters of target genes. In absence of ligand, RXR/RAR heterodimers associate with a transcriptionally repressive complex containing histone deacetylase activity that maintains chromatin in a compact and inactive state. The binding of RA to the RAR partner releases the co-repressors SMRT/N-CoR, and the associated mSIN3a/HDAC machinery. The conformational changes of RARs AF-2 helix evoked by ligand binding also results in the recruitment of histone acetyltransferases, such as CBP/p300 and p160 proteins, and the Mediator-like complex, TRAP/DRIP, to the promoter of the target gene. The co-activator proteins render the chromatin more accessible by acetylating core histones, presumably loosening up the local DNA-histone interactions. Subsequently, the DRIP/TRAP complexes target the basal transcription apparatus to the 'open' promoter near the RARs to allow for transcription initiation. Despite the clear deficiencies in our understanding of the transcriptional mechanisms of RAR function, it is nonetheless remarkable how rapidly we have come to appreciate the not entirely subtle effects of ligand binding to these receptors. The next few years should prove pivotal in our linking of the RARs and

associated factors to the basal transcription apparatus, and in the connection between histone acetylation and the nucleosomal remodeling machinery.

Figure 1-4. Co-Regulator Exchange Model for RAR transcription function. [Please refer to text for abbreviations].

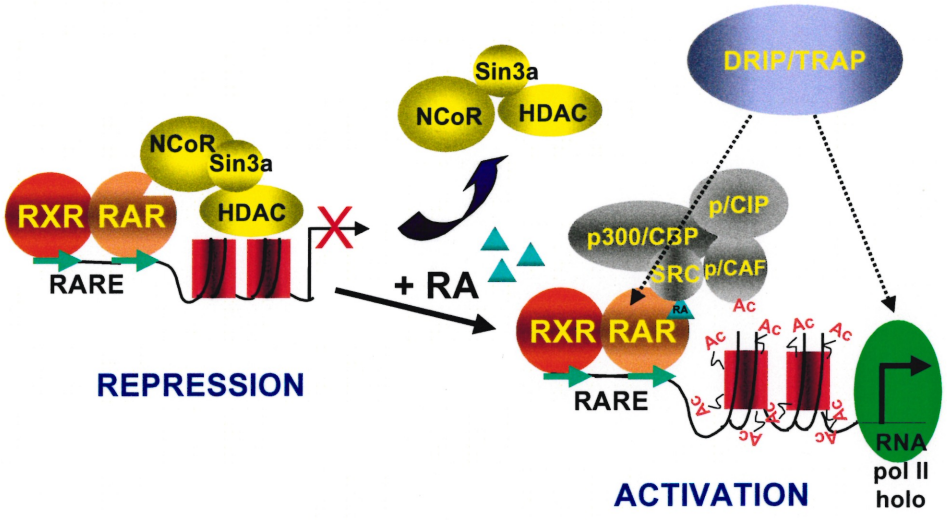

1.5. Genetic Analysis Of Retinoid Receptor Function During Mammalian Development

Early studies using dietary deprivation of vitamin A (VAD) during embryonic development in both rodents and avians have unequivocally demonstrated the crucial roles of the retinoids during development. Processes such as the differentiation of the genital and respiratory tracts, as well as heart, eye and CNS development have proven to be highly sensitive to vitamin A levels during development (Zile *et al.*, 2001). Upon the identification of the RARs and RXRs, it became imperative not only to examine their distribution during embryogenesis, but to undertake a systematic mutagenesis of these receptors in the mouse. After several years of intensive studies of the retinoid receptor

mutants, a consensus has emerged that the RARs and RXRs do indeed transduce the vitamin A signal, and that they seem to do so as heterodimers (Kastner *et al.*, 1995).

1.5.1. The Expression Of Retinoid Receptors During Development

The transcripts for the three RARs and RXRs genes are collectively distributed widely throughout mouse development. Individual RAR and RXR genes, however, often have non-overlapping and complimentary patterns of expression. In each of the retinoid receptor sub-families, there is one member that is almost ubiquitously expressed. For RARs, that member is RARα, while within the RXR family, RXRβ transcripts are found throughout the embryo (Dollé *et al.*, 1990, 1994; Mangelsdorf *et al.*, 1992; Ruberte *et al.*, 1990).

The earliest detectable expression of RARβ occurs during the mid to late primitive streak stages in the lateral mesodermal wings of the primitive streak, with increasing transcript abundance in the rostral-most region (Ruberte *et al.*, 1991). At this stage, RARβ transcripts are restricted to the mesenchyme, and are excluded from the overlying neuroepithelium. By early somitogenesis stages, RARβ expression shifts to a predominantly neuroepithelial restriction near the caudal hindbrain. As the embryo develops, this expression elaborates throughout the closed neural tube in the trunk region with an anterior limit in the post-otic hindbrain, near rhombomeres 6 and 7, and a posterior limit at the open caudal neural tube. Thus, RARβ transcripts are located throughout the presumptive spinal cord during its development, but are excluded from the CNS in areas where the neural tube remains open. Early expression also includes the foregut endoderm, lateral mesoderm, and the posterior heart. Subsequently, during organogenesis, RARβ transcripts are found in several regions of epithelial-mesenchymal interactions. These include mesenchymal tissues of the frontonasal process, tongue, mandible, and neural crest cells (Dollé *et al.*, 1989; Dollé *et al.*, 1990; Ruberte *et al.*, 1991). Additional expression domains of RARβ include the lateral and intermediate mesoderm, tracheal epithelium and associated mesenchyme, epithelium of the developing bronchi and genital tract, foregut epithelium and adjacent mesenchyme. Eye expression is restricted to the pigmented retina, vitreous body, and the condensed mesenchyme surrounding the eye. During limb morphogenesis, RARβ transcripts become localized in

the apical ectodermal ridge and in the interdigital mesenchyme, which eventually undergoes apoptosis to separate the digits (Dollé *et al.*, 1989; Ruberte *et al.*, 1990).

RARγ has a highly diffuse expression pattern during mid-streak stages (Ruberte *et al.*, 1990). Definitive expression is seen by E8 in all three germ layers of the open caudal neural tube region (Ruberte *et al.*, 1990; Ruberte *et al.*, 1991). RARγ transcripts are abundant in the neurectoderm of the open caudal neurofolds, the presomitic and lateral mesoderm, and the posterior endoderm. Therefore, RARγ is expressed in regions that exclude RARβ transcripts, particularly in the caudal embryo. By somitogenesis stages, RARγ transcripts begin to be expressed in the anterior areas of the embryo, such as the frontonasal mesenchyme and mandibular (first pharyngeal) arch mesenchyme. The development of the pharyngeal arches from E8.5-E10.5 is accompanied by strong RARγ expression in these structures (Dollé *et al.*, 1990; Ruberte *et al.*, 1990; Ruberte *et al.*, 1991). RARγ is specifically expressed in the largely neural crest cell-derived mesenchyme of the pharyngeal arches, and not in the overlying ectoderm. Other mesodermal derivatives expressing RARγ include the lateral plate and limb buds (Dollé *et al.*, 1989; Ruberte *et al.*, 1990).

Among the tissues expressing the highest levels of RARγ are in the precartilaginous mesenchymal condensations of both the axial and apendicular skeleton. During the ontogeny of the vertebrate, RARγ is initially expressed in the undifferentiated presomitic paraxial mesoderm, then becomes undetectable in the somites themselves, but is later greatly induced in the sclerotomal component of the differentiating somite. Expression within the sclerotome persists during its condensation into cartilage, and is subsequently downregulated as the first ossification centers appear. Interestingly, this pattern of expression in the precartilaginous condensations follows a cranio-caudal progression, being upregulated first in the cervical region, and accompanies the wave of sclerotome differentiation along the anterior-posterior axis. RARγ is also expressed in the mesenchyme surrounding the tracheal and bronchial epithelium, and is maintained during the formation of the cartilaginous tracheal rings and laryngeal cartilages. This expression of RARγ in mesenchymal condensations is also mirrored in the limb buds, where the initially diffuse RARγ expression throughout the limb bud mesenchyme is followed by

high expression in limb and digit precartilaginous condensations. Additional regions of RARγ expression include the epithelia of the oral cavity and foregut, genital tubercle mesenchyme, and in the dermal, epidermal and peridermal layers of the skin (Ruberte *et al.*, 1990).

RXRα and RXRγ display largely non-overlapping expression patterns during development. Although initially diffuse during early embryogenesis, RXRα becomes highly expressed in the viscera, liver, kidney, spleen and the epithelia of the digestive system and skin (Mangelsdorf *et al.*, 1992; Dollé *et al.*, 1994). In contrast, RXRγ transcripts are localized in the differentiating muscle lineages of the developing cranio-facial region, skeleton, and the limbs. Skeletal muscle expression is evident as early as E10, as the rostral-most somites begin to differentiate along their dorso-ventral axis into sclerotome and demamyotome (Mangelsdorf *et al.*, 1992). RXRγ transcripts are also localized in several discrete regions of the developing CNS, including the diencephalon, the corpus striatum, which contains basal ganglia, and the ventral horns of the spinal cord. Additional expression patterns include the retina, otic vesicle, and the pituitary and thyroid glands (Mangelsdorf *et al.*, 1992; Dollé *et al.*, 1994).

1.5.2. Vitamin A Deficiency Syndrome In Mammals

Early nutritional studies have established a fundamental role for vitamin A in the development and survival of mammals. The deprivation of retinoids from the diet of rats leads to several defects collectively referred to as the vitamin A deficiency (VAD) syndrome. In the adult, VAD leads a widespread transformation of various glandular or secretory epithelia into a keratinizing squamous epithelium (Table 1-1; Wolbach and Howe, 1925). This is often accompanied by the agenesis of several glandular organs, ocular malformations, male sterility due to the degeneration of seminiferous tubules, and eventually results in death. Furthermore, the deprivation of retinoids during pregnancy results in many congenital malformations in the resulting pups. The fetal VAD syndrome gives rise to defects involving the eye, heart, various glands, genito-urinary tract, and leads to the hyper-keratinization and squamous metaplasia of epithelia (Table 1-1; Wilson and Warkany, 1948, 1949; Wilson *et al.*, 1953; Dickman *et al.*, 1997). Although

Table 1-1. Defects induced by Vitamin A Deficiency (VAD) in adults and in fetuses during development. [Please refer text for references].

Adult (Post-Partum) VAD

- Growth retardation.
- Ocular defects: *corneal lesions due to keratinization, atrophy of the mucous glands of the conjunctiva, photoreceptor degeneration.*
- Atrophy of various glands: *submaxillary, parotid, lacrimal, Harderian, extraorbital, pancreas, thyroid, pituitary , thymus, testes, prostate.*
- Formation of keratinizing squamous epithelium in the following areas:
    - *Respiratory tract (larynx, trachea, bronchi, nasal septum, nares, sinuses)*
    - *Anterior alimentary tract (submaxillary, parotid, and salivary glands, pancreatic ducts, pharynx).*
    - *Genito-urinary tract (bladder, ureter, kidney, uterus and oviducts, epididymis, prostate, coagulating glands).*
    - *Eyes and associated glands (conjunctiva, meibomian gland ducts, cornea, lacrimal gland, harderian gland).*
    - *Thymus*

Fetal VAD

- Ocular defects: *coloboma, micropthalmia, eversion of the retina, defects of the lens and eye lids, post-lental membrane.*[*]
- Cardiac defects: *interventricular septal defect, aortico-pulmonary septal defect, spongy myocardium.*
- Aortic arch defects: *double outlet right ventricle, persistent truncus arteriosus, dextroposed aorta, absent ductus arteriosus.*
- Respiratory tract defects: *Agenic or hypoplastic left lung, hypoplastic right lung.*
- Kidney defects: *Ectopia, close apposition or fusion of kidneys, hydronephrosis.*
- Genito-urinary tract defects: *Ectopic termination of ureters, hypoplasia of ureters, hydroureter unilateral absence or hypopasia of genital tract, absence of seminal vesicles, agenesis or incomplete development of Mullerian ducts.*
- Cranio-facial defects: *Absent caudal cranial nerves, hypoplastic frontonasal region and mandibular arch.*
- Squamous metaplasia of epithelia.
- Diaphramatic hernia.
- Growth retardation.

[*] See Table 1-2 for a more detailed description of the ocular defects observed in fetal VAD.

affecting similar tissues as post-partum VAD, the defects resulting from fetal VAD are generally more severe than those observed for the post-partum VAD. Moreover, the fetal VAD syndrome involves additional abnormalities not previously associated with post-partum deficiency, such as diaphragmatic hernia, defects of the heart and aortic arches, agenesis or ectopia of various glands and genito-urinary tract, and the absence or hypoplasia of the lungs.

1.5.3. Single RAR Null Mutants

The deletion of any single one of the three RARs in the mouse leads to surprisingly few abnormalities, suggesting a partial functional redundancy among these genes. In addition to the targeted disruption of all isoforms of a given RAR type, several groups deleted specific RAR isoforms in an attempt to demonstrate isoform specificity in receptor function (Kastner *et al.*, 1995). The deletion of the entire RARα gene leads to growth deficiency and post-natal lethality, similar to that occurring with dietary retinoid deficiency (Lufkin *et al.*, 1993). Additional VAD-associated defects included male infertility due to lesions within the parenchyma of the testes. Interestingly, RARα knockout fetuses also displayed novel abnormalities not previously observed in VAD studies, such as cervical vertebral defects, which occurred at low frequencies, and a moderately penetrant soft-tissue syndactyly of the fore- and hindlimbs (Lohnes *et al.*, 1994; Lufkin *et al.*, 1993). Moreover, RARα1 knockout mice are healthy and fertile, demonstrating a complete overlap with the RARα2 isoform (Li *et al.*, 1993; Lufkin *et al.*, 1993).

RARβ null mice are even less affected than RARα mutants, as they are viable and display no obvious abnormalities in any organs nor the axial or apendicular skeleton (Ghyselinck *et al.,* 1997; Luo *et al.*, 1995). They did, however, display a fusion of the ninth and tenth cranial ganglia derived from the hindbrain, although it was seen only in one mutant embryo (out of eleven examined). The removal of RARβ function in the embryo did not affect its sensitivity to the cranio-facial, limb and vertebral defects elicited by excess RA (Luo *et al.*, 1995; Mendelsohn *et al.*, 1994b). Importantly, this indicates that RARβ is not critical for transducing the teratogenic retinoid signal, as has been previously supposed based on the RA inducibility of the RARβ2 promoter in

transgenic reporter mice (Balkan *et al.*, 1992; Mendelsohn *et al.*, 1991; Mendelsohn *et al.*, 1994b; Rossant *et al.*, 1991). Similarly, the mutation of RARβ2, which is the most prevalent RARβ isoform during embryogenesis and contains the prototypical RARE in its promoter, resulted in no phenotype (Mendelsohn *et al.*, 1994b). Thus, RARβ seems largely dispensable for mammalian development.

In contrast, the mutation of the RARγ gene led to several defects associated with VAD (Lohnes *et al.*, 1993). For example, most RARγ knock-out mice die soon after birth and the remaining pups display a severe growth deficiency, with most of them dying within three weeks of age. Other VAD-associated defects in RARγ$^{-/-}$ mice include male sterility due to a fully penetrant squamous metaplasia and keratinization of the glandular epithelia of the seminal vesicles and part of the prostate. Furthermore, the cranial prostate was atrophied in these mice, exacerbating the reduced male fertility phenotype. RARγ null fetuses also displayed glandular defects such as the absence of the Harderian glands, which lubricates the eyes. This gland is often hypoplastic in VAD rodents, but is believed to occur as a consequence of the widespread keratinization of the eye and surrounding tissues following retinoid deprivation (Wolbach and Howe, 1925). Defects occurring in RARγ$^{-/-}$ mutants that were not previously observed in deprivation studies include frequent malformations in the anterior axial skeleton, and abnormalities in the cartilaginous rings of the trachea (Lohnes *et al.*, 1993). Importantly, the removal of RARγ leads to the partial homeotic transformation of several cervical and upper thoracic vertebrae and to the malformation of the neural arches of these structures.

As is the case for RARα and RARβ genes, a large degree of functional overlap occurs between the two RARγ isoforms (Lohnes *et al.*, 1993; Subbarayan *et al.*, 1997). RARγ2 null mice are completely normal, while RARγ1 knock-outs display a limited subset of the defects exhibited by the total isoform null mouse. Particularly, RARγ1$^{-/-}$ mice are somewhat growth deficient (10% growth retarded compared to 40-80% seen in RARγ$^{-/-}$ mice) but are viable and fertile. Likewise, the glandular defects observed in RARγ total isoform null mutants were not seen in RARγ1$^{-/-}$ mice. However, some specificity in RARγ1 function does occur, particularly for the formation of the cricoid cartilage of the trachea, which was abnormal in almost all the RARγ1$^{-/-}$ mice (Subbarayan

et al., 1997). A low frequency of cervical vertebral malformations also occurred in RARγ1 null mice, supporting a primary role for this isoform in mediating the RARγ function.

In contrast to RARβ nulls, RARγ mutant mice are completely resistant to a subset of the teratogenic effects of exogenous RA when administered between E8.5 and E9 (Lohnes *et al.*, 1993). Particularly, RARγ null mice are resistant to axial truncations caused by excess retinoids during these stages. The importance of this gene in transducing this teratogenic event is emphasized by the reduced sensitivity of the $RAR\gamma^{+/-}$ mice relative to wild types to excess RA, indicating a strict gene dosage effect. The individual deletion of RARγ1 or RARγ2, however, did not limit the sensitivity of these mice to RA-induced caudal truncations (Subbarayan *et al.*, 1997). These results demonstrate, that RARγ is critically required for the transduction of at least some of the malformations induced by excess retinoids during development.

1.5.4. Double RAR Null Mutants

While the mutation of single RAR isoforms or genes failed to fully elicit a VAD phenotype, the role of the RARs in transducing the vitamin A signal was ultimately confirmed by the generation of double RAR mutants. Like VAD studies, RARαγ double mutant fetuses exhibited extreme growth retardation (Lohnes *et al.*, 1994). Several different developmental processes and tissues were affected by the loss of two RARs, and collectively, the combination of all RAR compound mutant phenotypes recapitulated the VAD syndrome. They can be broadly grouped according to the type of tissues affected, such as neural crest cells (NCCs), pharyngeal arch derivatives (which are largely NCC-derived), eye, the urogenital system, respiratory tract, and the heart (Table 1-2; Lohnes *et al.*, 1994; Mendelsohn *et al.*, 1994a). In addition, abnormalities not previously associated with the VAD syndrome were observed in the double null mutants. These included defects of some NCC and pharyngeal arch derivatives, neural tube closure defects, malformations of the axial and apendicular skeletal, and digit patterning defects.

NCC defects in RAR double nulls. NCCs are a transient pluripotent population of cells that originate from the lateral margins of the neural folds within the boundary defined by the surface and neural ectoderm. During neurulation, they detach from the

neural plate and migrate ventrally throughout the antero-posterior axis and ultimately give rise to an broad variety of tissues, including the cranial ganglia, peripheral sensory neurons, most cranio-facial skeletal elements and connective tissue, mesenchyme of the pharyngeal arches, the septae of the heart outflow tract, and tunic media of the aortic arches among others (Kaufman and Bard, 1999; Carlson, 1996).

NCCs are particularly sensitive to the effects of excess retinoids, and many of their derivatives are affected in RAR double knock-out mice and VAD rat fetuses (Moriss-Kay, 1993; Lohnes *et al.*, 1994; Means and Gudas, 1995; Mendelsohn *et al.*, 1994a; Wilson *et al.*, 1953). While RARαβ2, RARα1β2 and RARβ2γ have very minor, if any, cranio-facial defects, RARαγ mutants contained numerous deficiencies in these crest-derived structures (Lohnes *et al.*, 1994). RARαγ double mutants displayed losses in the frontal, nasal, premaxillary and vomer bones, which were often replaced by disorganized cartilaginous nodules, indicating a possible defect in the migration, proliferation and/or differentiation of NCCs (Table 1-2). Cranio-facial deficiencies were also observed in VAD fetuses (Table 1-1). Particularly, Dickman *et al.* (1997) described a high occurrence of hypoplasia of the frontonasal region in rats reared from VAD mothers. The RAR double mutants also displayed ectopic crest-derived cranial skeletal elements, which have been suggested to be homologous to the pila antotica and pterygoquadrate cartilage (Lohnes *et al.*, 1994). Interestingly, these structures are normally present in reptiles, and are thus thought to be atavisms created by the lack of proper retinoid signaling in the neural crest. This raises the possibility that the RARs have evolved novel roles within the mammalian lineage to modify a pre-existing ancestral vertebrae 'ground state' with respect to cranio-facial skeletal structures.

Additional crest defects included the loss of septae in the outflow tract of the heart and various deficiencies in eye structures, which were observed in RARαβ, RARβγ, and RARαγ double mutants (Table 1-2; Mendelsohn *et al.*, 1994a). The NCC-derived ocular and cardiac defects were particularly reminiscent of those occurring in VAD fetuses, supporting a role for the RARs in transducing the retinoid signal (Dickman *et al.*, 1997; Wilson *et al.*, 1953).

Pharyngeal arch defects in RAR double nulls. The pharyngeal arches are bilateral swellings that develop laterally along the antero-posterior axis from E8 to E11 during

mouse embryogenesis. They are composed of an inner core of mesenchyme surrounded by ectoderm on their surface and rostral foregut endoderm internally. Although the mesenchyme is initially composed of lateral and paraxial mesoderm, the outgrowth the arches is fueled by the population of NCCs, eventually giving rise to 5 arches (numbered 1,2,3, 4 and 6), four of which are visible externally (Sadler, 2000). The arches are separated by prominent clefts on their external surface called pharyngeal grooves, and endodermal pharyngeal pouches along their internal surface. The pharyngeal arches ultimately become incorporated within the body of the fetus, contributing to the development of the skeletal elements of the jaw and the various glands associated with the head and neck. The first pharyngeal arch plays an essential role in the formation of the cranio-facial region. It is composed of a mandibular prominence, which gives rise to the mandible or lower jaw, and a smaller maxillary prominence, that becomes incorporated in the facial region to form the upper jaw or maxillary, palatine and alisphenoid bones (Carlson, 1996; Sadler, 2000). Of these, the latter elements were either absent or hypoplastic, while the former remained unchanged in RARα or RARαγ double mutants. Skeletal structures derived from the second and third arches, such as the stapes and styloid process and hyoid bone, respectively, were either absent or hypoplastic and malformed in RAR double mutants, particularly in RARαγ nulls (Table 1-2; Lohnes *et al.*, 1994; Mendelsohn *et al.*, 1994a).

The sensory ganglia and muscles of the cranio-facial region are derived from the NCC population of the pharyngeal arches (Sadler, 2000). These NCC populations arise from the midbrain and hindbrain and migrate ventro-laterally into the swelling arches, where they eventually differentiate into the nerves and musculature of the face. The cranio-facial nerves are highly deficient in RARαβ double mutants (Dupé *et al.*, 1999), supporting a general defect in NCCs in the RAR double nulls.

The caudal pharyngeal pouches participate in the formation of the glands of the neck region such as the thymus, thyroid and parathyroid glands (Kaufman and Bard, 1999; Sadler, 2000). Several RAR double mutants display ectopias and hypoplasias of these tissues, indicating a deficiency in arch development (Table 1-2; Mendelsohn *et al.*, 1994a). Consistent with this, the examination of pharyngeal arch system at earlier stages (e.g. E9.5-10.5) reveals that the caudal-most arches are highly sensitive to RAR ablation,

being altogether absent or hypoplastic in RARαγ and RARαβ null embryos (Dupé *et al.*, 1999; Wendling *et al.*, 2001). Besides thymic, thyroid and parathyroid deficiencies, other cranial glands that are abnormal or lacking in RAR double mutants include the sublingual and submandibular (Mendelsohn *et al.*, 1994a), which are derived from endodermal buds of the tongue and mouth primordium, respectively, and the surrounding crest-derived cranial mesenchyme (Sadler, 2000). Moreover, pharyngeal arch-derived structures such as cranial nerves and several glands of the head and neck region are also affected in VAD manipulations (Table 1-1), supporting a critical role for vitamin A signaling in arch and NCC development (Dickman *et al.*,1997; Wilson *et al.*, 1953).

Ocular deficiencies in RAR double mutants. Eye development begins as a series of interactions between forebrain neurectoderm and the underlying NCC-derived mesenchyme that leads to the local evagination of the former tissue to form the optic vesicle (Sadler, 2000). This structure subsequently undergoes a ventral invagination to form the optic cup. The open neurectoderm of the optic cup, called the optic fissure, ultimately fuses and is populated by mesoderm invading to form a transient cover, the ventrolenticular membrane. Crest-derived mesenchyme migrating between the lens and surface ectoderm forms the corneal stroma, while the space between the cornea and the lens eventually gives rise to the anterior chamber. The neurectodermal derivatives of the eye include the retina, optic nerve and the epithelial covering of the iris, while the NCC-derived components are the sclera, corneal stroma, anterior chamber and vitreous body. The eyelids originate from mesenchymal outgrowths covered by ectoderm.

The removal of any two RARs causes several eye defects with varying degrees of severity depending on the receptors involved, but occurring at nearly complete penetrance (Table 1-2; Grondona *et al.*,1996; Lohnes *et al.*, 1994). RARαγ and RARβ2γ2 double nulls display the most severe ocular phenotype, while RARα1β2 and RARαβ2 mutants are less affected, indicating the importance of the RARγ gene in transducing the retinoid signal in eye development. Particularly, RAR double nulls display coloboma of the retina and optic nerve, hyperplasia and keratinization of the corneal epithelium, degeneration of the retina, agenesis or hypoplasia of the eyelids, and the lack of the cornea, conjunctiva, and anterior chamber of the eye (Table 1-2). These defects are also manifested by VAD fetuses, but at a lower frequency (Wilson *et al.*, 1953; Dickman *et*

al., 1997). RAR double mutants also present several eye abnormalities that are not found in VAD fetuses, such as the lack of lens formation and persistent corneal-lenticular stalk. Thus, retinoid signaling through the RARs are critical for the proper formation and maturation of diverse components of the eye.

Urogenital defects in RAR double null fetuses. The urogenital system develops from reciprocal inductions between mesonephros, or primitive kidney, and the surrounding mesenchyme (Sadler, 2000). The mesonephros performs the excretory functions of the embryo and is composed of a mesoderm-derived longitudinal tubule on each side of the embryo surrounded by intermediate mesoderm. Following reciprocol inductive interactions, the caudal portion of the mesonephros gives rise to the metanephros consisting of the uteric bud, which in turn generates the ureter, renal pelvis, the calyces, and the collecting tubules of the definitive kidney. The anterior portion of the mesonephros develops into the genital ridge following a similar set of inductive events involving the associated mesoderm.

RAR double mutants harbor a variety of defects in the urogenital system (Mendelsohn *et al.*, 1994a).These include kidney agenesis or hypoplasia, hydronephrosis, absent renal pelvis, ectopic or agenic ureters, hydroureter, agenesis of the uterus and cranial vagina, and agenesis of the vas deferens and seminal vesicles (Table 1-2). A close examination of RARαβ2 double mutants revealed that the kidney defects resulted from improper ureteric bud induction, which led to hypoplastic kidneys with reduced numbers of ureteric tubules (Mendelsohn *et al.*, 1999). In RARαγ mutants, the nephric tubules were dispersed randomly and formed in more caudal positions than normally, suggesting aberrant metanephric induction (Mendelsohn *et al.*, 1994a). Moreover, while all three RARs seem to be involved in urogenital development, there were some important differences in the urogenital structures affected by the loss of RARβ or RARγ in combination with RARα. RARαβ2 double nulls generally displayed more severe abnormalities of the female genital tract, while RARαγ mutants displayed male genital tract malformations at a higher frequency. RARγ single mutants also have male genital tract deficiencies, consistent with an essential role for this receptor in the development of the male urogenital system (Lohnes *et al.*, 1993). With the exception of kidney agenesis or hypoplasia, the majority of these defects were also noted in VAD fetuses (Table 1-1).

Respiratory tract defects in RAR double mutants. The respiratory system develops as an outgrowth of the ventral wall of the foregut. This outgrowth, referred to as the lung bud or respiratory diverticulum, enlarges to form the right and left main bronchi, which in turn are further divided into three and two secondary bronchi of the right and left lung primordia, respectively (Sadler, 2000). The bronchi eventually give rise to the lobes of the lungs, which are asymmetric, since the right side contains three and the left has two lobes. The high surface area of the lungs is achieved by the repeated branching of the secondary bronchi. As the lung bud expands caudally, it generates two longitudinal esophagotracheal ridges that ultimately fuse to form the esophagotracheal septum This structure separates the foregut along the dorso-ventral axis, with the esophagus located dorsally and the trachea and lung buds ventrally.

Of the RAR double mutants, only RARαβ2$^{+/-}$ and RARαβ2 double mutants display hypoplastic or unilateral loss of the lungs and a lack of the esophagotracheal septum (Table 1-2; Mendelsohn *et al.*, 1994a). Branching morphogenesis seems to arrest very early on in these mutants, either before or following the formation of the primary bronchi, resulting in agenic or hypoplastic lungs, respectively. VAD fetuses also display these defects, emphasizing the importance of retinoid signaling in lung branching morphogenesis (Table 1-1).

In addition, the tracheal and laryngeal cartilages are misshapen and severely fused in RAR double mutants (Table 1-2; Mendelsohn *et al.*, 1994a). The respiratory cartilage defects are fully penetrant and display their greatest expressivity in RARαβ2, RARα1γα2$^{+/-}$, and RARαγ mutants. However, in contrast to the lung defects, tracheal and laryngeal cartilage abnormalities are not observed in retinoid deprivation studies.

Cardiac and aortic arch defects in RAR double mutants. The heart develops from paired endothelial tubes derived from lateral plate mesoderm (LPM) that fuse at the midline during pre-somite stages to form a linear tube (Carlson, 1996; Fishman and Chien, 1997; Sadler, 2000). Subsequently, various morphogenetic movements direct the primitive heart tube to loop rightwards and generate a left-sided heart with four chambers, consisting of right and left ventricles and atria, along with the inflow and outflow tracts. The embryonic outflow tract communicates with the primitive ventricle and separates aortic and pulmonary blood flow via the NCC-derived aorticopulmonary

septum. This division fails to occur in RARαβ2 and RARαγ double mutants and leads to a single outflow vessel, referred to as persistant truncus arteriosus (Table 1-2; Mendelsohn *et al.*, 1994a). Additional cardiac defects observed in RAR double nulls include dextroposed aorta, high ventricular septal defect, and double outlet right ventricle. These abnormalities are all consistently observed in VAD fetuses (Wilson and Warkany, 1949; Dickman *et al.*, 1997), suggesting a strict requirement for retinoid signaling in the development of the cardiac outflow system.

RAR double mutants also displayed abnormalities in the great arteries derived from the paired aortic arches (Table 1-2). They are originate from endothelial condensations of the pharyngeal arch mesenchyme and connect to aortic sac at the most distal end of the outflow tract (Sadler, 2000). Although initially symmetric, aortic arch arteries are retained unilaterally during development, creating asymmetries in the aortic branch pattern. Most RAR double mutants displayed enormous variability in the stereotypical pattern of the aortic arch arteries, as do fetuses from VAD mothers (Dickman *et al.*, 1997; Mendelsohn *et al.*, 1994b; Wilson *et al.* 1953). It is important to note that at least part of the arch arteries, like the aorticopulmonary septum, are ultimately derived from cardiac NCC. Thus, this is consistent with a generalized effect of RAR ablation on this remarkable population of cells.

Another important cardiac deficiency resulting from RAR ablation is the loss of myocardial populations within the ventricles (Table 1-2). The myocardium originates from lateral plate mesoderm and forms the muscular component of the heart, as well as contributing to the septation of the atria and ventricles (Sadler, 2000). RARαγ mutants display a completely penetrant ventricular myocardial hypoplasia that leads to a spongy myocardial phenotype in fetuses. This condition is also characteristic of the fetal VAD syndrome (Table 1-1), indicating the importance of retinoid signaling in myocardial development.

Skeletal and other non-VAD-associated defects in RAR double mutants. In addition to the cranio-facial skeletal elements, the axial and apendicular skeletons are abnormal in RAR double mutants. The axial skeleton is composed of vertebrae that are derived from the sclerotomal compartment of the somites (Kaufman and Bard, 1999; Verbout, 1985). The anterior-most vertebrae form the occipital and basioccipital bones at

the base of the head. These are followed by the cervical vertebrae of the neck, the rib producing thoracic vertebrae, and the lumbar, sacral, and finally, caudal vertebrae.

As was discussed previously, single RAR nulls, particularly the RARγ mutants, display homeotic transformations and malformations of several cervical and some thoracic vertebrae (Lohnes *et al.*, 1993). Both the occurrence and the severity of these defects are greatly increased upon additional RAR ablation (see section 1.6.8.; Table 1-4; Lohnes *et al.*, 1994). This is especially evident for the allelic series involving the successive removal of RARα isoforms from the RARγ background. Interestingly, while the separate inactivation of RARα and RARβ2 resulted in mild or no vertebral defects, the combined mutation of both genes led to a synergistic effect on vertebral patterning. This indicates the importance of global levels of RAR signaling for normal vertebral development, and again demonstrates the large degree of redundancy inherent in retinoid receptor function. Despite the sensitivity of vertebral patterning to RAR signaling, axial defects were never observed in VAD studies (Wilson *et al.*, 1953; Dickman *et al.*, 1997). This suggests that VAD fetuses still retain residual retinoid activity sufficient to drive axial patterning, possibly supplied by maternal retinyl ester stores. Furthermore, it is impossible to generate a complete VAD mother, as this is incompatible with life.

The development of the apendicular skeleton is also affected in RAR double mutants (Lohnes *et al.*, 1994). These abnormalities include soft tissue syndactyly (fused digits) or webbed digits, polydactyly (extra digits), and ectrodactyly (digit loss) and occur only in RARαγ double mutant forelimbs. RARα and RARγ single mutants rarely display webbed digits (Lufkin *et al.*, 1993), while those occurring in RARα$\gamma^{+/-}$ double nulls are fully penetrate. In contrast, RARαB2 and RARβ2γ double mutants never displayed digit abnormalities. This is consistent with the expression of the RARα and γ, but not RARβ, in the condensing mesenchyme of the limb skeleton (Dollé *et al.*, 1989). Moreover, as with the vertebral defects, digit malformations have not been described in VAD fetuses.

The external ear develops from localized thickenings of surface ectoderm on either side of the caudal hindbrain (Kaufman and Bard, 1999; Sadler, 2000). These thickenings (otic placodes) subsequently invaginate to form the otic vesicles (otocysts). RARαγ double mutants display hypoplastic otocysts which lead to small and incomplete cartilaginous otic capsules (Lohnes *et al.*, 1994). Moreover, recent findings demonstrate

Table 1-2. Summary of the abnormalities occurring in RAR double null mutants. [Modified from Kastner *et al.*, 1995. (Please refer to text for references)].

RAR MUTANT ABNORMALITIES OBSERVED IN THE FETAL VAD SYNDROME

Abnormalities	**RAR Mutant Genotype**
Cardiac and aortic arch neural crest cell defects:	
• Persistent truncus arteriosus	$\alpha1\beta2$, $\alpha\beta2$, $\alpha\gamma$
• Dextroposed aorta	$\alpha1\beta2$, $\alpha1\gamma\alpha2^{+/-}$, $\alpha\gamma$
• High ventricular septal defect	$\alpha1\beta2$, $\alpha\beta2$, $\alpha1\gamma\alpha2^{+/-}$, $\alpha\gamma$
• Double outlet right ventricle	$\alpha1\gamma\alpha2^{+/-}$
• Patterning abnormalities of the arteries derived from aortic arches	$\alpha1\beta2$, $\alpha\beta2$, $\alpha1\gamma\alpha2^{+/-}$, $\alpha\gamma$
Other cardiac defects:	
• Thin ("spongy") myocardium	$\alpha\gamma$
Ocular neural crest cell defects:	
• Retrolenticular membrane	$\alpha\beta2$, $\alpha\gamma$
• Unfused eyelids	$\alpha1\gamma\alpha2^{+/-}$, $\alpha\gamma$
• Hypoplastic conjunctival sac	$\beta2\gamma$, $\alpha\gamma$
• Abnormal corneal stroma	$\beta2\gamma$, $\alpha\gamma$
• Absence of anterior chamber	$\beta2\gamma$, $\alpha\gamma$
• Agenesis of cornea, conjunctiva, and eyelids	$\alpha\gamma$
Other ocular defects:	
• Microphtalmia	$\alpha\gamma$
• Coloboma of the retina	$\alpha\gamma$
• Coloboma of the optic nerve	$\beta2\gamma$, $\alpha\gamma$
• Metaplasia and keratinization of the corneal epithelium	$\alpha\gamma$
• Abnormal lens fibers	$\alpha\gamma$
• Shortened ventral retina and ventral rotation of the lens	$\alpha\gamma$
• Pre-natal retinal dysplasia	$\alpha\gamma$
Cranio-facial neural crest cell defects:	
• Hypoplasia of frontonasal process and mandibular arch	$\alpha\gamma$
• Loss or disorganization of caudal-most cranial nerves and ganglia	$\alpha\beta$
Respiratory tract defects:	
• Agenic/hypoplastic left lung	$\alpha\beta2$
• Hypoplastic right lung	$\alpha\beta2$
• Absence of esophagotracheal septum	$\alpha1\beta2$, $\alpha\beta2$
Urogenital tract defects:	
• Agenic/hypoplastic ureter	$\alpha1\beta2$, $\alpha\beta2$, $\alpha\gamma$
• Ectopic ureter	$\alpha1\beta2$, $\alpha\beta2$
• Hydroureter	$\alpha\beta2$, $\beta2\gamma$
• Kidney hypoplasia	$\alpha1\beta2$, $\alpha\beta2^{+/-}$, $\alpha\beta2$, $\alpha1\gamma\alpha2^{+/-}$
• Caudally displaced kidney/Ectopia	$\alpha\beta2$, $\alpha\gamma$
• Hydronephrosis	$\alpha1\beta2$,$\alpha\beta2$, $\beta2\gamma$
• *Female:* Agenesis of oviduct and uterus (total or partial)	$\alpha1\beta2$, $\alpha\beta2$, $\alpha\gamma$
• *Female:* Agenesis of cranial vagina	$\alpha1\beta2$, $\alpha\beta2$, $\alpha\gamma$
• *Male:* Agenesis or dysplasia of vas deferens	$\alpha1\gamma\alpha2^{+/-}$, $\alpha\gamma$
• *Male:* Agenesis of seminal vesicles	$\alpha\gamma$
Diaphramatic hernia	$\alpha\beta2$

Table 1-2, *continued.* Summary of the abnormalities occurring in RAR double null mutants. [Modified from Kastner *et al.*, 1995. (Please refer to text for references)].

RAR MUTANT ABNORMALITIES NOT OBSERVED IN THE FETAL VAD SYNDROME

Abnormalities	RAR Mutant Genotype
Ocular defects:	
• Corneal-lenticular stalk	$\alpha1\gamma\alpha2^{+/-}$, $\alpha\gamma$
• Agenic lens	$\alpha\gamma$
• Post-natal retinal dysplasia	$\beta2\gamma2$
• Agenesis of Harderian gland	γ, $\beta2\gamma$, $\alpha1\gamma$, $\alpha1\gamma\alpha2^{+/-}$, $\alpha\gamma$
Cranio-facial defects:	
• Agenesis of frontal, nasal, premaxillar, and vomer bones	$\alpha\gamma$
• Agenesis or dysplasia of sublingual and submandibular glands and ducts	$\beta2$, $\alpha1\gamma$, $\alpha1\gamma\alpha2^{+/-}$, $\alpha\gamma$
• Supernumerary atavistic elements: *Pila antotica*	$\alpha1\gamma$, $\alpha\gamma$
Pterygoquadrate cartilage	$\beta2\gamma$, $\alpha\beta2$, $\alpha1\beta2$, $\alpha1\gamma\alpha2^{+/-}$, $\alpha\gamma$
Exencephaly	$\alpha\gamma$
Pharyngeal arch-derived glandular defects:	
• Hypoplastic medial thymus	$\alpha\beta2$
• Persistent cervical thymus	$\alpha\gamma$
• Ectopic accessory thymus bodies	$\beta2\gamma$, $\alpha1\beta2$, $\alpha\beta2^{+/-}$, $\alpha\beta2$, $\alpha1\gamma\alpha2^{+/-}$, $\alpha\gamma$
• Hypoplasia of thyroid	$\alpha1\beta2$, $\alpha\beta2$, $\alpha1\gamma\alpha2^{+/-}$, $\alpha\gamma$
• Ectopic thyroid	$\alpha\beta2$, $\alpha\gamma$
• Ectopic parathyroids	$\alpha1\beta2$, $\alpha\beta2$, $\alpha1\gamma\alpha2^{+/-}$, $\alpha\gamma$
Rhombencephalic (hindbrain) defects:	
• Loss of caudal rhombomeres	$\alpha\beta$, $\alpha\gamma$
• Hypoplastic and ectopic otocysts	$\alpha\beta$, $\alpha\gamma$
Skeletal defects:	
• Homeotic transformations and malformations of cervical vertebrae	α, γ, $\alpha\beta2$, $\beta2\gamma$, $\alpha1\gamma$, $\alpha\gamma$
• Malformed scapula	$\alpha\gamma$
• Agenesis of radius	$\alpha\gamma$
• Hypoplastic ulna	$\alpha\gamma$
• Agenesis of carpal bones	$\alpha\gamma$
• Syndactyly (soft tissue)	α, $\alpha\gamma$
• Polydactyly	$\alpha\gamma$
• Ectrodactyly	$\alpha\gamma$
Cartilage defects:	
• Malformed or fused laryngeal cartilages: *Thyroid cartilage*	$\alpha\beta2$, $\alpha1\gamma\alpha2^{+/-}$, $\alpha\gamma$
Arytenoid cartilage	$\alpha\beta2$, $\alpha1\gamma\alpha2^{+/-}$, $\alpha\gamma$
Cricoid cartilage	$\alpha1\beta2$, $\alpha\beta2$, $\alpha1\gamma\alpha2^{+/-}$, $\alpha\gamma$
• Malformed tracheal cartilage	$\alpha1\beta2$, $\alpha\beta2$, $\alpha1\gamma\alpha2^{+/-}$, $\alpha\gamma$
• Ectopic cranio-facial cartilage nodules	$\alpha1\beta2$, $\alpha\beta2$, $\alpha\gamma$
Urogenital tract defects:	
• Agenesis or aplasia of kidney	$\alpha\gamma$
• Absence of anal canal	$\alpha\beta2$

that RARαβ double null and RARαβ$^{+/-}$γ compound null mutants contain small ectopic otocysts caudal to the parental otic vesicles (Dupé *et al.*, 1999; Wendling *et al.*, 2001). In affected mutant embryos, the abnormal otocysts are always accompanied by hindbrain patterning defects, suggesting that the two process are linked. RAR signaling thus appears to play an important role in the induction of the otocyst and hindbrain patterning (see below).

RARs are also required for the proper closure of the neural tube, as RARαγ and RARαβ$^{+/-}$γ compound mutants show an externalized brain, or exencephaly (Lohnes *et al.*, 1994; Wendling *et al.*, 2001). These defects seem to result from a failure of the neural tube to close along the length of the hindbrain.

Thus, the sum of the genetic studies in the mouse have unequivocally established the importance of the RARs in mediating diverse retinoid-dependent processes, as well having demonstrated a great plasticity afforded by the functional overlap between the three RAR genes.

1.5.5. Single and Double RXR Null Mutants

As with the RARs, a systematic mutagenesis of the RXR gene family in the mouse germ line was undertaken to illuminate their function *in vivo*. Of the three RXR genes, only the mutation of RXRα has an overt phenotype late in embryogenesis and leads to embryo lethality between E13.5-E16.5 (Kastner *et al.*, 1994; Sucov *et al.*, 1994). The lethality is likely due to the cardiac defects and poor vascularization of the RXRα null homozygotes. Particularly, an abnormal thinning of the trabeculae is observed in the RXRα$^{-/-}$ hearts by E14.5, which accompanied a general reduction in the ventricular wall myocardium and ventricular septal defects. Detailed analyses of RXRα$^{-/-}$ embryonic hearts revealed that the myocardial loss was due to the precocious differentiation and maturation of cardiomyocytes (Kastner *et al.*, 1997b).

Interestingly, a single RXRα allele is sufficient for development, since RXRα$^{+/-}$/ RXRβ/RXRγ triple mutants are viable and essentially normal (Krezel *et al.*, 1996). The importance of RXRα in the transduction of the vitamin A signal is suggested by a study from Kastner and colleagues (1997b) showing an exacerbation of the ventricular

myocardial hypoplasia associated with VAD in RXRα/RXRβ double mutants. The myocardial deficiency in RXRα single and RXRα/RXRβ double nulls, as with RARαγ null mutants, is due to an aberrant differentiation of subepicardial myocytes comprising the wall of the ventricle. This gives rise to the "spongy" myocardial phenotype and becomes nearly fully penetrant in RXRα/RXRβ double mutants, likely reflecting a true deficiency in retinoid signaling in the heart.

Additional VAD-associated abnormalities included a slight but consistent growth retardation of $RXR\alpha^{+/-}$ juvenile mice, and bilateral microphthalmia (Kastner *et al.*, 1994). Particularly, in all $RXR\alpha^{-/-}$ embryos, a ventral shortening of the eye is often accompanied an abnormal thickening of the corneal stroma. This leads to a close positioning or even contact of the stroma with the lens, which in turn causes the severe reduction or absence of the anterior chamber of the eye. Also, the closure of the optic fissure is incomplete in RXRα null fetuses, resulting in a coloboma of the optic nerve.

An interesting observation regarding the $RXR\alpha^{-/-}$ mice is that they are completely resistant to limb defects evoked by excess RA (Sucov *et al.,* 1995), while single RAR mutants remain sensitive to this specific teratogenic abnormality (Lohnes *et al.,* 1993; Luo *et al.,* 1995; Mendelsohn *et al.,* 1994b). Thus, RXRα seems to be a limiting partner in the transduction of the excess RA signal in the apendicular skeleton.

The targeted mutation of RXRγ did not result in any obvious malformations. Indeed, $RXR\gamma^{-/-}$ mice are completely viable and fertile (Krezel *et al.*, 1996). With the exception of abnormal spermatogenesis, RXRβ nulls were also normal (Kastner *et al.*, 1996). A puzzling finding from these studies is that RXRγ seems to be completely unnecessary, as RXRα/RXRγ and RXRβ/RXRγ are no more affected than RXRα and RXRβ single mutants, respectively (Krezel *et al.*, 1996). Taken together, the level of redundancy among the RXRs is even more striking than that observed for the RARs, and perhaps reflects a universal ability of these two classes of receptors to heterodimerize with one another without preference.

1.5.6. Synergism Between The RAR and RXR Null Mutations

As discussed earlier, evidence from retinoid receptor dimerization and transfection studies hinted at a possible role for RAR and RXR heterodimerization in the transduction of the retinoid signal. This synergism has subsequently been noted *in vivo* with various RAR/RXR double null mutants in many retinoid-dependent processes (Kastner *et al.*, 1994, 1997a). For instance, while the outflow tract septation was normal in RXRα$^{-/-}$, and RARα$^{-/-}$ or RARγ$^{-/-}$ embryos, the removal of RARα or RARγ from the RXRα null background leads to septation defects and an increase in myocardial loss, demonstrating a high degree of synergism between the two receptor classes (Table 1-3; Kastner *et al.*, 1994, 1997a). Similarly, although single RXRα or even double RXR mutants displayed at most ocular and myocardial defects, RXRα/RAR (α, β, or γ) double nulls recapitulated the entire RAR double mutant syndrome (Table 1-3; Kastner *et al.*, 1994, 1997a). Significantly, the removal of just one RARα, RARβ, or RARγ allele from the RXRα null background results in some of the defects found in RAR double mutants (Tables 1-2 and 1-3). The loss of a single RXRα allele from the RARγ mutant background is sufficient to induce digit webbing, tracheal defects, and vertebral homeosis and malformations to a similar extent to that observed in RARαγ double null embryos (Kastner *et al.*, 1997a). As with the RXR double and triple mutant data, this indicates that RXRα fulfills all the requirements for RXRs in retinoid signaling during development. Accordingly, RXR/RAR double mutants composed of either RXRβ or RXRγ null alleles did not lead to any increase in the severity of RAR single mutant phenotypes, consistent with a predominant role for RXRα. Given that RXRα/RAR double mutants present the same spectrum of defects as RAR double mutants, and collectively recapitulate the fetal VAD syndrome, these observations support the notion that RXR/RAR heterodimers, and not RXR homodimers, transduce the vitamin A signal during embryogenesis.

Table 1-3. Synergism between RXRα and RARα, RARβ, and RARγ null mutations. [Modified from Kastner *et al.*, 1997a. (Please refer to text for references)].

Abnormalities	**RXRα (Xα) and RAR (Aα, Aβ, or Aγ) mutant genotype**						
	Xα/Aα$^{+/-}$	*Xα/Aα*	*Xα/Xβ*$^{+/-}$	*Xα/Xβ*	*Xα/Xγ*$^{+/-}$	*Xα/Xγ*	*Xα*
Ocular defects							
• Shortened ventral retina	+	++	+	+	++	+++	+
• Coloboma of the retina	np	np	np	np	np	x	np
• Thicker corneal stroma	+	+	+	++	++	+++	+
• Hypoplastic/agenic eyelids	+	+	+	++	++	+++	+
Cardiac and arterial defects							
• Myocardial deficiency	+++	+++	na	na	++	++	++
• Conotruncal septal defect	x	x	np	np	np	np	np
• Persistent truncus arteriosus	+	+++	np	++	np	++	np
• Abnormal arteries	+	+++	np	+	+	+	np
Respiratory tract defects							
• Hypoplasia of lungs	np	+++	np	np	np	np	np
• Lack of esophagotracheal septum	np	+++	np	np	np	np	np
Glandular defects							
• Agenesis of thymus	np	np	np	+	np	np	np
• Hypoplasia of submandibular gland	np	np	np	np	np	+++	np
Urogenital tract defects							
• Ageneis of Mullerian duct	++	+++	+	++	+	+	np
• Ectopic ureter	+	+++	++	+++	+	++	np
• Hypolasia of kidneys	np	+++	np	np	np	np	np
• Agensis of kidneys	+	np	np	np	np	np	np

Evaluation scheme based on expressivity and penetrance of the phenotype: +, moderately affected; ++, highly affected; +++, severely affected.
Abbreviations: na, not available; np, not present; x, present.

1.6. Retinoid Signaling And Antero-Posterior Patterning Of The Vertebrate Axis

1.6.1. The Organizer And Establishment Of The Vertebrate Antero-Posterior Axis

Classical studies in the early patterning of the amphibian embryo have revealed that the antero-posterior (A-P) axis is initiated by a particular group of cells in the dorsal marginal zone that straddles the middle of the amphibian blastula (reviewed in Gilbert, 1994; DeRobertis *et al.*, 2000). This special group of cells forms the dorsal blastopore lip which is endowed with the ability to recruit and organize surrounding tissues into dorsal mesodermal (mesendodermal) and neurectodermal fates, and subsequently impart it with an A-P character. This region is called Spemann's organizer (or simply, the organizer), whose appearance constitutes the first morphological sign of posterior identity, thereby defining the A-P axis. In the amphibian embryo, the organizer is capable of inducing an embryonic axis, complete with head and tail, when transplanted to the ventral region of a host embryo (DeRobertis *et al.*, 2000). Indeed, this ability to induce a complete ectopic axis has become the defining characteristic of vertebrate organizer tissue.

Recent work has led to important discoveries as to the molecular nature of the amphibian organizer. It seems that the organizer functions by dorsalizing the inherently ventral nature of tissues deposited before gastrulation, thus allowing the creation of axial (dorsal) mesoderm and the CNS. This is accomplished by the secretion of a diverse collection of molecules that are able to inhibit several key signaling pathways, such as those initiated by BMPs (bone morphogenetic proteins), which are divergent members of the TGFβ superfamily, and Wnt (Wingless/int-1-related) family members (reviewed in DeRobertis *et al.*, 2000). The antagonists secreted by the organizer include Wnt-specific inhibitors such as Frzb-1, Dickkopf-1 (Dkk-1), and Crescent; the BMP inhibitors Chordin, Follistatin, and Noggin; a TGFβ-specific inhibitor, Lefty/Antivin; and Cerberus, a multifunctional antagonist capable of inhibiting the activities of both Wnts and BMPs (DeRobertis *et al.*, 2000). The activity of these antagonists seem essential for at least one of the two requirements of the organizer, that is, the induction of anterior structures (Bouwmeester *et al.*, 1996; Glinka *et al.*, 1998).

As with amphibians, the first morphological sign of asymmetry in mammals occurs at the initiation of gastrulation, when the primitive ectoderm, known as the

epiblast, undergoes an epithelial to mesenchymal transition to form a groove of ingressing tissue called the primitive streak (or streak; reviewed in Beddington and Robertson, 1999; Hogan *et al.*, 1994; Tam and Behringer, 1997). This defines the future posterior region of the embryo. During subsequent stages, this structure elongates to the distal tip of the cup-shaped mammalian embryo. At the anterior extremity of the streak lies a specialized structure, referred to as the node, that seems to be homologous to the amphibian gastrula organizer. It can give rise to similar tissues as Spemann's organizer, such as the prechordal plate and notochord, which together constitutes axial mesendoderm (the dorsal-most mesodermal type), and definitive gut endoderm (Beddington and Robertson, 1999; Tam and Behringer, 1997). Furthermore, the node expresses many of the genes found in the amphibian organizer (Hogan *et al.*, 1994; Beddington and Robertson, 1998, 1999). Together, the mouse node and primitive streak generate all the mesoderm and definitive endoderm of the embryo via the ingression of epiblast cells, consistent with organizer function.

A more formal proof of the node being the functional equivalent of the amphibian organizer came when Beddington (1994) grafted one onto the epiblast of a recipient mouse embryo, which led to the formation of a second neural axis. However, in contrast to amphibians, the ectopic axis lacked anterior-most structures including forebrain. Thus, the mouse node is unable to support the complete formation of a secondary axis. Alternatively, when combined with extra-embryonic tissues, particularly, primitive anterior endoderm (anterior visceral endoderm or AVE), as well as epiblast, the node is able to fully induce an ectopic axis with anterior neural structures (Tam and Steiner, 1999). In another series of elegant experiments, Thomas and Beddington (1996) demonstrated that the AVE is required for the expression of early markers of the prospective forebrain. Importantly, evidence from this study, as well as that of others, suggest that the anterior neural tube is already patterned before the onset of gastrulation (reviewed in Beddington and Robertson, 1999; Stern, 2000). These landmark studies suggest, that although initially elusive, the mammalian organizer is more complex than that of amphibians, requiring the distinct activities of at least two separate tissues: the AVE and node. Thus, while the AVE occupies itself with anterior neural induction, the node induces more posterior regions of the axis, such as the trunk. Due to these separate

inducing activities, the AVE is often referred to as the head organizer, and the node as the trunk organizer.

1.6.2. The Posteriorization Of The Vertebrate Antero-Posterior Axis

A long held view of how the vertebrate axis acquires antero-posterior patterning contends that following the induction of an anterior neural state, signals act to posteriorize it. This two-step process, called activation-transformation, was initially proposed by Nieuwkoop almost half a century ago (Nieuwkoop, 1952; Nieuwkoop and Nigtevecht, 1954). Briefly, this model asserts that the neuraxis is induced by organizer activity (the activation step) and initially possesses only anterior neural character, which is subsequently regionalized by the activity of various posteriorizing signals, such as Wnts, Fgfs, and RA (the transformation step; reviewed in Stern, 2000).

The role of retinoids in promoting posterior fates along the A-P axis has gained much support from studies in *Xenopus laevis*, the preeminent model system for neural induction. RA drastically attenuates forebrain development in a dose-dependent manner, while expanding more posterior neural tissue concomitantly with the anterior shift in the expression of posterior neurectodermal markers (Durston *et al.*, 1989; Ruiz i Altaba and Jessell, 1991a, 1991b; Sive *et al.*, 1990; Sharpe, 1991). Moreover, the period at which RA is able to posteriorize the CNS is restricted to neurulation stages following gastrulation (Durston *et al.*, 1989; Papalopulu and Kitner, 1996; Sive *et al.*, 1990; Sharpe, 1991). This suggests that the embryo becomes sensitive to RA following the induction of neurectoderm by organizer activity. Consistent with this, naïve ectodermal explants from the amphibian blastula or gastrula become competent to respond to RA only after they have been induced to become neural tissue by Noggin, Follistatin, Chordin or Cerberus (Papalopulu and Kitner, 1996; Taira *et al.*, 1997; reviewed in DeRobertis *et al.*, 2000; Wilson and Hemmati-Brivanlou, 1997). This implies that normal retinoid signaling is crucial for the development of the posterior CNS (see section 1.6.3), but is not required for anterior neural patterning.

In the mouse, retinoid treatment following gastrulation also leads to a reduction in anterior fates (Simeone *et al.*, 1995; Avantaggiato *et al.*, 1996). RA treatment expands the expression of several midbrain and rostral hindbrain markers anteriorly, such as *pax-2,*

wnt-1, en-1, and *en-2*, along with a concomitant loss of forebrain markers *emx-1, emx-2, dlx-1*and *otx-2*, suggesting a posteriorization of cell fate in the CNS. Fetuses resulting from such treatments are microcephalic or even lack head structures altogether, demonstrating that the reduction in anterior development is extensive (Yasuda *et al.*, 1986; Kessel and Gruss, 1990). As with *Xenopus*, sensitivity of mouse embryos to retinoids is restricted to stages following gastrulation, and thus occurs subsequent to neural induction (Kessel and Gruss, 1990). These results therefore support a role for RA as a potent caudalizing factor in the regionalization of CNS development.

Fgf signaling also has the ability to posteriorize the A-P axis, and Fgfs have been championed by some groups as Nieuwkoop caudalizers in *Xenopus* (Amaya *et al.*, 1991, 1993; Cox and Hemmati-Brivanlou, 1995; Holowacz and Sokol, 1999; Kengaku and Okamoto, 1995; Lamb and Harland, 1995; Taira *et al.*, 1997). Like retinoids, Fgfs can induce *hox* gene expression in posterior neural tissue and mesoderm, thereby influencing the patterning along the A-P axis (see below; Kolm and Sive, 1995; Kolm *et al.*, 1997; Pownall *et al.*, 1996; Ruiz i Altaba and Jessell, 1991b; Sive and Cheng, 1991; Sive *et al.*, 1990; Sharpe, 1991). In addition, genetic studies in zebrafish demonstrates that Fgfs regulate the morphogenetic movements (convergent extension) that allow for posterior development (Griffin *et al.* 1995, 1998); which is a defining characteristic of the trunk organizer. Fgf signaling does this by regulating the products of the *no tail* and *spadetail* loci, which encode zebrafish homologs of the *brachyury* gene, a critical regulator of convergent extension movements in vertebrates (reviewed in Yamada, 1994).

Importantly, retinoids and Fgfs synergize in the posteriorization of both mesoderm and neurectoderm in *Xenopus* development, suggesting that caudalization involves an interaction between peptide growth factors and RA signaling (Cho and DeRobertis, 1990; Kolm and Sive, 1995; Kolm *et al.*, 1997; Ruiz i Altaba and Jessell, 1991; Sive and Cheng, 1991; Taira *et al.*, 1997). Kolm and colleagues (1997) propose that RA functions to caudalize the hindbrain, while Fgfs promote the posteriorization of the spinal cord in *Xenopus*. This is consistent with the enrichment of retinoids in the rostral spinal cord adjacent to the hindbrain, and the posterior-high expression gradient of Fgfs in the *Xenopus* gastrula and mouse primitive streak (Crossley and Martin, 1995; Isaacs *et al.*, 1992; Haub and Goldfarb, 1991; Hebert *et al.*, 1991; Niswander and Martin,

1992; Song and Slack, 1996; Wilkinson *et al.*, 1988). Therefore, instead of a single molecule mediating the transformation event of Nieuwkoop's two-step model, vertebrate A-P patterning requires a complex interplay between growth factors and retinoid signaling.

1.6.3. RA Signaling And Hindbrain Development

One of the most obvious manifestations of patterning along the A-P axis is the presence of segmented structures in the posterior brain and in paraxial mesoderm along the entire length of the embryo. The hindbrain (or rhombencephalon) is composed of eight segments, called rhombomeres (numbered r1 to r8), that lie caudal to midbrain and rostral to the spinal cord (Carlson, 1996; Kaufman and Bard, 1999; Gilbert, 1994). Rhombomeres consist of a series of depressions and bulges (sulci and gyri) whose boundaries are defined the restricted expression of several genes (Fig. 1-5; Cordes, 2001). Furthermore, they are transient structures that harbor neural crest cells that form the cranial ganglia and the inner ear, and ultimately give rise to the brain stem (medulla, pons, and cerebellum). Neural crest cells originating from the first three even-numbered rhombomeres migrate ventrally beneath the ectoderm to populate the first, second, and third pharyngeal arches, respectively. R3 and r5 seem to lack neural crest cells and are inhibitory to the migration of crest cells from adjacent rhombomeres (Cordes, 2001; Golding *et al.*, 2000; Trainor and Krumlauf, 2000).

Much evidence exists for a role of retinoid signaling in the patterning of the hindbrain, consistent with a transforming role for this putative morphogen along the A-P axis (Gavalas and Krumlauf, 2000). Retinoids are consistently enriched in the rostral part of the spinal cord immediately adjacent to the caudal hindbrain (Fig. 1-2; Maden *et al.*, 1998). Both anterior paraxial mesoderm (occipital and cervical somites) and overlying neurectoderm consistently have slightly higher levels of retinoids that more posterior regions. This accurately reflects the expression of Raldh2, a major RA biosynthetic enzyme (Fig. 1-2; Niederreither *et al.*, 1997). Furthermore, the RA-catabolizing enzymes Cyp26A1 and Cyp26B1 are expressed in the anterior (r2) and anterior to middle regions (r2-r6) of the hindbrain, respectively (Fujii *et al.*, 1997; MacLean *et al.*, 2001). This presumably creates a sharp gradient of RA diffusing from the rostral spinal cord into the

caudal hindbrain. RA distribution in the hindbrain region is therefore consistent with it being a planar and lateral mesodermal signal that patterns the neurectoderm according to a concentration landscape. Thus, if retinoid signaling does indeed impart a posterior character to the hindbrain, then altering the retinoid gradient should perturb patterning in predictable ways.

In agreement with this, there is an increasing posterior sensitivity to RA signaling along the developing hindbrain (Conlon and Rossant, 1992; Godsave *et al.*, 1998; Dupé and Lumsden, 2001; Wood *et al.,* 1994). Excess RA during post-gastrulation or early somitogenesis stages leads a dramatic foreshortening of the anterior hindbrain of mouse and *Xenopus* embryos (Conlon and Rossant, 1992; Godsave *et al.*, 1998; Kolm *et al.*, 1997; Marshall *et al.,* 1992). There is a co-linear response to exogenous RA in the hindbrain. For instance, the hindbrain expresses homeobox-containing transcription factors (*hox* genes) in a nested series along its A-P axis: *hoxb1, hoxb3, hoxb4,* and *hoxb5* are expressed in r4, r5-r6, r7-r8, and r8 and the spinal cord, respectively (reviewed in McGinnis and Krumlauf, 1992). The more posteriorly expressed *hox* genes respond to higher levels of exogenous RA, while anterior expressing genes require less RA (Conlon and Rossant, 1992; Godsave *et al.*, 1998; Marshall *et al.,* 1992; Wood *et al.,* 1994). Similarly, inactivation of Cyp26A1 in the mouse, a RA-catabolizing enzyme expressed in r2, leads to a mild posterior transformation of the anterior hindbrain, concomitant with a rostral expansion and enhanced *hoxb1* expression in r4 (Abu-Abed *et al.*, 2001; Sakai *et al.*, 2001). Also, small numbers of cells rostral to the r4 boundary express *hoxb1* ectopically in *cyp26A1*$^{-/-}$ embryos, reflecting a posteriorization of the hindbrain. This suggests that there is a sharp gradient of RA patterning the hindbrain along the A-P axis, with greater levels of retinoids required to instruct more posterior fates.

Predictably, the loss of RA signaling leads to an anteriorization of the hindbrain. Treating chick embryos with increasing levels of RAR antagonist BMS493 leads to a progressive loss of posterior rhombomeres and enlargement of anterior rhombomeres (Dupé and Lumsden, 2001). BMS493 treatment in the mouse also results in a caudal truncation of the hindbrain, with a greater loss of hindbrain structures occurring with treatments at earlier times (Wendling *et al.*, 2001). In the most extreme form of retinoid deprivation elicited by antagonist treatments, the caudal hindbrain becomes truncated

Figure 1-5. The effects of inhibition of RA signaling on hindbrain development.

The phenotypes were assessed by the expression patterns of various rhombomeric-restricted markers indicated below. High expression is indicated by the solid lines. Low expression is represented by the dashed lines. Otocysts are represented by the shaded ovals and normally develop at the r5/r6 boundary. Intermediate retinoid signaling leads to hypoplastic, and sometimes ectopic otocysts, while low levels of RA signaling leads to hypoplastic otocysts. ND, not determined. Abbreviations: mb, midbrain; ot, otocyst; r, rhombomere; sc, spinal cord; ot, otocysts. [Modified from Gavalas and Krumlauf, 2000].

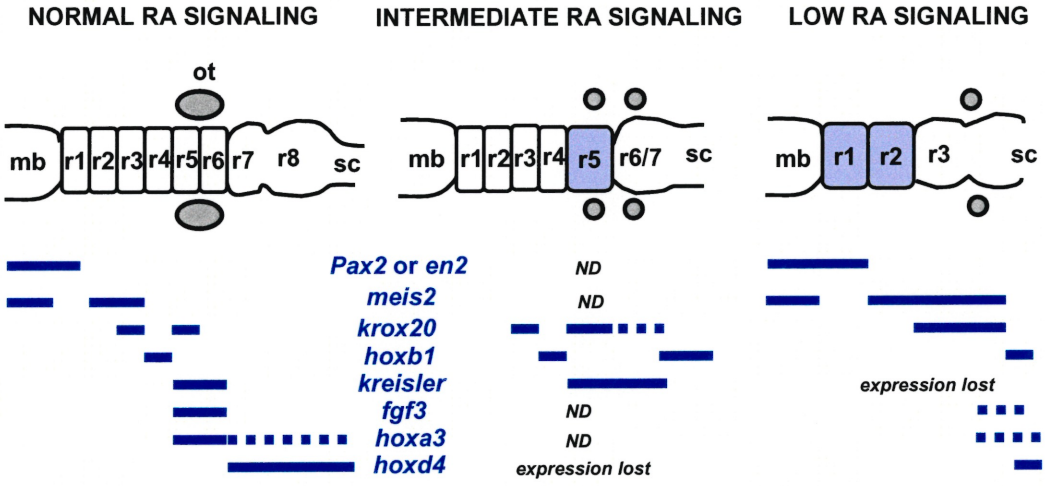

EXPERIMENT:	*RARβγ* double mutants, Dominant-negative *RAR*, Ectopic *Xcyp26A1*, *RAR* antagonist treatment E8.0 (mouse), Low concentration of *RAR* antagonist (chick).	VAD quails, VAD rats, *Raldh2* mutants, *RARαγ* double mutants, *RAR* antagonist treatment at E7.0 (mouse), High concentration of *RAR* antagonist (chick).
REFERENCES:	Dupé *et al.*, 1999. Blumberg *et al.*, 1997; Kolm *et al.*, 1997; van der Wees *et al.*, 1998; Hollemann *et al.*, 1998. Wendling *et al.*, 2001. Dupé *et al.*, 2001.	Gale *et al.*, 1999; Maden *et al.*, 1996; White *et al.*, 2000. Niederreither *et al.*, 1999, 2000. Wendling *et al.*, 2001. Dupé *et al.*, 2001.

below r4, while the remaining rhombomeres are expanded. This has also been observed in VAD quails and rats, RARαγ double null mutants, and *Raldh2*$^{-/-}$ mouse embryos, which represents the mouse equivalent of a near complete retinoid-deficient situation (Fig. 1-5; Gale *et al.*, 1999; Maden *et al.*, 1996; Niederreither *et al.*, 2000; Wendling *et al.*, 2001; White *et al.*, 2000b). These losses in the posterior rhombomeres have been confirmed with extensive molecular analyses of key hindbrain patterning genes (Fig. 1-5). In *Raldh2*$^{-/-}$ embryos, the expression of various *hox* genes, particularly *hoxa1, b1, a3,* and *b3*, are either highly reduced, or in the case of *hoxd4*, abolished altogether (Niethereither *et al.*, 1999, 2000). As *hoxd4* is the caudal-most expressing *hox* gene in the hindbrain, this is consistent with a deletion of the molecular identity of the posterior hindbrain. Similar losses in caudal rhombomeric markers occur in VAD quails and rats (Gale *et al.* 1999; Maden *et al.*, 1996; White *et al.*, 2000b).

Interestingly, RARαγ double mutants display as severe a phenotype as *Raldh2*$^{-/-}$ and VAD embryos with respect to hindbrain patterning, while RARαβ double mutants present a milder loss of posterior rhombomeres (Dupé *et al.*, 1999; Wendling *et al.*, 2001). Particularly, the hindbrains of RARαβ double mutants lack rhombomeres caudal to r6 and have an enlarged r5, indicating that there is still remains an intermediate degree of retinoid signaling in these mutants (Fig. 1-5). In agreement with these patterning defects, RARαβ double null mouse embryos often have a small unilateral or bilateral ectopic otocysts that form caudal to the original otocysts (Dupé *et al.*, 1999). These structures normally arise from the r5/r6 boundary, thus the ectopias may reflect a caudal shift of this boundary, and can be interpreted as an anteriorization of rhombomeric identity. Similar hindbrain phenotypes can be elicited in *Xenopus* with dominant-negative RARs or ectopic expression of Cyp26A1 (Fig. 1-5; Blumberg *et al.*, 1997; Hollemann *et al.*, 1998; Kolm *et al.*, 1997; van der Wees *et al.*, 1998). This includes the anterior transformation of much of the hindbrain, consistent with a requirement of RA signaling for posterior development.

Collectively, these studies indicate that a block in retinoid signaling leads to a loss of the caudal hindbrain and a respecification of the remaining rhombomeres to a more anterior identity. Moreover, the sensitivity to retinoid signaling appears to be greatest in the posterior hindbrain, with the rostral extremity of the hindbrain, at the junction of the

midbrain, and the spinal cord being relatively unaffected by aberrant retinoid signaling. Therefore, retinoids adequately fulfill the requirements of a caudalizing factor in the vertebrate hindbrain.

1.6.4. Somitogenesis

In addition to the hindbrain, another tissue that displays obvious metamerism is the mesoderm-derived somites. They are bilateral epithelial blocks of cells located on either side of the notochord, below the neural tube, and eventually give rise to the vertebrae (as well as other tissues) that are differentially patterned along the A-P axis. Somites, like all mesodermal tissues, are derived from epiblast cells ingressing through the primitive streak (Lawson *et al.*, 1991; Tam *et al.*, 2000). The cells fated to give rise to the paraxial mesoderm have been mapped to a rostro-lateral region of the epiblast, relative to the location of the primitive streak (Lawson *et al.,* 1991; Tam *et al.,* 1997, 2000). By mid-streak stages, presumptive paraxial mesoderm is found in the epiblast in a large lateral domain encompassing the rostral half of the primitive streak (Fig. 1-6a; see Appendix I for the staging of mouse embryos). As the streak elongates anteriorly, it impinges on these precursors in the epiblast, which then ingress through the anterior portion of the streak. Cranial paraxial mesoderm (somitomeres) is the first such population to move through the streak, followed by somitic paraxial mesoderm during late gastrulation stages. These ingressing cells migrate laterally and rostrally as they exit the streak and are deposited along the sides of the developing midline. Towards the end of gastrulation, the cells of the anterior streak contain precursors for the first six to ten pairs of somites and the paraxial mesoderm.

The primitive streak continues to generate paraxial mesoderm until it regresses completely by E8.5 in the caudal region of the mouse embryo (Fig. 1-6b; Tam and Tan, 1992; Tam *et al.*, 2000). Up to this point, all of the cervical and some thoracic level somites have been generated. Subsequently, there is a transition in cellular recruitment of paraxial mesoderm from the streak to the tail bud mesenchyme as the posterior neuropore (open caudal neural tube) closes. The tail bud then generates the remaining paraxial mesoderm (Tam, 1984). The mesenchymal cells of the tail bud behave very much like the primitive streak as they can generate diverse lineages in the caudal embryo, such as

hindgut endoderm, paraxial and lateral mesoderm, and neuroepithelium (Kanki and Ho, 1997; Tam, 1984). Moreover, the tail bud also shares the expression of several markers with the streak, such as *brachyury* (Wilkinson *et al.*, 1990; Hermann, 1991; Kispert and Herrmann, 1994), *wnt-3a* (Roelink and Nusse, 1991; Takada *et al.*, 1994) and *fgfr1* (Orr-Urteger *et al.*, 1991; Yamaguchi *et al.*, 1992). The loss of any of these genes leads to severe deficiencies in mesoderm formation, consistent with a critical role in primitive streak function (Beddington *et al.*, 1992; Ciruna *et al.*, 1997; Takada *et al.*, 1994; Wilkinson *et al.*, 1990; Yamaguchi *et al.*, 1994; Deng *et al.*, 1994). Interestingly, *brachyury* regulates a type of intercalary cell movement called convergent extension (Beddington *et al.*, 1992; Wilson and Beddington,1997; Wilson *et al.*, 1995; Tada and Smith; 2000; Yamada, 1994). Furthermore, *wnt3a* has been shown to directly regulate *brachyury* promoter activity in the mouse (Arnold *et al.,* 2000; Yamaguchi *et al.*, 1999), and Fgf signaling impacts on the expression of the *brachyury* in *Xenopus* (Kim *et al.*, 1998; Latinkic *et al.*, 1997) and chick (Dubrulle *et al.*, 2001). The regulation of this important morphogenetic protein is complex, as *brachyury* in turn induces the expression of *Wnt* family members (*Xwnt11*; Tada and Smith, 2000) and *Fgfs* (Casey *et al.*, 1998; Kim *et al.*, 1998), and itself (Conlon, *et al.,* 1996; Tada *et al.,* 1997) in *Xenopus*. Thus, a possible mechanism for generating paraxial mesoderm from tail bud mesenchyme involves convergent extension movements.

Paraxial mesoderm is deposited along both sides of the developing midline and subsequently, in its most rostral domain, begins to condense to form epithelial balls, the somites. This rostral paraxial domain contains the earliest ingressed paraxial mesodermal tissue, and thus initiates somitogenesis first via a mesenchymal to epithelial transition. Somites therefore develop in a cranio-caudal sequence, with the more mature somites being continually displaced cranially by the generation of new ones (Tam, 1986). Early embryological work demonstrated that somites are formed from presomitic mesoderm with a certain periodicity. In avians and mammals, a somite pair is generated every ninety minutes or so (reviewed in Pourquié, 2000). This rate is observed in different vertebrates, hinting at an underlying evolutionarily conserved mechanism for generating somites. Several theories have been put forth to explain the periodicity of somite formation. One that is currently enjoying much support is the clock and wavefront model (Pourquié,

2000; Tam *et al.*, 2000). This theory asserts that presomitic cells oscillate synchronously according to an internal clock, and then stop oscillating when they are reached by a progressing wavefront originating from the posterior embryo. The wavefront is thought to consist of an A-P gradient of maturation governed by a signaling process that propagates slowly up along the embryo. At the apex of the presomitic mesoderm, the autonomous clock segments the tissue in response to this wavefront.

Until recently, the molecular mechanisms governing somitogenesis were poorly understood. In what is a classic study, Palmeirim and colleagues (1997) elegantly show the expression of a basic helix-loop-helix transcription factor gene, *c-hairy*, in chicks as an anteriorly progressing wavefront within the presomitic mesoderm. This vertebrate homolog to the *Drosophila* pair rule gene, *hairy*, initiates expression throughout the presomitic mesoderm, but becomes progressively restricted anteriorly until its reaches the rostral presomitic mesoderm, where it is strongly expressed in the caudal half of both the newly forming and recently emerged somite (Fig. 1-6c). Each cycle of the *c-hairy* wavefront corresponds to the time required to form a somite (i.e. ninety minutes). An identical pattern of expression has been observed for a mammalian *hairy* gene, *HES1*, and a second chick *hairy* homolog, *c-hairy2* (Jouve *et al.*, 2000). Thus, the cyclical activation of the vertebrate *hairy* genes reflects the output of a segmental clock and provides molecular support for the clock and wavefront theory. Subsequent work revealed that several members of the Notch signaling pathway are also expressed in presomitic mesoderm and newly forming somites in patterns that presage the formation of somite boundaries (reviewed in Pourquié, 2000; Tam *et al.*, 2000). Furthermore, the loss of function of a number of members of the Notch signaling pathway leads to disorganized somitogenesis, consistent with a role in somite formation (Pourquié, 2000, and references therein).

Fgf signaling has been implicated in generating the somitogenesis wavefront and establishing somite identity by coordinating *hox* gene expression in the appropriate somites (Dubrulle *et al.*, 2001; Zakany *et al.*, 2001). *Fgfs* and their receptor, *fgfr1*, are normally expressed in the caudal unsegmented portion of the paraxial mesoderm, where they may regulate the differentiation status of presomitic mesoderm (Crossley and Martin, 1995; Dubrulle *et al.*, 2001; Haub and Goldfarb, 1991; Niswander and Martin,

Figure 1.6. Localization of tissue precursors in the mouse epiblast and tailbud and formation of somites.

(**A**) Fate map of the epiblast in mid to late primitive streak stages. The black line indicates the primitive streak. (**B**) Localization of tissue precursors in the mouse tailbud region at early somite stages. The dotted line indicates the notochord and floorplate. (**C**) Cyclic expression pattern of *c-hairy* in the presomitic mesoderm of chick embryos and the formation of somites. Depicted is one full oscillation of the somitogenesis cycle occurring in 90 minutes. *c-hairy* expression begins in a broad domain from the posterior embryo and progresses upwards as a narrowing wave. *c-hairy* expression becomes stabilized in the caudal portion of the somite. S_O, forming somite; S_I, most recently formed somite; S_{II}, older rostral somite. [Figures A and B modified from Tam *et al.*, 2000. Figure C modified from Pourquié *et al.*, 2000].

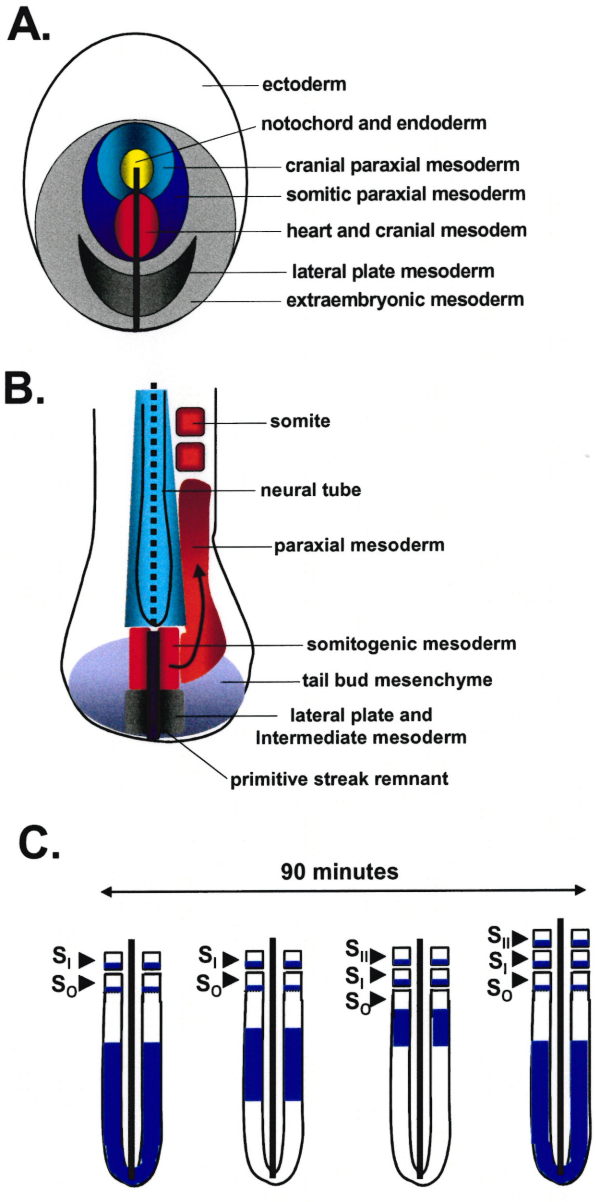

1992; Orr-Urteger *et al.*, 1991; Wilkinson *et al.*, 1988). Consistent with this, ectopic expression of FGF8 throughout the chick presomitic mesoderm abolishes somitogenesis and expands the expression of *brachyury*, a marker for naïve mesoderm. Likewise, the loss of *fgfr1* in the mouse also leads to a lack of somitogenesis (Ciruna *et al.*, 1997; Deng *et al.*, 1994; Yamaguchi *et al.*, 1994). A much more localized expression of FGF8 in the rostral presomitic mesoderm causes abnormally small somites to form, indicating an acceleration of either the somitogenesis clock or the propagation of the wavefront (Dubrulle *et al.*, 2001). As the cyclic expression of *hairy* is unaffected by local increases in FGF8 levels, this suggests that Fgf signaling contributes to the wavefront controlling the decision to undergo segmentation. Collectively, these observations suggest that Fgf signaling regulates segmentation in response to the somitogenesis clock, which in turn sets the axial level of *hox* expression, and therefore somite identity.

1.6.5. Hox Genes And Co-Linearity

As alluded to earlier, *hox* genes are expressed in a nested pattern along the A-P axis in both neurectoderm (hindbrain) and mesoderm (somites), and are believed to establish segment identity (Gaunt *et al.,* 1988, 1989). They are transcription factors characterized by the presence of a DNA binding motif called the homeobox, and display remarkable conservation during metazoan evolution (McGinnis and Krumlauf, 1992). The fly genome contains two separate homeotic gene complexes referred to as the Bithorax (BX-C) and Antennapedia (ANT-C) complexes. In the mouse, this basic set occurs in four separate clusters of linked *hox* genes, labeled *HoxA* through *HoxD*, that are found on different chromosomes (Fig. 1-7A; Graham *et al.,* 1989; McGinnis and Krumlauf, 1992; Krumlauf, 1994). It is believed that this resulted from at least two independent duplication events of an ancestral *Homeotic* gene complex (or *HOM-C*) during the divergence of the vertebrate and invertebrate lineages. As each cluster is imperfectly repeated four times in mammals with respect to insects, there may be as many as four copies of a given *hox* gene within the mammalian genome (Fig. 1-7A). These copies are referred to as paralogs, and share greater homologies with one another than with any other *hox* genes (McGinnis and Krumlauf, 1992). For example, *hoxa4, hoxb4,* and *hoxd4* are paralogs, while any of these genes are orthologs of the fly *deformed (dfd)* gene (Fig.

1-7A). Moreover, there is evidence to support the functional equivalence of paralogous *hox* members (Greer *et al.,* 2000).

Interestingly, the clustered distribution of *hox* genes in chromosomes reflects their spatio-temporal expression profile; a phenomenon referred to as co-linearity (McGinnis and Krumlauf, 1992; Krumlauf, 1994). That is, the entire cluster is transcribed in the same orientation such that the more 5' the position of a *hox* gene within a cluster, the later it becomes activated and the more caudal its expression along the A-P axis (Fig. 1-7B). This important property of *hox* gene function has been conserved in evolution as insects display an identical co-linearity in their *hox* gene counterparts (Graham *et al.*, 1989). Moreover, both the *Drosophila* and vertebrate *HOM-C* genes are involved in the specification of segment identity, indicating a true functional and structural homology with one another.

Hox genes are activated during late gastrulation (E7.5 in the mouse), presumably in the ingressing tissue of the primitive streak (Deschamps *et al.*, 1999; Krumlauf, 1994). This corresponds to the initiation phase of *hox* gene expression and is thought to establish the anterior boundaries of *hox* expression in paraxial mesoderm. Moreover, as somitogenesis proceeds in a cranial to caudal fashion, the earliest formed, and thus most anterior somites express the more 3' *hox* genes. This principal of co-linearity has been demonstrated by Duboule's group in an elegant series of transposition experiments within the *Hox D* cluster (Kmita *et al.,* 2000; van der Hoeven *et al.,* 1996). When 3' *hox* genes were placed in more 5' locations, they became activated later on in development and in more posterior locations along the axis, consistent with their new chromosomal location. These studies therefore established that position with a cluster determines the order of expression. More recent work points out that *hox* gene activation may be accomplished by a progressive escape from repression and corresponding accessibility to the transcriptional apparatus (Kondo and Duboule, 1999). The repressor element has been mapped by this group to some 40 kb upstream of the 5' most gene in the *HoxD* cluster and functions to keep the 5' *hox* genes repressed. This likely accounts for at least some aspects of the observed co-linearity of *hox* gene expression, as 3' more *hox* genes are further away from the repressor and thus escape its influence more readily.

Figure 1-7. Co-linearity in the structure and expression of Homebox gene complexes.

(**A**) Genomic organization of the Homeobox (Hox) gene complexes (HOM-C) in *Drosphila* (top) and the mouse. Mammalian genomes have four copies of the *Antennapedia* (ANT-C) and *Bithorax* (BX-C) complexes (*Hox A* to *D*) located on four separate chromosomes. A single complex spans 100 kb and includes paralogous groups 1 to 13. The color scheme indicates the mammalian genes that are homologous to the *Drosophila* HOM-C genes. The direction of transcription of the complexes is indicated by the arrow. In mammals, the 3' more *hox* genes are transcribed earlier, expressed in more anterior compartments, and display a greater response to retinoid treatments (i.e. respond more quickly and with lower doses of RA). *Drosophila* HOM-C genes: *lab, labial; pb, proboscipedia; dfd, deformed; scr, sex-combs reduced; antp, antennapedia; ubx, ultrabithorax; abd, abdominal.* (**B**) The expression domains of *Hox* genes along the antero-posterior axis constitutes a *Hox* code for vertebra identity. Solid transverse lines indicate the major segment modules of the vertebrate axis: Occipital, cervical, thoracic [vertebrosternal (identified by long processes or ribs) and non-vertebrosternal thoracic (identified by smaller ribs)], lumbar, and sacral. Dotted line identifies the caudal segments. [Figure A modified from Sadler, 2000. Figure B modified from Hogan *et al.*, 1994].

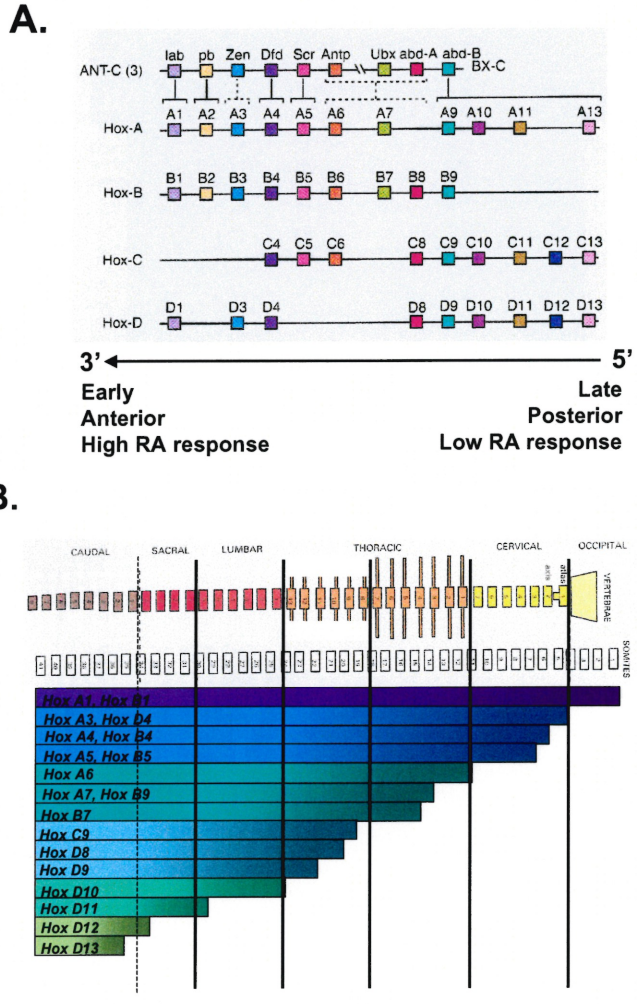

Indeed, the removal of the repressor element leads to a loss of co-linearity due to the premature activation of 5' *hox* genes.

Interestingly, recent findings suggest that *hox* gene expression in the maturing somite is actually transient and reflects the outcome of the somitogenesis clock (Dubrulle *et al.,* 2001; Zakany *et al.,* 2001). The formation of each somite is immediately preceded by a burst of *hox* gene activation, which becomes subsequently downregulated as the new somite forms. Based on these observations, the authors suggest that the segmentation clock enhances the transcription of *hox* genes in cells approaching the somite boundary, which then stabilizes the identity of the segments along the A-P axis. Thus, a refined model of co-linearity states that *hox* genes are transcriptionally activated during gastrulation by the progressive release of a silencing mechanism, and somite expression boundaries are then set by time-dependent bursts of *hox* gene activation by the segmentation clock.

1.6.6. Hox Genes And Vertebral Patterning

A hallmark of vertebrate design is the presence of somite-derived segments, the vertebrate, that possess unique regional morphologies along the A-P axis. These include seven cervical vertebrae, rib-producing thoracic vertebrae, seven of which fuse at the midline to form the rib cage (the vertebrosternal ribs), and the lumbar, sacral, and caudal vertebrae. Perhaps the most interesting property of the *hox* genes is that, due to co-linearity, unique combinations of *hox* gene expression occur within different axial structures (Fig. 1-7B; Burke *et al.*, 1995; Gaunt *et al.*, 1988, 1989; Kessel and Gruss, 1991). For example, the first somites express paralog group 1 genes, while more caudal somites express paralogous groups 1 and 2, followed by groups 1 through 4, and so on (Fig. 1-7B). This led Kessel and Gruss (1990) to propose the existence of a Hox code that defines vertebral identity. This states that the unique combination of *hox* gene expression within a vertebral segment defines it. Based on this model, one expects gain of function or loss of function experiments to perturb vertebral patterning in predictable ways. That is, the loss of more posterior paralogous genes results in somites containing a Hox code characteristic of more anterior segments, and should lead to anterior homeotic transformations of the vertebrae. While ectopic expression of more 5' *hox* genes should

lead to posterior homeotic transformations due to a posterior expansion of hox expression in more rostral somites. Indeed, the phenotype of any given *hox* knock-out correlates with it's anterior-most domain of expression, consistent with the Hox code model (reviewed in Krumlauf, 1994).

There also exits a high degree of redundancy in *hox* gene function. For example the loss of both *hoxa1* and *hoxb1* give rise to a more severe phenotype than either single mutants, affecting the pharyngeal arches, hindbrain patterning and hindbrain-derived cranial ganglia (Gavalas *et al.*, 1998, 2001). Likewise, the progressive loss of paralogous group 4 genes leads to a gene dosage-dependent increase in both the occurrence and the severity of the transformation of the second cervical vertebra (C2) to the identity of the first (C1; Horan *et al.*, 1995b). A particularly interesting observation from this study is that the group 4 *hox* compound nulls display a near complete transformation of most cervical vertebrae to the identity of the of C1, suggesting that some combinations of *hox* genes act to pattern entire regions of the A-P axis. Another example of synergy involves the mutation of paralog group 3 genes, whose rostral limit of expression reaches the somites that form the cervical vertebrae (Fig. 1-7B). The phenotypes of the *hoxd3* and *hoxa3* single mutants do not overlap, despite their similar expression profiles. In particular, the loss of *hoxd3* (Condie and Capecchi, 1993) results in an incomplete transformation of C1 to an occipital bone, while the targeted mutation of *hoxa3* leads to abnormalities of the hyoid bones of the skull and does not affect the cervical or occipital vertebrae (Chisaka and Capecchi, 1991). However, the combined mutation of both of these genes results in a gene-dosage dependent deletion of C1, and an exacerbation of hyoid bone deficiencies, demonstrating a remarkable degree of functional overlap (Condie and Capecchi, 1994).

The overexpression of *hox* genes leads to posterior homeotic transformations, due to the rostral expansion of their expression into more anterior segments. For instance, the ectopic expression of *hoxa1* in both mice (Zhang *et al.*, 1994) and fish (Alexandre *et al.*, 1996) leads to a posteriorization of the hindbrain, mimicking the action of retinoids. Likewise, driving *hoxd4* expression into the rostral-most cranial somites results in spectacular transformations of the occipital vertebrae to the identities of the more posterior cervical segments (Lufkin *et al.*, 1992). Other posterior homeotic

transformations of the axial skeleton can be elicited by the ectopic expression of *hoxb2* (Nonchev *et al.*, 1997), *hoxc6* (Jegalian and DeRobertis, 1992), *hoxb8* (Charité *et al.*, 1994), and *hoxc8* (Pollock *et al.*, 1992), consistent with a redefinition of the Hox code. Together, these gain- and loss-of-function experiments thus lend support for the existence of a Hox code patterning the segments along the A-P axis.

1.6.7. Retinoid Signaling And Hox Gene Regulation

The regulation of *hox* genes is remarkably dynamic and complex. Deschamps and colleagues (1999) have outlined three separate phases of *hox* gene function: initiation, establishment, and maintenance. As described above, initiation involves the activation of *hox* gene expression during gastrulation in the tissues ingressing through the primitive streak, including the presumptive paraxial mesoderm and overlying nascent neuroepithelium. Whereas establishment refers to the fine tuning of *hox* gene expression within their characteristic rhombomeric and somite boundaries. The maintenance phase of *hox* gene expression usually refers to a long term epigenetic mechanism that modifies the chromatin structure surrounding the *hox* clusters, and involves the activities of polycomb group and trithorax group genes (reviewed in Gould, 1997).

Interestingly, for certain *hox* genes the establishment mechanism involves cross regulation by paralogous *hox* members (Manzanares *et al.*, 2001; Morrison *et al.*, 1997; Packer *et al.*, 1998; Studer *et al.*, 1998). Several 3' *hox* genes have bipartite *hox* binding motifs that bind a heterodimer of Hox proteins along with another class of homeobox-containing factors, the Pbx proteins (Maconcochie *et al.*, 1997; Manzanares *et al.*, 2001; Popperl and Featherstone, 1992; Popperl *et al.*, 1995). In the case of the *hoxb1* gene, the auto-regulatory element has been shown to be critical for the establishment and maintenance of its expression in the hindbrain (Popperl *et al.*, 1995), and is mediated by both *hoxa1* and *hoxb1* genes (Studer *et al.*, 1998). Similar cross-regulatory motifs are required for the establishment of *hoxb2* (Maconochie *et al.*, 1997), *hoxa*3 (Manzanares *et al.*, 2001), *hoxa4* (Packer *et al.*, 1998), and *hoxb4* (Gould *et al.*, 1997, 1998) expression in the neurectoderm.

Several important observations support a key role for retinoid signaling in the initiation phase of *hox* gene expression. Among the earliest discoveries regarding retinoid

regulation of *hox* genes came from studies in human embryonal carcinoma cell lines. RA is able to efficiently activate *hox* genes in a co-linear fashion in these cell lines, with 3' more genes being more rapidly induced at with lower concentrations that 5' more genes (Moroni *et al.,* 1993; Simeone *et al.*, 1990, 1991). Subsequently, these findings have been extended *in vivo* in the mouse (Conlon and Rossant, 1992; Kessel and Gruss, 1991; Marshall *et al.,* 1992; Wood *et al.,* 1994), where it was found that RA treatment during late gastrulation rapidly induces 3' *hox* gene expression and anteriorizes their rostral expression boundaries. This response is co-linear, with the 3'-most *hox* genes being insensitive to retinoids after E7, and more 5' *hox* genes remaining sensitive to RA at progressively later times up until day 9 of gestation (Conlon and Rossant, 1992; Kessel and Gruss, 1991). Interestingly, the caudal-most expressing genes are refractory to excess RA, suggesting that retinoid signaling directly regulates the *hox* genes at the 3' end of the cluster (Conlon and Rossant, 1992).

Retinoids are enriched in the primitive streak of avians and mammals (see Fig. 1-2; section 1.2), consistent with a role in the activation of early-expressing *hox* genes. Furthermore, the mutation of Raldh2, a major RA biosynthetic enzyme, and VAD in avians and rodents, results in the down-regulation or absence of several 3' *hox* genes in their rostral expression domains (Fig. 1-5; section 1.6.3; Gale *et al.*, 1999; Maden *et al.*, 1996; Niederreither *et al.*, 1999, 2000; White *et al.*, 2000b). Similarly, RARαγ double null mutants and embryos treated with a RAR antagonist also display a loss of *hox* gene expression in the hindbrain. Importantly, the *hox* genes consistently down-regulated in these experiments include groups 1, 2 and 4, suggesting that some of these *hox* group members are directly regulated by retinoids (Dupé *et al.*, 2001; Wendling *et al.*, 2001).

More robust support for the function of retinoids in *hox* gene activation comes from the discovery of RAREs within the regulatory regions of most group 1 and 4 genes. Among the first RAREs to be isolated is the 3' DR5 type element of the *hoxa1* gene (Langston and Gudas, 1992). This enhancer is necessary for establishing the rostral limit of *hoxa1* expression and mediates the RA-inducibility of the gene (Frasch *et al.*, 1995; Langston and Gudas, 1992). Consistent with this, mice lacking the *hoxa1* 3' RARE fail to initiate the rostral *hoxa1* boundary and display reduced levels of *hoxa*1 transcripts (Dupé

et al., 1997). These mice are also compromised in the ability to induce *hoxa1* expression in response to RA treatment.

The *hoxb1* gene contains both 5' DR2 and 3' DR5 RAREs which are sufficient to recapitulate the early expression pattern of the *hoxb1* gene in transgenic mice (Marshall *et al.*, 1994; Ogura and Evans, 1995; Studer *et al.*, 1994). As with the *hoxa1* RARE, the targeted disruption of the *hoxb1* 3' RARE reveals its importance in establishing the early rostral expression boundary of *hoxb1* in the hindbrain, and in directing robust expression levels of this gene (Studer *et al.*, 1998). Likewise, the initiation of *hoxb4* expression in neurectoderm requires a RARE that responds to retinoid signals emanating from the cranial paraxial mesoderm (Gould *et al.*, 1998). Other similar RAREs have been described for the *hoxa4* (Packer *et al.*, 1998) and *hoxd4* (Morrison *et al.*, 1996, 1997; Popperl and Featherstone, 1993; Zhang *et al.*, 1997, 2000) loci, which mediate RA-induction and establish the proper anterior expression boundaries of these genes. An interesting corollary to these observations is that no RAREs have been reported for the group 3 paralogous genes, which begin to be expressed in sharp rostral domains a full day later than groups 1, 2, and 4 (Manzanares *et al.*, 2001). At least for the *hoxa3* locus, an auto-regulatory element consisting of two Hox/Pbx binding sites seems to mediate its expression in the neurectoderm, in agreement with its relatively late initiation during development (Manzanares *et al.*, 2001).

Thus, *hox* RAREs convey the universal ability to drive early abundant expression of *hox* genes within the neurectoderm. Moreover, they set the rostral limit of *hox* expression and are thus able to interpret positional information supplied by caudalizing signals from either the mesoderm or neural plate. Retinoid signaling therefore helps establish *Hox* co-linearity by directly activating the 3' most members of the complex within defined spatial-temporal domains.

1.6.8. Retinoid Receptors And Vertebral Patterning

A number of key experiments outlined above have established that retinoid signaling can pattern metameric structures within the neuroepithelium by regulating *hox* genes (section 1.6.3). This also holds true for the somite-derived vertebrae, which are also patterned by *hox* genes (Fig. 1-7B). Kessel and Gruss (1991) have shown that vertebral patterning is

particularly sensitive to excess retinoids from late gastrulation (E7-7.5) to early somitogenesis stages (E8.5) in the mouse. A subsequent analysis from Kessel (1992) discovered that excess RA can also elicit vertebral patterning defects at later stages, from E10.5 to E11.5. Moreover, early treatments affect the entire vertebral axis, while later treatments generally result in regional defects along the axial skeleton, such as lower cervical and upper thoracic regions transformations (Fig. 1-8 and Table 1-4). This reflects the establishment of paraxial mesoderm and rostro-caudal progression of somitogenesis during the early window (E7-E8.5), and the subsequent differentiation of somites to prevertebrae for the late window, which also occurs in an A-P sequence.

Retinoid sensitivity during the early period is associated with rostral expansions of the anterior expression boundaries of several *hox* genes within prevertebral condensations (Kessel and Gruss, 1991). These shifts occur concomitantly with posterior transformations of the thoracic and lower cervical vertebrae, consistent with their normal patterns of expression in this region. Thus, exogenous RA can affect vertebral patterning by altering the *Hox* code.

Surprisingly, the homeotic transformations elicited with RA during the late window are not associated with alterations of *hox* expression domains, suggesting the existence of a *hox*-gene independent mechanism for vertebral patterning (Kessel, 1992). As these transformations resemble those occurring with earlier retinoid treatments, Kessel (1992) described this phenomenon as a respecification of the vertebrae. The author also proposes that retinoids can affect vertebral identities at this late window by interfering with the mesenchymal transformation of the somite to sclerotome. However, it is important to bear in mind the complexities of *hox* gene regulation. As discussed earlier, once established, *hox* gene expression is maintained in part by a cross-regulatory mechanisms involving paralogous *hox* members. Thus, RA treatment during the late window can conceivably alter vertebral patterning *via* more subtle effects on *hox* genes, possibly involving *hox* gene cross-regulation. In this scenario, retinoids can alter the *hox* function within the forming vertebrae by destabilizing *hox* gene expression mechanisms. This remains, however, a highly speculative model given that altered *hox* expression was never observed in the prevertebrae following RA treatments during the late window.

Recently, a role for endogenous retinoid signaling in vertebral patterning is supported by mice harboring null mutations in *cyp26A1*, a RA-catabolizing enzyme, (Abu-Abed *et al.*, 2001; Sakai *et al.*, 2001). *Cyp26A1*$^{-/-}$ fetuses exhibit multiple posterior homeotic transformations throughout the entire cervical region, consistent with the effects of excess RA during early gestation periods (Fig. 1-8 and Table 1-4). For instance, *cyp26A1* null fetuses display the transformation of the seventh cervical vertebrae to the identity of the first thoracic segment (Fig. 1-8). Furthermore, the morphologies of the first and second cervical vertebrae resemble those of more caudal cervical segments, suggesting posterior homeotic transformations. Thus, the deletion of *cyp26A1* mimics the effects of exogenous retinoids on the vertebral skeleton, presumably due to the reduced catabolism of RA during early embryogenesis.

Additional support for a requirement of RA signaling in axial patterning comes from the vertebral defects displayed by various retinoid receptor null mice. The loss of RARγ leads to several anterior transformations of the cervical region, consistent with its high expression in the presomitic mesoderm and, at later stages, in the sclerotome (Fig. 1-8; Lohnes *et al.*, 1993; Ruberte *et al.*, 1990). Interestingly, vertebral defects resemble those occurring in the *hoxd4*-null mouse, a known RA-target gene (Horan *et al.*, 1995a). Indeed, *hoxd4/RARγ* double mutants display a much more severe phenotype than either mutants alone (Folberg *et al.*, 1999a). Although not as severe as group 4 compound mutants (Horan *et al.*, 1995b), the penetrance and expressivity of the anterior transformations of the second cervical vertebra to the identity of the first increases in the *hoxd4/RARγ* double mutants, consistent with RARs regulating the early expression of all group 4 genes. The mutation of RARα, on the other hand, leads to a very low frequency of vertebral homeosis (Lohnes *et al.*, 1994; Lufkin *et al.*, 1993), while RARβ nulls display no overt axial defects (Luo *et al.*, 1995). In contrast, any combination of RAR double mutants leads to significant increases in both anterior and posterior homeotic transformations and malformations of the cervical vertebrae relative to those observed in RARγ$^{-/-}$ mice (Fig. 1-8 and Table 1-4). These abnormalities reach their greatest expression in RARαγ double nulls, which often display a complete dyssymphysis of the neural arches (dorsal aspect of the vertebrae) in the cervical region. Due to these severe losses of vertebral structure, the identities of the cervical vertebrae are difficult to

Figure 1-8. Summary of the homeotic transformations elicited by excess RA, *cyp26A1* and RAR mutations in the mouse.

Normal cervical and thoracic vertebral pattern is indicated on the left. Red circle identifies the anterior arch which is normally present on C1. Small rounded yellow rectangles represent the *tuberculi anteriori* normally present on C6. Black lines projecting from the thoracic vertebrae represent ribs. Light grey blocks identify transformed vertebrae. Upward and downward arrows indicate posterior and anterior homeotic transformations, respectively. For late RA treatments, the normal C5 and C6 vertebrae are indicated next to the correspondingly transformed vertebrae elicited by RA at E10.5. Red upward arrow indicates posteriorization occurring with RA treatment at E11.5. BO, basioccipital bone, C, cervical vertebrae (numbered 1 to 7), T, thoracic vertebrae (numbered 1 to13, with 14 occasionally seen in RAR mutants). [Figure 1-8 is on the following page].

Fig. 1-8

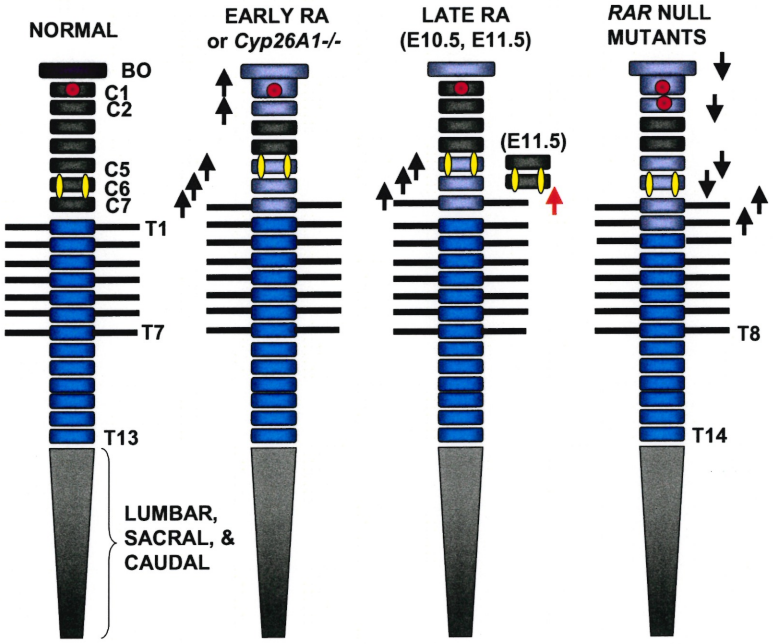

Table 1-4. Summary of the homeotic transformations affecting the cervical region of RA-treated embryos, *cyp26A1-/-*, and various RAR null mutants. Occurrence of defects is given as percentages. [Data obtained from Kessel and Gruss ,1991, and Kessel ,1992, for RA excess; Abu-Abed *et al.*, 2001, and Sakai *et al.*, 2001, for *Cyp26A1-/-*; Lohnes *et al.*, 1993, 1994, for *RAR* null mutants].

				RAR GENOTYPE					
	RA E7.3	***CYP26A1***	**RA E10.5/E11.5**	***RARγ***	***α1γ***	***α1γα2+/-***	***αγ***	***β2γ***	***αβ2***
Anteriorization:									
BO-C1 fusions				28	19	18	NA	22	0
C2→C1				17	31	64	NA	11	20
C6→C5				14	25	73	NA	0	80
C7→C6				14	25	73	NA	0	80
Posteriorizations:									
BO anomalies*	74	40	48/0						
C1→C2	57	40							
C2→C3	57	40							
C5→C6	50	80	44/0						
C6→C7	82	80	44/0						
C6→T1							33		
C7→T1 or T2	82	100	63/33		38	27	67		

* Basioccipital anomalies included fusions with exoccipital bones, fusions to neural aches of C1, fusion and presence of proatlas. NA, not applicable (due to the severity of the phenotype).

ascertain, but partial transformations of the second cervical vertebrae to the identity of the first are observed in less affected RARαγ mutants. Interestingly, while single RARβ null mutants lack vertebral defects, RARβ2γ and RARαβ2 show anterior homeotic transformations of the cervical vertebrae (Fig. 1-8). Furthermore, the removal of only one RXRα allele from the RARα or RARγ null background greatly increases the frequency of vertebral abnormalities seen in either RAR single mutants (Kastner *et al.*, 1997). This synergy suggests that effect of retinoid signaling in vertebral patterning is transduced by heterodimers between the RXR and RAR genes. Moreover, retinoid receptors seem to function largely redundantly in the patterning of the axial skeleton.

To conclude this section, I have described some of the key observations made within the last few years regarding the role of retinoid signaling in the caudalization of the vertebrate axis. This ability is shared across the vertebrate phylum, from amphibians to avians to mammals, and reflects the tight regulatory coupling of a linked group of genes, the *hox* genes. Retinoids, it seems, have been co-opted during evolution to activate the distal members of the *Hox* complexes and thus help establish their remarkable co-linearity with animal design. These simple molecules have incredible patterning abilities in both neural and mesodermal metameres, leading to an appreciation of the plasticity afforded by retinoid signaling in vertebrate morphogenesis.

1.7. Retinoid Signaling And Left-Right Axial Patterning

1.7.1. Heart Induction And Formation Of The Linear Heart Tube

The heart is the first major organ to develop and ultimately derives from anterior lateral plate mesoderm. Fate mapping of the mouse epiblast has restricted cardiac precursors to the cranial mesodermal domain located in the rostro-lateral half of the primitive streak region (Fig. 1-6A; Tam *et al.*, 1997). As the streak extends rostrally during gastrulation, the heart and cranial mesoderm precursors within the epiblast ingress through it and enter the nascent mesodermal stream, where they migrate anteriorly and laterally. These cells are among the first to gastrulate, resulting in cardiac precursors being found in the leading edge of the migrating mesodermal sheet immediately underneath the presumptive

cephalic neural plate. Moreover, the progenitors of the anterior (foregut) endoderm co-localize with heart mesodermal precursors in the epiblast and ingress through the streak at approximately the same time (Tam *et al.*, 1997). This establishes an early relationship between these two tissues, which is critical for the subsequent induction of the cardiogenic, or heart, field.

The heart field is defined as that region of the anterior embryo that is competent to form heart tissue in response to inducing signals, and is typically larger than the actual area that contains the cardiac progenitor cells (Redkar *et al.*, 2001; Tam and Schoenwolf, 1999). Early embryological studies determined that there are two tissues that are essential for defining the cardiac forming region in vertebrate embryos: the anterior endoderm and cephalic neural plate (reviewed in Schultheiss and Lassar, 1999). Grafting anterior or lateral portions of anterior endoderm in non-cardiac posterior mesodermal regions in the chick induces the expression of cardiogenic markers (Schultheiss *et al.*, 1995). Subsequent work has revealed that BMPs can mimic the heart inducing activity of embryonic anterior endoderm in the chick (Schultheiss *et al.,* 1997). Furthermore, the mutation of *BMP2* in the mouse results in severe cardiac defects, with a quarter of the mutants lacking heart tissue altogether (Zhang and Bradley, 1996).

Recently, a role of the antagonism of Wnt activity during cardiac mesoderm ingression has been shown to be required for heart induction. In particular, Wnt signaling from cranial mesoderm and neurectoderm restricts the formation of the heart field, which can be counteracted by over-expressing the Wnt antagonists Crescent and Dkk-1 (Marvin *et al.*, 2001; Schneider and Mercola, 2001; Tzahor and Lassar, 2001). Importantly, the ectopic expression of either Crescent or Dkk-1 in non-cardiogeneic mesoderm is sufficient to promote heart formation *in vivo* (Marvin *et al.*, 2001; Schneider and Mercola, 2001). Marvin and colleagues (2001) also show that in the chick, *crescent* is expressed in anterior endoderm during gastrulation, which agrees well with a putative role as an endogenous inducer of the heart field. Thus, a revised model of heart formation states that the induction of the heart is mediated by two separate signaling events. The first step involves the inhibition of Wnt signaling from cephalic neural tissue by the secretion of antagonists, such as Crescent and Dkk-1, from anterior endoderm to generate

the heart field. BMP signaling then acts on this broad field to promote the differentiation of heart tissue in a subset of cells.

Once heart induction has occurred, cardiac precursor cells form an extended crescent-shaped tissue ventral to the intestinal portal (open foregut); a structure referred to as the cardiac crescent (see Appendix I for mouse embryo staging). These lateral mesodermal wings form paired endothelial tubes converge at the midline and fuse to form a single medial heart vessel. This occurs at approximately 8 days of gestation in the mouse as the anterior neural tube begins to close (Sadler, 2000). As a consequence of the cephalic growth and closure of the anterior neuropore, the paired cardiac primordia, which are located on the ventral surface of the open foregut, are pulled cranially. At the same time, the embryo begins to fold laterally, dragging the cardiac primordia along with it, resulting in the cranio-caudal fusion of the heart tube.

1.7.2. Establishment Of The Left-Right Axis

Although superficially symmetrical, all vertebrates process intrinsic asymmetries in the development of many thoracic and abdominal organs along their left-right axis. The normal left-right arrangement of organs is called *situs solitis*, and with respect to cardiac development, gives a right to leftward displaced heart referred to as levocardia (Fig. 1-9A; Casey and Hackett, 2000; Majumder and Overbeek, 1999). Perturbations in the development of the left-right axis can lead to mirror-image reversals in the placement of the internal organs in the body cavity, a situation referred to as *situs inversus*. When this occurs, it may give rise dextrocardia, which is the development of the heart on the right instead of the left side. In dextrocardial hearts, the systemic ventricle, which distributes oxygenated blood from the lungs to the body, is the right ventricular chamber instead of the left (Fig. 1-9A). Likewise, in reversed *situs*, the pulmonary ventricle, which concerns itself with delivering oxygen-deprived blood to the lungs, is the left chamber as opposed to the right.

Situs defects are relatively common, in one estimate occurring at a frequency of 1/5000 births (Casey and Hackett, 2000). Most patients with complete *situs inversus* lead normal lives, however, reversals of a subset of the internal organs, called *heterotaxia*, is often lethal, principally due to complications arising from inadequate alignment of

outflow (conotrucus) and inflow (sinus venosus) regions of the heart. Despite the obvious clinical manifestations of *situs* defects, it is only within the last few years that progress has been made in identifying key regulators of left-right axis formation. The rapid evolution of this field has led to an impressive understanding of the mechanisms generating left-right asymmetry (Fig. 1-9B), including the regulatory modules directing laterality-specific gene expression (reviewed in Capdevilla *et al.*, 2000).

Among the most obvious signs of lateral asymmetry is the leftward positioning of the heart (Fig. 1-9A). Once the linear heart tube has formed, various signals direct it to undergo a stereotypical counter-clockwise torsion to give rise to a leftward displaced heart (Sadler, 2000). These same signals also impart lateral asymmetry to certain internal organs, including the lungs, stomach, spleen, and intestines, demonstrating a common mechanism underlying left-right (L-R) patterning. The establishment of the L-R axis involves a largely conserved cascade of signaling events, with important species differences, and can be subdivided into four overlapping stages. The first step involves the initial breaking of symmetry, which converts the initial A-P patterning to L-R asymmetry and is mediated by the node. Subsequently, L-R positional information is relayed from the node to the lateral plate mesoderm (LPM), and left-specific expression of laterality markers is established. The third phase involves the stabilization of the broad domains of side-specific expression via auto-regulatory and cross-regulatory interactions between laterality determinants. The last step of L-R axis formation is the interpretation of the side-specific information by the organ primordia and the establishment of asymmetric morphogenesis.

In mice, strong evidence exists for the role of a specialized group of monocilia present on the ventral surface of the node in the initial breaking of symmetry (Marszalek *et al.*, 1999; Nonaka *et al.*, 1998; Okada *et al.*, 1999; Takeda *et al.*, 1999). In an elegant series of experiments utilizing videomicroscopy, researchers from Hamada's group have demonstrated that nodal cilia rotate counter-clockwise, generating a net leftward flow of extracellular fluid across the ventral surface of the node (Nonaka *et al.*, 1998). The authors suggest that this motion, called the nodal flow, concentrates a secreted molecule initially expressed throughout the node to its left side. Once this laterality determinant reaches a threshold level, it triggers the expression of left-sided genes in tissues adjacent

to the left side of the node, namely the left LPM, and subsequently establishes left-right asymmetry. Consistent with this model, mice mutant for the kinesin motor proteins Kif3A or Kif3B, lack nodal cilia, do not produce the nodal flow, and display a randomization of organ *situs* (Marszalek *et al.*, 1999; Nonaka *et al.*, 1998; Takeda *et al.*, 1999). Likewise, the classical mouse mutant *inversus viscerum* (*iv*) harbors a mutation in a novel member of the dynein motor family, called left-right dynein, that renders the nodal cilia immobile (Okada *et al.*, 1999; Supp *et al.*, 1997). This mutant displays numerous *situs* defects, in agreement with a requirement of nodal cilia in left-right asymmetry. Another mouse mutant, called *inversion of embryonic turning* (*inv*), also displays randomized asymmetric development (Yokoyama *et al.*, 1993), and is associated with reduced rotation of the nodal cilia (Okada *et al.*, 1999). The *inv* locus is predicted to encode a large intracellular protein containing ankyrin repeats, suggesting a structural or scaffolding function (Mochizuki *et al.*, 1998). Unfortunately, this offers little insight as to the function of *inv* in L-R patterning, but it may mediate or stabilize the assembly of the nodal cilia. Thus, these studies suggest that, in mammals, the leftward nodal flow is the initial signal that breaks symmetry in the L-R axis by concentrating laterality determinants on the left side.

A likely candidate for a left-determining signaling molecule secreted by the node is a TGFβ family member, called appropriately enough, *nodal* (Conlon *et al.*, 1994). Although, initially expressed throughout the periphery of the node, *nodal* becomes up-regulated on the left side of the node by early somite stages before becoming expressed in a broad domain throughout the left LPM (Collignon *et al.*, 1996; Lowe *et al.*, 1996). This expression pattern is therefore consistent with the nodal flow model, whereby an initial asymmetry on the left side of the node region, becomes propagated throughout the left side of the embryo. In support of this, the left-specific expression of *nodal* is reversed or bilateralized in mouse models of *situs inversus*, *iv* and *inv*, which display disrupted nodal flow (Collingnon *et al.*,1996; Lowe *et al.*, 1996; Okada *et al.*, 1999).

The loss of Nodal function is lethal early in development due to a failure to gastrulate (Conlon *et al.*, 1994), however a recently published hypomorphic *nodal* mutation confirmed its role in left-right patterning (Lowe *et al.*, 2001). Particularly, *nodal* hypomorphs display right pulmonary isomerism as well as reversal of cardiac looping,

concomitant with the loss of expression of two important downstream targets of the laterality cascade, *lefty2* and *pitx2*, in the left lateral plate mesoderm (see below). Other *situs* defects in *nodal* hypomorphs included right-sided stomach and isomerization of the atria (Lowe *et al.*, 2001). Consistent with a role in L-R determination, the misexpression of *nodal* on the right LPM adjacent to the avian organizer (Levin *et al.*, 1995; Sampath *et al.*, 1997, 1998), and its ectopic expression in amphibians (Lohr *et al.*, 1997) and zebrafish (Rebagliati *et al.*, 1998) is sufficient to randomize the *situs* of several organs.

Nodal is an atypical member of the TGFβ superfamily of secreted molecules, and like all TGFβ ligands, signals through TGFβ receptors (reviewed in Goumans and Mummery, 2000). It is therefore not surprising that the mutation of *activin type IIB receptor (ActRIIB)*, a putative Nodal receptor, is associated with reversals in cardiac looping and right pulmonary isomerism, as well as other *situs* abnormalities (Oh and Li, 1997). Also supporting a role for TGFβ signaling in L-R patterning are the loss of function mutations in *smad5* (Chang *et al.*, 2000) and *smad2* (Heyer *et al.*, 1999), which are intracellular mediators of the TGFβ pathway (Goumans and Mummery, 2000)

The full effect of Nodal signaling seems to require essential co-factors from the EGF-CFC family of extracellular proteins (Ding *et al.*, 1998; Gaio *et al.*, 1999; Gritsman *et al.*, 1999; Schlange *et al.*, 2001; Yan *et al.*, 1999). Loss of function of *crypto* (or *cfc2*) phenocopies the A-P patterning defects in *nodal* mutants in the mouse (Ding *et al.*, 1998) and zebrafish (Gritsman *et al.*, 1999), while the loss of *cryptic* (or *cfc1*), another mammalian EGF-CFC gene, leads to randomized cardiac looping concomitant with the lack of *nodal, lefty2,* and *pitx2* expression in the left LPM (Gaio *et al.*, 1999; Yan *et al.*, 1999). Similar results are observed with an antisense knockdown of the chick *cfc1* gene (Schlange *et al.*, 2001).

Interesting differences exist between avians and mammals with respect to the initial breaking of symmetry (Fig. 1-9B). Monocilia have not been reported in the chick, but asymmetries in the expression patterns of certain signaling molecules occur significantly earlier in the chick perinodal region relative to equivalent stages in the mouse (Capdevila *et al.*, 2000). The chick embryo also expresses right-sided determinants along with the Nodal-driven left-specific pathway. Among these is another TGFβ signaling molecule, Activin βB, and its receptor, ActRIIA (Levin *et al.*, 1995,

1997). Activin signaling inhibits the expression of the morphogen Shh on the right side of Hensen's node. This leads to the restriction of Shh on the left side adjacent to the chick organizer, which then activates Nodal in a small domain lateral to the organizer (Levin *et al.* 1995, Pagan-Westphal and Tabin, 1998). Furthermore, Activin induces the expression of *fgf8* on the right side, which in turn prevents the inappropriate activation of *nodal* on the right (Boetteger *et al.*, 1999). Thus, in the chick, Activin signaling initiates left-specific *nodal* expression by inhibiting *shh* and activating *fgf8* on the right (Figure 1-9B). By comparison, the expression of Activin receptors, Fgf8 and Shh are not asymmetric in mouse, although their mutations do affect left-right patterning (Izraeli *et al.*, 1999; Meyers and Martin, 1999; Oh and Li, 1997; Tsukui *et al.*, 1999). The generation of a hypomorphic *fgf8* mutation results in reversals in heart looping and right pulmonary isomerism, concomitant with the loss of expression of *nodal* and other laterality determinants (Meyers and Martin, 1999). Thus, while *fgf8* is a right determinant in the chick, its role in the mouse is to activate the left-specific laterality cascade.

Recent developments in the mouse suggest a role for Shh signaling in the activation of the laterality cascade in the left LPM. The mutation of *smoothened (smo)*, which encodes a putative Shh co-receptor and effector, results in axial and L-R patterning defects along with aberrant expression of *nodal, lefty1/lefty2*, and *pitx2* (Zhang *et al.*, 2001). Importantly, as *nodal* expression remains intact in the node of $smo^{-/-}$ embryos, but is entirely abolished in the LPM, Shh signaling may also be involved in the transfer of *nodal* expression from the node to left LPM (Zhang *et al.*, 2001). However, *shh* mutants also lack axial structures such as the notochord and floorplate, which normally function as a midline barrier that prevents left-specific information from traversing to the right (see below). Thus, the bilateral expression of *nodal* and other left determinants in $shh^{-/-}$ embryos may be due to loss of midline tissues, resulting in a porous barrier to the rightward flow of laterality determinants. Shh has therefore evolved two ways in regulating left-specific information: in avians, asymmetric *shh* expression in the left perinodal region activates *nodal* and the left laterality cascade, whereas in the mouse, *shh* functions not only to restrict established laterality information to the left side, but to activate *nodal* in the left LPM as well (Fig. 1-9B). These interesting differences may

reflect the inherently different morphologies of gastrulation in birds and mammals (Beddington and Robertson, 1998).

The transfer of laterality information from the organizer to lateral plate mesoderm seems to involve paraxial mesoderm (Pagan-Westphal and Tabin, 1998). In chicks, Shh is able to induce *nodal* expression in a small region immediately adjacent to Hensen's node. An additional factor is then require to transfer this small *nodal* domain to the much broader left-sided expression throughout the left LPM. In a search for left-specific factors that are able to promote Nodal signaling, several groups identified a Cerberus-related molecule called Caronte (Car; Rodriguez-Esteban *et al.*, 1999; Yokouchi *et al.*, 1999; Zhu *et al.*, 1999). This BMP antagonist is indeed expressed asymmetrically in a small domain in the left paraxial mesoderm, adjacent to *shh*-expressing cells near the node. Car promotes the left-sided pathway presumably by antagonizing the activity of BMPs in the chick lateral mesendoderm, which inhibit Nodal signaling possibly by the competition for intracellular mediators, such as Smad5. Thus, Car releases Nodal inhibition by BMPs in the left LPM, allowing its expansion throughout this domain.

Once *nodal* expression becomes established in the left LPM, its activity is restricted there by the action of antagonist molecules, encoded by the *lefty* genes. Lefty2 defines a novel class of TGFβ signaling factors and is specifically expressed in the left LPM in response to Nodal signaling (Levin *et al.*, 1997; Meno *et al.*, 1996; Sampath *et al.*, 1997). Like *nodal*, *lefty2* expression is found in the right LPM in *iv* and *inv* mutants (Meno *et al.*, 1996), and its misexpression in chicks or frogs results in *situs* defects (Levin *et al.*, 1997; Sampath *et al.*, 1997). Moreover, *lefty2* expression is absent in *nodal* hypomorphs, suggesting it acts downstream of Nodal signaling (Lowe *et al.*, 2001). However, the loss of function of *lefty2* in both mice and zebrafish results in excess mesoderm formation due to a grossly expanded primitive streak (Meno *et al.*, 1999); a phenotype that the authors argue is opposite to that of *nodal* mutants. In agreement with this, *nodal* expression is expanded in *lefty2*$^{-/-}$ mouse embryos.

Insights into the mechanistic basis of this cross-regulatory relationship comes from the analysis of the *nodal* and *lefty2* promoter regions (Adachi *et al.*, 1999; Norris and Robertson, 1999; Saijoh *et al.*, 1999). Interestingly, both the *nodal* and *lefty2* promoters contain a conserved early asymmetric enhancer. Crossing transgenic reporter

mice harboring these asymmetric enhancers into the *iv* and *inv* mutant backgrounds leads to bilateralized or right-sided expression, demonstrating they indeed function as asymmetric regulatory modules (Adachi *et al.*, 1999; Norris and Robertson, 1999; Saijoh *et al.*, 1999). The *nodal/lefty2* left-specific enhancer contains binding sites for FAST transcription factors, which are the downstream effectors of the TGFβ signaling pathway (Goumans and Mummery, 2000). This suggests that the early asymmetric expression of *nodal* and *lefty2* is controlled by TGFβ signaling. Moreover, the targeted deletion of the *nodal* asymmetric enhancer abolishes reporter expression in the left LPM but not the node, suggesting it functions as an autoregulatory element for Nodal signaling in the left LPM (Norris and Robertson, 1999). Also, the overexpression of *lefty2* in zebrafish inhibits *nodal* expression (Meno *et al.*, 1999). These results hint at the existence of an inhibitory feedback loop between Lefty2 and Nodal, and a positive autoregulatory loop driving *nodal* expression. Thus, to summarize this data, Nodal is able to activate *lefty2,* which in turn antagonizes Nodal signaling through the competition for common receptors at the cell surface (Fig. 1-9B). The subsequent decrease in Nodal receptor occupation leads to a loss of *nodal* autoregulation via its asymmetric enhancer.

The most downstream component of the laterality cascade is the Nodal target gene *pitx2*, which encodes a novel bicoid-type homeobox transcription factor. This gene was initially cloned as *RIEG*, as its haploinsufficiency gives rise to Rieger's syndrome in humans (Semina *et al.*, 1996). Subsequently, this gene was cloned in other vertebrates and found to be expressed in the left LPM immediately prior to cardiac looping (Campione *et al.*, 1999; Logan *et al.*, 1998; Piedra *et al.*,1998; Ryan *et al.*, 1998). Later on, *pitx2* is highly expressed asymmetrically in several developing organs and is thus suspected to play a major role in the asymmetric development of organs (Hjalt *et al.*, 2000; Semina *et al.*, 1996). The misexpression of *pitx2* on the right side in chicks and frogs is sufficient to cause reversals in heart and gut looping (Campione *et al.*, 1999; Logan *et al.*, 1998; Piedra *et al.*,1998; Ryan *et al.*, 1998). *Pitx2* is efficiently induced by Nodal misexpression on the right side, suggesting it acts as a downstream component of the Nodal-driven laterality cascade (Fig. 1-9B). Strong support for this comes from the *pitx2* promoter, which like that of *lefty2* and *nodal,* contains critical Nodal response elements (FAST binding sites) that mediate its left-specific expression in the LPM

(Shiratori *et al.*, 2001). Furthermore, *pitx2* expression is randomized in *iv* mice, consistent with it being a distal component of the L-R pathway (Piedra *et al.*, 1998; Campione *et al.*, 2001).

The targeted disruption of *pitx2* leads to the asymmetric development of several organs such as the atria, lungs, stomach and gut (Kitamura *et al.*, 1999; Lin *et al.*, 1999; Lu *et al.*, 1999). Interestingly, the levels of Pitx2 seem to impart positional information to different organs. The progressive ablation of the three *pitx2* isoforms (*pitx2a, pitx2b,* and *pitx2c*) increases the number of organs affected (Gage *et al.*, 1999). Also, a recent study by Liu and colleagues (2001) describes a gene-dosage requirement of the major *pitx2* isoform, *pitx2c*, in the asymmetric development of different organs. For example, while the establishment of the left atrial chamber requires low levels of functional Pitx2c, the asymmetric development of the lungs and gut is easily perturbed by even the slightest decreases in *pitx2c* dosage

Additional targets of Nodal signaling in the left LPM include the zinc finger transcription factor Snail-related (SnR) and the homeobox-containing factor, Nkx3-2 (Schneider *et al.*, 1999). SnR is initially expressed bilaterally in precardiac mesoderm, but becomes progressively restricted to the right side of both mouse and chick embryos (Isaac *et al.*, 1997; Sefton *et al.*, 1998). In the chick, SnR represses *pitx2* expression on the right side, thereby keeping the left-side transcriptionally distinct from the right (Fig. 1-9B; Patel *et al.*, 1999). Furthermore, Nodal signaling appears to suppress *SnR* expression on the left, which in turn allows for robust left-specific *pitx2* expression. *Pitx2* expression thus appears to be regulated by Nodal in two ways: direct activation through the early asymmetric enhancer, and indirectly via the inhibition of the pitx2 repressor, SnR.

Nkx3-2 is expressed on the left LPM in response to nodal signaling and is thought to mediate the asymmetric development of organs in response to the L-R pathway (Schneider *et al.*, 1999). Interestingly, the analysis of the *pitx2* promoter revealed the presence of NK2 binding sites, which are required for the maintenance of *pitx2* expression. Thus, *nkx3-2* may regulate organ asymmetries by maintaining robust *pitx2* in the left LPM and its derivatives during organogenesis (Fig. 1-9B). Taken together, these results suggest that the asymmetric development of organs involves the transfer of

laterality information from the left LPM to *pitx2*. This is mediated both directly and indirectly by Nodal.

The maintenance of left-specific information involves midline tissues such as the notochord and floorplate, which act as a molecular barrier preventing the rightward flow of left determinants (Fig. 1-9B; Capdevila *et al.*, 2000). As alluded to earlier, a prediction from this midline barrier model asserts that any perturbation of the midline function will result in a bilateralization of left-specific determinants due to their unrestricted diffusion towards the right. Consistent with this, the loss of members of the Shh pathway, such as *shh* (Meyers and Martin, 1999; Tsukui *et al.*, 1999), *HNF-3β* (Collignon *et al.*, 1996), and *smo* (Zhang *et al.*, 2001), disrupt midline development and display a randomization of *situs* concomitant with bilateralized *nodal, lefty2*, and *pitx2* expression. Interestingly, a second *lefty* gene, *lefty1*, is expressed in midline tissues, particularly in the left half of the floorplate (Meno *et al.*, 1997). *Lefty1* and *lefty2* constitute a divergent sub-family of TGFβ signaling molecules and are closely linked on mouse chromosome 1 (Meno *et al.*, 1997). However, the regulatory mechanisms governing *lefty1* and *lefty2* expression are entirely different. While an asymmetric enhancer directs *lefty2* expression on the left side, the asymmetric expression of *lefty1* is regulated by a combination of bilateral enhancers and a right-sided specific silencer (Saijoh *et al.*, 1999). Targeted deletion of *lefty1* confirms its role in L-R development as mutants display *situs* defects in association with the bilateral expression of *nodal, lefty2* and *pitx2* (Meno *et al.*, 1998). Moreover, as *nodal, lefty2* and *pitx2* all contain FAST-binding sites in their asymmetric enhancers, *lefty1* can presumably inhibit their expression directly. Thus, *lefty1* seems to function as the molecular mediator of the midline barrier. Collectively, these results demonstrate that signaling from the midline keeps left-specific information from diffusing to the right, and thus prevents the laterality cascade from degrading with time. A summary of the key players in the L-R pathway is depicted in Figure 1-9B.

Figure 1-9. Establishment of asymmetries in the left-right axis.

(**A**) Drawing of the ventral view of the heart during cardiac looping morphogenesis. Normal (*situs solitus)* heart looping is indicated on top and mirror-image reversal (*situs inversus*) is depicted on the bottom. Blood flows from the inflow tracts at the bottom (sinus venosus) to the outflow tracts (bulbis cordis, conotrucus, and aortic arches) at the top. Normal looping of the heart involves a rightward rotation of the linear heat tube leading to the mature four chambered hear with septation (levocardia). In *situs inversus*, the direction of cardiac looping is reversed leading to the formation of the systemic ventricle (red) on the right and the pulmonary ventricle (yellow) on the left (dextrocardia). (**B**) Outline of L-R signaling pathway in chicks (right) and mice (left). Differences between chicks and mice include the presence of nodal cilia (depicted by short black curved lines), and the existence of the midline barrier in the mouse. The initial breaking of symmetry in the chick involves asymmetric expression of Shh in response to activin signaling, whereas in the mouse the nodal cilia act to concentrate Nodal on the left periphery of the organizer. Shh signaling is subsequently transmitted to Nodal via the BMP antagonist Caronte (Car), which is expressed in the paraxial mesoderm (presomitic mesoderm and somites). In addition, Shh may also activate Nodal in a small domain lateral to the mouse organizer. Once Nodal expression is established, it activates Pitx2, which drives organ asymmetry. Auto-regulatory and cross-regulatory interactions between Nodal and Lefty members limit Nodal signaling to the left LPM. In the mouse, Lefty1 expression in the left prospective floorplate defines a midline barrier that inhibits Nodal signaling in that tissue. This maintains the expression of the laterality determinants on the left side, leading to the asymmetric development of the various organs. Please refer to text for detailed explanations. Abbreviations: LPM, lateral plate mesoderm, pfp, prospective floorplate, ps, primitive streak, psm, presomitic mesoderm, so, somite. [Figure A modified from Majumder and Overbeek, 1999. Figure B modified from Meyers and Martin, 1999. (Figure 1-9 is on the following page)].

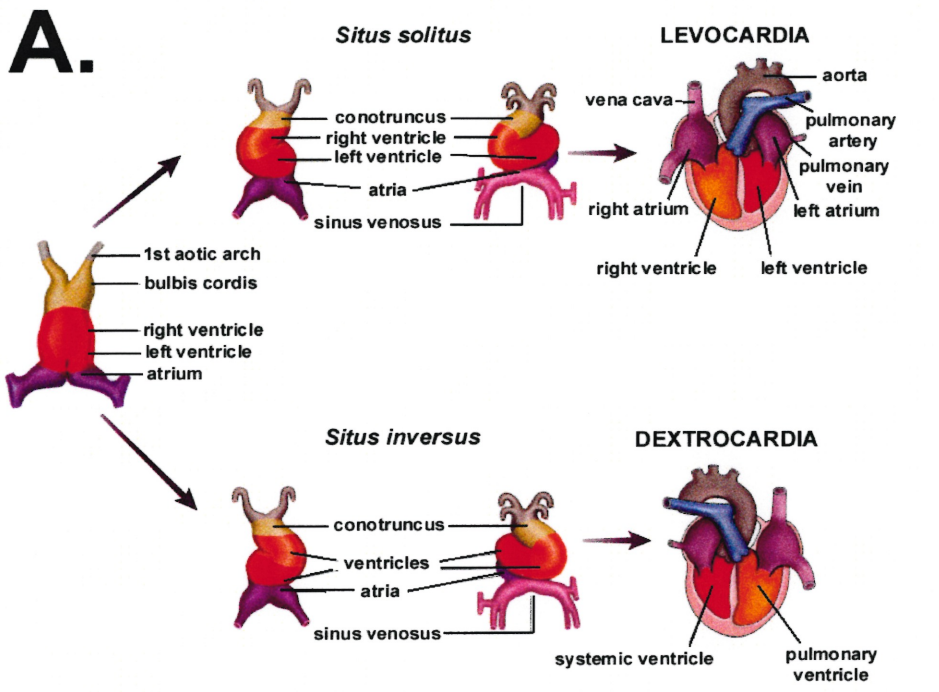
A.
Situs solitus
LEVOCARDIA
conotruncus
right ventricle
left ventricle
atria
sinus venosus
vena cava
aorta
pulmonary artery
pulmonary vein
left atrium
right atrium
right ventricle
left ventricle
1st aotic arch
bulbis cordis
right ventricle
left ventricle
atrium
Situs inversus
DEXTROCARDIA
conotruncus
ventricles
atria
sinus venosus
systemic ventricle
pulmonary ventricle

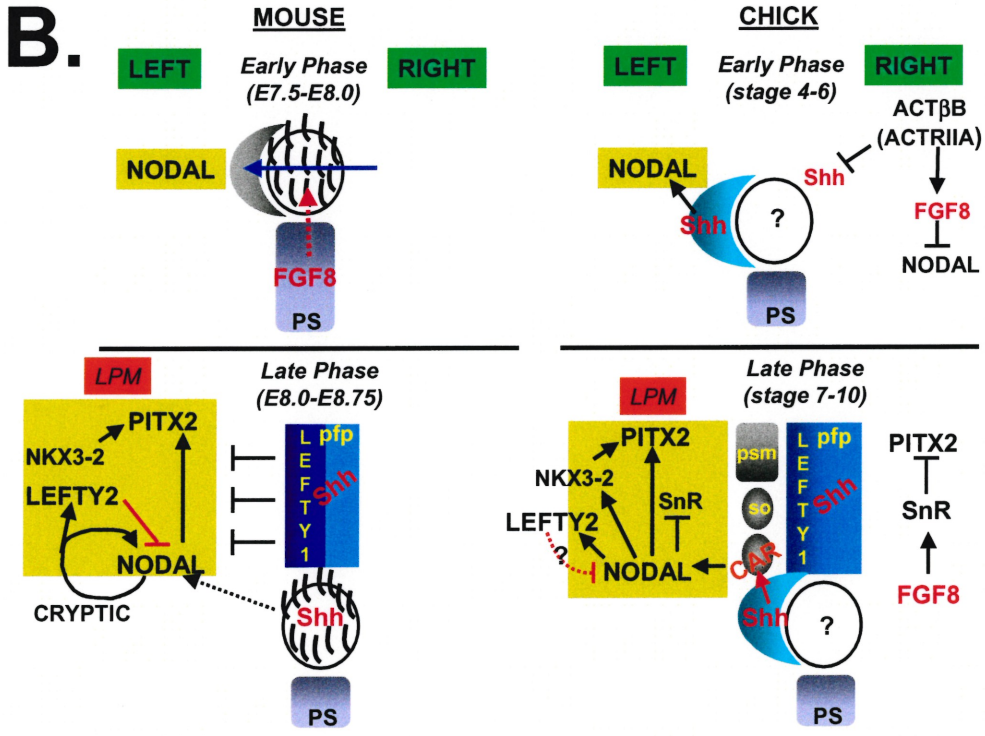
B.
MOUSE
LEFT
Early Phase (E7.5-E8.0)
RIGHT
NODAL
FGF8
PS
CHICK
LEFT
Early Phase (stage 4-6)
RIGHT
ACTβB (ACTRIIA)
NODAL
Shh
Shh
?
FGF8
NODAL
PS
LPM
Late Phase (E8.0-E8.75)
PITX2
NKX3-2
LEFTY2
NODAL
CRYPTIC
L E F T Y 1
pfp
Shh
Shh
PS
LPM
Late Phase (stage 7-10)
PITX2
NKX3-2
LEFTY2
SnR
NODAL
psm
so
L E F T Y 1
pfp
Shh
CAS
Shh
?
PS
PITX2
SnR
FGF8

1.7.3. Retinoid Signaling And Left-Right Axis Formation

Early nutritional studies have established a role for retinoid signaling in cardiac development (Smith and Dickman, 1997). The deprivation of retinoids during avian development results in abnormal or reversed cardiac looping, thinned myocardial wall, and the loss of posterior heart structures (Heine *et al.*, 1985; Dersch and Zile, 1993; Kotetskii, 1998, 1999). Moreover, excess retinoids in quails and mammals, including primates, gives rise to similar heart defects including cardiac malpositioning, and *situs inversus* or heterotaxia of organs in the thoracic region (Dickman and Smith, 1996; Hendrickx *et al.*, 1980; Miura *et al.*, 1990; Shenefelt, 1972; Thompson *et al.*, 1969; Van Maldergem *et al.*, 1992; Yasui *et al.*, 1998).

Cardiac *situs* in mice is particularly sensitive to exogenous RA during gastrulation, with treated mice displaying atrial isomerism and abnormal heart looping (Yasui *et al.*, 1998). Interestingly, aberrant retinoid signaling in avians can perturb the asymmetric expression of various extracellular proteins surrounding the heart, including hLAMP-1 and Flectin (Smith *et al.*, 1997; Tsuda *et al.*, 1996). These were among the first studies linking *situs* defects resulting from abnormal retinoid signaling with reversals in the expression of L-R axial markers. Subsequently, several groups examined the effects of aberrant retinoid signaling on the expression of the newly discovered laterality determinants (Chazaud *et al.*, 1999; Tsukui *et al.*, 1999; Wasiak and Lohnes, 1999; Zile *et al.*, 2000). Excess RA administered during late gastrulation stages in the mouse embryos results in reversal of *situs* and is associated with bilateralization of *nodal, lefty2,* and *pitx2* expression (Chazaud *et al.*, 1999; Tsukui *et al.*, 1999; Wasiak and Lohnes, 1999). Importantly, excess retinoids do not affect *lefty1* expression in the prospective floorplate, suggesting that the midline barrier function within the floorplate is largely intact. Alternatively, VAD quails display a loss of *nodal* and *pitx2*, but do not affect earlier asymmetric signals such as *shh, caronte, activin receptor IIa,* and *fgf8*, consistent with a disruption of left-specific signaling in the LPM (Zile *et al.*, 2000). Similar effects can be evoked by RAR-antagonist treatment in mice (Chazaud *et al.*, 1999), suggesting that retinoids normally pattern the L-R at stages subsequent to the initial breaking of symmetry. Collectively, these results argue that retinoid signaling regulates L-R axis development principally through the maintenance of the left-specific laterality pathway

driven by *nodal.* These findings are also consistent with a role for retinoids in providing competence to the embryo to respond to left-specific cues.

The disruption of the retinoid receptors revealed a physiological requirement for RA signaling certain aspects of heart development, but failed to demonstrate a role for these receptors in looping morphogenesis (section 1.5.4). This may reflect the inherent redundancy in RAR signaling, which as we have seen can be quite extensive. In support of this, both RAR antagonists (Chauzaud *et al.,* 1999) and retinoid deprivation (Zile *et al.*, 2000) have indeed demonstrated a requirement for normal retinoid signaling in directing laterality development. It thus remains possible that the RARs do indeed mediate an effect on L-R patterning; an idea which invites our inquiries.

1.8. Hypothesis

This introduction described the breadth of retinoid signaling during vertebrate development, with particular emphasis on key regulatory events in axial patterning. During the course of my studies, I have attempted to address several outstanding questions with respect to the timing and role of the retinoid receptors during A-P and L-R development. Based on the observation that RARγ is essential for the transduction of the teratogenic effects of excess RA on the caudal embryo (Lohnes *et al.,* 1993), I reasoned that this receptor may also be required to elicit the effects of retinoid excess on vertebral patterning. Furthermore, as vertebral patterning displays a biphasic sensitivity to exogenous retinoids, this experiment allowed an assessment of the developmental period at which RARγ normally functions to pattern vertebrae. A second question addressed during my studies pertains to the problem of identifying the primary tissue affected by excess retinoids at E8.5 that leads to axial trunctions. Given that the RARγ null mice are resistant to these caudal truncations, I hypothesized that by examining various tissue-specific markers in RAR$\gamma^{-/-}$ versus wild type embryos following RA treatment, I would determine where the primary lesion occurs in response to the teratogen. Lastly, given that our understanding of RAR function remains incomplete due to the large degree of functional overlap between the different receptors, I reasoned that novel roles for these

receptors would be revealed by circumventing RAR redundancy. To this end, I have employed a gene replacement approach to bypass RAR redundancy and demonstrated new roles for these receptors in cardiac looping morphogenesis.

CHAPTER 2

ARTICLE

Contribution Of Retinoic Acid Receptor Gammma To Retinoid-Induced Craniofacial And Axial Defects

Angelo Iulianella and David Lohnes

Institut de Recherches Clinique de Montréal,110 Avenue des Pins, Montréal , Québec, Canada, H2W 1R7, and Programme de biologie moléculaire, Université de Montréal

Developmental Dynamics **Volume 209, Pages 92-104, 1997**

ABSTRACT

Exogenous retinoic acid (RA) administered during mouse embryogenesis can alter the pattern of the axial skeleton during two developmental periods: an early window (7 to 8.5 days post-coitum; dpc) and a late window (9.5 to 11.5 dpc). Treatment during the early window results in vertebral homeotic transformations (predominantly posteriorizations) concomitant with rostral shifts in Hox gene expression, while treatment at the later window results in similar transformations without detectable alterations in Hox gene expression patterns. Mice null for retinoic acid receptor gamma (RARγ) exhibit axial defects, including homeosis of several vertebrae, therefore establishing a role for this receptor in normal axial specification. RARγ null mutants are also completely resistant to RA-induced spina bifida, which occurs in wild type embryos treated at 8.5 - 9.0 dpc, suggesting that this receptor specifically transduces at least a subset of the teratogenic effects of retinoids.

To further investigate the role of RARγ on RA-induced defects during the early and late windows of retinoid-sensitive vertebral patterning, RARγ heterozygotes were intercrossed, pregnant females treated with vehicle or RA at 7.3, 10.5 or 11.5 dpc and full term fetuses assessed for skeletal defects. Relative to wild type littermates, RARγ null mutants treated at 7.3 dpc were markedly resistant to RA-induced embryo lethality, craniofacial malformations and neural tube defects. Furthermore, while RARγ null mutants were modestly resistant to certain vertebral malformations elicited by RA treatment at 7.3 dpc, they exhibited more pronounced resistance following treatment at 10.5 and 11.5 dpc. Moreover, several of the vertebral defects inherent to the RARγ null phenotype were abolished by RA treatment specifically at 10.5 dpc, suggesting that RARα and/or RARβ isoforms may substitute for certain RARγ functions, and that RARγ may elicit its normal effects on vertebral morphogenesis at this developmental stage.

INTRODUCTION

Vitamin A and its derivatives (retinoids) play central roles in vertebrate development and in the maintenance of various tissues in the adult (reviewed in Sporn et al. 1994). Rodents fed a vitamin A deficient (VAD) diet display weight loss, sterility, squamous metaplasia of various tissues including the respiratory tract, alimentary tract, genito-urinary tract, and eyes and related glands, and eventually die (Wolback and Howe, 1925). Moreover, pregnant dams deprived of vitamin A give rise to fetuses exhibiting various congenital defects involving the eye, genito-urinary and respiratory tracts, and heart and aortic arch derivatives, among others (Wilson et al., 1953 and references therein). With the exception of blindness, all of the defects generated by post-partum VAD can be prevented and/or reversed by treatment of animals with retinoic acid (RA; Thompson et al., 1964), thereby establishing that RA is a principal active metabolite of vitamin A.

The identification of retinoic acid receptors (RARs) allowed for a genetic analysis of the varied developmental and physiological roles of retinoid signaling (reviewed in Chambon, 1996; Sucov and Evans, 1995). Differential promoter usage and alternative splicing leads to generation of N-terminal variant isoforms for each of the three RARs (RARα1 and α2, RARβ1-β4, RARγ1 and γ2). RARs function as ligand-inducible transcription regulators by binding to specific sequences (RA response elements; RAREs) present in the promoter/enhancer region of target genes, but do so only as heterodimers with another class of receptors, the retinoid x receptors (RXRα, β, γ). RARs can be activated by both all-trans retinoic acid and the stereoisomer, 9-*cis* retinoic acid. RXRs, which can function as transcription regulators in certain contexts as homodimers, are activated only by 9-cis RA (Heyman et al., 1992; Mangelsdorf and Evans, 1995).

Targeted disruption of the various RARs has revealed specific as well as redundant functions for these receptors (reviewed in Kastner et al., 1995; Sucov and Evans, 1995). In addition to certain defects related to postpartum VAD, RARγ null mice display axial malformations, including vertebral homeotic transformations, not previously observed in dietary deprivation studies (Lohnes et al., 1993). RARγ disruption in combination with RARα or β2 ablation leads to increasing penetrance and expressivity of

the axial defects associated with the RARγ null phenotype. Furthermore, RARαβ2 and RARα1β double mutants, but not single mutants, also exhibit vertebral transformations and malformations, indicating a degree of functional redundancy among the RARs with respect to vertebral morphogenesis (Luo et al., 1996; Lohnes et al., 1994; Mendelsohn et al., 1994a).

Excess RA can alter vertebral identities at specific times during development. Treatment at 7.3 to 8.5 days post coitum (dpc) results in multiple homeotic transformations of the vertebral column which are accompanied by alterations in the anterior expression boundary of some Hox genes (Kessel and Gruss, 1991). The observation that the vertebral defects of certain Hox null mutants phenocopy certain of the axial transformations of RARγ null and RAR double mutant fetuses further supports the contention that RARs affect vertebral specification *via* regulation of Hox gene expression *in vivo* (Lohnes et al., 1993; Lohnes et al., 1994). However, RA administration at 9.0-11.5 dpc can also "respecify" vertebral patterns without detectable alterations in Hox gene expression (Kessel, 1992), suggesting that alternative mechanisms of retinoid-dependent vertebral morphogenesis exist.

RARγ null mutants are completely resistant to RA-induced spina bifida, indicating that this receptor plays a specific role in retinoid teratogenesis (Lohnes et al., 1993). The present study was undertaken to determine if this receptor is critically required for the transduction of other retinoid-induced skeletal defects. To this end, females from RARγ heterozygous intercrosses were treated with RA at either the early (7.3 dpc) or late (10.5 or 11.5 dpc) windows of RA-sensitive vertebral specification, and the resulting wild type, heterozygous, and null mutant fetuses assessed for skeletal defects. While some differences in axial patterning were observed between RARγ mutants and wild type fetuses treated with RA at 7.3 dpc, mutants were highly resistant to the neural tube defects and cranial-facial malformations elicited by treatment during this developmental window. In contrast to treatment during the early retinoid-sensitive window, RARγ ablation had a significant influence on axial patterning following RA exposure at 10.5 and 11.5 dpc. Furthermore, several of the vertebral defects associated with the RARγ null phenotype were abrogated by RA exposure specifically at 10.5 dpc,

suggesting that this receptor may normally function in vertebral morphogenesis during this developmental stage.

MATERIALS AND METHODS

Animals and Treatment. The RARγ null mice used in this study have been previously described (Lohnes et al., 1993). RARγ heteozygotes were mated overnight and females examined the following morning for the presence of a vaginal plug; noon of the day of plug was considered as 0.5 dpc. Pregnant females were dosed by oral gavage with vehicle or all-trans retinoic acid dissolved in corn oil to a final delivery of 10 mg/kg maternal weight at 7.3 dpc or 100 mg/kg at 10.5 or 11.5 dpc.

Pregnant females were sacrificed at 18.5 dpc by cervical dislocation and fetuses obtained *via* cesarean section and stored at -20°C. Placental DNA was utilized for genotype assignment by either genomic Southern blot as previously described (Lohnes et al., 1993) or by PCR. In the latter case, primers specific for RARγ sequences (5'-CAGAGCACCAGCTCGGAGGA-3' and 5'-CTTCACAGGAGCTGACCCCA-3') which flank the Neo integration site of the targeted locus were used to amplify a 120 bp product specific for the wildtype allele. The primer 5'-GGCCGGAGAACCTGCGTGCAATCC-3', comprising sequences complementary to the 5' coding region of the Neo gene, was employed with the first oligonucleotide to amplify an approximately 600 bp product specific for the disrupted allele. The PCR conditions used were 94°C for 30 seconds, 55°C for 10 sec, and 72°C for 1 minute for 25 cycles. Amplification products were resolved on a 1.5% agarose gel and visualized by ethidium bromide staining.

Whole Mount Skeletal Preparations. Fetuses were skinned, eviscerated, and dehydrated in 100% ethanol. Carcasses were then stained overnight with 0.03% alcian blue (Sigma) in 80% ethanol:20% glacial acetic acid (v/v) to detect cartilaginous elements. Specimens were then dehydrated in 100% ethanol, cleared in 2% aqueous potassium hydroxide for 6 hours, rinsed once in tap water, and stained overnight with 0.1% alizarin red S (Sigma) to detect ossified structures. Clearing was effected by several changes of 20% glycerol in 1% potassium hydroxide over one week, followed by 50%

glycerol:50% ethanol (v/v) for 2-3 weeks. Specimens were scored under a dissecting microscope and photographed with ASA 400 color film (Kodak).

Statistical analysis. The effect of RA-treatment on viability was assessed by comparing observed versus expected genotype distribution using *Chi* squared analysis (Sokal and Rohlf, 1981).

RESULTS

RARγ Mutants Are Resistant To The Lethality Of Excess RA

As previously described (Kessel and Gruss, 1991; Kessel, 1992), treatment of dams with RA at 7.3, 10.5 and 11.5 dpc resulted in a high resorbtion frequency and reduced litter sizes (data not shown). Treatment at 7.3 dpc resulted in significant lethality of wildtype offspring relative to RARγ null mutants, as judged by deviation from the expected Mendelian distributions (Table 2-1). A more moderate, although not statistically significant, effect was also observed following treatment at 10.5 dpc.

Table 2-1

TABLE 1. Viability of RA-Treated Fetuses at 18.5 dpc

	Genotype distribution of fetuses from RARγ+/− intercrosses[a]		
RA treatment	$RAR\gamma^{+/+}$	$RAR\gamma^{+/-}$	$RAR\gamma^{-/-}$
7.3 dpc[b]	20 (0.6)*	72 (2)	38 (1.1)
10.5 dpc[c]	27 (0.7)	78 (2)	37 (1.0)
11.5 dpc[c]	28 (1.1)	52 (2)	25 (1.0)

[a]Ratios were normalized with respect to heterozygotes.
[b]10 mg RA/kg maternal body weight.
[c]100 mg RA/kg maternal body weight.
*Significantly different from the expected Mendelian distribution ($P < 0.05$).

Craniofacial And Neural Tube Defects Elicited By RA Treatment At 7.3 dpc

In accordance with previous studies (Kessel and Gruss, 1991; Morriss-Kay, 1993), *in utero* exposure to RA at 7.3 dpc resulted in a high frequency of offspring exhibiting presumptive neural tube defects, notably anencephaly and exencephaly (Fig. 2-1h). Fetuses lacking overt neural tube defects often displayed a spectrum of additional craniofacial malformations involving reduction or agenesis of skeletal elements. For simplicity, anencephaly and exencephaly were compiled together and craniofacial defects arbitrarily scored as severe or moderate; severe craniofacial malformations included agenesis of rostral facial skeletal elements (e.g. Fig. 2-1i) and microcephaly, while moderate malformations included hypoplasia or dysplasia of rostral skeletal elements (not shown). Because anencepthaly and exencephaly result in severe craniofacial malformations likely secondary to perturbation of neural tube closure, specimens exhibiting these pathologies were not considered in the latter analysis.

Anencephaly and exencephaly could be readily assessed upon cesarean section at 18.5 dpc. Following genotype assignment, RARγ null mutants were found to exhibit a five-fold decrease in the incidence of these RA-induced defects relative to heterozygous and wild type littermates (Table 2-2). Analysis of skeletal preparations likewise revealed a 50-60% reduction in the frequency of severe and moderate craniofacial malformations in RARγ null mutants relative to control littermates (Table 2-2; note that although specimens with neural tube defects were excluded from analysis of these defects, all specimens were included in the calculation of the frequency of craniofacial defects and therefore the resistance of RARγ null mutants to these malformations is understated). The consequence of RARγ ablation on the induction of craniofacial malformations also appeared to be stage-specific, as the frequency and severity of such defects elicited by RA treatment at 10.5 or 11.5 dpc did not differ with respect to genotype (e.g. cleft palate; Fig. 2-2e and f).

Analysis Of Vertebral Defects: Assignment Of Vertebral Patterns

Vertebral patterns were assigned essentially as previously described (Kessel, 1992; Kessel and Gruss, 1991), and will be only briefly reiterated here. Normal wild type mice

have a highly invariant vertebral pattern consisting of seven cervical vertebrae (denoted C1 to C7), thirteen thoracic vertebrae (denoted T1 to T13), seven of which are normally fused to the sternum (vertebrosternal thoracic vertebrae), six lumbar vertebrae (denoted L1 to L6) and three or four sacral vertebrae fused together to form the sacral bone (S1 to S4). Caudal vertebrae were not considered in the present study.

A number of morphogenic criteria can be used to distinguish certain of these vertebral elements. In the cervical region, the atlas (C1) is the only vertebra lacking a vertebral center and possessing a ventral ossified tubercle, the anterior arch of atlas (e.g. Fig. 2-2g; AAA). The neural arches of C1 are also larger than those of more caudal cervical vertebrae. The axis (C2) possesses neural arches intermediate in size to the atlas and more caudal cervical vertebrae, and is further characterized by the presence of two vertebral centers, including the axis dens which projects rostrally from C2 and is considered homologous to the body of the atlas. C3 to C5 are very similar, possessing closed or nearly closed transverse foramen, while C6 is distinguished by the presence of ventrally protruding tuberculi anterior. The seventh cervical vertebra lacks transverse foramen and may possess minor rib anlage extending from the transverse process; the latter finding is a normovariant. All thoracic vertebrae are characterized by the presence of ribs projecting from the lateral processes, the first seven (T1 to T7) being attached to the sternum. In addition, the second thoracic vertebra is characterized by the presence of an prominent spinous process on its dorsal aspect.

Exposure of embryos to RA at 7.3 dpc resulted in a number of defects of the axial skeleton, several of which were interpretable as homeotic transformations by virtue of altered vertebral morphologies. In treated wild type offspring, the frequency of these transformations agreed well with previous reports (Table 2-2; Kessel and Gruss, 1991). Ablation of RARγ, however, had a significant impact on the frequency and/or severity of several of these defects.

Following treatment at 7.3 dpc, sixty-five percent of treated wild type offspring exhibited evidence for an occipital vertebra (a proatlas), manifested as a moderate or extensive ossified neural arch-like structure between, and often fused to, the exoccipital bone and the atlas (Fig. 2-1a and c). Thirty-five percent of these wild type fetuses also exhibited a ventral tubercle reminiscent of an ectopic anterior arch of atlas (Fig. 2-1b and

Figure 2-1. Skeletal and neural tube defects induced by RA treatment at 7.3 dpc.

(a-f) Lateral view of the cervical and upper thoracic region of the axial skeleton of wildtype (a-c) and RARγ null mutant (d-f) fetuses treated with RA at 7.3 dpc. Note the evidence for both partial (a, c, and e) and complete proatlases (b, f) induced by RA treatment at this stage (indicated by P). AAA* indicates an ectopic anterior arch ventral to the first vertebra in (b, f), and, together with the occipital proatlantal neural arch structure (P in a, b, c, e and f), was considered as evidence for induction of a complete proatlas. Curved arrow indicates proatlas-exoccipital fusions in (a, c, and e). Long arrow in (a and b) indicates neural arch fusions of cervical vertebrae, whereas the short arrow points to ectopic ossifications. C2 bifidus is indicated by short arrow in (b). Extensive ribs on C7 are indicated by a large star in (a, c), whereas minor ectopic rib anlage on C6 are indicated by a small star in (b, e). Note the reduction of cervical vertebrae from 7 to 6 in (b, d-f) and the presence of tuberculi anterior (TA) on C5 in (b, e and f). S, supraoccipital bone; T1, first thoracic vertebra. (g-i) Lateral view of craniofacial malformations induced by RA treatment at 7.3 dpc. (g) Untreated wildtype fetus. (h) treated wildtype fetus displaying anencephaly (denoted by a large star) and a complete proatlas with an associated ectopic anterior arch (denoted by AAA*). Large arrow in (h) indicates fusions of the proatlas and C1. (i) RA-treated RARγ-null mutant fetus displaying severe rostral craniofacial malformations (large star), and hypoplasia of the frontal bone (small star); note also the presence of a partial proatlas (P). AAA, anterior arch of atlas; Pb, parietal bone; E, exoccipital bone; F, frontal bone; I, interparietal bone; M, mandible; N, nasal bone; O, otic capsule; S, supraoccipital bone; T, tympanic ring; X, maxillary bone.

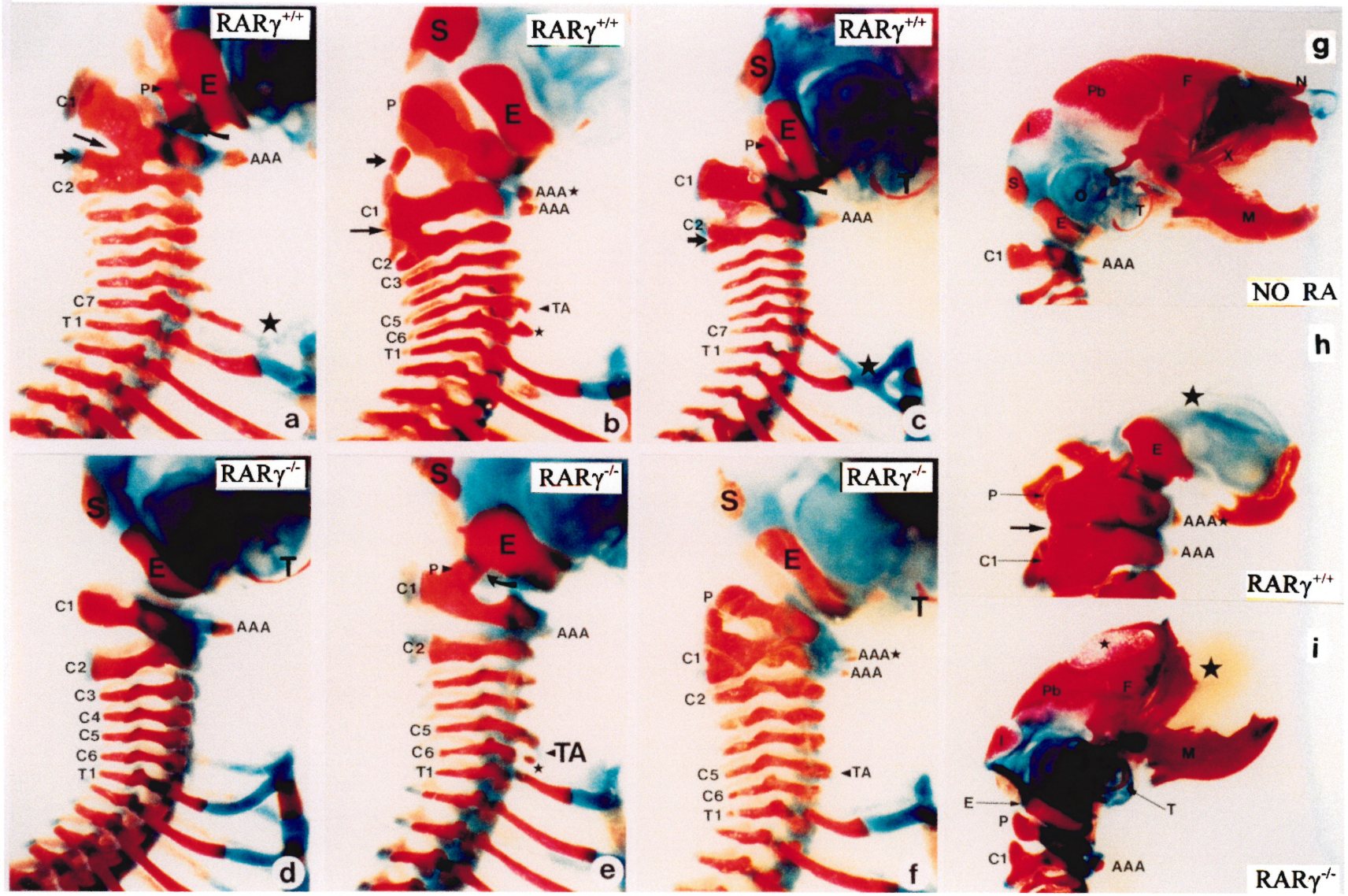
RARγ+/+
RARγ+/+
RARγ+/+
RARγ-/-
RARγ-/-
RARγ-/-
RARγ+/+
RARγ-/-
NO RA
a
b
c
d
e
f
g
h
i
S
E
P
T
C1
C2
C3
C4
C5
C6
C7
T1
AAA
AAA★
TA
Pb
F
N
I
X
O
M

2-1h); this latter characteristic was arbitrarily considered as evidence for the generation of a complete proatlas. In contrast, only 5% of RA-treated RARγ mutant littermates exhibited a full proatlantal phenotype (Fig. 2-1f), with heterozygotes presenting an intermediate frequency (Table 2-2). It should be noted that untreated RARγ null mutants exhibit a similar phenotype, interpreted as an anterior transformation of C2 to a C1 identity (Lohnes et al., 1993; also compare Figs. 2-1f and 2-2j). However, the dens axis is retained in RARγ null mutants exhibiting a C2 to C1 transformation (Lohnes et al., 1993), whereas this structure is lost upon RA-induction of a full proatlas (see Kessel et al., 1990 for discussion). In the present study, treated RARγ mutants exhibiting supernumerary anterior arch of atlas-like structures were also lacking the dens axis in all but one instance, indicating that induction of a full proatlas occurs at a much lower frequency in the mutant background.

Treatment with RA at 7.3 dpc also resulted in posterior homeotic transformations of C3, C4 or C5 to a C6 identity, as evidenced by the appearance of tuberculi anterior on one or more of these vertebrae in the majority of wildtype specimens analyzed (Fig. 2-1b; Table 2-2). Although 68% of RARγ null offspring exhibited tuberculi anterior on C5 (Fig. 2-1f), stronger posteriorization effects (i.e. tuberculi anterior on C3 or C4) were observed only in wildtype and heterozygous offspring. This likely reflects the complete resistance of RARγ null offspring to severe reduction of the cervical region, as, unlike controls, none of the null mutants exhibited fewer than six cervical vertebrae (e.g. Figs. 2-1d-f; Table 2-2).

The finding of six cervical vertebrae, irrespective of the presence of a proatlas, is indicative of a posterior transformation of C7 to a thoracic identity (Table 2-2; Fig. 2-1b, d-f; Kessel and Gruss, 1991). Extensive ectopic rib anlage on C5, 6 or 7 were also considered as evidence for transformation of these vertebrae to thoracic identities (Figs. 2-1a and c; Table 2-2). By these criteria, RA treatment at 7.3 dpc resulted in posterior transformation of C7 to a thoracic identity in the majority of all offspring independent of genotype. However, RARγ mutants never exhibited more extensive posteriorization events (i.e. cervical ribs on C5 or C6) occasionally found in wildtype and heterozygous offspring (Table 2-2); again, this finding likely reflects the resistance of mutants to the loss of cervical elements seen in control fetuses.

Table 2-2

TABLE 2. Skeletal Defects Induced by RA Treatment at 7.3 dpc[a]

	RARγ$^{+/+}$ (48)[b]	RARγ$^{+/-}$ (58)	RARγ$^{-/-}$ (38)	Transformation
Malformations				
Anencephaly/exencephaly	12 (25)	20 (34)	2 (5)	
Cranio-facial malformations				
Moderate	10 (21)	9 (16)	3 (8)	
Severe	9 (19)	16 (28)	4 (11)	
Proatlas-exoccipital fusion	5 (10)	16 (28)	10 (26)	
C1-proatlas fusion	7 (15)	18 (31)	10 (26)	
Cervical vertebral fusions[c,d]	13 (27)	15 (26)	18 (47)	
Transformations				
Basioccipital-AAA fusion[c]	—	—	2 (5)	
Proatlas				
Evidence for	14 (29)	31 (53)	15 (39)	
Complete	17 (35)	13 (22)	2 (5)	Occipital to cervical
Tuberculum anterior				
Absent	5 (10)	—	1 (3)	
C3	1 (5)	1 (2)	—	C3 to C6
C4	1 (2)	4 (7)	—	C4 to C6
C5	33 (69)	41 (71)	26 (68)	C5 to C6
C6	8 (17)	12 (21)	11 (29)	
Rib anlage on C5 or C6				
Absent/small	35 (73)	37 (64)	28 (74)	
Extensive	5 (10)	11 (19)[e]	—	C5/C6 to T1
Rib anlage on C7				
Absent/small	5 (10)	4 (7)	7 (18)	
Extensive	3 (6)	6 (10)	3 (8)	C7 to T1
Processus spinosus				
Absent	3 (6)	4 (7)	3 (8)	
T1	12 (25)	21 (36)	6 (16)	T1 to T2
T2	33 (68)	30 (52)	29 (76)	
T3	—	3 (5)	—	T3 to T2
Cervical vertebrae				
3 to 5	3 (6)	4 (7)	—	C4, 5 or 6 to T
6	37 (77)	44 (76)	28 (74)	C7 to T1
7	8 (17)	10 (17)	10 (26)	
Ribs[f]				
12	3 (6)	6 (10)	3 (8)	
13	37 (77)	45 (78)	32 (84)	
14	8 (17)	7 (12)	3 (8)	
Vertebrosternal ribs				
6	8 (17)	5 (9)	1 (3)	T7 to T8
7	32 (67)	47 (81)	31 (82)	
8[c]	8 (17)	6 (10)	6 (16)	T8 to T7 or C7 to T1
Lumbar vertebrae[f]				
5	24 (50)	36 (62)	19 (50)	
6	24 (50)	22 (38)	19 (50)	
Presacral vertebrae				
<24	4 (8)	5 (9)	—	
24	15 (31)	26 (45)	16 (42)	
25	24 (50)	23 (40)	15 (39)	
26	5 (10)	4 (7)	7 (18)	
Vertebral patterns				
C3–5/T13/L5/S3/4	—	1 (2)	—	C to T, L to S
C3–5/T13/L6/S3/4	3 (6)	1 (2)	—	C to T, L to S
C3–5/T14/L5/S3/4	—	1 (2)	—	C to T, L6 to S1
C3–5/T14/L6/S3/4	—	1 (2)	—	C to T
C6/T12/L5/S3/4	1 (2)	3 (5)	—	C7 to T1, T to L, L to S
C6/T12/L6/S3/4	2 (4)	2 (4)	1 (3)	C7 to T1, T to L, L to S
C6/T13/L5/S3/4	14 (29)	23 (40)	15 (39)	C7 to T1, T13 to L1, L to S
C6/T13/L6/S3/4	13 (27)	11 (19)	9 (24)	C7 to T1, T13 to L1, L6 to S1
C6/T14/L5/S3/4	8 (17)	4 (7)	2 (5)	C7 to T1, L6 to S1
C6/T14/L6/S3/4	—	1 (2)	1 (3)	C7 to T1
C7/T12/L6/S3/4	—	1 (2)	2 (5)	T13 to L1, L6 to S1
C7/T13/L5/S3/4	2 (4)	6 (10)	2 (5)	L6 to S1
C7/T13/L6/S3/4	5 (10)	3 (5)	—	

[a]Numbers in parentheses indicate percentages. AAA: anterior arch of the atlas.
[b]Includes 28 fetuses from wildtype intercrosses.
[c]RARγ null-associated defects.
[d]Neural arch fusions between C1–C2, C2–C3, C3–C4, or C4–C5.
[e]Two specimens showed a C5 to T1 transformation (i.e., extensive rib anlage on C5).
[f]Transformations were assigned according to vertebral patterns.

More caudal homeotic transformations induced by RA treatment at 7.3 dpc included gain or loss of thoracic vertebrae, as indicated by rib counts; the presence of the spinous process on the eight, rather than ninth, vertebral element; the presence of six or eight, rather than seven, vertebrosternal ribs and the presence of five lumbar vertebrae instead of six. As discussed previously (Kessel and Gruss, 1991), deviations in the number of ribs from thirteen may be interpreted as either a posterior transformation of the seventh cervical segment to a thoracic identity in the case of six cervical vertebrae, fourteen ribs and six lumbar vertebrae, or an anterior homeotic transformation of L1 to a thoracic identity in the case of seven cervical vertebrae, fourteen ribs and five lumbar vertebrae. RA treatment at 7.3 dpc appeared to result in several transformations along the axial skeleton occurring concomitantly within a single specimen. For example, six cervical, thirteen thoracic and five lumbar vertebrae implies a posterior transformation of C7 to a thoracic identity, transformation of the last thoracic vertebra to a lumbar identity and transformation of the last two lumbar vertebrae to sacral identities, culminating in the loss of two presacral vertebrae.

Interpretation of these vertebral patterns (Table 2-2) revealed that RARγ mutants exhibited a lower frequency of the formation of an ectopic fourteen rib relative to wildtypes (8% versus 17% respectively), and a three-fold reduction of the C6/T14/L5 vertebral pattern (Table 2-2). Other transformations affected by RARγ ablation included a six-fold reduction of T7 to T8 transformation, and a modest attenuation of transformation of the first thoracic vertebra to a T2 identity. The frequencies of other homeotic transformations and vertebral patterns were not appreciably different in the RARγ null background compared to controls.

Skeletal Defects Induced By RA Administration At 10.5 And 11.5 dpc

Following RA treatment at 10.5 or 11.5 dpc, forelimb and/or hindlimb malformations were evident in all offspring from heterozygous intercrosses. The frequency and severity of these defects did not vary with genotype (Fig. 2-2a-c). Fetuses also exhibited defects of the axial skeleton, several of which resembled homeotic transformations induced by RA exposure at 7.3 dpc. However, unlike earlier treatment, vertebrae were affected in a

regionalized fashion, with defects generally induced in a cranial-caudal manner with respect to the developmental stage of exposure. In wildtype offspring, the nature and frequency of these axial malformations agreed well with previous work (Kessel, 1992). RARγ null specimens, however, were markedly resistant to certain of these RA-induced defects.

At 10.5 dpc, RA treatment induced fusions between the basioccipital and exoccipital bones in approximately half of all wildtype and heterozygous specimens examined whereas RARγ null mutant littermates never displayed this defect (Fig. 2-2d-f ; Table 2-3). A number of homeotic transformation of the axial skeleton were also attenuated by RARγ ablation. Following treatment at 10.5 dpc, mutants were only slightly resistant to posterior homeotic transformation of C5 to C6, as evidenced by the presence of ectopic tuberculi anterior on C5 (Fig. 2-2h; Table 2-3). However, whereas the majority of affected wildtype specimens exhibited a bilateral shift of tuberculi anterior to C5 with concomitant transformation of C6 to a C7 identity (assessed by loss of both tuberculi anterior and closed transverse foramen), only one null mutant displayed such a bilateral transformation (Table 2-3). Furthermore, 21% of wildtype specimens, but no mutants, displayed C5 to C6 and C6 to C7 transformations following treatment at 11.5 dpc. In a similar manner, the presence of extensive cervical ribs on C7 induced by treatment at 10.5 (e.g. Fig. 2-2h) or 11.5 dpc was approximately three-fold less frequent in mutants relative to wildtype controls (Table 2-3). RARγ therefore appears to play a significant role in posterior transformation of C5 through C7, as well as events involved in abnormal development of more rostral somite derivatives (i.e. fusion of basioccipital and exoccipital bones) induced by excess RA at 10.5 and 11.5 dpc.

RARγ also appeared to influence specification of more posterior vertebrae, as mutants treated at 10.5 dpc exhibited a ten fold increase in the incidence of anterior transformation of L1 to T14 relative to wildtype controls (Table 2-3). Following treatment at 11.5 dpc, RARγ mutants also exhibited a five-fold increase in anterior transformation of L2 to a thoracic phenotype (i.e. T15/L4) compared to wildtype littermates (Table 2-3). Thus, contrary to the trend observed in the cervical region, mutants exhibited increases in RA-induced anterior homeotic transformation of lumbar

Figure 2-2. Defects induced by RA treatment at 10.5 and 11.5 dpc.

(a-c) Forelimbs from untreated wildtype (a) or wildtype (b) and RARγ null mutants (c) treated with RA at 10.5 dpc. Note that all treated limbs exhibited similar defects. H, humerus; R, radius; S, scapula; U, ulna. (d-f) Ventral view of the base of the skull from an untreated wildtype, or wildtype (e) and RARγ null mutant (f) treated with RA at 10.5 dpc. Fusion of the basioccipital (B) and exoccipital (E) bones (indicated by the short arrows in e) was only manifested in the treated wildtype specimen. Cleft palate (star in e, f) and other craniofacial defects did not differ between wildtypes and mutants (e.g. compare reductions and malformations of alisphenoid (A), basisphenoid (BS) and palatial bone (P) in e and f); T, tympanic ring. (g-l) Lateral view of cervical region of an untreated wildtype control (g), wildtype specimen treated with RA at 10.5dpc (h) and RARγ null mutants treated at 10.5 dpc (I) or 11.5 dpc (j-l). Note the tuberculum anterior (TA) on C5 instead of C6 and an extensive rib on C7 (large star) in (h) and (I). Fusion of the neural arches of are denoted by long arrows in (I, k and l). Note the C2 to C1 anterior transformation indicated by an ectopic anterior arch of atlas (AAA*) in (j and l). E, exoccipital bone; S, supraoccipital bone; T, Tympanic ring. (m-o) Dorsal view of the thoracic region of an untreated wildtype fetus (m), or wildtype (n) and RARγ null fetuses (o) treated at 11.5 dpc. Note the extensive fusions of the thoracic vertebrae from T3 to T8 in the wildtype specimen (large bracket in n) compared to more moderate fusions in the RARγ null mutant (bracket in o).

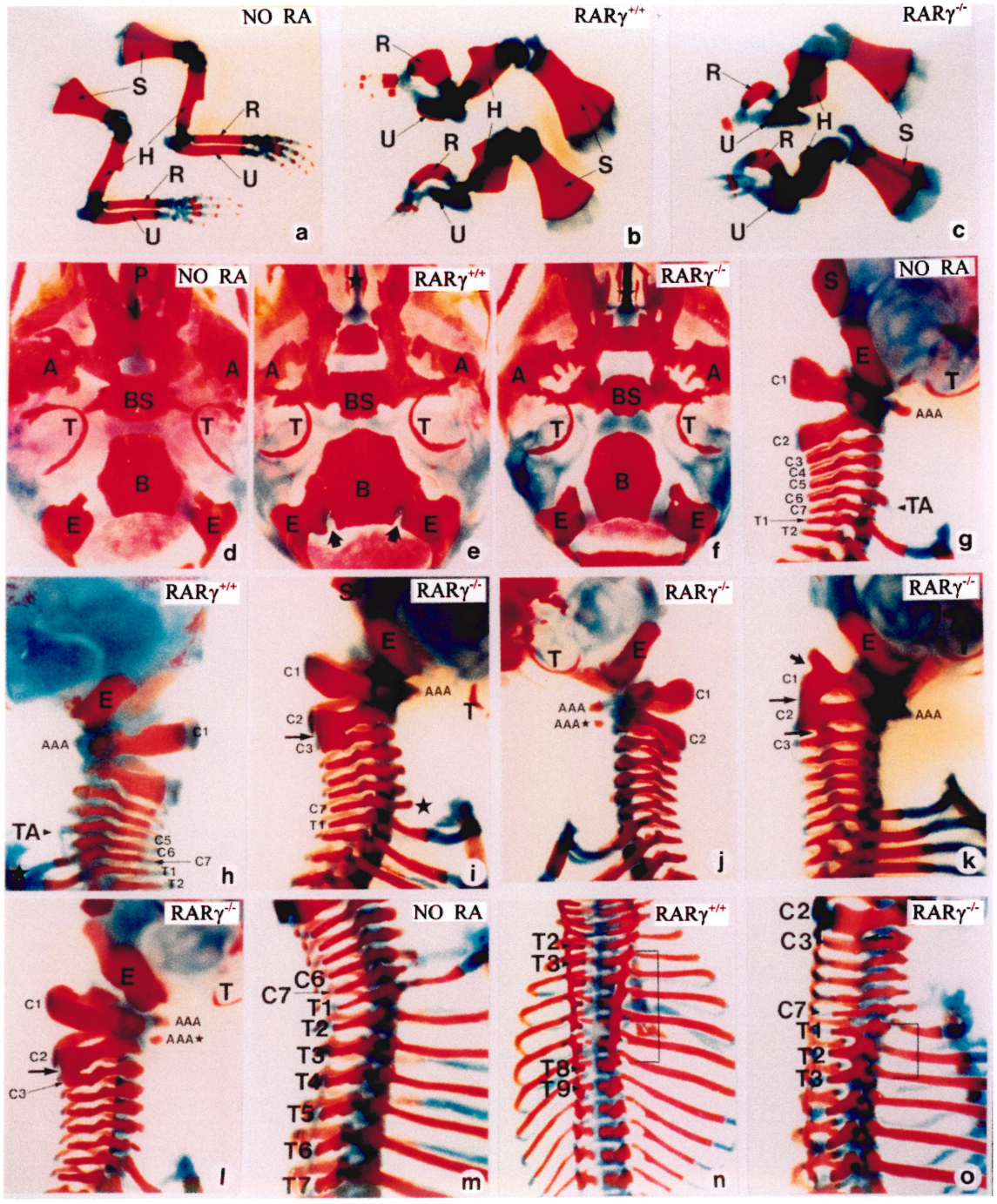
NO RA
RARγ+/+
RARγ-/-
S
R
H
U
a
b
c
P
A
BS
T
B
E
d
e
f
C1
AAA
C2
C3
C4
C5
C6
C7
T1
T2
TA
g
h
i
j
k
AAA★
l
m
n
o
T2
T3
T8
T9
C2
C3
C7
T1
T2
T3
T4
T5
T6
T7

vertebrae. However, in contrast to previous reports (Lohnes et al., 1993), we have observed that 11% of untreated RARγ null offspring exhibited L1 to T14 transformations, as evidenced by minor rib anlage on the 21st vertebral element (Table 2-3 and data not shown). Thus, the increase in anterior transformation of lumbar to thoracic identities observed in the null background could be due to additive events between RARγ disruption and RA treatment. Given the experimental nature of these studies, it is likely that these events are highly related.

A low frequency of untreated wildtype controls in both our and others (Kessel, 1992) studies exhibited L6 to sacral transformations, as evidenced by T13/L5 or T14/L4 vertebral patterns, and this phenotype was attenuated following treatment with RA specifically at 10.5 (Table 2-3; Kessel, 1992). Intriguingly, RARγ null mutants never exhibited this particular transformation irrespective of treatment, despite the fact that all specimens were littermate-derived, and therefore of comparable genetic background. Although we cannot exclude the existence of a closely linked modifier co-segregating with the RARγ locus, the curative effect specific to wildtype specimens treated at 10.5 dpc, the lack of this phenotype in RARγ null littermates, and the finding of anterior transformation of L1 to T14 in the mutant background, all suggest that RARγ does indeed influence vertebral patterning in this region of the axial skeleton. The discrepancy between this observation and previous reports may be attributed to background effects, as our current colony (which is 129Sv-C57BL/6 hybrid) has been backcrossed to C57BL/6 several times. Such modifying events have been noted in a number of knockout studies, including genes involved in axial patterning (Ramirez-Solis et al., 1993), notably RARα (Lufkin et al., 1993; Lohnes et al., 1994). Generation and analysis of RARγ null offspring on genetically homogeneous backgrounds may reveal further roles for this receptor.

RA treatment at 11.5 dpc resulted in additional malformations of the axial skeleton, including fusions of the ventro-lateral portion of the neural arches of thoracic vertebrae and dyssymphysis or fusion of the vertebral bodies of thoracic or lumbar vertebrae. These defects were classified as either severe or moderate depending on the number of vertebrae involved and the extent of the malformation (Table 2-3). Relative to

Table 2-3

TABLE 3. Vertebral Patterns Induced by RA Treatment at 10.5 and 11.5 dpc

	RA at 10.5 dpc			RA at 11.5 dpc			Untreated		
	$RAR\gamma^{+/+}$ (29)	$RAR\gamma^{+/-}$ (49)	$RAR\gamma^{-/-}$ (33)	$RAR\gamma^{+/+}$ (33)	$RAR\gamma^{+/-}$ (40)	$RAR\gamma^{-/-}$ (25)	$RAR\gamma^{+/+}$ (21)	$RAR\gamma^{-/-}$ (27)	Transformation
Malformations									
Basioccipital-exoccipital fusion	13 (45)	26 (53)	—	—	1 (3)	—	—	—	
C1 Bifidus[a]	—	—	—	—	—	1 (4)	—	2 (7)	
Neural arch fusions[a,b]	—	—	1 (3)	4 (12)	—	9 (36)	—	3 (11)	
C1 or C2 malformed[a,c]	—	—	2 (6)	—	—	8 (32)	—	7 (26)	
Vertebral malformations[d]									
Moderate	—	—	—	2 (6)	12 (30)	4 (16)	—	—	
Severe	—	—	—	10 (30)	1 (3)	—	—	—	
Transformations									
Basioccipital-AAA fusion[a,e]	—	—	2 (6)	—	—	2 (8)	—	2 (7)	
Anterior arch on C2[a]	—	—	—	—	—	4 (16)	—	4 (15)	C2 to C1
Tuberculum anterior									
Absent	—	—	—	5 (15)	11 (28)	3 (12)	—	—	
C5	10 (34)	4 (8)	1 (3)	7 (21)	—	—	—	—	C5 to C6, C6 to C7
C5 and C6	1 (3)	11 (22)	7 (21)	—	—	—	—	—	C5 to C6
C6	18 (62)	34 (69)	24 (73)	21 (64)	29 (72)	20 (80)	21 (100)	27 (100)	
C7[a]	—	—	1 (3)	—	—	2 (8)	—	—	C7 to C6
Rib anlage on C7									
Absent/small	20 (69)	25 (51)	29 (88)	29 (88)	36 (90)	24 (96)	21 (100)	27 (100)	
Extensive	9 (31)	24 (49)	4 (12)	4 (12)	4 (10)	1 (4)	—	—	C7 to T1
Ribs[f]									
13	28 (97)	47 (96)	23 (70)	9 (27)	6 (15)	—	21 (100)	24 (89)	
14	1 (3)	2 (4)	10 (30)	23 (70)	33 (83)	21 (84)	—	3 (11)	
15	—	—	—	1 (3)	1 (3)	9 (16)	—	—	
Vertebrosternal ribs									
7	29 (100)	49 (100)	30 (91)	33 (100)	39 (97)	17 (68)	21 (100)	22 (81)	
8[a]	—	—	3 (9)	—	1 (3)	8 (32)	—	5 (19)	T8 to T1
Lumbar vertebrae[f]									
4	—	—	—	5 (15)	10 (25)	4 (16)	—	—	
5	2 (7)	2 (4)	10 (30)	21 (64)	25 (63)	21 (84)	5 (24)	3 (11)	
6	27 (93)	47 (96)	23 (70)	7 (21)	5 (13)	—	16 (76)	24 (89)	
Vertebral patterns									
C7/T13/L5/S3/4	1 (3)	—	—	3 (9)	1 (3)	—	5 (24)	—	L6 to S1
C7/T13/L6/S3/4	27 (93)	47 (96)	23 (70)	7 (21)	5 (13)	—	16 (26)	24 (89)	
C7/T14/L4/S3/4	—	—	—	4 (12)	9 (23)	—	—	—	L1 to T14, L6 to S1
C7/T14/L5/S3/4	1 (3)	2 (4)	10 (30)	18 (55)	24 (60)	21 (84)	—	3 (11)	L1 to T14
C7/T15/L4/S3/4	—	—	—	1 (3)	1 (3)	4 (16)	—	—	L1 to T14, L2 to T15

[a]$RAR\gamma$ null-associated vertebral defects.
[b]Neural arch fusions between C1–C2, C2–C3, or C4–C5.
[c]Dyssymphysis of the neural arches and enlargement of C2 neural arch.
[d]Split vertebral bodies and neural arch fusions of thoracic and/or lumbar vertebrae.
[e]AAA: anterior arch of the atlas.
[f]Vertebral transformations were assigned according to vertebral patterns.

wildtype controls, RARγ mutants exhibited a low incidence of only moderate thoracic vertebral malformations involving fusions of, at most, 3 vertebrae (e.g. Fig. 2-2o). In contrast, approximately one third of wildtype littermates displayed more severe fusions which often involved six or more vertebrae (Fig. 2-2n; Table 2-3).

Certain Aspects Of The RARγ Null Phenotype Are Abolished By RA Treatment

RARγ null offspring exhibit skeletal defects including malformations and homeotic transformations of several vertebral elements (Lohnes et al., 1993). Characteristic transformations include anteriorization of C2 to a C1 identity, C6 to a C5 identity, C7 to a C6 identity, and T8 to a T7 identity (the former transformation is considered incomplete, as the dens axis, a C2-specific structure, is unperturbed). Our present results have also documented L1 to T14 anterior homeotic transformation in RARγ null mutants. Axial malformations characteristic of RARγ null mutants include fusions of the neural arches of C1 through C4 and of the basioccipital bone and anterior arch of atlas.

As stated above, our colony has been outcrossed to a C57/B6 background, but is still 129Sv-C57BL/6 hybrid, necessitating a re-evaluation of RARγ null-specific axial defects. With the exception of fusion of the basioccipital bone to the anterior arch of atlas, which occurred at a lower frequency than previous reports, and the finding of L1 to T14 transformation, the incidence and nature of the vertebral anomalies in RARγ offspring agreed well with the original report (Table 2-3 and Lohnes et al., 1993).

The frequency of most malformations characteristic of the RARγ null phenotype were unaffected by RA treatment at 11.5 dpc (e.g. C2 to C1 in Fig. 2-2j and l; Table 2-3). Fusions of the neural arches of cervical vertebrae (Fig. 2-2k, l, and o), which occurred in 36% of treated mutant offspring, was higher than untreated RARγ null controls. This may be due to an effect of RA superimposed on the RARγ null phenotype, since wildtype specimens treated at 11.5 dpc also displayed similar vertebral fusions (Table 2-3). In marked contrast, RA-treatment at 10.5 dpc markedly attenuated several of the skeletal defects induced by RARγ ablation (Table 2-3). In particular, anterior transformation of C2 to a C1 identity was never observed, and the incidence of T8 to T7 transformation was reduced by 50%. The frequencies of other vertebral defects, including cervical

neural arch fusions and malformations of C1 and C2, were also greatly reduced, being observed in only two RARγ null specimens (e.g. Fig. 2-2i). Defects not attenuated by RA treatment at 10.5 dpc in the RARγ mutant background included fusion of the basioccipital bone and anterior arch of atlas, and anterior transformations of T7 to T6 and L1 to T14.

The extreme malformations of cervical vertebrae frequently resulting from RA treatment at 7.3 dpc confounded clear assessment of RARγ null-associated skeletal defects. Although most mutants with two vertebrae characteristic of C1 exhibited morphological criteria consistent with the induction of a proatlas (see above), at least one specimen had an apparent C2 to C1 transformation, as the dens axis was present on the second vertebral element (data not shown). Treatment at 7.3 dpc also resulted in fusions of the neural arches in wild type mice (e.g., Fig. 2-1a and b). However, the incidence of these malformations was consistently higher in treated RARγ null mutants relative to wild type controls (Table 2-2), again suggesting an additive effect between RA treatment and the cervical vertebral fusions inherent to the RARγ null phenotype, and that these latter defects are not attenuated by treatment at 7.3 dpc.

DISCUSSION

Previous studies have demonstrated that RARγ specifically transduces the teratogenic effect of RA on the caudal neural tube at 8.5 - 9.0 dpc. We have extended this initial observation, and present evidence that RARγ also contributes to rostral neural tube defects and malformations of the axial skeleton induced by excess RA.

RARγ Contributes To Retinoid-Induced Embryolethality

RARγ null embryos, compared to control littermates, were resistant to the embryo lethality evoked by excess RA, particularly at 7.3 dpc. Since expression of RARγ at this stage has not been reported, it is difficult to speculate as to the nature of this effect. Our results, however, clearly imply that this receptor is expressed at this stage, and is capable of transducing the retinoid signal at least in a pharmacological setting. In agreement with a role for this receptor in retinoid toxicity, others have also noted that RARγ null

mice are resistant to certain pharmacological effects of post-partum RA excess (Look et al., 1995).

A Role For RARγ In Craniofacial And Neural Tube Defects

A proportion of RARα/γ double null mutants exhibit exencephaly at term due to an open rhombencephalon which arises prior to 9.5 dpc (Lohnes et al., 1994). Involvement of RARγ in neural tube defects is also presented here, as null mutants were markedly resistant to exencephaly and anencephaly following RA administration at 7.3 dpc. Interestingly, RARγ mutants are also resistant to neural tube defects (spina bifida) induced by RA at more caudal levels at later developmental stages (Lohnes et al.,1993). Whether these findings are indicative of a common RARγ-dependent event awaits elucidation of the molecular mechanism(s) of retinoid-induced neural tube defects.

Neural crest cells (NCC) have long been recognized to be a target of retinoid excess (reviewed in Morriss-Kay, 1993; Ito and Morita, 1995). Consistent with this is our finding that RARγ null mice were partially resistant to retinoid-induced craniofacial defects, the basis of which likely reflect malformations of mesenchymal NCC derivatives. Defects of mesectodermal origin also underly many of the craniofacial malformations observed in RAR double null mutants (Lohnes et al., 1994), as well as cardiac outflow tract defects and abnormalities of aortic arch derivatives found both in RAR double null mutants and VAD rat and quail embryos (Mendelsohn et al., 1994a; Thompson et al., 1964; Dersch and Zile, 1993; Luo et al., 1996). However, as previously discussed (Mendelsohn et al., 1994a), the window of opportunity for rescue of these VAD-imposed defects by exogenous retinoid administration is consistent with a role for the RARs during migration or postmigration phases of NCC ontogenesis. In contrast, since the time of retinoid administration in the present study (7.3 dpc) is prior to the onset of NCC migration (Bronner-Fraser, 1995), our findings suggest that RARγ plays a role in teratogenic events at earlier stages of NCC development. However, since not all RAR or RXR null combinations have been investigated, it is unclear whether these receptors do indeed play a physiological role in premigratory NCC. In this regard, recent studies documenting hindbrain abnormalities (primarily loss of rhombomeres 4 through 8) and associated NCC deficits in VAD quail embryos clearly suggests that the retinoid signal

plays critical roles in the morphogenesis of the CNS and certain NCC populations at early developmental stages (Maden et al., 1996).

RARγ And Limb Defects

Ablation of RARγ did not alter the severity or frequency of limb defects induced by RA treatment at 10.5 or 11.5 dpc. Induction of these malformations is also not attenuated by disruption of RARα1, RARβ (all isoforms) or RARα1/β (Luo et al., 1995; 1996). Since both RARα and RARγ are uniformly expressed in the limb bud mesenchyme at these stages of treatment (Dollé et al., 1989), these findings suggest that RARα isoforms, in the absence of RARγ, may suffice to transduce the teratogenic retinoid signal leading to limb defects. This possibility is consistent with the observation that RARα/γ double null mutants exhibit limb malformations (Lohnes et al., 1994). However, as RARβ is expressed during early limb development in a region overlapping the zone of polarizing activity, and RARβ2 promoter activity has been noted in the ectodermal ridge (Mendelsohn et al., 1991), a role for this receptor in RA-induced limb defects cannot be excluded. Alternatively, since RXRα null embryos are completely resistant to retinoid-induced limb defects (Sucov et al., 1995), it is possible that this particular teratogenic outcome is elicited by 9-cis RA signaling via RXR homodimers. Further studies, focusing on RAR double null mutants, may address these questions.

RARγ And Vertebral Malformations

Following treatment at 10.5 dpc, RARγ null embryos were found to be completely resistant to RA-induced fusions of the basioccipital and exoccipital bones, and markedly resistant to fusions of the neural arches of thoracic and lumbar vertebrae. A number of mouse mutants have been described which exhibit vertebral fusions similar to the latter malformations, including *Rf* (rib fusions; Mackensen and Stevens, 1960), *rh* (rachiterata; Theiler et al., 1974) and *rv* (rib-vertebrae; Theiler and Varnum, 1985), to name a few. The basis for the vertebral defects observed in these developmental mutants is likely mesenchymal, and a similar mechanism may apply to the RARγ-dependent RA-induced fusions as this receptor is highly expressed in sclerotome at the time of treatment. These

phenotypic similarities suggest that the genes encoded by these loci could conceivably be in the retinoid signaling pathway, or converge on common downstream effectors. However, as these genes have not yet been isolated, a molecular assessment of this hypothesis cannot be presently undertaken.

RARγ And Vertebral Specification

RA treatment of wild-type mouse embryos at 7.0 - 8.5 dpc results in homeotic transformations along the entire vertebral column concomitant with anteriorization of the expression domains of certain Hox genes (Kessel and Gruss, 1991). That Hox genes could be direct RA targets is supported by the finding of functional RAREs in the promoter/enhancer region of some RA-responsive Hox family members (Langston and Gudas, 1992; Popperl and Featherstone, 1993; Studer et al., 1994; Ogura and Evans, 1995; reviewed in Marshall et al., 1996). Furthermore, HOX transcripts, particularly 3' paralog members, are upregulated by RA in teratocarcinoma cells (Simeone et al., 1990; Simeone et al., 1991), and disruption of either RARα or γ in F9 embryocarcinoma cells attenuates induction of certain of these genes (Boylan et al., 1993; Boylan et al., 1995). A further link between Hox genes and a role for RA in specification of the axial skeleton comes from the observation that RARγ disruption results in phenocopies of certain Hox null mutants; anterior transformation of C2 to a C1 identity is observed in RARγ, Hoxb-4 and Hoxd-4 null offspring (Ramirez-Solis et al., 1993; Horan et al., 1995), whereas T8 to T7 transformation is seen in both RARγ and Hoxc-8 null mice (Le Mouellic et al., 1992). Disruption of RARγ in combination with RARα or RARβ2 isoforms generally results in an increase in the expressivity and penetrance of RARγ null-associated axial defects, and in the appearance of novel transformations several of which are also highly similar to malformations characteristic of certain additional Hox null fetuses (Lohnes et al., 1994 and references therein).

RARγ transcripts are detected at 8.5 dpc in all germ layers posterior to the open caudal neuropore prior to somite condensation (Ruberte et al., 1990), suggesting that this receptor may function during somitogenesis, *via* a Hox gene-dependent mechanism, to specify somite identity. However, RARγ transcripts are also abundantly expressed in sclerotome at later stages (9.5 - 11.5 dpc; Dollé et al., 1990). During this latter period,

excess RA can act to "respecify" vertebral identities in the absence of detectable qualitative or quantitative changes in Hox gene expression (Kessel, 1992).

In the present study, RA treatment of RARγ null embryos at 10.5 dpc resulted in a reduction in the incidence of certain vertebral defects inherent to the RARγ null phenotype, as mutants never exhibited C2 to C1 transformations and the frequency of T8 to T7 transformation and malformations of cervical vertebae (including neural arch fusions) was greatly reduced compared to untreated RARγ null specimens. Paradoxically, the incidence of certain RARγ null-associated defects, such as T8 to T7 transformation and cervical neural arch fusions, increased relative to untreated mutants following RA-exposure at 11.5 dpc. In these cases, however, wild-type littermates exhibited similar defects, suggesting an additive effect between RA-induced malformations and lesions due to ablation of RARγ. This latter finding further supports the observation that treatment specifically at 10.5 dpc is necessary to attenuate certain of the vertebral defects evoked by loss of RARγ.

These findings are indicative of at least two possible mechanisms for RARγ function. In the first instance, the axial defects characteristic of RARγ null offspring may reflect a role for this receptor in Hox gene-dependent vertebral specification during gastrulation which is subsequently altered by RA treatment at 10.5 dpc, resulting in a more normal vertebral pattern. Alternatively, RARγ may function during the later RA-sensitive Hox gene-independent window of vertebral morphogenesis, with the remaining RARs fullfilling certain roles of RARγ in the presence of excess RA. While we cannot exclude that a similar curative effect also occurred following exposure to RA at 7.3 dpc, RA-induced malformations were greatly influenced by RARγ ablation following treatment at 10.5 and 11.5 dpc, whereas, with few exceptions, mutants exposed at 7.3 dpc showed comparatively little resistance. In this respect, it should be noted that previous studies have shown that RARγ null mutants are not resistant to vertebral homeotic transformation following RA administration at 8.5 - 9.0 dpc (Lohnes et al., 1993). Finally, expression of the RA-responsive Hoxb-4 gene is not apparently altered in untreated RARγ null mutants (P. Dollé and P. Chambon, personal communication). Taken together, these observations suggest that RARγ functions during the latter period

of RA-sensitive vertebral development, possibly by affecting sclerotome formation and/or migration.

This model does not exclude the possibility that RARγ also affects vertebral specification by regulation of Hox gene-dependent pathways, nor does it exclude a role for the RARs in affecting Hox gene expression during somitogenesis. Many Hox genes involved in vertebral specification are expressed not only during somitogenesis, but also exhibit persistent expression in sclerotome. In the developing limb, it has been proposed that certain Hox genes may function during two periods, the first corresponding to events related to proliferation and the second pertaining to the realization of the final form of skeletal elements (Morgan and Tabin, 1994); a similar mechanism may relate to the early and late windows of RA-sensitive vertebral specification. Furthermore, although Hox transcript distribution is not apparently altered following RA treatment at 9.5 - 11.5 dpc, subtle changes in their domain or level of expression cannot be excluded, as previously discussed (Kessel et al., 1992). It is also conceivable that RARγ may function during this period by altering the expression of other components of the Hox transcription machinery, such as Pbx and related genes (Chang et al., 1995, and references therein). The outcome of such a hypothetical situation would likely be altered Hox functionality in the absence of detectable changes in Hox gene expression, a possibility we are currently addressing.

Implications For Functional Specificity Of The RARs

The overlapping expression patterns of the RARs (Dollé et al., 1990; Ruberte et al., 1991) and the synergistic effects of combinatorial RAR null mutation (Lohnes et al., 1994; Mendelsohn et al., 1994a; Grondona et al., 1996; Luo et al., 1996) suggests that RARα and/or RARβ isoforms serve to attenuate the RARγ null phenotype in RA treated mutants. However, several transformations inherent to the RARγ null background were not abrogated by treatment at any of the stages tested. This suggests either that the correct window for RA administration was not examined or that the remaining RARs do not exhibit the correct expression pattern. Alternatively, these defects may reflect RARγ function(s) that cannot be fulfilled by any other receptor. One such example is fusion of

the basioccipital bone to the anterior arch of atlas. In this regard, the frequency of this defect is not increased following ablation of RARα or β2 isoforms from the RARγ null background (Lohnes et al., 1994; Mendelsohn et al., 1994a). These observations suggest that RARγ performs a specific function intrinsic to the normal ontogenesis of the first hypochordal bar, a transient embryonic structure the persistence of which likely underlies the fusion between the anterior arch of atlas and the basioccipital bone (see Lohnes et al. 1993 for discussion). Consistent with this possibility is the finding that following treatment at 7.3 dpc, one of the few transformations significantly attenuated by loss of RARγ was the induction of a full proatlas. Our criteria for this particular transformation was the presence of an ectopic anterior arch of atlas associated with the proatlas. Since the origin of this supernumerary anterior arch is likely due to abnormal persistence of the first hypochordal bar (Kessel et al., 1990), this further suggests that RARγ plays a specific role in the specification of this particular structure in both loss (receptor ablation) and gain of function (RA excess) situations. Whether these findings are indicative of true functional specificity or the lack of expression of other RARs in the appropriate tissues will require alternative approaches, such as gain of function.

ACKNOWLEDGEMENTS

The authors thank Pierre Chambon for the RARγ null mouse line, Marie-Claude Marchand for expert technical assistance and Christian Charbonneau for assistance with photography. This work was supported by a grant from the Medical Research Council of Canada and an MRC scholarship to D.L.

REFERENCES

Boylan, J.F., Lohnes, D., Taneja, R., Chambon, P., and Gudas, L.J. (1993) Loss of retinoic acid receptor gamma function in F9 cells by gene disruption results in aberrant Hoxa-1 expression and differentiation upon retinoic acid treatment. *Proc. Natl. Acad. Sci. U.S.A.* **90**: 9601-9605.

Boylan, J.F., Lufkin, T., Achkar, C.C., Taneja, R., Chambon, P., and Gudas, L.J. (1995) Targeted disruption of retinoic acid receptor alpha (RAR alpha) and RAR gamma results in receptor-specific alterations in retinoic acid-mediated differentiation and retinoic acid metabolism. *Mol. Cell. Biol.* **15**: 843-851.

Bronner-Fraser, M. (1995) Origins and developmental potential of the neural crest. *Exp. Cell Res.* **218**: 405-417.

Chambon, P. (1996) A decade of molecular biology of retinoic acid receptors. *FASEB J.***10**:940-954.

Chang, C.P., Shen, W.F., Rozenfeld, S., Lawrence, H.J., Largman, C., and Cleary, M.L. (1995) Pbx proteins display hexapeptide-dependent cooperative DNA binding with a subset of Hox proteins. *Genes Dev.* **9**: 663-674.

Dersch, H., and Zile, M.H. (1993) Induction of normal cardiovascular development in the vitamin A-deprived quail embryo by natural retinoids. *Dev. Biol.* **160**: 424-433.

Dollé, P., Ruberte, E., Kastner, P., Petkovich, M., Stoner, C.M., Gudas, L.J., and Chambon, P. (1989) Differential expression of genes encoding alpha, beta and gamma retinoic acid receptors and CRABP in the developing limbs of the mouse. *Nature* **342**: 702-705.

Dollé, P., Ruberte, E., Leroy, P., Morriss-Kay, G., and Chambon, P. (1990) Retinoic acid receptors and cellular retinoid binding proteins. I. A systematic study of their differential pattern of transcription during mouse organogenesis. *Development* **110**: 1133-1151.

Grondona, J.M., Kastner, P., Gansmuller, A., Décimo, D., Chambon, P., and Mark, M. (1996) Retinal dysplasia and degeration in RAR beta-2/RAR gamma-2 compound mutant mice. *Development* **122**: 2173-2188.

Heyman, R.A., Mangelsdorf, D.J., Dyck, J.A., Stein, R.B., Eichele, G., Evans, R.M., and Thaller, C. (1992) 9-cis retinoic acid is a high affinity ligand for the retinoid X receptor. *Cell* **68**: 397-406.

Horan, G.S., Kovacs, E.N., Behringer, R.R., and Featherstone, M.S. (1995) Mutations in paralogous Hox genes result in overlapping homeotic transformations of the axial skeleton: evidence for unique and redundant function. *Dev. Biol.* **169**: 359-372.

Ito, K., and Morita, T. (1995) Role of retinoic acid in mouse neural crest cell development in vitro. *Dev. Dyn.* **204**:211-218.

Kastner, P., Mark, M., and Chambon, P. (1995) Nonsteroid nuclear receptors - what are genetic studies telling us about their role in real life. *Cell* **83**: 859-869.

Kessel, M. (1992) Respecification of vertebral identities by retinoic acid. *Development* **115**: 487-501.

Kessel, M., Balling, R., and Gruss, P. (1990) Variations of cervical vertebrae after expression of a Hox-1.1 transgene in mice. *Cell* **61**: 301-308.

Kessel, M., and Gruss, P. (1991) Homeotic transformations of murine vertebrae and concomitant alteration of Hox codes induced by retinoic acid. *Cell* **67**: 89-104.

Langston, A.W., and Gudas, L.J. (1992) Identification of a retinoic acid responsive enhancer 3' of the murine homeobox gene Hox-1.6. *Mech. Dev.* **38**: 217-227.

Le Mouellic, H., Lallemand, Y., and Brulet, P. (1992) Homeosis in the mouse induced by a null mutation in the Hox-3.1 gene. *Cell 69*: 251-264.

Lohnes, D., Kastner, P., Dierich, A., Mark, M., LeMeur, M., and Chambon, P. (1993) Function of retinoic acid receptor γ (RARγ) in the mouse. *Cell* **73**: 643-658.

Lohnes, D., Mark, M., Mendelsohn, C., Dollé, P., Dierich, A., Gorry, P., Gansmuller, A., and Chambon, P. (1994) Function of the retinoic acid receptors (RARs) during development (I). Craniofacial and skeletal abnormalities in RAR double mutants. *Development* **120**: 2723-2748.

Look, J., Landwehr, J., Bauer, F., Hoffmann, A.S., Bluethmann, H., and Lemotte, P. (1995) Marked resistance of RARγ-deficient mice to the toxic effects of retinoic acid. *Am. J. Physiol.- Endo. and Met.* **32**: E91-E98.

Lufkin, T., Lohnes, D., Mark, M., Dierich, A., Gorry, P., Gaub, M.P., LeMeur, M., and Chambon, P. (1993) High postnatal lethality and testis degeneration in retinoic acid receptor alpha mutant mice. *Proc.Natl. Acad. Sci. U.S.A.* **90**: 7225-7229.

Luo, J., Pasceri, P., Conlon, R.A., Rossant, J., and Giguère, V. (1995) Mice lacking all isoforms of retinoic acid receptor beta develop normally and are susceptible to the teratogenic effects of retinoic acid. *Mech. Dev.* **53**: 61-71.

Luo, J.M., Sucov, H.M., Bader, J.A., Evans, R.M., and Giguère, V. (1996) Compound mutants for retinoic acid receptor (RAR) beta and RAR-alpha-1 reveal developmental functions for multiple rar-beta isoforms. *Mech. Dev.* **55**: 33-44.

Mackensen, J.A., and Stevens, L.C. (1960). Rib fusions, a new mutation in the mouse. *J. Hered.* **51**: 264-268.

Maden, M., Gale, E., Kostetskii, I., and Zile, M. (1996) Vitamin A-deficient quail embryos have half a hindbrain and other neural defects. *Curr. Biol.* **6**: 417-426.

Mangelsdorf, D.J., and Evans, R.M. (1995) The RXR heterodimers and orphan receptors. *Cell* **83**: 841-850.

Marshall, H., Morrison, A., Studer, M., Popperl, H., and Krumlauf, R. (1996) Retinoids and Hox genes. *FASEB J* **10**: 969-978.

Mendelsohn, C., Ruberte, E., LeMeur, M., Morriss-Kay, G. and Chambon, P. (1991) Developmental analysis of the retinoic acid-inducible RAR-beta 2 promoter in transgenic animals. *Development* **113**: 723-734.

Mendelsohn, C., Lohnes, D., Décimo, D., Lufkin, T., LeMeur, M., Chambon, P., and Mark, M. (1994a) Function of the retinoic acid receptors (RARs) during development

(II). Multiple abnormalities at various stages of organogenesis in RAR double mutants. *Development* **120**: 2749-2771.

Mendelsohn, C., Mark, M., Dollé, P., Dierich, A., Gaub, M.P., Krust, A., Lampron, C., and Chambon, P. (1994b) Retinoic acid receptor beta 2 (RAR beta 2) null mutant mice appear normal. *Dev. Biol.* **166**: 246-258.

Morgan, B.A., and Tabin, C. (1994) Hox genes and growth - early and late roles in limb bud morphogenesis. *Development (Suppl.)*: 181-186.

Morriss-Kay G (1993) Retinoic acid and craniofacial development: molecules and morphogenesis. *Bioessays* **15**: 9-15.

Ogura, T., and Evans, R.M. (1995) Evidence for two distinct retinoic acid response pathways for HOXB1 gene regulation. *Proc. Natl. Acad. Sci. U.S.A.* **92**: 392-396.

Popperl, H., and Featherstone, M.S. (1993) Identification of a retinoic acid response element upstream of the murine Hox-4.2 gene. *Mol. Cell. Biol.* **13**: 257-265.

Ramirez-Solis, R., Zheng, H., Whiting, J., Krumlauf, R., and Bradley, A. (1993) Hoxb-4 (Hox-2.6) mutant mice show homeotic transformation of a cervical vertebra and defects in the closure of the sternal rudiments. *Cell* **73**: 279-294.

Ruberte, E., Dollé, P., Krust, A., Zelent, A., Morriss-Kay, G., and Chambon, P. (1990) Specific spatial and temporal distribution of retinoic acid receptor gamma transcripts during mouse embryogenesis. *Development* **108**: 213-222.

Ruberte, E., Dollé, P., Chambon, P., and Morriss-Kay, G. (1991) Retinoic acid receptors and cellular retinoid binding proteins. II. Their differential pattern of transcription during early morphogenesis in mouse embryos. *Development* **111**: 45-60.

Simeone, A., Acampora, D., Arcioni, L., Andrews, P.W., Boncinelli, E., and Mavilio, F. (1990) Sequential activation of HOX2 homeobox genes by retinoic acid in human embryonal carcinoma cells. *Nature* **346**: 763-766.

Simeone, A., Acampora, D., Nigro, V., Faiella, A., D'Esposito, M., Stornaiuolo, A., Mavilio, F., and Boncinelli, E. (1991) Differential regulation by retinoic acid of the homeobox genes of the four HOX loci in human embryonal carcinoma cells. *Mech. Dev.* **33**: 215-227.

Sokal, R.R., and Rohlf, F.J. (1981) In *Biometry (second edition)*(eds. J. Wilson and S. Cotter), pp 152-154. W.H. Freeman and Co., San Francisco.

Sporn, M.B., Roberts, A.B., and Goodman, D.S. (1994) In *The Retinoids (second edition)* (eds. Sporn, M.B., Roberts, A.B., and Goodman, D.S.), pp 319-350. Raven Press, New York.

Studer, M., Popperl, H., Marshall, H., Kuroiwa, A., and Krumlauf, R. (1994) Role of a conserved retinoic acid response element in rhombomere restriction of Hoxb-1. *Science* **265**: 1728-1732.

Sucov, H.M., and Evans, R.M. (1995) Retinoic acid and retinoic acid receptors in development. *Mol. Neurobiology* **10**: 169-184.

Sucov, H.M., Izpisua-Belmonte, J.C., Ganan, Y., and Evans, R.M. (1995) Mouse embryos lacking RXR alpha are resistant to retinoic-acid-induced limb defects. *Development* **121**: 3997-4003.

Theiler, K., Varnum,D., and Stevens, L.C. (1974) Development of rachiterata, a mutation in the house mouse with 6 cervical vertebrae. *Z. Anat. Entwickl-Gesch.* **145**: 75-80.

Theiler, K., and Varnum, D. (1985) Development of rib-vertebrae: a new mutation in the house mouse with accessory caudal duplications. *Anat. Embryol.* **173**: 111-116.

Thompson, J.N., Howell, J. McC., and Pitt, G.A.J. (1964) Vitamin A and reproduction in rats. *Proc. Royal Soc.* **159**: 510-535.

Wilson, J.C., Roth, C.B., and Warkany, J. (1953) An analysis of the syndrome of maternal vitamin A deficiency. Effects of restoration of vitamin A at various times during gestation. *Am. J. Anat.* **92**: 189-217.

Wolbach, S.B., and Howe, P.R. (1925) Tissue changes following deprivation of fat-soluble A vitamin. *J. Exp. Med.* **42**: 753-777.

CHAPTER 3

ARTICLE

A Molecular Basis for Retinoic Acid-Induced Axial Truncation

Angelo Iulianella[§†], Barbara Beckett[¶], Martin Petkovich[¶#] and David Lohnes[§‡†]

[§]Programme de biologie moléculaire, Université de Montréal, ¶Cancer Research Laboratories, #Departments of Pathology and Biochemistry, Queen's University, Kingston, Ontario, ‡Division of Experimental Medicine, McGill University, and †the Institut de Recherches Cliniques de Montréal, 110 Avenue des Pins, ouest, Montréal, Québec, Canada, H2W 1R7

***Developmental Biology*, Volume 205, Pages 33-48, 1999**

ABSTRACT

Dietary deprivation and gene disruption studies clearly demonstrate that biologically active retinoids, such as retinoic acid, are essential for numerous developmental programs. Similar ontogenic processes are also affected by retinoic acid excess, suggesting that the effects of retinoid administration reflect normal retinoid-dependent events. In the mouse, exogenous retinoic acid can induce both anterior (anencephaly, exencephaly) and posterior (spina bifida) neural tube defects depending on the developmental stage of treatment. Retinoic acid receptor γ (RARγ) mediates these effects on the caudal neural tube at 8.5 days post-coitum, as RARγ null mice are completely resistant to spina bifida induced by retinoic acid at this stage. We therefore used this null mouse as a model to examine the molecular nature of retinoid-induced caudal neural tube defects by using a panel of informative markers and comparing their expression between retinoic acid treated wild type and RARγ null embryos.

Our findings indicate that treatment of wild type embryos led to a rapid and significant decrease in the caudal expression of all mesodermal markers examined (e.g. *brachyury, wnt-3a, cdx-4*). In contrast, somite, neuroepithelial, notochord, floorplate, and hindgut markers were unaffected. RARγ null mutants exhibited normal expression patterns for all markers examined, consistent with the notion that mesodermal defects underlie the etiology of retinoid-induced spina bifida.

We also found that caudal somitic, but not posterior pre-somitic, embryonic tissues contained detectable bio-active retinoids, an observation which correlated with the ability of the latter tissues to rapidly clear exogenous RA. Interestingly, transcripts encoding *mP450RAI*, a cytochrome P450, the product of which is believed to catabolize retinoic acid, were abundant in the retinoid-poor region of the caudal embryo. *mP450RAI* was rapidly induced by retinoic acid treatment in vivo, consistent with previous data suggesting that it plays a critical role in retinoid signaling. These data suggest that nascent mesoderm is highly sensitive to retinoic acid, and that mP450RAI serves to tightly regulate retinoid levels in the caudal embryo. These findings also raise the possibility that RA may play a role in the generation of posterior mesoderm derivatives in part by affecting *brachyury* expression.

INTRODUCTION

Retinoids (vitamin A and its derivatives) play important roles in the maintenance of various tissues in the adult vertebrate and are essential for diverse embryological processes (reviewed in Sporn *et al.* 1994). Rodents fed a vitamin A deficient (VAD) diet show weight loss, sterility and squamous metaplasia of various tissues including the respiratory, alimentary, and genito-urinary tracts, and eyes and related glands (Wolbach and Howe, 1925). Likewise, VAD during embryogenesis results in fetuses exhibiting a spectrum of congenital defects involving the eye, genito-urinary and respiratory tracts, among other tissues (Wilson *et al.* 1953). Retinoic acid (RA) can prevent or reverse all of the defects generated by post-partum VAD (with the exception of blindness) indicating that RA (or closely related derivatives) is the principal active metabolite of vitamin A (Wilson *et al.* 1953). Moreover, studies using VAD rats supplemented with RA as a model for the effects of stage-specific retinoid-deficiency also suggest that RA can fulfill the developmental requirements for vitamin A (Dickman *et al.* 1997).

A molecular dissection of the retinoid signaling pathway became possible with the identification of the RA receptors (RARs; reviewed in Chambon, 1996). In addition to the three separate RAR types (RARα, β, and γ), differential promoter usage and alternative splicing generates N-terminal variant isoforms for each gene (RARα1 and α2, RARβ1-β4, RARγ1 and γ2). RARs function as ligand-inducible transcriptional regulators in conjunction with a retinoid x receptor partner (RXRα, β, γ; Leid *et al.* 1993; Mangelsdorf and Evans, 1995). While RARs are activated by both all-trans and 9-cis RA, RXRs, which can homodimerize and function as transcriptional regulators in certain contexts, are activated only by 9-cis RA (Mangelsdorf and Evans, 1995; Heyman *et al.* 1992).

Targeted mutagenesis of the RARs has been employed to establish the roles of each of these receptors in vivo (Kastner *et al.* 1995; Sucov and Evans, 1995). While disruption of a single RAR isoform results in little or no apparent abnormality, mice devoid of all RARα or RARγ isoforms exhibit several defects similar to those observed in post-partum VAD studies (Lohnes *et al.* 1993; Lufkin *et al.* 1993). In contrast, RAR compound null fetuses recapitulate essentially all aspects of the fetal VAD syndrome, as

well as a number of additional malformations not previously associated with such dietary deficiency studies (Luo *et al.* 1996; Mendelsohn *et al.* 1994; Lohnes *et al.* 1994). Moreover, the penetrance and expressivity of the abnormalities observed in RAR single null offspring are significantly increased in RXRα/RARγ compound mutants, suggesting that RXR/RAR heterodimers transduce the retinoid signal in vivo, at least during development (Kastner *et al.* 1997). These observations offer convincing evidence that the RARs are the principle transducer of the retinoid signal, although a considerable degree of functional redundancy appears to exist among these receptors.

Pharmacological doses of RA leads to diverse congenital malformations, the precise nature of which depends on the dosage and developmental stage of exposure (Morriss-Kay *et al.* 1994;; Kessel and Gruss, 1991). In contrast to the apparent functional redundancy among the RARs during normal development, specific retinoid receptors are clearly involved in transducing subsets of the teratogenic effects of RA. This is evidenced by the observation that RARγ null embryos are completely resistant to the lumbosacral truncations and spina bifida caused by RA administration at 8.5 days post coitum (dpc) (Lohnes *et al.* 1993). More recently, we have also found that RARγ null mutants are highly resistant to RA-induced anencephaly and exencephaly at 7.3 dpc, supporting a role for this receptor in retinoid-induced anterior neural tube defects (Iulianella and Lohnes, 1997). Similar studies have also shown a critical role for RXRα in mediating the teratogenic RA signal leading to limb defects (Sucov and Evans, 1995b).

Neural tube defects (NTD) are prevalent congenital disorders in the human population, afflicting 1-4 newborns in every 1000 (Copp, 1994a; Copp and Bernfield, 1994). Although the molecular basis underlying these disorders are poorly understood, retinoid signaling is clearly required for normal development of the neural tube, as exemplified by the high incidence of exencephaly in RARα/γ double null mutants (Lohnes et al. 1994). Aberrant retinoid signaling has also been implicated in the etiology of spina bifida in the *curly tail (ct)* mouse mutant. In afflicted *ct/ct* embryos, RARγ and RARβ transcripts are downregulated in the posterior neuropore (PNP) and hindgut, respectively (Chen *et al.*, 1995), and the extent of this decrease is associated with the severity of the delay in PNP closure which is believed to be the underlying basis for the spina bifida observed in this mutant (Brook *et al.* 1991). Moreover, RA can exacerbate

or attenuate the incidence of NTD in *ct/ct* offspring depending on the dose and time of administration in a manner which correlates with normalization of RARβ and γ transcripts (Chen *et al.* 1995). Finally, as described above, RARγ specifically transduces RA-induces spina bifida, demonstrating a specific and unique role for this receptor in this teratogenic outcome.

In the present study, the RARγ-null mouse was used to investigate the mechanistic and molecular nature of RA-induced spina bifida by comparing the expression of tissue-specific markers between wildtype and RARγ-null mutant embryos treated with RA. We report that, in a situation of RA excess, RARγ specifically effects gene expression in posterior mesoderm at 8.5 dpc. Using a sensitive reporter cell assay, we also observed that caudal somite-containing tissues are relatively enriched in diffusible active retinoids at 8.5-9.5 dpc, whereas pre-somitic embryonic tissues are devoid of bioavailable RA at all stages examined. Furthermore, in contrast to somitic regions, caudal tissues rapidly cleared exogenous RA. This observation correlated closely with the expression of *mP450RAI*, a cytochrome P450 family member capable of metabolizing RA to more polar derivatives. These data suggest that nascent mesoderm populations are highly sensitive to variations in retinoid level, and also raise the possibility that RA plays a role in events critical to the normal differentiation of posterior mesoderm during late gastrulation.

MATERIALS AND METHODS

Embryos And RA Treatment

The RARγ null mice used in this study have been previously described (Lohnes *et al.* 1993). RARγ heterozygous and null embryos were generated from $RAR\gamma^{+/-}$ intercrosses. Wildtype embryos were derived either from the above matings, from intercrosses of wildtype stock from the RARγ colony (C57BL/6–129Sv hybrid), or from CD-1 intercrosses; no appreciable differences in gene expression profiles were noted between any of these backgrounds. Mice were mated overnight and females were examined the following morning for the presence of a vaginal plug; noon of the day of plug was considered as 0.5 dpc. Pregnant females were dosed by oral gavage with all-trans RA

dissolved in corn oil to a final delivery of 100mg/kg at 8.4 dpc. Pregnant females were sacrificed 4, 8, or 24 hours post-treatment and embryos dissected in phosphate buffered saline (PBS), fixed overnight in 4% paraformaldehyde, dehydrated through a methanol series and stored at -20°C in 100% methanol. Yolk sacs were lysed according to (Hogan *et al.* 1994) and used to establish genotype by PCR as described previously (Iulianella and Lohnes, 1997).

In Situ *Hybridization Analysis*

Similarly staged embryos (according to somite number) were pooled by genotype and time of exposure to RA and rehydrated through a methanol series. The *mP450RAI* cDNA (Abu-Abed *et al.* 1998) was used to generate a digoxygenin-labeled riboprobe by linearizing with EcoRI and transcribing with T7 RNA polymerase. The *brachury, shh, wnt-3a, HNF-3β, pax-3, follistatin*, and *cdx-4* riboprobes were generated as previously described (Gamer and Wright, 1993; Albano *et al.* 1994; Goulding *et al.* 1991; Sasaki and Hogan, 1993; Parr *et al.* 1993; Echelard *et al.* 1993; Wilkinson *et al.* 1990). Whole mount *in situ* hybridizations were performed according to (Wilkinson, 1992).

After *in situ* hybridization, embryos were cleared, photographed under a dissecting microscope, post-fixed in 4% paraformaldehyde/0.2% glutaraldehyde at 4°C for 30 minutes, rinsed in several changes of PBS and embedded in Paraplast (Fisher). Sectioning was performed on a Jung RM 2055 microtome at 7μm and sections processed according to(Hogan *et al.* 1994). Whole mount *in situ* hybridization specimens and sections were photographed with 64T Ektachrome film (Kodak).

Generation And Analysis Of Representative cDNA

To quantify differences in gene expression, caudal tissue (posterior to the closed neural tube) of treated and untreated individual embryos was dissected and used for the generation of representative cDNA by PCR essentially as previously described (Sauvageau *et al.* 1994). Briefly, RNA was prepared by lysis in a 5M guanidium isothiocyanate solution and precipitated using a linear polyacrylamide carrier. Reverse transcription was carried out at 37°C for 10 minutes in a 10μl volume using 100 units of MMLV reverse transcriptase (Gibco-BRL) and 0.2μg/μl of a primer

(5'GATGTCGTCCAGGCCGCTCTGGACAAAATATGAATTCT $T(T)_{21}$-3') under standard reaction conditions. Homopolymeric A tailing of the cDNA was accomplished using 8mM dATP and 7.5 units of terminal deoxynucleotidyl transferase (Gibco-BRL) at 37°C for 15 minutes. PCR was performed according to (Sauvageau *et al.* 1994), using the same primer as employed for the reverse transcription. Controls consisted of caudal tissue extracts that were not reverse transcribed, but were subsequently subjected to tailing and amplification reactions. One fifth (10µl) of the PCR reaction was run on a 1% agarose gel and stained with ethidium bromide to visualize product.

Alkali Southern blots were prepared using Gene Screen Plus membranes (NEN-Dupont) according to the manufacturer's directions. Hybridizations were performed overnight at 42°C in a formamide-based buffer (40% formamide, 0.9M sodium chloride, 50mM sodium phosphate, 2mM EDTA, 4X Denhardts, 0.1% SDS) supplemented with 0.1mg/ml denatured salmon sperm DNA with approximately 10^6 cpm/ml of denatured probe prepared by random priming. Sequences used to generate the probes were derived from the cDNAs employed for *in situ* hybridization by appropriate restriction digestion followed by agarose electrophoresis and isolation by Gene Clean (Bio 101). Blots were washed in 2X SSC/0.1% SDS three times at 65°C, followed by three washes in 0.2X SSC/0.1% SDS at the same temperature.

Following autoradiography, densitometry was performed using the Alpha Imager IS-1000 software package, version 2.0 (Alpha Innotech corporation, San Leandro, CA, USA). Values were normalized with respect to β-actin and expressed as fold change relative to untreated controls. Statistical analysis was performed by Student's t-test.

Determination Of Retinoid Bioavailability

Retinoid bioavailability in embryonic tissues was assessed using F9 embryonal carcinoma cells transfected with a RA-responsive Lac Z reporter construct previously described (Wagner *et al.* 1992). Caudal pre-somitic and adjacent somite-containing tissues were dissected from 8.5 to 11.5 dpc embryos and placed onto the reporter cell monolayers (~90% confluence) in 96-well plates. For 9.5 to 11.5 dpc embryos, two somitic samples were taken at different axial levels; one containing the most recently formed somites, the other being immediately rostral to the first somite-containing section.

In order to keep the explant size constant, the number of somites contained within each sections varied from 4-6, with the first section containing fewer somites but including some condensing pre-somitic paraxial mesoderm, while the more rostral sample included 6 somites. Tissues were incubated on the monolayers overnight according to Wagner *et al* (Wagner *et al.* 1992). The samples were then washed in PBS and fixed with 4% paraformaldehyde on ice for 10 minutes, followed by two washes with PBS. Samples were then stained for β-galactosidase activity as described (Lim and Chae, 1989), and photographed using 64T Ektachrome film.

To determine the ability of somitic and caudal tissues to clear exogenous retinoids, pregnant CD1 females were treated with 100mg RA/kg at 8.4 dpc and embryos dissected 3.5 or 6 hours post-treatment. Caudal and rostral explants were then assayed for RA bioavailabilty as described above.

RESULTS

Wildtype mouse embryos treated with exogenous RA (100mg/kg maternal weight) at 8.5 dpc exhibit caudal axial dysmorphogenesis (Kapron-Bras and Trasler, 1988a; Kessel and Gruss, 1991). In contrast, RARγ null embryos are completely resistant to this effect, with heterozygotes exhibiting an intermediate phenotype (Lohnes *et al.* 1993). However, RARγ mutants still exhibit homeotic transformations following treatment, suggesting that this receptor specifically transduces retinoid-induced axial truncations. Thus, the RARγ null mouse is a useful model to examine the molecular nature underlying this defect.

We pursued this by comparing the effect of RA excess on the expression of genes in wildtype and RARγ null mutant embryos. Genes investigated were either specific to lineages potentially involved in this defect and/or encoded products known to be essential for normal development of the caudal embryo. These included *brachyury* and *wnt-3a*, whose transcripts are expressed in the primitive streak, associated nascent mesoderm and neuroepithelium. *Brachyury* is also expressed in the notochord (Parr *et al.* 1993; Roelink and Nusse, 1991; Wilkinson *et al.* 1990; Kispert and Herrmann, 1994). Mutation of either of these loci leads to caudal axial truncations similar to that evoked by RA treatment (Takada *et al.* 1994; Beddington *et al.* 1992). *Cdx-4* was chosen as an

additional primitive streak, nascent mesoderm, and caudal neuroepithelium marker (Gamer and Wright, 1993). *Shh* and *HNF-3β* are expressed in the floorplate, notochord, and hindgut, and are critical for axial patterning (Chiang *et al.* 1996; Ang and Rossant, 1994; Echelard *et al.* 1993; Sasaki and Hogan, 1993). *Pax-3* transcripts are localized in the dorsal somite, the neuropithelilum and the presumptive neural crest lineage (Goulding *et al.* 1991), and mutation of this gene leads to NTD, including spina bifida (Copp, 1994a). *Follistatin* was examined as an additional somite marker (Albano *et al.* 1994).

Pregnant dams from RARγ heterozygote intercrosses were dosed with RA at 8.4 dpc and RARγ null, heterozygote, and wildtype embryos were examined for the expression of the above transcripts 4, 8, or 24 hours later. For all the *in situ* hybridization analysis, a minimum of 4 similarly staged embryos for each genotype were examined, with all experiments being performed at least twice. Whenever possible, littermates for each genotype were compared, thus controlling for subtle differences in maternal RA-absorption and clearance kinetics. The results of all *in situ* hybridization experiments were consistent for all embryos of a given genotype and were independent of minor variations in staging.

RA Attenuates Markers Of Nascent Mesoderm

In untreated mice at 8.5 dpc *brachyury* transcripts are principally located in the notochord, the primitive streak remnant and in nascent mesoderm, with lower expression in neural plate and hindgut endoderm (Wilkinson *et al.* 1990; Kispert and Herrmann, 1994); Fig. 3-1A,E). In contrast, in wildtype embryos examined 24 hours post-treatment expression was observed only in the notochord, which was, however, highly dysmorphic in the caudal region (compare Fig 3-1A to 3-1B). Treatment also resulted in truncation of the axis (compare Fig. 3-1B to 1A) as well as abnormal tail flexion (large arrow in Fig. 3-1B), a defect which precedes spina bifida in other mouse models (Brook *et al.* 1991; Copp, 1994; Copp and Bernfield, 1994). In contrast, RARγ$^{-/-}$ littermates did not display overt axial defects and showed no differences in *brachyury* expression relative to untreated controls (compare Fig. 3-1A to 3-1D). RARγ$^{+/-}$ embryos showed an intermediate decrease in expression with accompanying caudal flexion defects (large arrow, Fig. 3-1C), consistent with the partial resistance of these heterozygotes to RA-

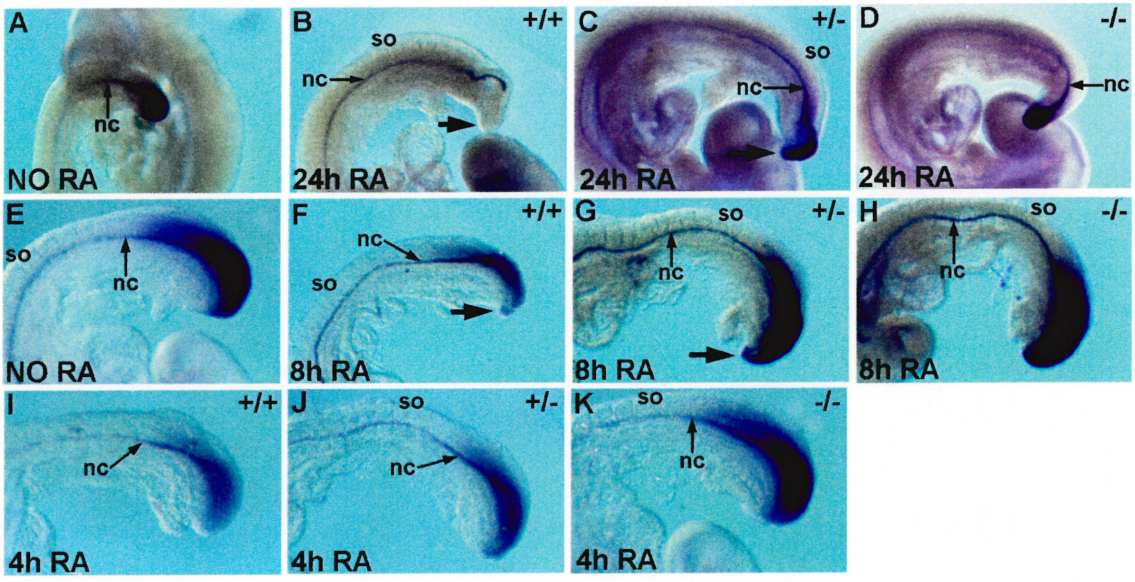

Figure 3-1. *Brachyury* expression is rapidly downregulated by RA treatment.

Pregnant dams from RARγ$^{+/-}$ intercrosses were treated with RA at 8.4 dpc and embryos collected 24 (B-D), 8 (F-H) or 4 hours (I-K) post-gavage. RA treatment resulted in a complete extinction of caudal expression in wildtype embryos 24 hours post treatment (B, compare to untreated embryo in A) and a significant repression at 8 or 4 hours post-exposure (F, and I respectively; compare to untreated specimen in E). RARγ$^{-/-}$ embryos were completely resistant to this effect at all stages examined (D, H, K) whereas heterozygotes exhibited an intermediate response (C, G, J). The large arrow denotes the tail flexion defect evident in wildtype and heterozygous offspring 24 (B, C) or 8 (G, I) hours after gavage. nc, notochord; so, somite.

induced spina bifida (Lohnes *et al.* 1993). Untreated RARγ$^{-/-}$ embryos exhibited *brachyury* expression comparable to control wildtype specimens (data not shown).

The long lapse between treatment and analysis of expression confounded clear assessment of whether this was a primary effect. Therefore we examined embryos exposed to RA for shorter periods and found that *brachyury* transcripts were consistently downregulated 8 or 4 hours post-treatment in wild-type embryos (compare Figs. 3-1E to F or I), with tail flexion defects apparent after 8 hours of exposure (large arrow in Fig. 3-1F). As observed with longer treatment times, RARγ$^{-/-}$ littermates were completely resistant to this effect (Fig. 3-1H and K compare to E), while RARγ heterozygotes showed an intermediate response (Figs. 3-1G and J). Embryos examined 4 hours post-treatment did not exhibit any gross morphological abnormalities, such as the tail flexion defects observed 8 and 24 hours after RA exposure, suggesting that the decrease in *brachyury* preceded overt dysmorphogenesis.

To more precisely compare the effects of RA on *brachyury*, a PCR-based technique was used to derive representative cDNAs from pre-somitic caudal tissue from single embryos, as described in Materials and Methods. Analyses were performed in triplicate from independent embryos (untreated or 4 or 8 hours after RA gavage), the hybridization signal quantified by densitometry and normalized relative to β-actin signals. Consistent with the *in situ* hybridization data, this analysis confirmed a reproducible and significant decline in *brachyury* transcripts 4 and 8 hours post-treatment (Fig. 3-2).

Like *brachyury*, null mutation of *wnt-3a* leads to caudal axial truncations (Takada *et al.* 1994). Moreover, a hypomorphic allele of *wnt-3a* (*vestigial tail*) is associated with a relatively mild caudal truncation, demonstrating a gene dosage effect and further illustrating a critical role for this gene product in the generation or maintenance of posterior mesoderm (Greco *et al.* 1996). In the caudal embryo at 8.5 dpc, *wnt-3a* is expressed in the primitive streak remnant, the neuroepithelium encompassing the PNP and the underlying mesenchyme (Roelink and Nusse, 1991). In this expression domain, RA treatment resulted in a downregulation of expression 8 (Fig. 3-3A, B) or 4 hours (data not shown) post-exposure in wildtype, relative to RARγ$^{-/-}$ specimens (note that for this

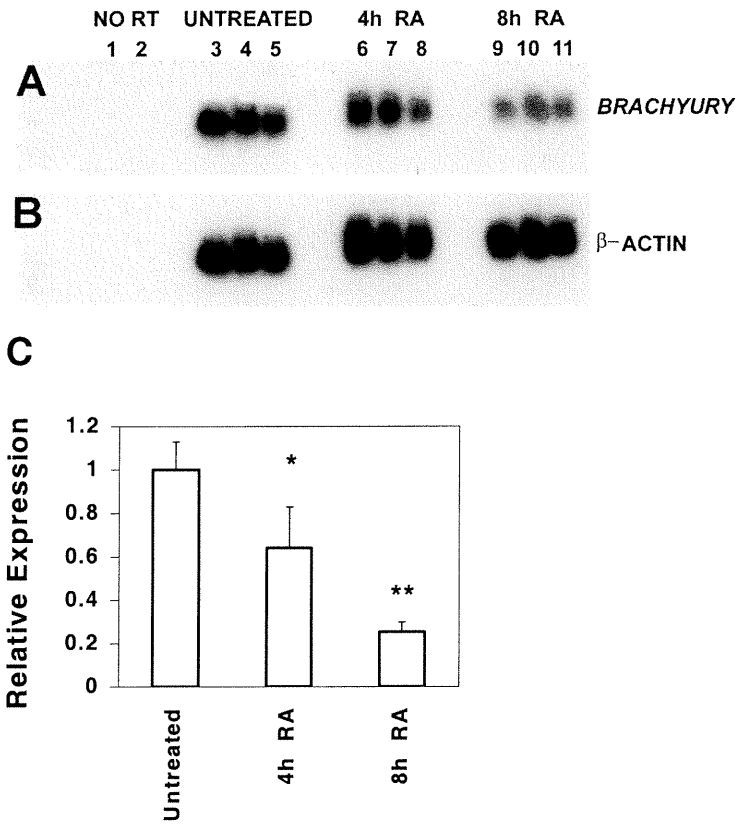

Figure 3-2. Semi-quantitative analysis of *brachyury* expression.

Representative cDNAs from untreated embryos (lanes 3-5), or from samples 4 (lanes 6-8) or 8 hours (lanes 9-11) following RA treatment were generated from individual embryos as described in materials and methods No RT indicates no reverse transcriptase controls prepared using untreated (lane 1) or RA-treated (lane 2; 8 hours RA exposure) specimens. Southern blots were hybridized to either *brachyury* (A) or *β-actin* (B) probes. (C) Densitometric scanning was performed and the *brachyury* signal normalized with respect to expression of *β-actin*. Results were plotted relative to the ratio obtained from untreated embryos. Error bars indicate standard deviation from the mean. Significantly different from untreated embryos *, $p<0.05$; **, $P<0.01$ by Student's t-test.

and all other *in situ* analysis described below, expression in RARγ null embryos, with or without RA, was comparable to that in untreated wildtypes; data not shown). As with *brachyury*, gene dosage effects were also observed, with heterozygotes exhibiting an intermediate decline in *wnt-3a* transcripts (data not shown).

Cdx-4 is a homeobox-containing gene belonging to the *caudal* gene family. At 8.5 dpc, *cdx-4* transcripts are detected in caudal mesoderm and neuroectoderm including the primitive streak remnant, presomitic paraxial and lateral plate mesoderm and hindgut endoderm (Gamer and Wright, 1993). As with *brachyury* and *wnt-3a*, *cdx-4* transcript levels decreased in wildtype embryos 8 hours following RA treatment, while expression was unaffected in RARγ null littermates (Figs. 3-3C and 3-3D, respectively).

To determine whether the above observations were secondary to effects on other lineages, the expression of additional genes were examined. At 8.5 dpc, *shh* and *HNF-3β* both label floorplate, notochord, hindgut endoderm and the ventral midline of the midbrain. Moreover, both gene products are essential for normal axial patterning (Chiang *et al.* 1996; Ang and Rossant 1994). Embryos examined 8 hours post-treatment did not show any overt differences in *shh* or *HNF-3β* expression between wildtype and RARγ$^{-/-}$ embryos (Fig. 3-3E-3-3H), suggesting that there is no acute perturbation of notochord, floorplate or hindgut endoderm populations which could cause secondary effects on the caudal embryo.

Pax-3 is expressed in the dorsal somite, neuroepithelium and presumptive neural crest cell populations in 8.5 dpc embryos (Goulding *et al.* 1991). Mice mutant for this gene (*splotch*) develop spina bifida due to an accumulation of neural crest cells at the tip of the open PNP, thereby delaying its closure (Moase and Trasler, 1990). Moreover, RA can interact with the *spotch* allele leading to an enhanced or decreased incidence of spina bifida depending on the timing and dose of RA administered (Kapron-Bras and Trasler, 1984, 1985; Kapron-Bras *et al.* 1988). However, no differences in *pax-3* expression were observed between wildtype and RARγ$^{-/-}$ embryos 8 hours post-treatment (Fig. 3-3I and 3-3J). Likewise, RA treatment did not affect *follistatin* expression, which is expressed in all somites at 8.5 dpc (data not shown; Albano *et al.* 1994). These data suggest that

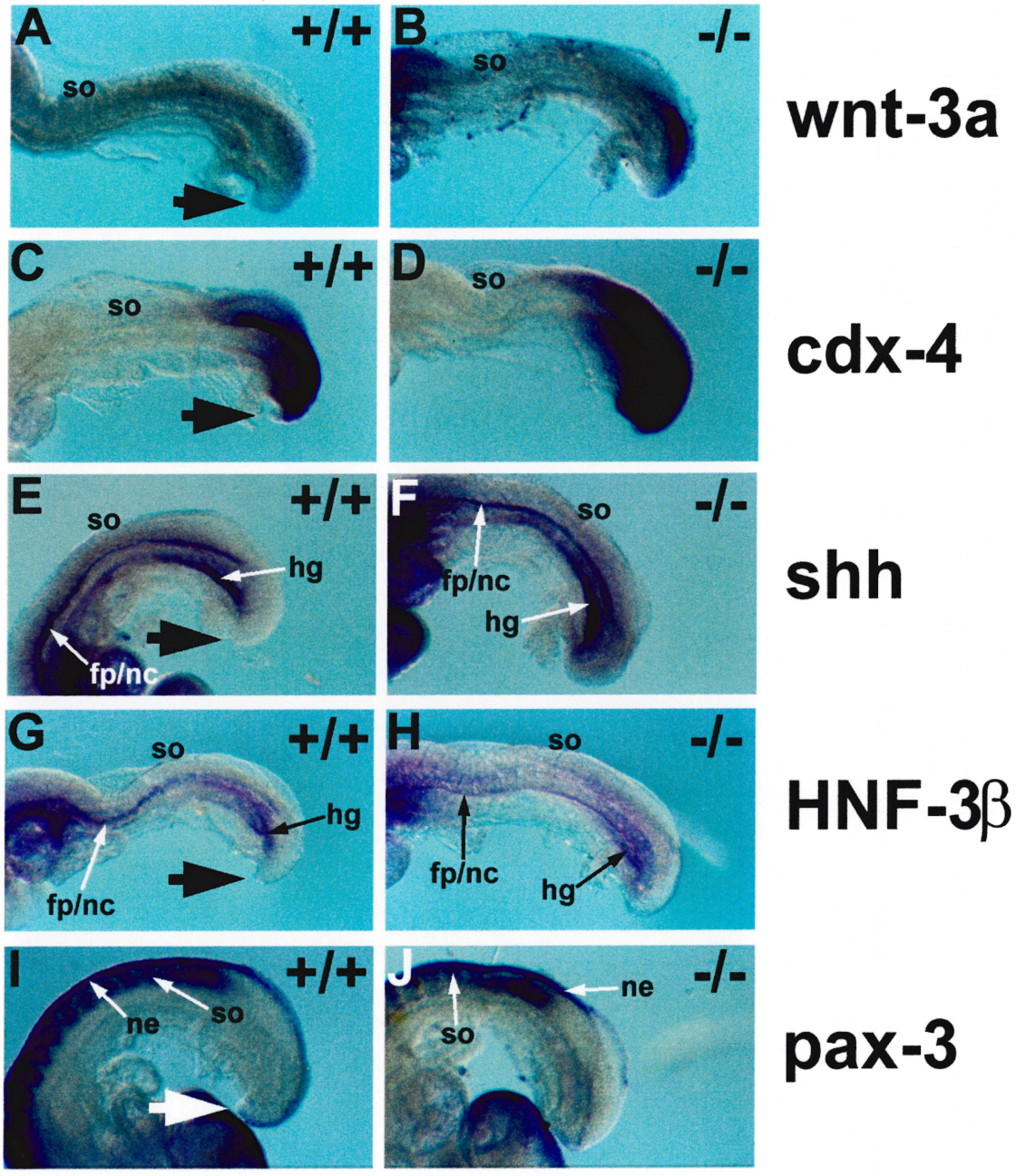

Figure 3-3. RA specifically downregulates markers of nascent mesoderm.

Whole mount *in situ* hybridization of wildtype (A, C, E, G, I) or RARγ$^{-/-}$ littermates (B, D, F, H, J) 8 hours following RA treatment. In wildtype, but not RARγ$^{-/-}$ embryos, RA repressed expression of *wnt-3a* (A compare to B) and *cdx-4* (C, compare to D). Identical treatment did not alter *shh* (E, F), *HNF-3β* (G, H) or *pax-3* (I, J) expression in wildtypes relative to null specimens. The large arrow (A, C, E, G, I) indicates the tail flexion defect induced in wildtype embryos. fp/nc, floorplate/notochord; hg, hindgut; ne, neuroepithelium; so, somite.

perturbation of these somitic and neuroepithelial populations by RA administration does not underlie the posterior dysmorphogenesis caused by retinoid excess.

To determine more specifically which tissues were affected by RA, transverse sections of embryos 8 hours post-treatment were examined for *brachyury* or *cdx-4* expression. In the open PNP region, treatment reduced *brachyury* expression on neuroepthelium and mesoderm underlying the neural plate in wild types relative RARγ$^{-/-}$ embryos (compare ne and me in Figs. 3-4A-C to E-G). Likewise, hindgut endoderm showed a pronounced RARγ-dependent decrease in *brachyury* transcripts (compare hg in Fig. 3-4A-C to E-G). Message was still evident in the notochord of wild type embryos, although it was clearly affected by treatment (Fig. 3-1B and data not shown), consistent with previous results (Yasuda *et al.* 1990; Tibbles and Wiley, 1988). Differences between the genotypes were particularly striking in the rostral-most region of the PNP, where the signal was undetectable in wild types (with the exception of the notochord) but clearly evident in a normal distribution in RARγ$^{-/-}$ mutants (compare Fig. 3-4A to E). Interestingly, *brachyury* message in the primitive streak region of wild type embryos was not extinguished by acute RA exposure (Fig. 3-4D), although expression was completely attenuated 24 hours post-treatment (Fig. 3-1B).

Examination of sections from specimens hybridized for *cdx-4* confirmed that treatment also attenuated this message in an RARγ-dependent manner (compare Figs. 3-4I -N). However, in this case, these effects appeared to be more modest and restricted to rostral derivatives, including the somatopleure and neuroepithelium at the level of the closed neural tube (compare sop and ne in Fig. 3-4I to L). In contrast, in the open PNP, expression in the neural folds (ne, Fig. 3-4J and M) neural plate, and caudal mesoderm (ne and me, Fig. 3-4K and N) appeared equivalent between wild type and null mutants. Caudal sections of embryos hybridized with *shh* or *HNF-3β* did not reveal any overt differences inexpression between wild type and RARγ$^{-/-}$ specimens (data not shown), in agreement with whole mount analysis (Fig. 3-3E-H).

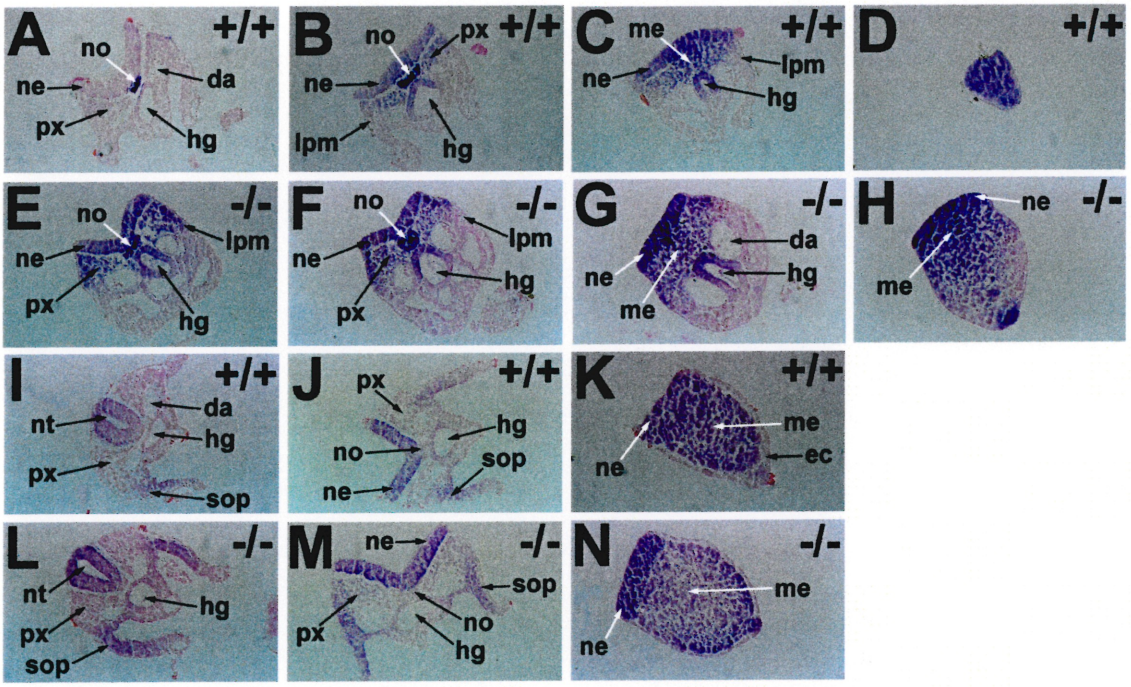

Figure 3-4. RARγ-mediated downregulation of *brachyury* and *cdx-4* expression.

Transverse sections (rostral-caudal sequence) through the caudal region of RA-treated (8 h) embryos from whole mounts hybridized with antisense *brachyury* (A-H) or *cdx-4* (I-N) probes. (A-D) *Brachyury* expression in sections from treated wildtype embryos. (E-H) Equivalent sections from treated RARγ$^{-/-}$ embryos. In wildtype embryos, at the rostral most level of the posterior neuropore, *brachyury* expression was evident in notochord (no) only (A), compared to expression in neuroepithelium (ne), hindgut endoderm (hg), and paraxial (px) and lateral plate mesoderm (lpm) in RARγ $^{-/-}$ mutants (E). At more caudal levels, expression was observed in mesoderm, dorsal hindgut endoderm and neuroepithelium in wildtypes but the signal was consistently diminished in intensity relative to RARγ null littermates (compare B and C to F and G). Staining was also observed in wildtypes in the primitive streak regions which, however, remained less intense than in the null mutants (D, compare to H). (I-N) Sections of wholemounts from treated wildtype (I-K) or RARγ$^{-/-}$ littermates (L-N) hybridized with a *cdx-4* probe. At the level of the closed neural tube and rostral posterior neuropore, wildtypes (I, J) exhibited reduced expression in the neuroepithelium (nt or ne), paraxial mesoderm (px) and somatopleure (sop) compared to null mutants (L, M). In contrast, comparable expression was observed in the neuroepithelium and mesoderm (me) in the primitive streak region between the two genotypes (K, compare to N). da, dorsal aorta; ec, ectoderm; hg, hindgut; lpm, lateral plate mesoderm; me, mesoderm; ne, neuroepithelium; no, notochord; nt, neural tube; px, paraxial mesoderm; sop, somatopleure. Magnification 160X (B, C, E, F, I), 180X (A, G, H, K, L, N), and 200X (D, J, M).

Retinoid Bioavailability In The Caudal Embryo

The finding that RA rapidly attenuated the expression of posterior mesodermal markers prompted us to examine *in vivo* bioactive retinoid distribution in the caudal embryo using a reporter assay previously described (Fig. 3-5). At all stages investigated (8.5 - 11.5 dpc), caudal tissue did not release detectable levels of biologically active retinoids (Fig. 3-5A, C, F, and I; a minimum of five explants were examined for each stage. Note that the few positive cells in these micrographs are background inherent to these reporter cells; Wagner *et al.,* 1992, and data not shown). In contrast, at 8.5 dpc all somite-level tissues elicited a positive response (Fig. 3-5B, n = 17). At 9.5 dpc, β-galactosidase activity was observed in somite samples from both axial levels (Figs. 3-5D and E) with a markedly lower, but reproducible, response from 10.5 dpc explants (Figs. 3-5G and H). Assays using 11.5 dpc samples exhibited little or no activity, irrespective of axial level examined. Therefore, retinoid bioavailability was apparently greatest in 8.5 and 9.5 dpc posterior somite-level tissues, with levels decreasing at 10.5 and 11.5 dpc.

To determine the distribution of exogenous RA, pregnant dams from wild type intercrosses were treated with 100mg RA/kg and dissected 3.5 or 6 hours later and caudal and somitic samples assayed as described above. At 3.5 hours post-treatment, all caudal and somitic samples examined exhibited high levels of RA (Fig. 3-6C and D; compare to untreated controls in 3-6A and B; n = 9. Note also the different magnifications used between untreated and treated samples). By 6 hours post-treatment a dramatic reduction in signal was seen in caudal tissue, while reporter cells incubated with somite-containing explants continued to exhibit a strong response (compare Fig. 3-6E to F; n = 8).

mP450RAI; A Novel Mechanism For The Regulation Of Retinoid Bioavailability

The RA bioassay data suggested the existence of a system capable of catabolizing RA selectively in the caudal embryo. Recently, a novel RA hydroxylase, *P450RAI* (CYP26), has been isolated from several vertebrate species. All homologues are able to oxidize RA into more polar derivatives, including 4-oxo-, 4-hydroxy-, and 18-hydroxy-RA, suggesting that this enzyme may inactivate RA (Fujii *et al.* 1997; White *et al.*, 1996, 1997). To determine if this cytochrome could play a role in RA metabolism observed in the caudal embryo, we examined its expression from 8.5 to 11.5 dpc. In wild type 8.5 to

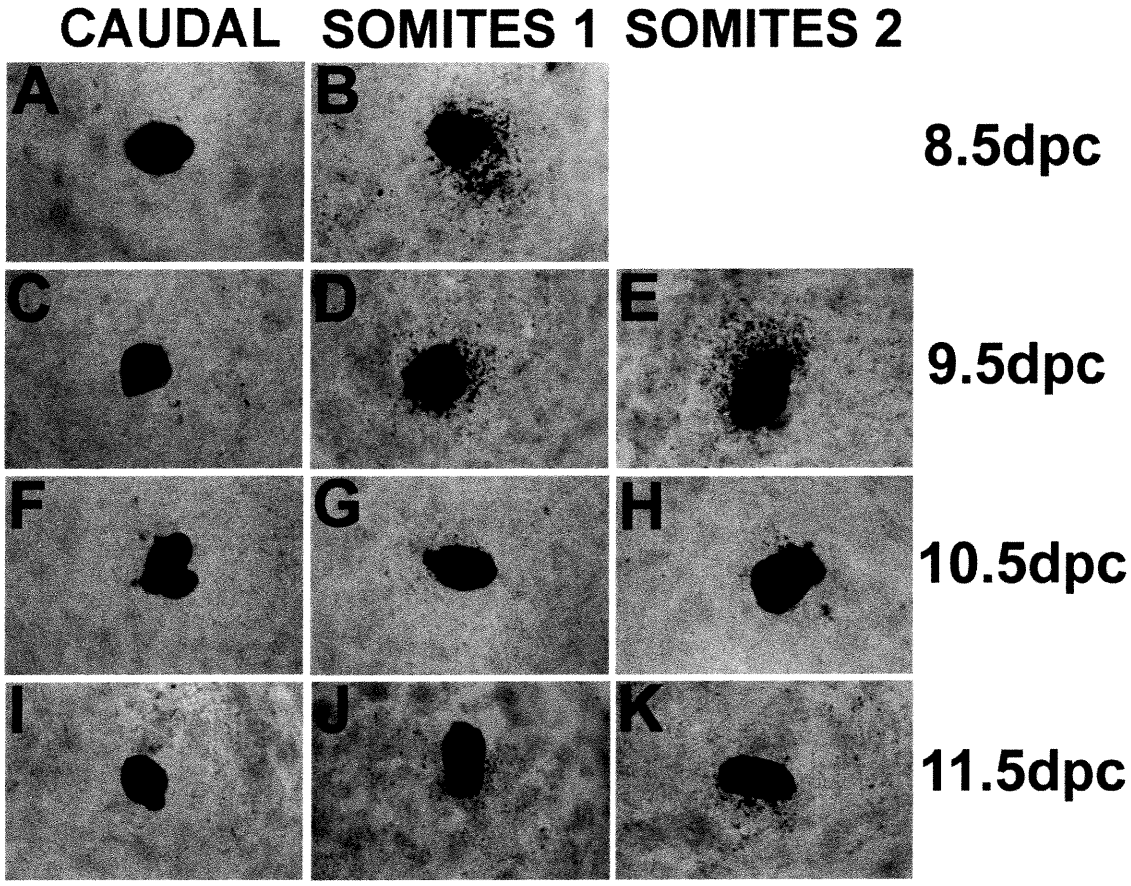

Figure 3-5. Bioavailable retinoid distribution in the caudal embryo.

Tissue at the level of the posterior neuropore (CAUDAL; A, C, F, I) and adjacent somite-containing tissues (SOMITES 1; B, D, G, J) were dissected from 8.5 to 11.5 dpc embryos. An additional more rostral explant (SOMITES 2; E, H, K) was dissected from 9.5 to 11.5 dpc specimens. After overnight culture on reporter cells, explants and cells were fixed and stained for β-galactosidase activity. CAUDAL explants were negative for bioavailable retinoids at all stages tested (A, C, F, I). In contrast, at 8.5 and 9.5 dpc both somite-containing explants contained bioavailable RA (B, D, E) which declined at 10.5 and 11.5 dpc (G, H, J, K). Magnification 100X.

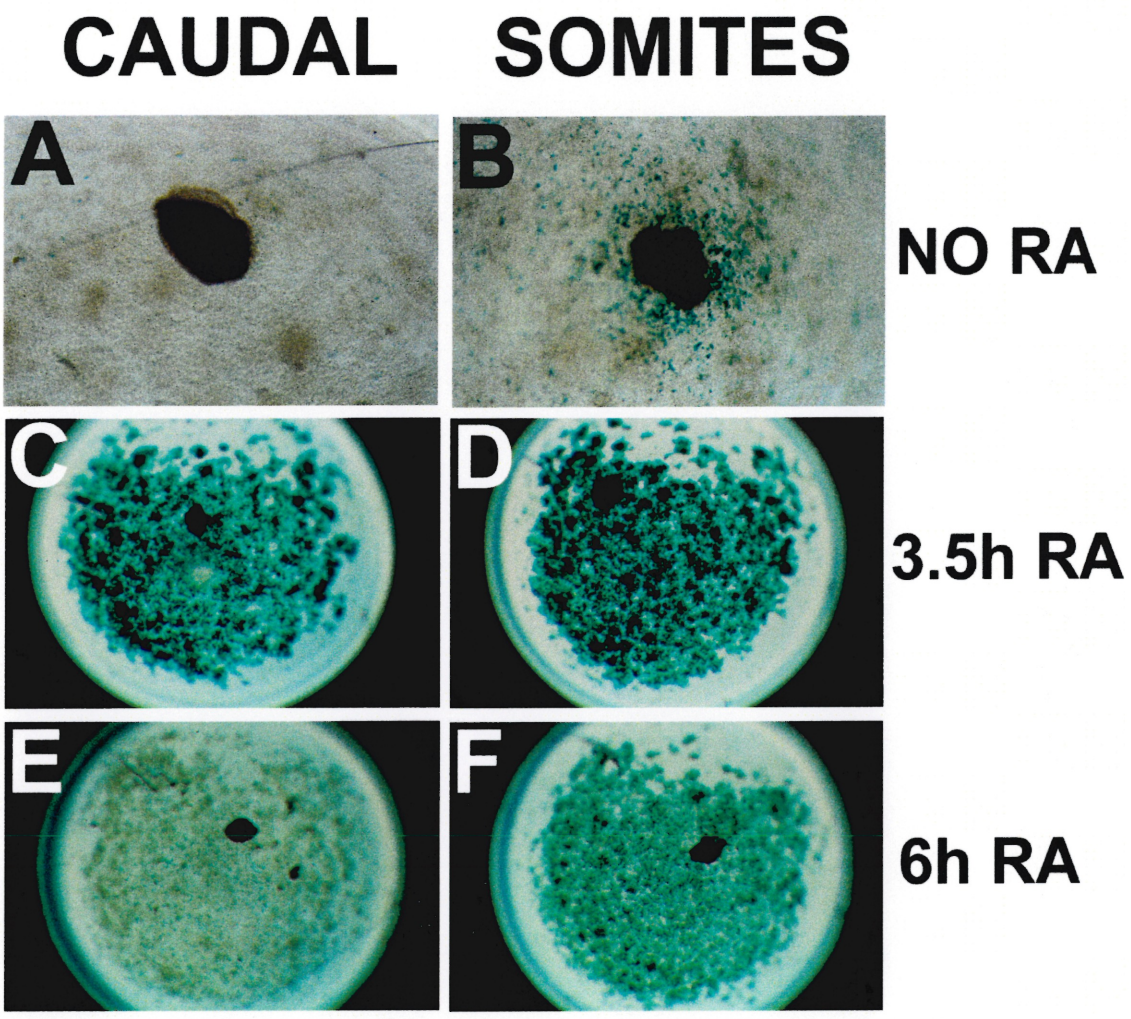

Figure 3-6. The caudal embryo preferentially catabolizes RA.

Bioactive retinoids were assayed from untreated caudal pre-somitic tissues (CAUDAL; A) or adjacent somite-containing tissues (SOMITES; B) from untreated 8.5 dpc wildtype embryos or from equivalent tissues dissected from embryos 3.5 (C, D) or 6 hours (E, F) following RA gavage. Treatment resulted in high levels of reporter cell response from explants from either axial level 3.5 hours post-treatment (C, D; compare to A, B). However, by 6 hours post-treatment, pre-somitic explants had cleared nearly all bioavailable RA (E) while adjacent somite-containing samples continued to elicit a strong response (F). Magnification 100X (A, B) and 50X (C-F).

9.0 dpc embryos (12 to 18 somites), *mP450RAI* transcripts were evident in caudal neuroepithelium, hindgut endoderm and the mesenchyme immediately underlying the neural plate of the open PNP (Figs. 3-7A, B). At 9.5 dpc (22-26 somites), strong expression continued in the nascent mesoderm at the caudal extremity of embryo, and in the neuroepithelium of the caudal PNP (Fig. 3-7C). In slightly older embryos (9.75 dpc; 28-32 somites), message diminished and was restricted to the neuroepithelium and underlying mesoderm in the region surrounding the posterior neurocoel (Fig. 3-7D). At 10.5 dpc, as PNP closure progressed, message abundance declined with expression restricted to the caudal-most tip of the embryo (Fig. 3-7E). At 11.5 dpc, after PNP closure, only a low level of *mP450RAI* message was observed in a few cells in the dorsal region of the tailbud (Fig. 3-7F). Consistent with previous studies (Fujii *et al.* 1997), *mP450RAI* was also detected in more cranial regions and in limb buds (data not shown).

The murine *P450RAI*, like the human and zebrafish homologues, is upregulated by RA *in vitro* (Abu-Abed *et al.,* 1998; White *et al.* 1996, 1997). Consistent with this, we observed a strong induction *mP450RAI* message by RA in 8.5 dpc wild type embryos as early as 4 hours post-treatment (Fig. 3-8B, compare to the untreated control in 3-8A. Note that RAR$\gamma^{-/-}$ embryos exhibited a similar induction; data not shown). Treatment resulted in abundant transcripts throughout the caudal embryo, with a sharp anterior limit of expression in the mesoderm, where transcripts were detected up to, but excluding, the most recently formed somite (so in Fig. 3-8B). Message in the neuroepithelium extended to a sightly more rostral level in the closed neural tube (Fig. 3-8B). At 8 hours posttreatment, *mP450RAI* was still induced, but was apparently receding from the anterior domains of expression seen 4 hours after gavage (compare Fig. 3-8C and D). Consistent with these findings, representative cDNA analysis indicated that RA elicited a 23- or 20-fold increase in *mP450RAI* abundance at 4 or 8 hours posttreatment, respectively (data not shown).

Transverse sections were examined to more precisely define *mP450RAI* distribution and RA-induced expression patterns. Consistent with whole mount analysis, untreated samples did not exhibit expression at the level of the closed neural tube or the rostral limit of the PNP (Figs. 3-8D and E). Weak expression was observed in the

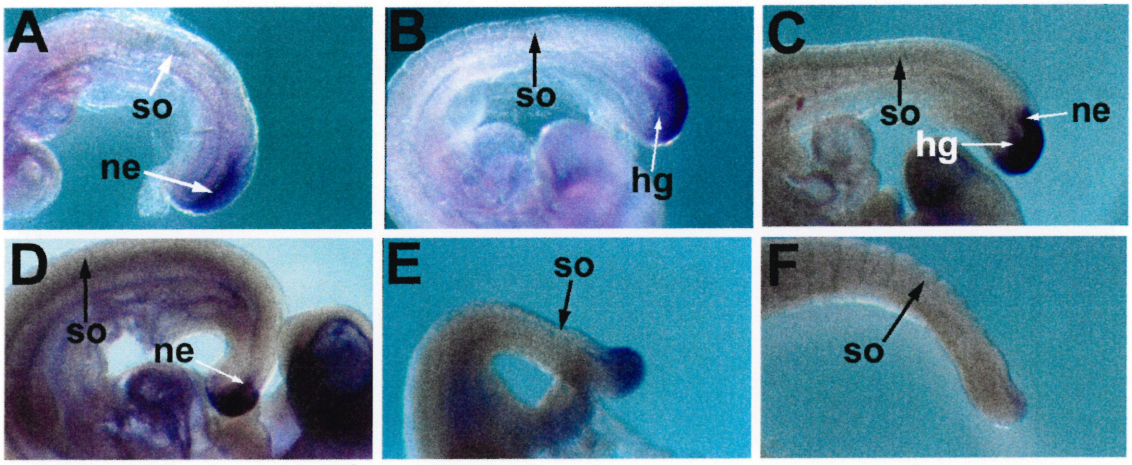

Figure 3-7. *mP450RAI* exhibits dynamic expression in the caudal embryo.

Whole mount *in situ* hybridization of an antisense *mP450RAI* riboprobe to 8.5 dpc (A), 8.75 dpc (B), 9.5 dpc (C), 9.75 dpc (D), 10.5 dpc (E), and 11.5 dpc (F) embryos. *mP450RAI* transcripts were detected in the neuroepithelium and underlying mesenchyme of the posterior neuropore at 8.5 dpc (A), with similar high level expression at 8.75-9.75 dpc (B-D). Expression subsequently declined in the tail bud during posterior neuropore closure at 10.5 dpc, and was barely detectable in the dorsal tail bud at 11.5 dpc (F).

Figure 3-8. Caudal expression of *mP450RAI* was rapidly upregulated by RA.

Whole mount *in situ* hybridization analysis (A-C) and transverse sections (D-O) of *mP450RAI* expression. (A-C) Whole mount analysis of untreated (A), or embryos 4 (B) or 8 (C) hours following RA gavage. RA induced *mP450RAI* transcripts throughout the posterior embryo up to the level of the most recently formed somite 4 hours posttreatment (B, compare to A). (C) *mP450RAI* expression declined 8 hours postgavage relative to the pattern of expression observed at 4 hours in the anterior domain of induced expression (C, compare to B). The large arrow in C indicates a caudal flexion defect. (D-O) *mP450RAI* expression in transverse section of 8.5 dpc wildtype embryos without (D-I) or 4 hours following RA-treatment (J-O). In untreated specimens, *mP450RAI* transcripts were not detected in any tissues at the level of the closed posterior neural tube (D) or the anterior region of the posterior neuropore (E). Weak expression was observed in neuroepithelium (ne) of the posterior neuropore at more caudal levels (F) with signal appearing in the underlying mesoderm (me; G, H) and hindgut endoderm (hg; G) in the caudal embryo. In the primitive streak region, staining was observed in the epithelium and underlying mesodm (H, J). RA treatment induced ectopic expression in the closed neural tube at the level of the most recently formed somite (nt in J, compare to D). Ectopic *mP450RAI* expression was observed in neuroepithelium and pre-somitic paraxial mesoderm immediately caudal to the most recently formed somite (px in K; compare to D). RA also induced expression throughout the posterior neuropore region in neuroepithelium, mesoderm, and dorsal hindgut endoderm (L-N). Sections through the primitive streak region showed induced *mP450RAI* expression throughout the embryos (O compare to I). da, dorsal aorta; hg, hindgut; lpm, lateral plate mesoderm; me, mesoderm; ne, neuroepithelium; no, notochord; nt, neural tube; px, paraxial mesoderm; so, somite. Magnification 95X (A-C), 180X (E-G, J, M-O), and 200X (D, H, I, K, L).

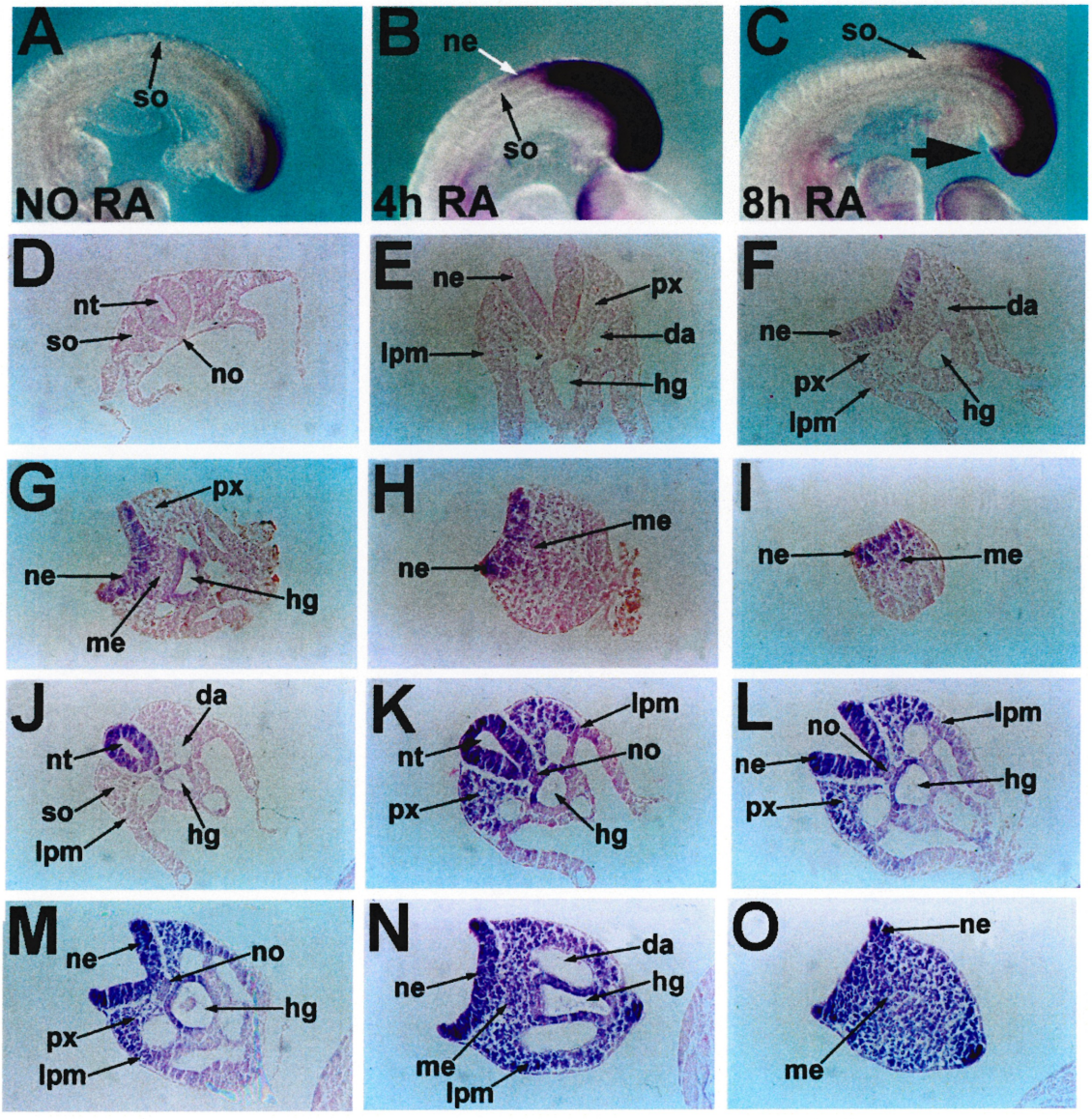
A
so
NO RA
B
ne
so
4h RA
C
so
8h RA
D
nt
so
no
E
ne
px
lpm
da
hg
F
da
ne
px
lpm
hg
G
px
ne
hg
me
H
me
ne
I
ne
me
J
da
nt
so
lpm
hg
K
lpm
nt
no
px
hg
L
no
lpm
ne
hg
px
M
ne
no
hg
px
lpm
N
da
ne
hg
me
lpm
O
ne
me

neuroepithelium in the open PNP, with signal increasing in strength at more caudal levels (ne, Figs. 3-8F-I). Posterior sections also exhibited expression in dorsal mesoderm underlying the neural plate (me, Figs. 3-8G-I) with a weak signal in the caudal-most regions of the hindgut endoderm (hg Fig. 3-8G). Following RA treatment, expression of *mP450RAI* was observed in the neuroepithelium of the closed neural tube at the level of the most recently formed somite (nt, Fig. 3-8J; note, however, absence of expression in the somite). At slightly more caudal levels, transcripts were also observed in pre-somitic paraxial mesoderm (px, Fig. 3-8K), as well as in the closed neural tube and hindgut. Thus, a discrete boundary of *mP450RAI* expression was established between the most recently formed somite and pre-somitic mesoderm. In the rostral PNP, expression was induced in the neuroepithelium and underlying mesoderm as well as notochord and dorsal hindgut endoderm (Fig. 3-8L, compare to 3-8E). In more caudal sections, transcripts were induced throughout the mesoderm, the neural plate, and hindgut endoderm relative to untreated controls (compare Figs. 3-8M and N to 3-8G and H). Message was also induced throughout the embryo in the primitive streak region (compare Figs. 3-8O and I).

DISCUSSION

A Molecular Basis For Retinoid-Induced Axial Truncation

Wild-type mouse embryos exposed to excess RA at 8.5 dpc exhibit vertebral transformations and caudal axial truncations associated with spina bifida (Tibbles and Wiley, 1988; Kessel and Gruss, 1991). The latter event absolutely requires the presence of RARγ, but not RARβ or RARα1, clearly illustrating a unique role for this receptor in eliciting a subset of the teratogenic outcomes induced by RA (Lohnes *et al.* 1993; Lufkin *et al.* 1993; Luo *et al.* 1995). In the present study, we demonstrate that these RARγ-dependent defects occur *via* an impact on posterior mesoderm, as evidenced by the rapid downregulation of *brachyury, wnt-3a* and *cdx-4* expression. These effects preceded overt morphogenetic alterations, such as tail flexion defects, which occurred upon prolonged development following treatment. In contrast to wild type embryos, *RARγ* null mutants exhibited normal expression for all markers examined. Moreover, $RAR\gamma^{+/-}$ embryos

displayed an intermediate effect on expression of mesodermal markers, consistent with the partial resistance of these heterozygotes to RA-induced axial truncation (Lohnes *et al.* 1993).

The lack of an effect of acute RA exposure on *shh* or *HNF-3β* expression suggests that retinoid-induced axial truncation is not due to effects on floorplate, notochord, or hindgut populations. Somitic mesoderm and presumptive neural crest populations were likewise unaffected as judged by *pax-3* and *follistatin* expression. Interestingly, a mutation of *pax-3* in the mouse (*splotch*) results in neural tube defects, including spina bifida, due to a delay in PNP closure caused by aberrant neural crest cell migration (Moase and Trasler, 1990, 1991; Serbedzija and McMahon, 1997). Our present data suggest that the previously described interaction between the *splotch* allele and retinoids (Kapron-Bras and Trasler, 1984, 1985; Kapron-Bras *et al.* 1988) may be explained by the effect of RA on posterior mesoderm.

Several lines of evidence suggest that attenuation of *brachyury* expression is a primary event in RA-induced axial defects. When administered at the correct stage, RA results in defects identical to those observed in *brachyury (T/T)* mutants (Wilkinson *et al.* 1990; Beddington *et al.* 1992). This response of *brachyury* to RA is rapid, occurring within 4 h, and requires RARγ, consistent with the role for this receptor in retinoid-induced axial truncation (Lohnes *et al.,* 1993). In *Xenopus*, ectopic expression of the *brachyury* homologue *Xbra* in animal caps is sufficient to induce mesoderm formation, and RA has been shown to have profound effects on subsequent mesodermal patterning in this species (Brennan, 1992; Bain *et al.* 1996; Ruiz i Altaba and Jessell, 1991; O'Reilly *et al.* 1995; Cunliffe and Smite, 1992). Moreover, posterior *wnt-3a* expression is extinguished at 8.5-9.5 dpc in *T/T* embryos (Rashbass *et al.* 1994) suggesting that the attenuation of *wnt-3a* in the present study is secondary to reduced *brachyury* expression. Likewise, attenuation of *cdx-4* may also be a secondary event, as it was affected in a modest fashion relative to other mesodermal markers. Taken together, these observations strongly suggest that the axial malformations induced by RA are due to insufficient *brachyury* activity, consistent with a role for this gene product in posterior mesoderm (Smith, 1997; Papaioannou and Silver, 1998; Beddington *et al.* 1992).

During gastrulation, *brachyury* transcripts are found in the primitive streak, nascent mesoderm, and notochord as well as dorsal hindgut endoderm and ventral neural plate (Kispert and Herrmann, 1994; Wilkinson *et al.* 1990). Recent studies suggest the existence of separable elements capable of directing *brachyury* expression either in the primitive streak and nascent mesoderm, or in the notochord (Clements *et al.* 1996). Our results suggest that, in a situation of RA excess, *RARγ* affects *brachyury* transcription specifically from the former element, as notochordal expression was not extinguished (although the notochord was malformed as early as eight hours post-treatment). The insensitivity of the notochord expression is not due to the possibility that RA simply prevents *do novo* mesoderm formation, since rostral domains of *brachyury* expression (e.g., presomitic mesoderm) are clearly affected by acute exposure. The effect of RA on *brachyury* is also not likely due to a general cytotoxic event as certain markers, such as *cdx-4*, were only sightly attenuated, and *mP450RAI* was actually induced. We also found no evidence for widespread cell death following acute exposure, and morphogenetic defects manifest only after effects on mesodermal markers have initiated. It therefore seems possible that RA, through RARγ, inhibits *brachury* expression.

Although our data suggest that RA interferes with a specific element directing a subset of *brachyury* expression, the nature of this effect is unknown. In this regard, in *Xenopus*, FGF signaling has been implicated in posterior mesoderm generation, and may form an autoregulatory loop with *Xbra* (Isaacs, 1997; Latinkic *et al.* 1997; Schulte-Merker and Smith, 1995; Isaacs *et al.* 1994). One component of the FGF signaling pathway is the transcription factor AP-1 (Dong *et al.* 1996; Kim *et al.* 1998). Blocking endogenous AP-1 activity or FGF signaling in *Xenopus* embryos results in severe posterior defects concomitant with disruption of *Xbra* expression (Schulte-Merker and Smith, 1995; Isaacs *et al.* 1994; Kim *et al.* 1998). As retinoids can inhibit AP-1 activity in diverse models (Karin *et al.* 1997; Handel, 1997), the attenuation of *brachyury* expression observed in the present study could conceivably occur *via* such a trans-repression mechanism. However, in the mouse, FGF signaling has not been implicated in inducing or maintaining *brachyury* expression (Schmidt *et al.* 1997; Ciruna *et al.,* 1997). Nonetheless, the lack of a demonstrated relationship between FGF and *brachyury* in the mouse may be due to the presence of functionally redundant FGFs and FGFRs in the

caudal embryo. Alternatively, AP-1 signaling may be required for *brachyury* expression independent of FGF signaling, and the effects of RA on this transcription factor during development remain to be established.

mP450RAI *Regulates RA Levels In The Caudal Embryo*

Despite the profound effects of RA treatment on posterior mesoderm, we were unable to detect endogenous retinoid activity emanating from caudal tissue at any embryonic stage examined. In contrast, adjacent somite-level explants contained readily detectable RA, particularly evident at 8.5-9.5 dpc, consistent with previous studies (Rossant *et al.* 1991; Balkan *et al.* 1992). The localization of RA in these regions has been associated with the expression of class IV alcohol dehydrogenase (class IV ADH), an enzyme capable of catalyzing the oxidation of retinol to retinaldehyde, the rate-limiting step in RA metabolism (Ang *et al.* 1996).

Application of exogenous RA resulted in a saturation of both caudal and posterior somitic tissues as early as 3.5 hours post-treatment, again in agreement with previous in vivo studies (Rossant *et al.* 1991; Balkan *et al.* 1992). We also found that, following treatment, caudal, but not posterior somitic, explants cleared essentially all exogenous RA by 6 hours post-treatment, suggesting the presence of an RA-metabolizing system preferentially localized in the caudal embryo. Indeed, in agreement with previous reports (Fujii *et al.* 1997), we observed coincident expression of *P450RAI* (*mP450RAI*) in this region. *mP450RAI* encodes a cytochrome P450 family member capable of metabolizing RA to more polar derivatives, principally by oxidation at C-4 or C-18 positions (Fujii *et al.* 1997; White *et al.* 1996, 1997; Abu-Abed *et al.* 1998). At 8.5 dpc, *mP450RAI* transcripts were observed in the primitive streak region and neuroectoderm associated with the open posterior neuropore. Interestingly, expression of this gene peaked at 8.5-9.5 dpc, and declined to almost undetectable levels shortly after neural tube closure.

Like the zebrafish and human homologues, murine *P450RAI* has been found to be RA inducible *in vitro* (White *et al.* 1996, 1997; Abu-Abed *et al.* 1998). Consistent with these data, we found that *mP450RAI* was strongly and rapidly induced in all tissues posterior to the most recently formed somite in 8.5dpc embryos. This contrasts with prior studies which reported a decline in expression of this gene in the caudal embryo

following treatment (Fujii *et al.* 1997). This discrepancy is likely due to the use of a lower dose of RA and/or a longer delay (12-24 h), as we have found that *P450RAI* induction is remarkably transient, already having begun to recede 8 hours post-treatment. Also, in contrast with previous studies (Abu-Abed *et al.,* 1998) we noted similar RA regulation in RARγ-null embryos, suggesting that this receptor is not critically required for induction of *P450RAI in vivo*. Whether this is indicative of cell-type-specific gene regulation or other mechanisms is unknown.

RA metabolism is closely associated with the expression of P450RAI in diverse cell lines (White *et al.* 1997; Abu-Abed *et al.* 1998), suggesting that P450RAI may act to limit retinoid signaling *via* catabolic inactivation of RA. However, certain of its products, such as 4-oxo-RA, have been reported to have potent biological activity (Gaemers *et al.* 1996; Pijnappel *et al.* 1993). In the present study, expression of *mP450RAI* coincided with rapid clearance of RA, suggesting either that the immediate products of this enzyme are not active *in vivo* or that they are rapidly converted (or cleared) to inert metabolites. This finding, together with the rapid and transient induction of *mP450RAI*, is consistent with this enzyme playing a critical role in a feedback loop to regulate RA bioavailability, at least in the caudal embryo. Such a mechanism is further supported by the finding of functional RAREs in the promoter region of *P450RAI* homologues from several vertebrate species (J. White and M.Petkovich, manuscript in preparation).

Implications For Retinoid Signaling

The lack of detectable biologically active retinoids in the caudal embryo, together with the expression pattern of *mP450RAI,* suggest that this enzyme may function to create regions devoid of retinoid signaling (see also Fujii *et al.,* 1997). In this scenario, the axial dysmorphogenesis induced by RA may represent a teratogenic outcome unrelated to normal RA-dependent events. However, several lines of evidence suggest that retinoid signaling functions in the caudal embryo at 8.5 dpc. First, class IV ADH (a candidate enzyme for the rate-limiting step in RA biosynthesis) is expressed in this region just prior to initiation of neural tube closure, and persists in paraxial mesoderm at 8.5 dpc (Ang *et al.* 1996, 1997). Second, caudal expression of *mP450RAI* at 8.5 dpc is modestly affected

in RARα1/γ double null embryos (our preliminary observations), indicating that these receptors are liganded. Finally, RARγ disruption results in homeosis of caudal thoracic and lumbosacral vertebrae, which may reflect altered *hox* gene expression in the primitive streak during late gastrulation (Iulianella and Lohnes, 1997; Lohnes *et al.* 1993; 1994). Taken together, these findings are indicative of active retinoid signaling in the primitive streak region at 8.5 dpc.

Our inability to detect biologically active retinoids in this tissue may reflect either limiting amounts of RA (perhaps in a very restricted population) which may be rapidly turned over by *P450RAI*. Consistent with this, the developing eye and limb bud also express *P450RAI* (Fujii *et al.* 1997), yet are profoundly affected by RAR disruption (Lohnes *et al.* 1994; Mendelsohn *et al.* 1994). Thus, *mP450RAI* expression does not necessarily abolish normal retinoid signaling; rather, it may serve to limit the effects of RA to specific populations and/or specific times.

Our present results suggest that RA may normally act to attenuate *brachyury* expression. As *mP450RAI* expression is highest in the primitive streak region, it may restrict RA levels in this area, allowing normal *brachyury* expression and subsequent mesoderm allocation from the streak (Wilson and Beddington, 1997). At more rostral levels, less differentiated mesoderm would encounter RA diffusing from posterior somites (Fig. 5), which would inhibit *brachyury* expression concomitant with differentiation. In agreement with this, transcripts for both *brachyury* (Wilkinson *et al.,* 1990) and *mP450RAI* (Fig. 7) diminish after 9.5 dpc, consistent with increased RA (due to reduced *mP450RAI*) attenuating *brachyury* expression at the tailbud stage. Also in conformity with this proposal is the observation that *brachyury* and *mP450RAI* are colocalized at 8.5 dpc, both showing the highest expression in caudal/dorsal domains (compare, e.g., Fig. 4H and 8N). Taken together with the rapid response of *brachyury* to exogenous RA, these observations suggest that retinoids may normally affect posterior mesoderm formation via regulation of *brachyury* expression.

ACKNOWLEDGEMENTS

The authors wish to thank Christian Charbonneau for assistance with photography, Prof. Pierre Chambon for the RARγ null mutant founder mice and Drs. Peter Gruss, Andrew McMahon, Bernhard Herrmann, Brigid Hogan and Christopher Wright for the gifts of cDNAs. This work was supported by grants to D.L. from the March of Dimes Birth Defects Foundation (FY98-0562) and the Medical Research Council of Canada. D.L. is a Medical Research Council of Canada Scholar.

REFERENCES

Abu-Abed, S.S., Beckett, B.R., Chiba, H., Chithalen, J.V., Jones, G., Metzger, D., Chambon, P. and Petkovich, M. (1998). Mouse p450RAI (CYP26) expression and retinoic acid-inducible retinoic acid metabolism in F9 cells are regulated by retinoic acid receptor gamma and retinoid x receptor alpha. *J. Biol. Chem.* **273**, 2409-2415.

Albano, R.M., Arkell, R., Beddington, R.S. and Smith, J.C. (1994). Expression of inhibin subunits and follistatin during postimplantation mouse development: decidual expression of activin and expression of follistatin in primitive streak, somites and hindbrain. *Development* **120**, 803-813.

Ang, H.L., Deltour, L., Hayamizu, T.F., Zgombic-Knight, M. and Duester, G. (1996). Retinoic acid synthesis in mouse embryos during gastrulation and craniofacial development linked to class IV alcohol dehydrogenase gene expression. *J. Biol. Chem.* **271**, 9526-9534.

Ang, H.L. and Duester, G. (1997). Initiation of retinoid signaling in primitive streak mouse embryos: spatiotemporal expression patterns of receptors and metabolic enzymes for ligand synthesis. *Dev. Dyn.* **208**, 536-543.

Ang, S.L. and Rossant, J. (1994). HNF-3 beta is essential for node and notochord formation in mouse development. *Cell* **78**, 561-574.

Bain, G., Ray, W.J., Yao, M. and Gottlieb, D.I. (1996). Retinoic acid promotes neural and represses mesodermal gene expression in mouse embryonic stem cells in culture. *Biochem. Biophys. Res. Commun.* **223**, 691-694.

Balkan, W., Colbert, M., Bock, C. and Linney, E. (1992). Transgenic indicator mice for studying activated retinoic acid receptors during development. *Proc. Nat. Acad. Sci. USA* **89**, 3347-3351.

Beddington, R.S., Rashbass, P. and Wilson, V. (1992). *Brachyury*-a gene affecting mouse gastrulation and early organogenesis. *Development (Suppl.)* 157-165.

Brennan, S.M. (1992). Retinoic acid prevents accumulation of a mesoderm-specific mRNA in the amphibian embryo. *Mech. Dev.* **38**, 17-24.

Brook, F.A., Shum, A.S., Van Straaten, H.W. and Copp, A.J. (1991). Curvature of the caudal region is responsible for failure of neural tube closure in the curly tail (ct) mouse embryo. *Development* **113**, 671-678.

Chambon, P. (1996). A decade of molecular biology of retinoic acid receptors. *FASEB J.* **10**, 940-954.

Chen, W.H., Morriss-Kay, G.M. and Copp, A.J. (1995). Genesis and prevention of spinal neural tube defects in the curly tail mutant mouse: involvement of retinoic acid and its nuclear receptors RAR-beta and RAR-gamma. *Development* **121**, 681-691.

Chiang, C., Litingtung, Y., Lee, E., Young, K.E., Corden, J.L., Westphal, H. and Beachy, P.A. (1996). Cyclopia and defective axial patterning in mice lacking sonic hedgehog gene function. *Nature* **383**, 407-413.

Ciruna, B.G., Schwartz, L., Harpal, K., Yamaguchi, T.P. and Rossant, J. (1997). Chimeric analysis of fibroblast growth factor receptor-1 (fgfr1) function: a role for fgfr1 in morphogenetic movement through the primitive streak. *Development* **124**, 2829-2841.

Clements, D., Taylor, H.C., Herrmann, B.G. and Stott, D. (1996). Distinct regulatory control of the brachyury gene in axial and non-axial mesoderm suggests separation of mesoderm lineages early in mouse gastrulation. *Mech. Dev.* **56**, 139-149.

Copp, A.J. (1994). Genetic models of mammalian neural tube defects. *Ciba Found. Symp.* **181**, 118-134.

Copp, A.J. and Bernfield, M. (1994). Etiology and pathogenesis of human neural tube defects: insights from mouse models. *Curr. Opin. Pediatr.* **6**, 624-631.

Cunliffe, V. and Smith, J.C. (1992). Ectopic mesoderm formation in xenopus embryos caused by widespread expression of a brachyury homologue. *Nature* **358**, 427-430.

Dickman, E.D., Thaller, C. and Smith, S.M. (1997). Temporally-regulated retinoic acid depletion produces specific neural crest, ocular and nervous system defects. *Development* **124**, 3111-3121.

Dong, Z., Xu, R.H., Kim, J., Zhan, S.N., Ma, W.Y., Colburn, N.H. and Kung, H. (1996). Ap-1/jun is required for early xenopus development and mediates mesoderm induction by fibroblast growth factor but not by activin. *J. Biol. Chem.* **271**, 9942-9946.

Echelard, Y., Epstein, D.J., St-Jacques, B., Shen, L., Mohler, J., McMahon, J.A. and McMahon, A.P. (1993). Sonic hedgehog, a member of a family of putative signaling molecules, is implicated in the regulation of CNS polarity. *Cell* **75**, 1417-1430.

Fujii, H., Sato, T., Kaneko, S., Gotoh, O., Fujii-Kuriyama, Y., Osawa, K., Kato, S. and Hamada, H. (1997). Metabolic inactivation of retinoic acid by a novel p450 differentially expressed in developing mouse embryos. *EMBO J.* **16**, 4163-4173.

Gaemers, I.C., van Pelt, A.M., van der Saag, P.T. and de Rooij, D.G. (1996). All-trans-4-oxo-retinoic acid: a potent inducer of in vivo proliferation of growth-arrested a spermatogonia in the vitamin A-deficient mouse testis. *Endocrinology* **137**, 479-485.

Gamer, L.W. and Wright, C.V. (1993). Murine cdx-4 bears striking similarities to the drosophila caudal gene in its homeodomain sequence and early expression pattern. *Mech. Dev.* **43**, 71-81.

Goulding, M.D., Chalepakis, G., Deutsch, U., Erselius, J.R. and Gruss, P. (1991). Pax-3, a novel murine DNA binding protein expressed during early neurogenesis. *EMBO J.* **10**, 1135-1147.

Greco, T.L., Takada, S., Newhouse, M.M., McMahon, J.A., McMahon, A.P. and Camper, S.A. (1996). Analysis of the vestigial tail mutation demonstrates that wnt-3a gene dosage regulates mouse axial development. *Genes Dev.***10**, 313-324.

Handel, M.L. (1997). Transcription factors AP-1 and NF-kappa b: where steroids meet the gold standard of anti-rheumatic drugs. *Inflam. Res.* **46**, 282-286.

Heyman, R.A., Mangelsdorf, D.J., Dyck, J.A., Stein, R.B., Eichele, G., Evans, R.M. and Thaller, C. (1992). 9-cis retinoic acid is a high affinity ligand for the retinoid x receptor. *Cell* **68**, 397-406.

Hogan, B., Beddington, R., Costantini, F. and Lacy, E. (1994). In "Manipulating the Mouse Embryo. A Laboratory Manual." Cold Spring Harbor Laboratory Press, New York.

Isaacs, H.V., Pownall, M.E. and Slack, J.M. (1994). efgf regulates xbra expression during xenopus gastrulation. *EMBO J.* **13**, 4469-4481.

Isaacs, H.V. (1997). New perspectives on the role of the fibroblast growth factor family in amphibian development. *Cell. Mol. Life Sci.* **53**, 350-361.

Iulianella, A. and Lohnes, D. (1997). Contribution of retinoic acid receptor gamma to retinoid-induced craniofacial and axial defects. *Dev. Dyn.* **209**, 92-104.

Kapron-Bras, C.M. and Trasler, D.G. (1984). Gene-teratogen interaction and its morphological basis in retinoic acid-induced mouse spina bifida. *Teratology* **30**, 143-150/

Kapron-Bras, C.M. and Trasler, D.G. (1985). Reduction in the frequency of neural tube defects in splotch mice by retinoic acid. *Teratology* **32**, 87-92.

Kapron-Bras, C.M. and Trasler, D.G. (1988a). Histological comparison of the effects of the splotch gene and retinoic acid on the closure of the mouse neural tube. *Teratology* **37**, 389-399.

Kapron-Bras, C.M. and Trasler, D.G. (1988b). Interaction between the splotch mutation and retinoic acid in mouse neural tube defects in vitro. *Teratology* **38**, 165-173.

Karin, M., Liu Zg and Zandi, E. (1997). AP-1 function and regulation. *Curr. Opin. Cell Biol.* **9**, 240-246.

Kastner, P., Mark, M. and Chambon, P. (1995). Nonsteroid nuclear receptors: what are genetic studies telling us about their role in real life? *Cell* **83**, 859-69: 12.

Kastner, P., Mark, M., Ghyselinck, N., Krezel, W., Dupe, V., Grondona, J.M. and Chambon, P. (1997). Genetic evidence that the retinoid signal is transduced by heterodimeric RXR/RAR functional units during mouse development. *Development* **124**, 313-326.

Kessel, M. and Gruss, P. (1991). Homeotic transformations of murine vertebrae and concomitant alteration of hox codes induced by retinoic acid. *Cell* **67**, 89-104.

Kim, J., Lin, J.J., Xu, R.H. and Kung, H.F. (1998). Mesoderm induction by heterodimeric AP-1 (c-jun and c-fos) and its involvement in mesoderm formation through the embryonic fibroblast growth factor/xbra autocatalytic loop during the early development of xenopus embryos. *J. Biol. Chem.* **273**, 1542-1550.

Kispert, A. and Herrmann, B.G. (1994). Immunohistochemical analysis of the brachyury protein in wild-type and mutant mouse embryos. *Dev. Biol.* **161**, 179-193.

Latinkic, B.V., Umbhauer, M., Neal, K.A., Lerchner, W., Smith, J.C. and Cunliffe, V. (1997). The xenopus brachyury promoter is activated by fgf and low concentrations of activin and suppressed by high concentrations of activin and by paired-type homeodomain proteins. *Genes Dev.* **11**, 3265-3276.

Leid, M., Kastner, P., Durand, B., Krust, A., Leroy, P., Lyons, R., Mendelsohn, C., Nagpal, S., Nakshatri, H., Reibel, C. *et al.* (1993). Retinoic acid signal transduction pathways. *Ann. New York Acad. Sci.* **684**, 19-34.

Lim, K. and Chae, C.B. (1989). A simple assay for DNA transfection by incubation of the cells in culture dishes with substrates for beta-galactosidase. *Biotechniques* **7**, 576-579.

Lohnes, D., Kastner, P., Dierich, A., Mark, M., LeMeur, M. and Chambon, P. (1993). Function of retinoic acid receptor gamma in the mouse. *Cell* **73**, 643-658.

Lohnes, D., Mark, M., Mendelsohn, C., Dolle, P., Dierich, A., Gorry, P., Gansmuller, A. and Chambon, P. (1994). Function of the retinoic acid receptors (RARs) during development (I). craniofacial and skeletal abnormalities in RAR double mutants. *Development* **120**, 2723-2748.

Lufkin, T., Lohnes, D., Mark, M., Dierich, A., Gorry, P., Gaub, M.P., LeMeur, M. and Chambon, P. (1993). High postnatal lethality and testis degeneration in retinoic acid receptor alpha mutant mice*Proc. Nat. Acad. Sci. USA* **90**, 7225-7229.

Luo, J., Pasceri, P., Conlon, R.A., Rossant, J. and Giguere, V. (1995). Mice lacking all isoforms of retinoic acid receptor beta develop normally and are susceptible to the teratogenic effects of retinoic acid. *Mech. Dev.* **53**, 61-71.

Luo, J., Sucov, H.M., Bader, J.A., Evans, R.M. and Giguere, V. (1996). Compound mutants for retinoic acid receptor (RAR) beta and RAR alpha 1 reveal developmental functions for multiple RAR beta isoforms. *Mech. Dev.* **55**, 33-44.

Mangelsdorf, D.J. and Evans, R.M. (1995). The RXR heterodimers and orphan receptors. *Cell* **83**, 841-50: 13.

Mendelsohn, C., Lohnes, D., Decimo, D., Lufkin, T., LeMeur, M., Chambon, P. and Mark, M. (1994). Function of the retinoic acid receptors (RARs) during development (II). multiple abnormalities at various stages of organogenesis in RAR double mutants. *Development* **120**, 2749-2771.

Moase, C.E. and Trasler, D.G. (1990). Delayed neural crest cell emigration from sp and spd mouse neural tube explants. *Teratology* **42**, 171-182.

Moase, C.E. and Trasler, D.G. (1991). N-cam alterations in splotch neural tube defect mouse embryos. *Development* **113**, 1049-1058.

Morriss-Kay, G., Ward, S. and Sokolova, N. (1994). The role of retinoids in normal development and retinoid-induced malformations. *Arch. Toxicol.* (Supp) **16**:112-117.

O'Reilly, M.A., Smith, J.C. and Cunliffe, V. (1995). Patterning of the mesoderm in xenopus: dose-dependent and synergistic effects of brachyury and pintallavis. *Development* **121**, 1351-1359.

Papaioannou, V.E. and Silver, L.M. (1998). The t-box gene family. *Bioessays* **20**, 9-19.

Parr, B.A., Shea, M.J., Vassileva, G. and McMahon, A.P. (1993). Mouse wnt genes exhibit discrete domains of expression in the early embryonic CNS and limb buds. *Development* **119**, 247-261.

Pijnappel, W.W., Hendriks, H.F., Folkers, G.E., van den Brink, C.E., Dekker, E.J., Edelenbosch, C., van der Saag, P.T. and Durston, A.J. (1993). The retinoid ligand 4-oxo-retinoic acid is a highly active modulator of positional specification. *Nature* **366**, 340-344.

Rashbass, P., Wilson, V., Rosen, B. and Beddington, R.S. (1994). Alterations in gene expression during mesoderm formation and axial patterning in brachyury (t) embryos. *Int. J. Dev. Biol.* **38**, 35-44.

Roelink, H. and Nusse, R. (1991). Expression of two members of the wnt family during mouse development--restricted temporal and spatial patterns in the developing neural tube. *Genes Dev.* **5**, 381-388.

Rossant, J., Zirngibl, R., Cado, D., Shago, M. and Giguere, V. (1991). Expression of a retinoic acid response element-hsplacz transgene defines specific domains of transcriptional activity during mouse embryogenesis. *Genes Dev.* **5**, 1333-1344.

Ruiz i Altaba A and Jessell, T. (1991). Retinoic acid modifies mesodermal patterning in early xenopus embryos. *Genes Dev.***5**, 175-187.

Sasaki, H. and Hogan, B.L. (1993). Differential expression of multiple fork head related genes during gastrulation and axial pattern formation in the mouse embryo. *Development* **118**, 47-59.

Sauvageau, G., Lansdorp, P.M., Eaves, C.J., Hogge, D.E., Dragowska, W.H., Reid, D.S., Largman, C., Lawrence, H.J. and Humphries, R.K. (1994). Differential expression of homeobox genes in functionally distinct cd34+ subpopulations of human bone marrow cells. *Proc. Nat. Acad. Sci. USA* **91**, 12223-12227.

Schmidt, C., Wilson, V., Stott, D. and Beddington, R.S. (1997). T promoter activity in the absence of functional t protein during axis formation and elongation in the mouse. *Dev. Biol.* **189**, 161-173.

Schulte-Merker, S. and Smith, J.C. (1995). Mesoderm formation in response to brachyury requires fgf signalling. *Curr. Biol.* **5**, 62-67.

Serbedzija, G.N. and McMahon, A.P. (1997). Analysis of neural crest cell migration in splotch mice using a neural crest-specific lacz reporter. *Dev. Biol.* **185**, 139-147.

Smith, J. (1997). Brachyury and the t-box genes. *Current Opinion in Genetics* and *Development* **7**, 474-480.

Sporn, M.B., Roberts, A.B. and Goodman, D.S. (1994). In "The Retinoids". Raven Press, New York.

Sucov, H.M. and Evans, R.M. (1995). Retinoic acid and retinoic acid receptors in development. *Mol. Neurobiology* **10**, 169-184.

Sucov, H.M., Izpisua-Belmonte, J.C., Ganan, Y. and Evans, R.M. (1995). Mouse embryos lacking RXR alpha are resistant to retinoic-acid-induced limb defects. *Development* **121**, 3997-4003.

Takada, S., Stark, K.L., Shea, M.J., Vassileva, G., McMahon, J.A. and McMahon, A.P. (1994). Wnt-3a regulates somite and tailbud formation in the mouse embryo. *Genes Dev.***8**, 174-189.

Tibbles, L. and Wiley, M.J. (1988). A comparative study of the effects of retinoic acid given during the critical period for inducing spina bifida in mice and hamsters. *Teratology* **37**, 113-125.

Wagner, M., Han, B. and Jessell, T.M. (1992). Regional differences in retinoid release from embryonic neural tissue detected by an in vitro reporter assay. *Development* **116**, 55-66.

White, J.A., Guo, Y.D., Baetz, K., Beckett-Jones, B., Bonasoro, J., Hsu, K.E., Dilworth, F.J., Jones, G. and Petkovich, M. (1996). Identification of the retinoic acid-inducible all-trans-retinoic acid 4-hydroxylase. *J. Biol. Chem.***271**, 29922-29927.

White, J.A., Beckett-Jones, B., Guo, Y.D., Dilworth, F.J., Bonasoro, J., Jones, G. and Petkovich, M. (1997). cDNA cloning of human retinoic acid-metabolizing enzyme (hP450RAI) identifies a novel family of cytochromes p450. *J. Biol. Chem.***272**, 18538-18541.

Wilkinson, D.G., Bhatt, S. and Herrmann, B.G. (1990). Expression pattern of the mouse t gene and its role in mesoderm formation. *Nature* **343**, 657-659.

Wilkinson, D.G. (1992). In "In Situ Hybridization. A Practical Approach". IRL Press, New York.

Wilson, J.C., Roth, C.B. and Warkany, J. (1953). An analysis of the syndrome of maternal vitamin A deficiency. Effects of restoration of vitamin A at various times during gestation. *Am. J. Anat.* **92**, 189-217.

Wilson, V. and Beddington, R. (1997). Expression of t protein in the primitive streak is necessary and sufficient for posterior mesoderm movement and somite differentiation. *Dev. Biol.* **192**, 45-58.

Wolbach, S.B. and Howe, P.R. (1925). Tissue changes following deprivation of fat-soluble A vitamin. *J. Exp. Med.* **42**, 753-777.

Yasuda, Y., Konishi, H., Kihara, T. and Tanimura, T. (1990). Discontinuity of primary and secondary neural tube in spina bifida induced by retinoic acid in mice. *Teratology* **41**, 257-274.

CHAPTER 4

ARTICLE

Chimeric Analysis Of Retinoic Acid Receptor Function During Cardiac Looping

Angelo Iulianella[1,2] and David Lohnes[1,2,3]

[1]Laboratory of Molecular and Cellular Biology, Institut de Recherches Cliniques de Montréal; and [2]Programme de biologie moléculaire, Université de Montréal; [3]Division of Experimental Medicine, McGill University.

Manuscript submitted to *Developmental Biology*

ABSTRACT

Retinoids (vitamin A and its derivatives) play essential roles during vertebrate development. Vitamin A deprivation during development leads to severe congenital malformations affecting many tissues including diverse neural crest cell populations and the heart. The vitamin A signal is transduced by the retinoic acid receptors (RARα, RARβ, and RARγ). However, these receptors exhibit considerable functional redundancy, as judged by the phenotypes of RAR single and double null mutants. To circumvent this redundancy, a ligand-binding RARγ mutant (RARγE) was targeted to the endogenous RARγ locus resulting in a gene replacement in mouse embryonic stem (ES) cells. Chimeric embryos derived from hemizygous RARγE ES cells displayed several defects similar to those found in certain RAR double null mutants, including hypoplasia or absence of the caudal pharyngeal arches and myocardial deficiencies. The latter defects were not due to abnormal cardiac specification as affected hearts still expressed chamber-specific markers in an appropriate manner. The chimeras also displayed cardiac looping anomalies which were associated with a reduction of Pitx2. In addition to supporting a role for RAR signaling in late looping morphogenesis and cardiomyocyte development, this study illustrates the utility of using a dominant-negative gene substitution approach to circumvent the functional redundancy inherent to RAR signaling.

INTRODUCTION

Vitamin A plays critical roles in vertebrate development, as initially evidenced by vitamin A deprivation (VAD) studies. VAD in rodents or birds leads to complex congenital defects involving the eye, genito-urinary system, several neural crest cell derivatives, hindbrain patterning and heart and associated vessels (Wilson *et al.*, 1953; Maden *et al.*, 1996; Heine *et al.*, 1985; Dickman *et al.*, 1997; Zile, 1998). Most of these defects can be reversed by exogenous retinoic acid (RA), demonstrating that RA can fulfill embryonic vitamin A requirements (Dersch and Zile, 1993; Dickman *et al.*, 1997; Kostetskii *et al.*, 1998, 1999).

Retinoids are required for several aspects of heart development, including anterior-posterior patterning of the heart tube, normal development of the myocardium and proper cardiac looping (reviewed in Smith and Dickman, 1997; Zile, 1998). Interestingly, excess RA in quails gives rise to similar cardiac defects including malpositioning, situs inversus, and cardiac bifida (Dickman and Smith, 1996). The notable difference is that RA excess truncates the anterior portion of the heart tube and expands posterior cardiac markers anteriorly, whereas VAD elicits posterior truncations (Xavier-Neto *et al.*, 1999; Liberatore *et al.*, 2000). This is consistent with a requirement for retinoid signaling in the development of the posterior linear heart tube. Indeed, bio-active retinoids are enriched in the atrial and sinus venosus region of the early heart, coincident with the expression of the major RA-synthesizing enzyme, Raldh2 (Moss *et al.*, 1998). In agreement with this, targeted disruption of *raldh2* in the mouse results in a loss of posterior cardiac structures, including the atria and sinus venosa, a thin myocardial wall, and a dilated ventricle which fails to undergo cardiac looping (Niederreither *et al.*, 1999, 2001).

Considerable progress has been made in our understanding of the molecular determinants of left-right asymmetry in vertebrates. Organ *situs* is controlled by an evolutionarily conserved cascade of signaling molecules leading to the activation of the left-specific determinants *nodal*, *lefty2*, and *pitx2* in the left lateral plate mesoderm (LPM ; reviewed in Mercola, 1999; Capdevila *et al.*, 2000). The misexpression of *nodal*, *lefty2*, or *pitx2* on the right LPM can result in situs defects, as can the loss of these left

side determinants (Logan *et al.*, 1998; Lowe *et al.*, 2001; Piedra *et al.*, 1998; Ryan *et al.*, 1998; Yoshioka *et al.*, 1998). The left-right pathway can be modified by retinoid signaling, as the treatment of mouse embryos with excess RA, or a RAR antagonist, results in aberrant heart looping concomitant with the misexpression of *nodal*, *lefty2*, and *pitx2* (Chazaud *et al.*, 1999; Tsukui *et al.*, 1999; Wasiak and Lohnes, 1999). Consistent with this, VAD quail embryos display a loss of *nodal* and *pitx2* expression and heart looping defects (Zile *et al.*, 2000). *Raldh2*$^{-/-}$ mouse embryos, which are largely RA deficient, also display an arrest in looping, although they exhibit normal *nodal* and *pitx2* expression (Niederreither *et al.*, 2001).

The vitamin A signal is transduced by the retinoic acid receptors (RARα, β and γ; reviewed in Chambon, 1996). RARs are ligand-dependent transcription factors that bind to retinoic acid response elements (RAREs) in the promoter regions of target genes as a heterodimer with a retinoid x receptor (RXRα,β and γ) partner. Loss of a single *RAR* leads to mild congenital malformations which do not recapitulate the fetal VAD phenotype (Lohnes *et al.*, 1993; Lufkin *et al.*, 1993; Luo *et al.*, 1995). However, double *RAR* mutants are severely affected and collectively display all the features of developmental VAD (Lohnes *et al.*, 1994; Mendelsohn *et al.*, 1994; Kastner *et al.*, 1995). Combinations of *RAR* and *RXRα* null mutants also recapitulate the fetal VAD phenotype, consistent with the vitamin A signal being conveyed by RXR/RAR heterodimers (Kastner *et al.*, 1994, 1997). Furthermore, *RXRα* null, and certain *RAR* double mutants exhibit several cardiac abnormalities, including reduced myocardium and lack of outflow tract septation (Kastner *et al.*, 1994, 1997; Mendelsohn *et al.*, 1994; Sucov *et al.*, 1994). Although these studies demonstrate that RAR/RXR heterodimers transduce the retinoid signal during embryogenesis, these data also underscore a high degree of functional overlap among the RARs.

To circumvent redundancy among the RARs, we have generated a cell line in which we substituted one *RARγ* allele with a ligand-binding deficient receptor. The advantages of this approach are multiple. First, it bypasses the cumbersome genetics needed to generate triple RAR null mutants. Second, it allows for specific inhibition of RAR signaling within a defined spatial-temporal context, in this case the RARγ expression domain. Finally, chimeric approaches can allow an inference as to the

primary site of RAR function for a given defect. In this regard, we show that RAR function in foregut endoderm is likely required for the development of the caudal pharyngeal arches, consistent with previous work (Dupé *et al.*,1999; Wendling *et al.*, 2001). We also describe a novel role for retinoid signaling in late cardiac looping morphogenesis, which was associated with a reduction in Pitx2 expression. These results demonstrate the utility of the targeted expression of a dominant negative RAR to circumvent functional redundancy in RAR signaling in the mouse and show a previously unsuspected role for retinoid signaling in late cardiac looping events.

MATERIALS AND METHODS

Gene Replacement

A dominant negative mouse *RARγ2* cDNA was created using the oligonucleotide 5'-CACAATGCTGGCTTTGAACCCCTTACAGACCTCG-3' for site-directed mutagenesis using the Transformer Kit (Clontech) resulting in a glycine to glutamic acid change at amino acid position 305 in the ligand binding domain. The mutated *RARγ2* cDNA (henceforth referred to as *RARγE*) was subcloned into a targeting vector containing a bifunctional thymidine kinase-neomycin (*TK-Neo*) selection cassette driven by the phosphoglucose kinase (PGK) promoter and flanked by *loxP* sites. These sequences were cloned into a Not I site engineered within exon5 of the *RARγ* locus resulting in the destruction the initiator ATG for the endogenous *RARγ2* gene. The targeting construct contained 1.5kb of homologous genomic sequences upstream and 5.8kb downstream of the integration site. An expression vector encoding diptheria toxin A chain (DT-A; Yagi *et al.*, 1990) was subcloned 3'of *RARγ* genomic sequences for negative selection.

R1 ES cells were cultured on mitotically inactivated murine embryonic fibroblasts under standard conditions (Wurst and Joyner, 1993). Cells were electroporated with 25 μg of linearized targeting vector and selected with G418 for 8-10 days. Genomic DNA from resistant colonies was restricted with Eco RI and targeted clones were identified using a 350bp Rsa I-Bam HI probe external to the targeting vector (probe 1, Fig. 1). Targeted clones were expanded and the *TK-Neo* cassette was excised by transient transfection with a *Cre* recombinase expression vector (Gu *et al.*, 1993). Desired

recombinants were identified by restriction with Eco RV and hybridization with 1.6kb Bam H1-Eco RI probe (probe 2, Fig. 4-1).

Generation Of Chimeric Embryos

Two independently targeted ES cell clones were used to generate chimeric embryos by standard injection of either C57BL/6 or ROSA26 host blastocysts (Hogan *et al.*, 1994; Zambrowicz *et al.*, 1997); embryos derived from either host exhibited similar defects. Embryos were dissected at E9.5 to E10.5 in PBS and fixed overnight in freshly prepared 4% paraformaldehyde (PFA) in PBS at 4°C. Some embryos were subsequently dehydrated through a methanol series in PBS/0.1% Tween-20 and stored at –20°C for whole-mount *in situ* hybridization. For histology, embryos were dehydrated through an ethanol series, embedded in paraffin, sectioned at 7 μm, and deparafinized and processed for hematoxylin and eosin staining. Some embryos generated from ROSA26 blastocysts were fixed in 4% PFA at room temperature for 1 to 2 hours, rinsed in PBS, and stained for β-galactosidase activity overnight at 37°C as described (Hogan *et al.*, 1994). Embryos were then embedded and sectioned as above.

Immunohistochemistry

Embryos were fixed in 4% PFA in PBS overnight at 4°C, and processed for staining as described above. Sections were deparafinized, rehydrated through an ethanol series, fixed in 10 mM sodium citrate buffer, and immunohistochemistry performed as described previously (Lanctot *et al.*, 1999). Briefly, following fixation specimens were blocked in 10% goat serum in PBS/0.2% Tween-20 and reacted with rabbit anti-mouse primary antibodies against either Pitx2 (P2R10; Hjalt *et al.*, 2000) or ANF (Santa Cruz). Samples were then rinsed in PBS/0.2% Tween-20, blocked as above, incubated with biotinylated anti-rabbit secondary antibody (Vector Labs), and subsequently with horse radish peroxidase-coupled streptavidin (NEN Life Sciences). Reactivity was revealed with diamino benzidine (Sigma) in PBS for 6-8 minutes. Specimens were counterstained with methyl green (Sigma) before mounting.

Whole-Mount In Situ *Hybridization*

Whole-mount *in situ* hybridization was performed as described previously (Wilkinson, 1992). Digoxigenin-labeled RNA probes were synthesized from vectors containing ventricular myosin light chain 2 (*MLC2v*; O'Brien *et al.*, 1993; Bruneau *et al.*, 2001), *Tbx5* (Bruneau *et al.*, 1999), or *eHand* (Srivastava *et al.*, 1995). Expression was visualized by staining for anti-digoxygenin-coupled alkaline phosphatase using either BM purple (Roche) or NBT/BCIP.

RESULTS

Replacement Of RARγ2 With A Dominant Negative Receptor

The *RARγE* cDNA was targeted to exon 5 of the *RARγ* locus to provide a restricted expression of the dominant negative receptor (Fig. 4-1). *Tk-Neo* sequences were subsequently removed by transient Cre recombinase expression and desired recombinants were characterized as described in Figure 4-1A. Expression of the dominant negative *RARγ* was confirmed by sequencing of RT-PCR products from ES cells (data not shown).

Two independent clones were injected into host blastocysts and the offspring from several litters examined at 3 weeks of age for coat color contribution. The resulting chimeras contained no more than ~30% ES cell coat coloration, suggesting that strong contribution of RARγE cells was embryo lethal. Consistent with this, RARγE chimeric embryos exhibited numerous defects, many of which have been previously seen in retinoid receptor double null offspring or in *Raldh2* null embryos (Kastner *et al.*, 1995; Chambon, 1996; Dupé *et al.*, 1999; Mendelsohn *et al.*, 1994; Niederreither *et al.*, 1999). These included pharyngeal arch hypoplasia, axial truncation, micropthalmia and heart defects (data not shown and see below).

The contribution of RARγE cells during embryogenesis was examined by injecting ES lines into ROSA26 recipient blastocysts. ROSA26 embryos express β-gal ubiquitously throughout development, and is a useful means to assess ES cell contribution (Zambrowicz *et al.*, 1997). RARγE ES cells contributed to all embryonic tissues (e.g. Fig. 4-2D, E, G, and H, and data not shown), with strong contributions to certain populations correlating with specific phenotypes. Control injections of wild type

Figure 4-1. Gene replacement of RARγ with the RARγE cDNA.

(A) A schematic representation of the RARγ locus is depicted on the top. Dark grey boxes indicate exons 5 and 8 of the RARγ2 isoform, and the DNA binding domain for both RARγ1 and RARγ2, respectively. The targeting vector is shown below the RARγ locus, and contains the RARγE cDNA, a thymidine kinase-Neomycin resistance (TK-Neo) bifunctional fusion gene flanked by Lox P sites (represented by black triangles), and the diptheria toxin A chain (DTA) 3' to targeting sequences for negative selection. Sequences are not drawn to scale. The targeted locus is shown below the targeting vector. The integration results in the destruction of the endogenous ATG of RARγ2. Depicted at the bottom is the floxed-out locus with TK-Neo sequences removed by Cre recombinase. Probe 1 is a 350bp BamHI-RsaI fragment 5' to targeting sequences and was used as an external probe to identify targeted clones. Probe 2 is an internal 1.6kb BamHI-EcoRI used to confirm the removal of TK-Neo sequences by Cre recombinase. B, BamHI; E, EcoRI; K, KpnI; Rv, EcoRV; Xh, XhoI. (B) Southern blot confirming the genomic integrity of targeted and floxed-out alleles. The initial targeting event was identified by EcoRI genomic digests and hybridization to probe 1 (lane 5 vs 1). The internal probe (probe 2) hybridizes to a 5.1kb EcoRI band in the targeted locus and a 1.6kb band upon the removal of TK-Neo sequences (lanes 17 and 21). Targeted alleles digested with EcoRV hybridized to a 1.8kb fragment with probe 2, while floxed-out alleles displayed a 5.8kb EcoRV fragment (lanes 20 and 24), confirming the loss of the selection cassette. Hybridization of probe 1 to EcoRV-digested genomic sequences of the targeted allele revealed a 6.5kb fragment, which was shifted to 7.8kb upon the loss of TK-Neo (lanes 8 and 12). In the targeted allele, probe2 hybridized to 6kb BamHI band with the removal the intervening TK-Neo sequences resulting in an increase to 9.5kb, which co-migrated with the wild type fragment (lanes 14, 18 and 22).

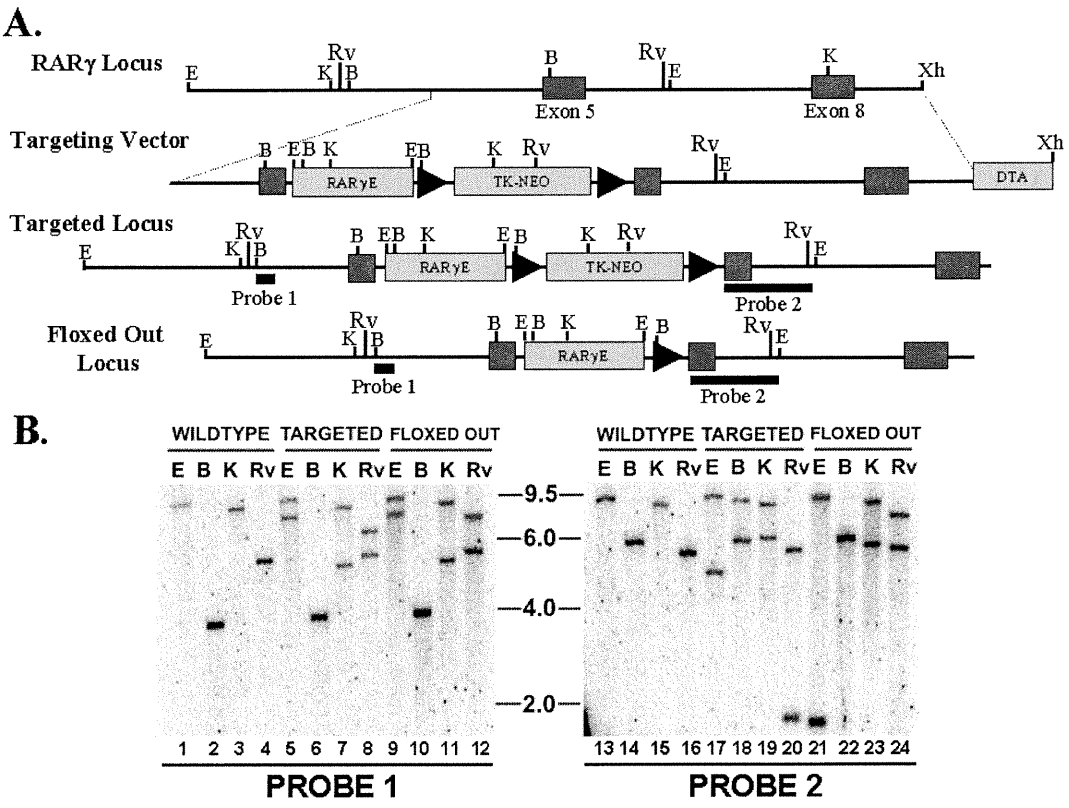
A.
RARγ Locus
Targeting Vector
Targeted Locus
Floxed Out Locus
Exon 5
Exon 8
RARγE
TK-NEO
DTA
Probe 1
Probe 2
B.
WILDTYPE TARGETED FLOXED OUT
E B K Rv E B K Rv E B K Rv
9.5
6.0
4.0
2.0
1 2 3 4 5 6 7 8 9 10 11 12
13 14 15 16 17 18 19 20 21 22 23 24
PROBE 1
PROBE 2

parental ES cells never gave rise to such abnormalities. Below we describe defects in cardiac and pharyngeal arch development in these chimeras.

RAR Function Is Required For Development Of The Caudal Pharyngeal Arches

Pharyngeal arch development is retinoid-dependent. RAR antagonist-treated embryos, RARα/RARβ and RARα/RARγ null offspring exhibit absent or hypoplastic pharyngeal arches caudal to the 2nd arch (Dupé *et al.*, 1999; Wendling *et al.*, 2000, 2001). The phenotype of mice null for *raldh2*, an enzyme essential for the generation of most embryonic RA, also supports a critical role for retinoid signaling in the pharyngeal arches (Niederreither *et al.*, 1999). Based on these data, and the pattern of expression of RARγ (Ruberte *et al.*, 1990), RARγE chimeras were examined for pharyngeal arch defects.

Wild type embryos at E10.5 have four externally discernable pharyngeal arches, which consist of a largely neural crest cell-derived mesenchymal component surrounded by ectoderm on their external surface and endoderm lining their interior border (Fig. 4-2B and C). Aortic arches are found within the interior of branchial arches 1- 4 and are evident in 2nd through 4th branchial arches in section Fig. 4-2C (a2-a4). Strong contribution of RARγE cells to the pharyngeal arches was frequently associated with a hypoplastic 3rd arch and absent 4th arch (e.g. Fig. 4-2F, compare with 4-2C). In affected embryos, aortic arches were hypoplastic or absent in the 2nd branchial arch and reduced in the 3rd arch (Fig. 4-2F). One chimera displayed agenic and hypoplastic caudal arches on the right side only (Fig. 4-2G-I). This unilateral arch deficiency involved the loss of the fourth pharyngeal arch and hypoplasia of the 3rd pouch (B4 and P3, respectively; Fig. 4-2I), and was associated with a greater mutant cell contribution in the right relative to the left side of the embryo. In contrast, the pharyngeal arches on the left side developed essentially normally, with the exception of the loss of the 4th aortic arch (a4; Fig. 4-2I, compare with 2C). In this regard, it is interesting to note that, although the mesenchyme of these pharyngeal arches was largely RARγE-derived, the underlying endoderm was predominantly wild type (compare Fig. 4-2I with 4-2C). This suggests that RAR function in pharyngeal endoderm is necessary and sufficient to direct pharyngeal arch development, with the exception of the development of the aortic arches.

Figure 4-2. RARγE chimeric embryos display pharyngeal arch defects.

(A, B) Frontal and left side views of an E10.5 wild type embryo, respectively. Frontal (D,G) and left side (E, H) views of RARγE←→ROSA26 chimeric embryos stained for β-galactosidase (β-gal) activity. The chimera in D and E shows greater RARγE cell contribution, while the chimera in G and H shows strong wild type contribution, particularly in the pharyngeal arch region (arches are numbered). Scale bar in (A) is 250μm. (C, F, I) Frontal sections through the pharyngeal regions of wild type (C) and chimeric (F, I) embryos. The wild type section was stained with eosin and the chimera in (C) was counter-stained with eosin following β-gal staining. The chimera in (I) was sectioned after x-gal staining and mounted without counterstaining. RARγE contribution to the pharyngeal endoderm correlated with a loss of caudal pharyngeal arches and aortic arches (F). The population of wild type cells (blue) in the endoderm was associated with caudal pharyngeal arch development (I). bc, bulbis cordis, fb, forelimb bud, la, left atrium, lv, left ventricle, rv, right ventricle, o, outflow tract, 1, first pharyngeal arch, 2, second pharyngeal arch. B1-B4, first to fourth pharyngeal arches, a2-a4, second to fourth aortic arches, P3-P4, third and fourth pharyngeal pouches. Scale bar in (C) is 100μm.

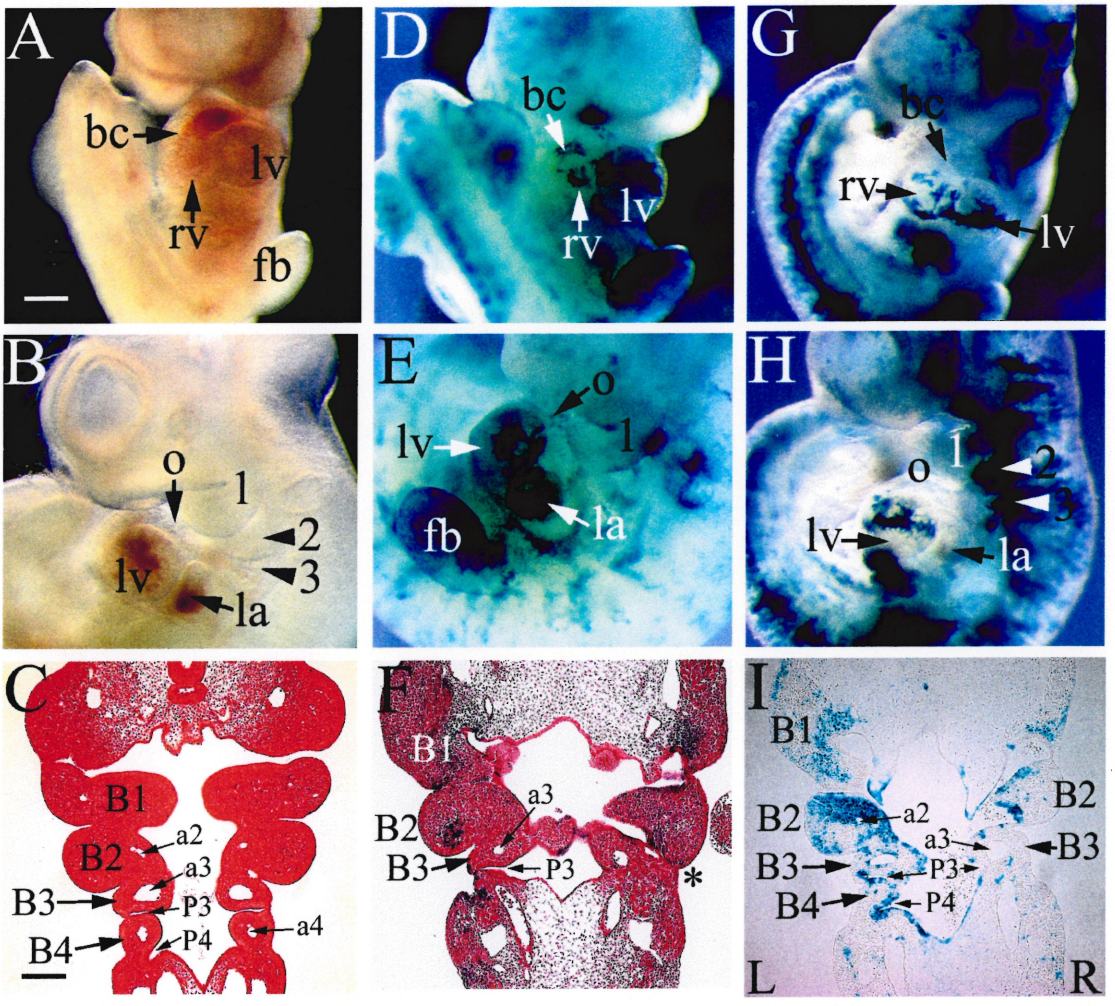
A
bc
lv
rv
fb
D
bc
lv
rv
G
bc
rv
lv
B
o
l
2
3
lv
la
E
o
lv
l
fb
la
H
o
l
2
3
lv
la
C
B1
B2
a2
a3
B3
P3
a4
P4
B4
F
B1
a3
B2
B3
P3
*
I
B1
B2
B2
a2
a3
B3
B3
P3
B4
P4
L
R

Cardiac Positioning Defects In RARγE Chimeras

Aberrant heart looping can be induced by VAD in avians (Heine *et al.*, 1985; Dersch and Zile, 1993; Dickman and Smith, 1996). Although cardiac looping defects have never been described in any retinoid receptor null mutants, RA excess or RAR antagonist treatment can affect cardiac looping concomitant with altered expression of several markers of the left-right signaling pathway, including *nodal*, *lefty2* and *pitx2* (Chazaud *et al.*, 1999; Tsukui *et al.*, 1999; Wasiak and Lohnes, 1999). A role for retinoid signaling in looping morphogenesis is further supported by the finding that *raldh2* null embryos exhibit a block in cardiac looping (Niederreither *et al.*, 1999, 2001). Consistent with these observations, 28% of all chimeras examined in the present study displayed some form of heart defects, the majority of which consisted of ventricular malpositioning, evident in 14% of all embryos examined (e.g. Fig. 4-2E, 4-4C-H, and 4-5C-G). Cardiac looping defects ranged from a slight misalignment of the ventricles to a severe block in cardiac looping (e.g. Fig. 4-3C, D), and rarely, a complete reversal of heart looping (e.g. Fig. 4-3L). As these data were derived from all embryos generated, irrespective of chimerism, they are an under-representation of the incidence of cardiac defects evoked by RARγE.

Pitx2, a member of the bicoid family of homeobox-containing transcription factors, is a downstream effector of the left-right pathway (Logan *et al.*, 1998; Piedra *et al.*, 1998; Ryan *et al.*, 1998; Yoshioka *et al.*, 1998; Campione *et al.*, 2001). It is expressed in the left LPM and left side of the linear heart tube during early somite stages and demarcates the left-ventral side of the heart throughout cardiac development (Hjalt *et al.*, 2000; Campione *et al.*, 2001). Aberrant retinoid signaling has been shown to affect *pitx2* expression concomitant with abnormal heart looping (Chazaud *et al.*, 1999; Tsukui *et al.*, 1999; Wasiak and Lohnes, 1999). Moreover, in VAD quails, aberrant looping morphogenesis is associated with reductions in *nodal* and *pitx2* expression (Zile *et al.*, 2000). We therefore examined the expression of Pitx2 protein in RARγE←→ ROSA26 chimeras.

In controls at E9.5, Pitx2 was expressed in the ectoderm of the frontonasal mass and the mandibular arch, in the left splanchnopleure, and at lower levels in the caudal aspect of the left wall of the atrium and conotruncus consistent with previous data (Fig. 4-3A; Hjalt *et al.*, 2000; Campione *et al.*, 2001). In the E9.5 chimera in Figure 4-3C, D, a

rightward looping of the bulbis cordis was initiated, but the ventricle failed to complete the looping that normally positions it on the left side (compare Fig. 4-3C with 4-3A; Fig. 4-3D with 4-3B). The heart of this chimera was largely composed of RARγE cells, with the exception of strong wild type contribution to the posterior wall of the left atrium, part of the dorsal aspect of the bulbis cordis, and the myocardium separating the left atrium from the ventricular chamber (red arrowheads in Fig. 4-3C, D). Interestingly, the left posterior atrial wall of the chimera, which was largely wild type, maintained Pitx2 expression, whereas adjacent splanchnopleure, consisting mainly of RARγE cells, exhibited reduced Pitx2 (Fig. 4-3C, compare with Fig. 4-3A). This effect was specific to the left LPM derivatives and heart as Pitx2 in the ectoderm of the mandibular arch, derived mostly from RARγE cells, was unaffected (red asterix in Fig. 4-3C compare to Fig. 4-3A).

Pitx2 expression at E10.5 continues to be asymmetric in several developing organs, including the heart and primitive stomach (black arrowheads; Fig. 4-3E and 4-3F). In more ventral sections, Pitx2 was expressed in left dorsal wall of the ventricle and the atrioventricular canal (Fig. 4-3F and 4-3K). Abnormal ventricular looping was observed in chimeras at E10.5 in which the ventricles were positioned more dorsally and anteriorly than in controls (Fig. 4-3G-J; compare to Fig. 4-3E, F). These anomalies were associated with a downregulation of Pitx2 expression in the left heart and the left stomach primordium, which were mostly composed of RARγE cells (black arrowheads in Fig. 4-3I, J; compare to Fig. 4-3E, F). Loss of Pitx2 in the heart was not always associated with RARγE cell contribution, as the chimera in Figure 4-3G,H displayed a loss of Pitx2 in the heart despite considerable wild type cell contribution (red arrowheads; Fig. 4-3G, H).

Two chimeras displayed a complete reversal of heart looping with a normal left-positioned stomach lumen (Fig. 4-3L). This defect was associated with a lack of Pitx2 expression in the heart and stomach, although expression in the buccopharyngeal ectoderm was unaffected (Fig. 4-3L, compare to 4-3K).

Figure 4-3. PITX2 expression in RARγE chimeras.

(A,B) Immunohistochemistry of frontal sections of E9.5 wild type embryo using PITX2-specific antibodies showing PITX2 expression (brown) in the splanchnopleure (spl), dorsal-caudal region of the heart, the ectoderm of the first pharyngeal arch (red asterix), and in the left side of the conotruncus (ct) and in the myocardial wall of the left atrium. (B) More ventral section than (A). (C,D) Frontal sections of E9.5 RARγE←→ROSA26 displaying weak PITX2 expression in the splanchnopleure. Note high levels of PITX2 in the first arch ectoderm of chimeras (red asterix in C, compare to A). Red arrowheads identify regions of strong wild type cell contribution in the chimeras. (E, F) Frontal sections of E10.5 wild type embryos showing PITX2 expression in the left wall of the ct, left atrium (la), and left side of the stomach primordium (st). Black arrowheads point to left-specific PITX2 expression. (G, H and I, J) Frontal sections of two different RARγE←→ROSA26 chimeras showing reduced PITX2 expression in the stomach primordium and left side of the heart. Red arrowheads in (G, H, and I) identify regions of strong wild type cell contribution (dark blue). Black asterix in (I, J) identifies the dorsal region of a chimeric heart that is largely derived from RARγE cells. Scale bar in (A) is 80μm. (K) Frontal section of an E10.5 wild type embryo displaying PITX2 expression in the left myocardial wall of the ct and in the atrioventricular canal (avc; black arrowheads). Note also the expression in the region of the stomach, and the buccopharyngeal ectoderm. (L) Comparable section of a RARγE←→ C57BL/6 chimera displaying a reversal in heart looping. PITX2 expression was absent or highly reduced in the left heart and stomach, while it remained strong in the buccopharyngeal region. Note the position of the stomach in (L) was comparable to the control (K). avc, atrioventricular canal, bc, bulbis cordis, ct, conotruncus, la, left atrium, ra, right atrium, spl, splanchnopleure, st, stomach primordium, tr, trabeculae, v, ventricle, All embryos were counterstained with methyl green. Scale bar in (K) is 160μm.

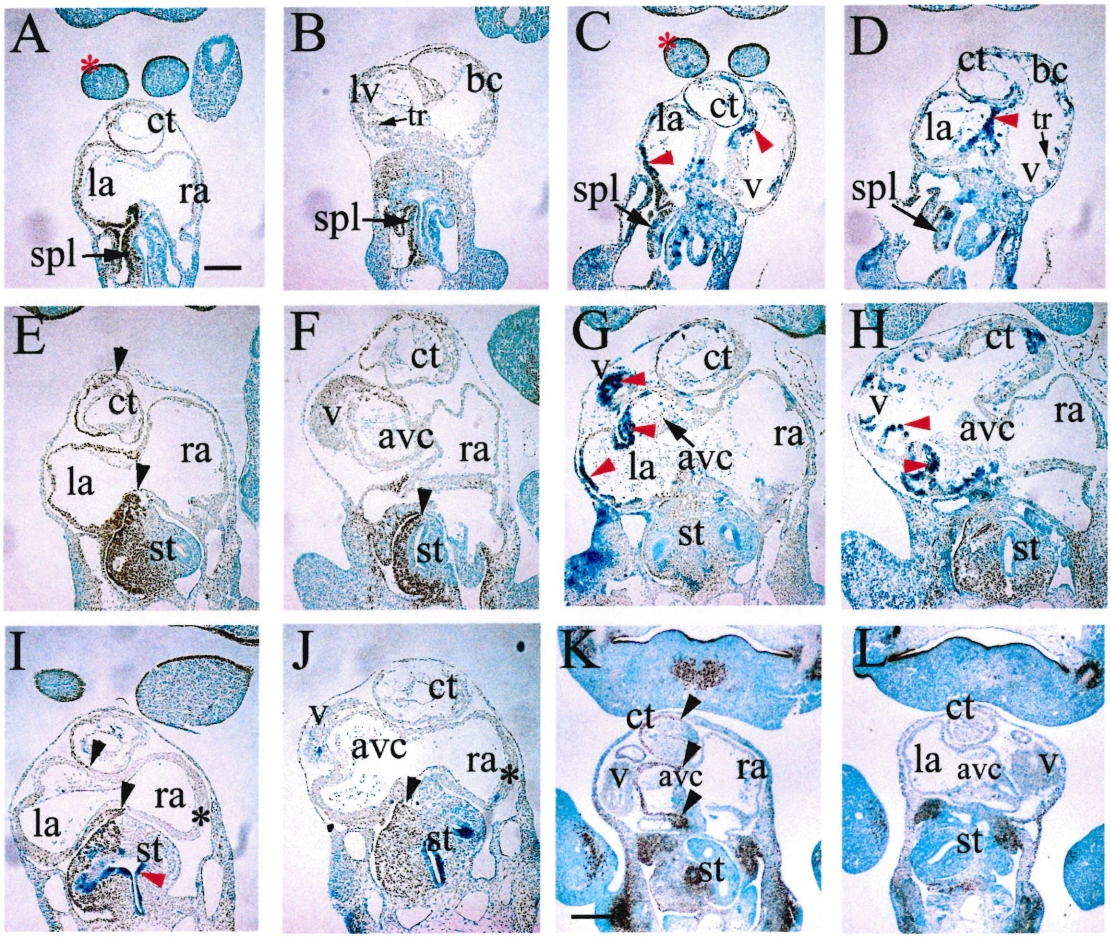
A
ct
la
ra
spl
B
lv
bc
tr
spl
C
la
ct
spl
v
D
ct
bc
la
tr
v
spl
E
ct
ra
la
st
F
ct
v
avc
ra
st
G
v
ct
ra
la
avc
st
H
ct
v
avc
ra
st
I
ra
la
st
J
v
ct
avc
ra
st
K
ct
v
avc
ra
st
L
ct
la
avc
v
st

Trabecular Deficiency In RARγE Chimeras

The myocardium develops as a thin layer of cells surrounding the ventricle and subsequently projects proliferating myoblastic strands of cells in response to signals from the endocardium; these cells become the future trabecular system of the heart (Fig. 4-4A, B; Challice and Viragh, 1973; Fishman and Chien, 1997; Gassmann *et al.*, 1995; Kaufman, 1992; Lee *et al.*, 1995; Meyer and Birchmeier, 1995). The thin peripheral myocardial layer begins to thicken at E11.5-12.5 until it gives rise to a dense compact layer by E14.5-16.5 that forms the ventricular wall. Several retinoid receptor mutants and VAD fetuses exhibit deficiencies in ventricular myocardium (Wilson *et al.*, 1953; Sucov *et al.*, 1994; Kastner *et al.*, 1994, 1997; Mendelsohn *et al.*, 1994). Consistent with this, we observed a severe deficiency in ventricular myocardium in chimeras as early as E9.5 (tr in Fig. 4-3D, compare with 4-3B). In *RXRα* mutants, and to a lesser extent *RARαγ* mutants, myocardial hypoplasia becomes apparent only after E11.5 (Sucov *et al.* 1994; Kastner *et al.*, 1994, 1997), therefore the deficiencies observed in RARγE chimeras represent a more severe perturbation of cardiomyocyte development.

To characterize this ventricular myocardial deficiency further, ANF expression was assessed. ANF is initially expressed on the ventral surface of the heart at E8 (Christoffels *et al.*, 2000; Zeller *et al.*, 1987). By E9.5, ANF expression becomes stronger on the outer curvature of the left ventricle and begins to be expressed in the developing lateral-dorsal myocardium of the atria. At E10.5, ANF expression becomes elaborated in the developing trabeculae of the left ventricle and in the atria, and is down-regulated in the right ventricle (Fig. 4-4C, D).

E10.5 chimeras displaying reduced trabeculation maintained ANF expression in the migrating myoblastic strands in the left ventricle (Fig. 4-4G, I, compare with Fig. 4-4D). This trabecular deficiency varied between affected chimeras, with the specimen in Figure 4-4H, I showing a much greater reduction than the chimera in Figure 4-4E-G. The myocardial deficiency was apparent as early as E9.5 in a chimera displaying a nearly completely mutant heart, which displayed a block in looping morphogenesis (Fig. 4-4K, compare to control in 4-4J). These results suggest that RARγE contribution to the heart resulted in reduced ventricular trabeculation, although myocardial specification was not overtly perturbed as ANF expression was unaffected. Moreover, RARγE-derived tissue

Figure 4-4. Trabecular deficiency in RARγE chimeras.

(A, B) Frontal sections of hematoxylin-eosin stained E10.5 wild type hearts. (C, D) Immunohistochemistry showing ANF expression (brown) in E10.5 wild type hearts. ANF was expressed in the myocardial wall of the atria (C) and was more abundant in the developing trabeculae (tr) and wall of the left ventricle (lv; D). (E-G) Serial frontal sections of an E10.5 RARγE←→ ROSA26 chimera showing a moderate reduction in the trabeculae. (H-I) Serial frontal sections of a chimera displaying a severe reduction in trabeculation and hypoplastic left ventricle. Ventricular specification was unaffected as ANF expression was still strong in the left ventricle (I). Note the prevalence of wild type (β-gal positive) cells associated with increased trabeculation (red asterix in F and I). (J) Frontal section of E9.5 wild type embryo showing ANF expression in the wall and early trabeculae of the left ventricle (lv) and the bulbis cordis (bc). (K) Comparable section of a E9.5 RARγE←→ROSA26 displaying abnormal cardiac positioning and a reduction in the myocardium and ANF expression. The greatest reduction was observed in the bulbis cordis, which failed to complete a rightward loop (J, K). The relative lack of β-gal positive cells in the chimera indicates a largely RARγE-derived heart. avc, atrioventricular canal, bc, bulbis cordis, ct, conotruncus, la, left atrium, ra, right atrium, lv, left ventricle, rv, right ventricle, tr, trabeculae, SV, sinus venosus. Scale bar in (A) is 80μm.

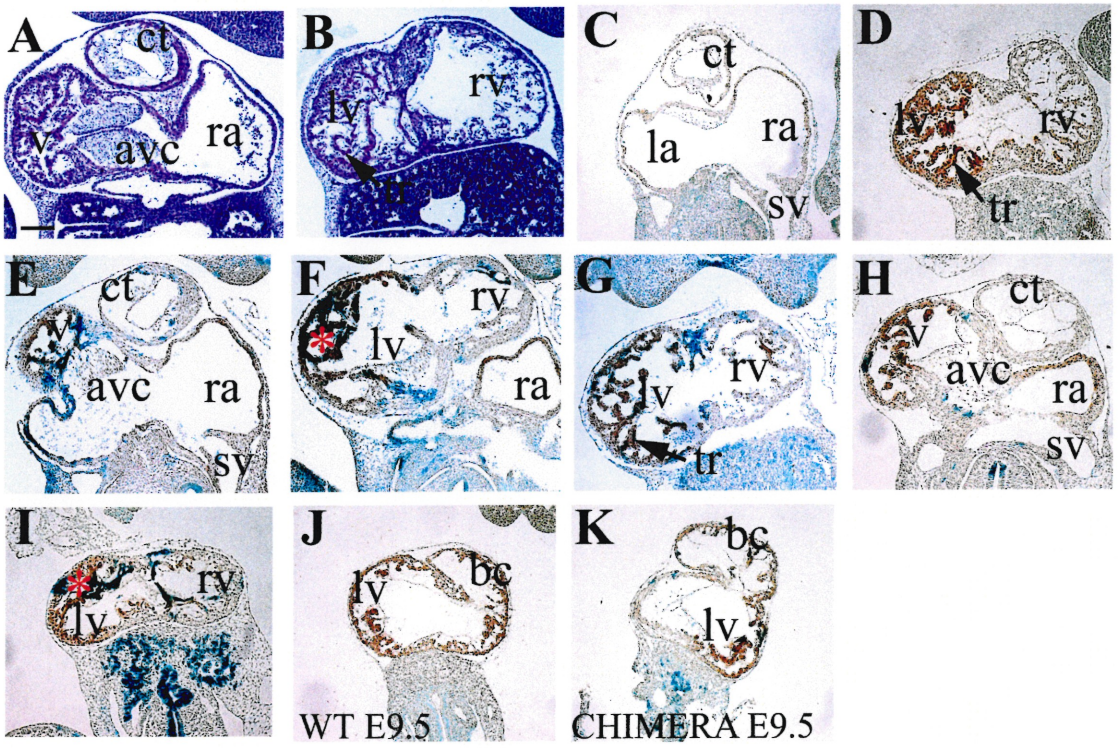
A
ct
v
avc
ra
B
rv
lv
tr
C
ct
la
ra
sv
D
lv
rv
tr
E
ct
v
avc
ra
sv
F
rv
lv
ra
G
rv
v
tr
H
ct
v
avc
ra
sv
I
rv
lv
J
bc
lv
WT E9.5
K
bc
lv
CHIMERA E9.5

still formed trabeculae, consistent with previous studies suggesting a non cell-autonomous requirement for retinoid signaling in this process (Chen *et al.*, 1998; Tran and Sucov, 1998).

Chamber Specification In RARγE Chimeras

Given that ANF expression was largely normal in the chimeras irrespective of the severity of cardiac defects, we examined the expression of additional cardiac markers including *ventricular myosin light chain 2* (*MLC2v*), *tbx5*, and *eHand.*

MLC2v is initially detected in the cardiac crescent at E7.5 (Lyons *et al.*, 1990; O'Brien *et al.*, 1993). In the linear heart tube, *MLC2v* expression is strongest in the medial region fated to give rise to the ventricles (O'Brien *et al.*, 1993; Christoffels *et al.*, 2000). Strong expression is maintained in the ventricles and proximal outflow tract at E9.5-E10.5, with lower levels seen in the atrioventircular canal (Christoffels, *et al.*, 2000; Fig.4-5A, B and data not shown). *MLC2v* was not altered in chimeras displaying overt cardiac looping defects at E9.5 (Fig. 4-5C-H, compare to 4-5A, B) nor at E10.5 (data not shown).

EHand expression is restricted to the anterior and posterior domains of the linear heart tube (Srivastava *et al.*, 1995). These regions give rise to the outflow tract and left ventricle, respectively, which strongly express *eHand* at E10.5 (Srivastava *et al.*, 1995; Fig. 4-6A, B). The outer curvature of the outflow tract also expresses *eHand*, but transcripts were excluded from the right ventricle, inner curvature of the heart and the atria. No differences in *eHand* expression were observed in E10.5 chimeras with overt heart defects (Fig. 4-6C-H).

Tbx5 is expressed as a posterior high gradient in the linear heart tube (Chapman *et al.*, 1996; Bruneau *et al.*, 1999). At E9.5, *tbx5* transcripts are detected in the presumptive right and left ventricles and in both atrial chambers, with greater expression in the left ventricle relative to the right (Chapman *et al.*, 1996; Bruneau *et al.*, 1999; Fig. 4-7A-C). Thus, *tbx5* is a lineage marker for cardiac structures arising from the posterior heart tube (Christoffels *et al.*, 2000). However, as with other chamber-specific markers, no difference in *tbx5* expression was detected in affected chimeras (Fig. 4-7D-F).

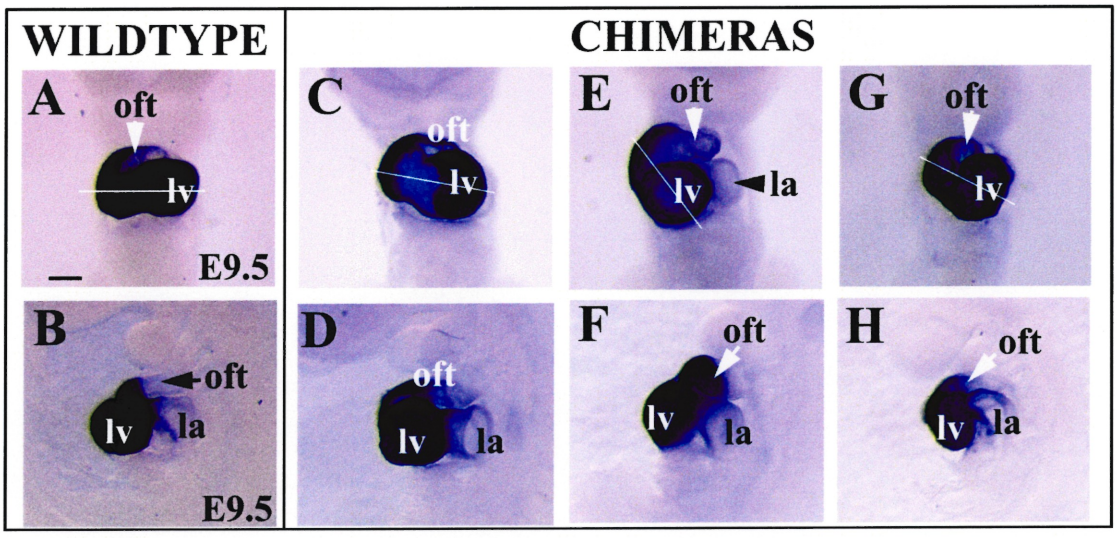

Figure 4-5. MLC2v expression is not affected in RARγE chimeras.

(A-H) *In situ* hybridization of MLC2v in E9.5 embryos. Frontal (A) and left (B) views of wild type controls showing MLC2v expression throughout the ventricles and proximal outflow tract (oft). (C, E, G) Frontal views of three E9.5 RARγE←→C57BL/6 chimeras displaying various degrees of abnormal cardiac looping. White bar traces the axis along the presumptive right and left ventricles. (D, F, H) Left side views of the same chimeras displaying looping anomalies. bc, bulbis cordis, la, left atrium, ra, right atrium, lv, left ventricle. rv, right ventricle, oft, outflow tract. Scale bar in (A) is 400μm.

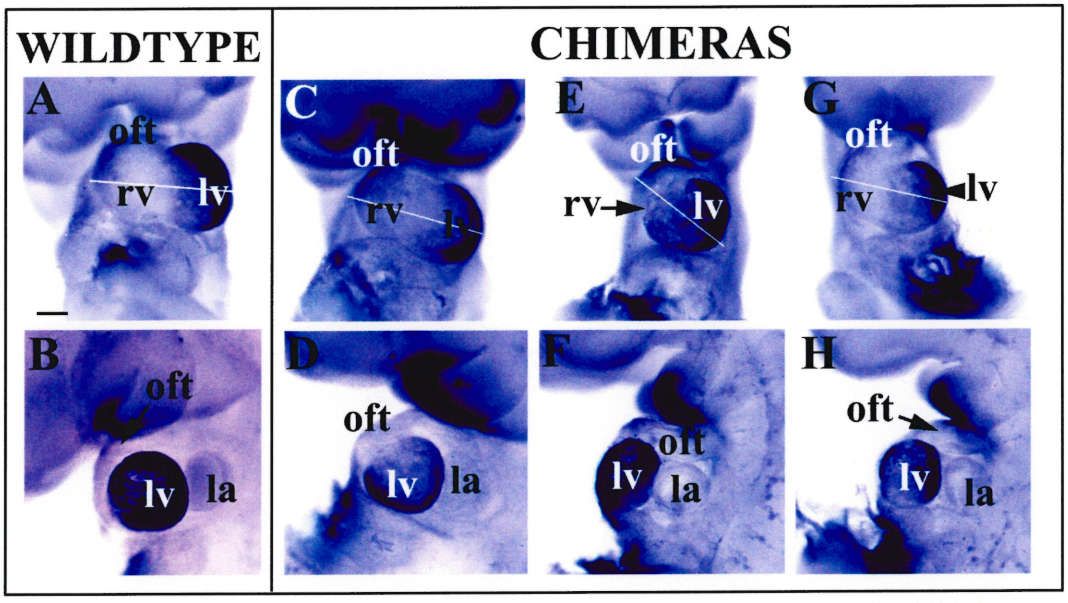

Figure 4-6. Expression of eHand is not affected in RARγE chimeras.

Frontal (A) and left(B) views of eHand expression in E10.5 wild type embryos in the left ventricle (lv) and outer curvature of the outflow tract (oft). (C, E, G) Frontal views of three RARγE ←→ C57BL/6 chimeras displaying abnormal looping, indicated by the white line. (D, F, H) Left side views of the chimeras in C, E, and G, respectively, demonstrating strong eHand expression in the left ventricle. la, left atrium, lv, left ventricle, rv, right ventricle, oft, outflow tract. Scale bar in (A) is 400μm.

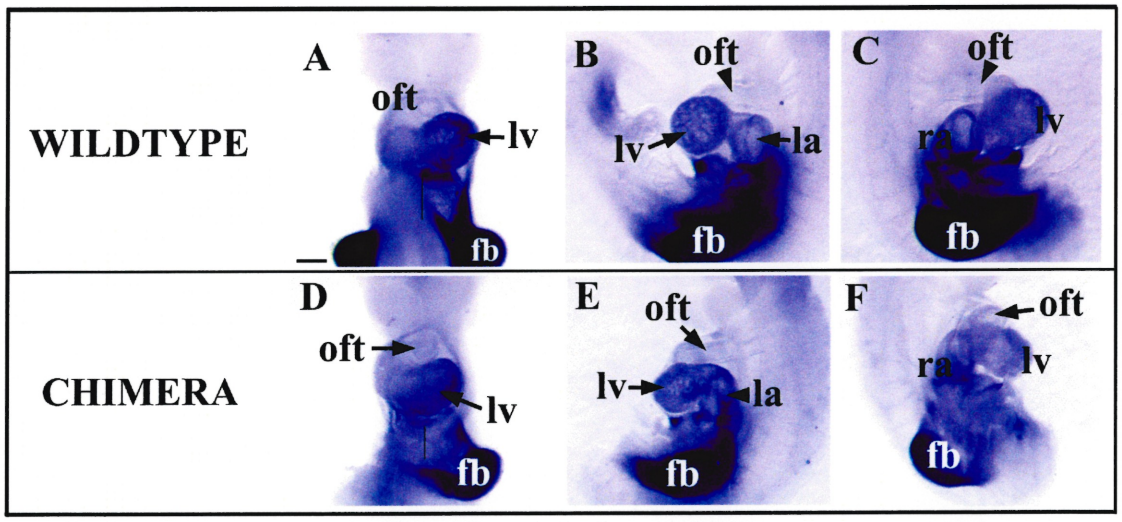

Figure 4-7. Expression of Tbx5 is not altered in RARγE chimeras.

(A-F) *In situ* hybridization of Tbx5 in E9.5 wild type (A-C) and a RARγE chimeric embryos (D-F). Frontal (A), left (B), and right (C) views of a wild type embryo showing Tbx5 expression in the ventricles and atria (lv, la, ra). Expression was more intense in the left ventricular segment than in the right ventricle (A). Non-cardiac expression included the forelimb bud and flank mesoderm. Frontal (D), left (E) and right (F) views of Tbx5 expression in a RARγE←→C57BL/6 chimera displaying a medially displaced ventricle (D compare to A) and an anterior-ventral shift of the proximal outflow tract (F compare to C). Black vertical lines in (A, D) identify the midline of the embryo. Fb, forelimb bud, la, left atrium, ra, right atrium, lv, left ventricle, rv, right ventricle, oft, outflow tract. Scale bar in (A)is 400μm.

DISCUSSION

Retinoid signaling plays key roles in vertebrate embryogenesis. Results from the targeted mutagenesis of the RARs has suggested a considerable degree of functional redundancy among this receptor family (Kastner *et al.*, 1995; Chambon, 1996). The present study attempted to circumvent this problem by substituting RARγ with a dominant negative receptor in ES cells. We present evidence that this mutant interferes specifically with retinoid-dependent events and gives rise to a more severe myocardial phenotype than previously observed with any combinations of *RAR* or *RXR* null mice. Furthermore, we demonstrate a novel role for retinoid signaling in late cardiac looping morphogenesis involving the laterality effector, Pitx2.

A Novel Model For Retinoid Signaling Deficiency In The Mouse

A dominant negative RARα was previously created by modeling an inherited mutation in the ligand-binding domain of thyroid hormone receptor α that leads to generalized thyroid hormone resistance (Saitou et al., 1994, 1995;Yamaguchi et al., 1998). We have created the corresponding mutation in the mouse RARγ cDNA, which we referred to as RARγE, and targeted it to the RARγ locus in ES cells. Chimeras generated from these cell lines displayed pharyngeal arch defects and deficiencies in ventricular myocardium similar to those observed in certain RAR double null embryos (Mendelsohn et al.,1994; Wendling et al., 2000, 2001). As one copy of the RARγE gene sufficed to elicit these effects, this suggests that it functions as a potent dominant negative. Based on studies of the cognate thyroid hormone receptor α mutant, this may occur by a lack of ligand binding and strong association with co-repressors (Yoh et al., 1997).

The RARγE Mutation Inhibits Retinoid Signaling In The Pharyngeal Arches

Pharyngeal arch development is dependent on retinoid signaling. Pan-RAR antagonist treatment, or the combined disruption of certain *RAR* genes all lead to hypoplastic or agenic caudal pharyngeal arches and associated structures (Dupé *et al.*, 1999; Wendling *et al.*, 2000, 2001). Contribution of RARγE cells appeared to reproduce several of these

defects, consistent with the pattern of expression of RARγ (Ruberte *et al.*, 1990), and the behavior of RARγE as a dominant negative receptor specific to RA signaling.

As RARγE was targeted to the RARγ locus, it was expected to be expressed in the pharyngeal arches. Indeed, the caudal-most arches were hypoplastic or lacking altogether in all strong chimeras examined at E10.5. Furthermore, population of RARγE cells in the arch mesenchyme was associated with a reduction or loss of the cognate aortic arches, as has been noted previously in *RAR* double mutants and RAR antagonist-treated embryos (Dupé *et al.*, 1999; Wendling *et al.*, 2000). Interestingly, wild type contribution to the pharyngeal endoderm was associated with normal caudal pharyngeal arch development, despite RARγE-derived arch mesenchyme. This suggests that RAR signaling in the pharyngeal endoderm is necessary and sufficient to direct most aspects of pharyngeal arch development, irrespective of the source of arch mesenchyme. Consistent with this, Wendling and colleagues (2000) ascribed a requirement for retinoids in the endoderm of the pharynx for the proper development of the caudal-most pharyngeal arches. Our chimeric analysis thus provides further support for RAR-dependent endodermal signaling in pharyngeal arch development.

Retinoid Signaling Is Required For Normal Cardiac Looping

Retinoid signaling is required for proper cardiac looping morphogenesis (Niederreither *et al.*, 1999, 2001; Smith and Dickman, 1997; Zile, 1998). These studies suggest that retinoids regulate the effectors of the laterality cascade or affect the ability of the heart to interpret this information (Dersch and Zile, 1993; Zile *et al.*, 2000). Consistent with this, RARγE chimeric embryos often displayed defects associated with aberrant cardiac looping. Frequently, hearts initiated proper rightward looping but had misplaced ventricles or outflow tracts, ranging from varying degrees of incomplete looping to an arrest in morphogenesis, and on rare instances, a complete reversal of cardiac looping was observed. At least certain of these anomalies may be due to the failure of the proximal outflow tract to displace completely to the left despite initiating looping correctly, in agreement with prior work in VAD quails (Zile *et al.*, 2000).

Certain retinoid receptor null mutants exhibit a thin myocardial wall due to precocious ventricular cardiomyocyte differentiation, and absence of outflow tract

septation (Mendelsohn *et al.*, 1994; Kastner *et al.*, 1994, 1997; Sucov *et al.*, 1994). However, these studies failed to support a role for these receptors in cardiac looping morphogenesis, as suggested by the outcome of VAD in avians (Dersch and Zile, 1993; Heine *et al.,* 1985; Kostetskii *et al.,* 1998; Zile *et al.,* 2000). A possible explanation for this discrepancy is that there remains sufficient retinoid signaling in the compound RXR/RAR mutants to direct cardiac laterality.

VAD quail embryos display abnormal cardiac looping concomitant with a down-regulation of expression of *nodal* and *pitx2* in the left LPM, whereas the asymmetric determinants *actRIIA*, *shh, fgf8, caronte,* or *lefty1* are unaffected (Zile et al., 2000). *Pitx2* is considered to be an important determinant of organ situs, presumably interpreting signals from the laterality cascade (Semina et al., 1996; Logan et al., 1998; Piedra et al., 1998; Ryan et al., 1998; Kitamura et al., 1999; Lin et al., 1999; Liu et al., 2001; Lu et al., 1999). In support of this, the loss of *pitx2* is associated with situs abnormalities of the lungs, gut and posterior heart components (Kitamura et al., 1999; Lin et al., 1999; Liu et al., 2001). Furthermore, the dosage of Pitx2 protein was recently suggested to be critical for organ situs (Liu et al., 2001). As with VAD quail embryos, we also observed a loss of Pitx2 expression in the derivatives of the left LPM and in the hearts of chimeras displaying looping defects, with the greatest decrease in occurring in a chimera that had undergone a complete reversal of heart situs. The contribution of RARγE cells in LPM-derived tissues, such as the splanchnopleure and stomach, was always associated with a loss of Pitx2, suggesting a cell-autonomous requirement for retinoid signaling in the LPM. However, the loss of Pitx2 in the hearts was not strikingly correlated with RARγE contribution, suggesting a non-cell autonomous requirement for retinoid signaling in the heart (see below).

Our results differ from those described for the *raldh2* null mutant, which does not exhibit altered *pitx2* expression despite a block in cardiac looping (Niederreither *et al.*, 2001). A possible explanation for this discrepancy may be that the severe deficiency in retinoid signaling in the *raldh2* mutant results in a block in heart looping due to mechanical constraints imposed by the loss of posterior cardiac tissue. Moreover, *pitx2* expression was examined a full day earlier in *raldh2* mutants than in the present study

(Niederreither *et al.,* 2001). Thus it is possible that *pitx2* is affected by loss of RA signaling only at later stages.

All known components of the retinoid signaling pathway are expressed symmetrically throughout early embryogensis, and RA distribution has no known laterality bias at the stages relevant to heart looping (Fujii *et al.*, 1997; Niederreither *et al.*, 1997; Rossant *et al.*, 1991; Ruberte *et al.*, 1990, 1991; Maden *et al.*, 1998). Thus, retinoid signaling is unlikely to be directly involved in the establishment of the left-right axis but may be involved in maintaining expression of the left-specific effectors, or to provide competence to interpret this information, as suggested previously (Zile *et al.* , 2000). In support of this, recent work provides a precedent for the regulation of *pitx2* at stages subsequent to looping involving a maintenance mechanism (Shiratori *et al.*, 2001). The *pitx2* asymmetric enhancer contains Nodal and Nkx2-5 response elements, and the deletion of the latter element results in a loss of reporter activity at later stages (Shiratori *et al.*, 2001). Thus, *pitx2* requires signals to ensure its continued expression within the LPM and its derivatives later on in development. Our results suggest that retinoid signaling contributes to the maintenance of *pitx2* expression, possibly indirectly by rendering cells within the LPM competent to respond of the left determinants.

Heart looping involves a complex series of morphogenetic processes leading to a dextral-looped heart with the correct positioning of the outflow tract and the atria (reviewed in Manner, 2000). Briefly, this process involves the transformation of the linear heart tube to a dextral c-shaped loop that subsequently undergoes a rightward rotation in the ventricular region and the displacement of the outflow tract to the right of the body. The latter two processes convert the initial c-shaped heart loop to an s-shape one (Manner, 2000). Both these processes seemed to be affected by altered retinoid signaling as RARγE chimeras displayed medially positioned ventricles and abnormal ventro-anterior shift of the outflow tracts. This suggests that retinoid signaling can affect later aspects of looping, possibly through altered *pitx2* expression. On rare instances we observed a complete reversal of cardiac looping in association with a severe reduction of *pitx2* expression in the left LPM and its derivatives, and the heart. The rarity of this defect may reflect the relatively late expression of RARγE within the LPM, as the dominant negative was targeted to the RARγ locus. Given that the expression of *RARγ* in

the nascent LPM begins at approximately E8.25 (Ruberte *et al.*, 1990), and is therefore closely juxtaposed to the initiation of cardiac looping, the occasional chimera may express RARγE during looping morphogenesis, leading to the observed reversals. Alternatively, the rarity of this defect may reflect a artefactual lesion in development that is expected to occasionally occur following blastocyst injection. Taken together, the present study suggests that the inhibition of RAR function in the LPM at stages subsequent to the initiation of heart looping affects late aspects of looping morphogenesis.

RAR Signaling And Myocardial Development

Disruption of certain of the retinoid receptors leads to myocardial deficiencies, particularly of the compact layer (Mendelsohn *et al.*, 1994; Kastner *et al.*, 1994, 1997; Sucov *et al.*, 1994). This may reflect a non cell-autonomous requirement for retinoid signaling, as embryos containing hearts composed mostly of RXRα$^{-/-}$ cells display normal myocardial development (Chen *et al.*, 1998; Tran and Sucov, 1998). Our results also demonstrate a requirement of RAR signaling in myocardial development, as myoblastic invasion of the ventricles was compromised in chimeras containing strong RARγE contribution to the heart, although the mutant cells could form trabeculae. The myocardial deficiency observed in our study was more severe that that noted for the RXRα mutation, likely reflecting a greater inhibition of retinoid signaling occurring in RARγE chimeras relative to RXRα null mutants. Consistent with this, the loss of *raldh2* leads to an even greater deficiency in myocardial development, being evident as early as E9 (Niederreither *et al.*, 2001). Similarly, the loss of myocardium in RARγE chimeras occurred much earlier relative to retinoid receptor null mutations (obvious by E11.5; Kastner *et al.,* 1997). Furthermore, chimeric hearts required considerable contribution mutant cells to evoke trabecular hypoplasia, suggesting that localized signaling from wild type cardiac tissue can rescue the deficiency in retinoid signaling. Paracrine signaling underlies the development of the trabeculae (reviewed in Fishman and Chien, 1997), and the presence of a limited number of wild type cells within chimeric hearts seems sufficient to allow myoblasts to invade ventricle lumen, albeit in a compromised manner.

Our study is consistent with a non cell-autonomous function for retinoid signaling in the heart, as previously suggested (Chen *et al.*, 1998; Tran and Sucov, 1998).

The expression of *MLC2v, eHand, tbx5* and ANF was not altered in chimeras exhibiting cardiac defects, demonstrating that chamber specification was not overtly affected. Cardiac-specific transcription was also largely unaffected in *raldh2*$^{-/-}$ mutants, with the exception of loss of *tbx5* expression, despite the severe defects in this mutant (Niederreither *et al.*, 2001). Retinoid signaling thus appears to be required for myocardial development and posterior heart development, but not for the patterning of the ventricles and outflow tract *per se*.

We describe a novel approach to circumvent functional redundancy of the RARs by a gene-swap approach. Chimeras exhibited a number of defects typical of other models of retinoid signaling deficiency, suggesting a specific inhibition of RAR function. The restricted expression of the dominant negative RAR, in combination with chimeric analysis, offers a viable means to examine retinoid-dependent ontogenic processes, and should reveal further roles for retinoid signaling during mammalian embryogenesis.

ACKNOWLEDGEMENTS

The authors thank Drs. Tord Hjalt and Jeffrey C. Murray for the gift of the Pitx2 antibody, Dr. Benoit Bruneau for his generous advice and plasmids encoding cardiac-specific markers, and Drs. Andras Nagy and Janet Rossant for R1 ES cells. We are grateful to Dr. Qinzhang Zhou at the IRCM transgenic facility for his assistance with blastocyst injections and embryo reimplantation. We also acknowledge Georges Nemer and Alexandre Marcil for reagents and advice for immunohistochemistry. A.I. is a recipient of a studentship from the Medical Research Council of Canada in conjunction with the Spina Bifida and Hydrocephalus Association of Ontario. D.L. is a chercheur-boursier (Junior 2) of the Fonds de la Recherches en Santé de Québec. This work was supported by a grant to D.L. from the Canadian Institutes of Heath Research.

REFERENCES

Bruneau, B. G., Bao, Z. Z., Fatkin, D., Xavier-Neto, J., Georgakopoulos, D., Maguire, C. T., Berul, C. I., Kass, D. A., Kuroski-de Bold, M. L., de Bold, A. J., Conner, D. A., Rosenthal, N., Cepko, C. L., Seidman, C. E., and Seidman, J. G. (2001). Cardiomyopathy in Irx4-deficient mice is preceded by abnormal ventricular gene expression. *Mol. Cell. Biol.* **21**, 1730-1736.

Bruneau, B. G., Logan, M., Davis, N., Levi, T., Tabin, C. J., Seidman, J. G., and Seidman, C. E. (1999). Chamber-specific cardiac expression of Tbx5 and heart defects in Holt- Oram syndrome. *Dev. Biol.* **211**, 100-108.

Campione, M., Ros, M. A., Icardo, J. M., Piedra, E., Christoffels, V. M., Schweickert, A., Blum, M., Franco, D., and Moorman, A. F. (2001). Pitx2 expression defines a left cardiac lineage of cells: evidence for atrial and ventricular molecular isomerism in the iv/iv mice. *Dev. Biol.* **231**, 252-264.

Capdevila, J., Vogan, K. J., Tabin, C. J., and Izpisua Belmonte, J. C. (2000). Mechanisms of left-right determination in vertebrates. *Cell* **101**, 9-21.

Challice, C. E. and Viragh, S. (1973). The architectural development of the early mammalian heart. *Tissue Cell* **6**, 447-462.

Chambon, P. (1996). A decade of molecular biology of retinoic acid receptors. *FASEB J.* **10**, 940-954.

Chapman, D. L., Garvey, N., Hancock, S., Alexiou, M., Agulnik, S. I., Gibson-Brown, J. J., Cebra-Thomas, J., Bollag, R. J., Silver, L. M., and Papaioannou, V. E. (1996). Expression of the T-box family genes, Tbx1-Tbx5, during early mouse development. *Dev. Dyn.* **206**, 379-390.

Chazaud, C., Chambon, P., and *Dollé*, P. (1999). Retinoic acid is required in the mouse embryo for left-right asymmetry determination and heart morphogenesis. *Development* **126**, 2589-2596.

Chen, J., Kubalak, S. W., and Chien, K. R. (1998). Ventricular muscle-restricted targeting of the RXRalpha gene reveals a non-cell-autonomous requirement in cardiac chamber morphogenesis. *Development* **125**, 1943-1949.

Christoffels, V. M., Habets, P. E., Franco, D., Campione, M., de Jong, F., Lamers, W. H., Bao, Z. Z., Palmer, S., Biben, C., Harvey, R. P., and Moorman, A. F. (2000). Chamber formation and morphogenesis in the developing mammalian heart. *Dev. Biol.* **223**, 266-278.

Dersch, H. and Zile, M. H. (1993). Induction of normal cardiovascular development in the vitamin A- deprived quail embryo by natural retinoids. *Dev. Biol.* **160**, 424-433.

Dickman, E. D. and Smith, S. M. (1996). Selective regulation of cardiomyocyte gene expression and cardiac morphogenesis by retinoic acid. *Dev. Dyn.* **206**, 39-48.

Dickman, E. D., Thaller, C., and Smith, S. M. (1997). Temporally-regulated retinoic acid depletion produces specific neural crest, ocular and nervous system defects. *Development* **124**, 3111-3121.

Dupé, V., Ghyselinck, N. B., Wendling, O., Chambon, P., and Mark, M. (1999). Key roles of retinoic acid receptors alpha and beta in the patterning of the caudal hindbrain, pharyngeal arches and otocyst in the mouse. *Development* **126**, 5051-5059.

Fishman, M. C. and Chien, K. R. (1997). Fashioning the vertebrate heart: earliest embryonic decisions. *Development* **124**, 2099-2117.

Fujii, H., Sato, T., Kaneko, S., Gotoh, O., Fujii-Kuriyama, Y., Osawa, K., Kato, S., and Hamada, H. (1997). Metabolic inactivation of retinoic acid by a novel P450 differentially expressed in developing mouse embryos. *EMBO J.* **16**, 4163-4173.

Gassmann, M., Casagranda, F., Orioli, D., Simon, H., Lai, C., Klein, R., and Lemke, G. (1995). Aberrant neural and cardiac development in mice lacking the ErbB4 neuregulin receptor. *Nature* **378**, 390-394.

Gu, H., Zou, Y. R., and Rajewsky, K. (1993). Independent control of immunoglobulin switch recombination at individual switch regions evidenced through Cre-loxP-mediated gene targeting. *Cell* **73**, 1155-1164.

Harvey, R. P. (1998). Cardiac looping-an uneasy deal with laterality. *Semin. Cell Dev. Biol.* **9**, 101-108.

Heine, U. I., Roberts, A. B., Munoz, E. F., Roche, N. S., and Sporn, M. B. (1985). Effects of retinoid deficiency on the development of the heart and vascular system of the quail embryo. *Virchows Arch. B Cell Pathol. Incl. Mol. Pathol.* **50**, 135-152.

Hjalt, T. A., Semina, E. V., Amendt, B. A., and Murray, J. C. (2000). The Pitx2 protein in mouse development. *Dev. Dyn.* **218**, 195-200.

Hogan B., Constantini, F., Lacy, P., and Beddington, R.S.P. (1994). Manipulating the mouse embryo: A laboratory manual, Second Edition. Cold Spring Harbor Laboratory Press, USA.

Kastner, P., Grondona, J. M., Mark, M., Gansmuller, A., LeMeur, M., Decimo, D., Vonesch, J. L., *Dollé*, P., and Chambon, P. (1994). Genetic analysis of RXR alpha developmental function: convergence of RXR and RAR signaling pathways in heart and eye morphogenesis. *Cell* **78**, 987-1003.

Kastner, P., Mark, M., and Chambon, P. (1995). Nonsteroid nuclear receptors: what are genetic studies telling us about their role in real life? *Cell* **83**, 859-869.

Kastner, P., Mark, M., Ghyselinck, N., Krezel, W., Dupé, V., Grondona, J. M., and Chambon, P. (1997). Genetic evidence that the retinoid signal is transduced by heterodimeric RXR/RAR functional units during mouse development. *Development* **124**, 313-326.

Kaufman, M. H. (1992).The Atlas of Mouse Development. Academic Press, San Diego.

Kitamura, K., Miura, H., Miyagawa-Tomita, S., Yanazawa, M., Katoh-Fukui, Y., Suzuki, R., Ohuchi, H., Suehiro, A., Motegi, Y., Nakahara, Y., Kondo, S., and Yokoyama, M. (1999). Mouse Pitx2 deficiency leads to anomalies of the ventral body wall, heart, extra- and petiocular mesoderm and right pulmonary isomerism. *Development* **126**, 5749-5758.

Kostetskii, I., Jiang, Y., Kostetskaia, E., Yuan, S., Evans, T., and Zile, M. (1999). Retinoid signaling required for normal heart development regulates GATA- 4 in a pathway distinct from cardiomyocyte differentiation. *Dev. Biol.* **206**, 206-218.

Kostetskii, I., Yuan, S. Y., Kostetskaia, E., Linask, K. K., Blanchet, S., Seleiro, E., Michaille, J. J., Brickell, P., and Zile, M. (1998). Initial retinoid requirement for early avian development coincides with retinoid receptor coexpression in the precardiac fields and induction of normal cardiovascular development. *Dev. Dyn,* **213**, 188-198.

Lanctot, C., Gauthier, Y., and Drouin, J. (1999). Pituitary homeobox 1 (Ptx1) is differentially expressed during pituitary development. *Endocrinology* **140**, 1416-1422.

Lee, K. F., Simon, H., Chen, H., Bates, B., Hung, M. C., and Hauser, C. (1995). Requirement for neuregulin receptor erbB2 in neural and cardiac development. *Nature* **378**, 394-398.

Liberatore, C. M., Searcy-Schrick, R. D., and Yutzey, K. E. (2000). Ventricular expression of tbx5 inhibits normal heart chamber development. *Dev. Biol.* **223**, 169-180.

Lin, C. R., Kioussi, C., O'Connell, S., Briata, P., Szeto, D., Liu, F., Izpisua-Belmonte, J. C., and Rosenfeld, M. G. (1999). Pitx2 regulates lung asymmetry, cardiac positioning and pituitary and tooth morphogenesis. *Nature* **401**, 279-282.

Liu, C., Liu, W., Lu, M. F., Brown, N. A., and Martin, J. F. (2001). Regulation of left-right asymmetry by thresholds of Pitx2c activity. *Development* **128**, 2039-2048.

Logan, M., Pagan-Westphal, S. M., Smith, D. M., Paganessi, L., and Tabin, C. J. (1998). The transcription factor Pitx2 mediates situs-specific morphogenesis in response to left-right asymmetric signals. *Cell* **94**, 307-317.

Lohnes, D., Kastner, P., Dierich, A., Mark, M., LeMeur, M., and Chambon, P. (1993). Function of retinoic acid receptor gamma in the mouse. *Cell* **73**, 643-658.

Lohnes, D., Mark, M., Mendelsohn, C., *Dollé*, P., Dierich, A., Gorry, P., Gansmuller, A., and Chambon, P. (1994). Function of the retinoic acid receptors (RARs) during

development (I). Craniofacial and skeletal abnormalities in RAR double mutants. *Development* **120**, 2723-2748.

Lowe, L. A., Yamada, S., and Kuehn, M. R. (2001). Genetic dissection of nodal function in patterning the mouse embryo. *Development* **128**,1831-1843.

Lu, M. F., Pressman, C., Dyer, R., Johnson, R. L., and Martin, J. F. (1999). Function of Rieger syndrome gene in left-right asymmetry and craniofacial development. *Nature* **401**, 276-278.

Lufkin, T., Lohnes, D., Mark, M., Dierich, A., Gorry, P., Gaub, M. P., LeMeur, M., and Chambon, P. (1993). High postnatal lethality and testis degeneration in retinoic acid receptor alpha mutant mice. *Proc. Natl. Acad. Sci. U S A* **90**, 7225-7229.

Luo, J., Pasceri, P., Conlon, R. A., Rossant, J., and Giguere, V. (1995). Mice lacking all isoforms of retinoic acid receptor beta develop normally and are susceptible to the teratogenic effects of retinoic acid. *Mech. Dev.* **53**, 61-71.

Lyons, G. E., Schiaffino, S., Sassoon, D., Barton, P., and Buckingham, M. (1990). Developmental regulation of myosin gene expression in mouse cardiac muscle. *J. Cell. Biol.* **111**, 2427-2436.

Maden, M., Gale, E., Kostetskii, I., and Zile, M. (1996). Vitamin A-deficient quail embryos have half a hindbrain and other neural defects. *Curr. Biol.* **6**, 417-426.

Maden, M., Sonneveld, E., van der Saag, P. T., and Gale, E. (1998). The distribution of endogenous retinoic acid in the chick embryo: implications for developmental mechanisms. *Development* **125**, 4133-4144.

Manner, J. (2000). Cardiac looping in the chick embryo: a morphological review with special reference to terminological and biomechanical aspects of the looping process. *Anat. Rec.* **259**, 248-262.

Mendelsohn, C., Lohnes, D., Decimo, D., Lufkin, T., LeMeur, M., Chambon, P., and Mark, M. (1994). Function of the retinoic acid receptors (RARs) during development (II). Multiple abnormalities at various stages of organogenesis in RAR double mutants. *Development* **120**, 2749-2771.

Mercola, M. (1999). Embryological basis for cardiac left-right asymmetry. *Semin. Cell Dev. Biol.* **10**, 109-116.

Meyer, D. and Birchmeier, C. (1995). Multiple essential functions of neuregulin in development. *Nature* **378**, 386-390.

Moss, J. B., Xavier-Neto, J., Shapiro, M. D., Nayeem, S. M., McCaffery, P., Drager, U. C., and Rosenthal, N. (1998). Dynamic patterns of retinoic acid synthesis and response in the developing mammalian heart. *Dev. Biol.* **199**, 55-71.

Niederreither, K., McCaffery, P., Drager, U. C., Chambon, P., and *Dollé*, P. (1997). Restricted expression and retinoic acid-induced downregulation of the retinaldehyde dehydrogenase type 2 (RALDH-2) gene during mouse development. *Mech. Dev.* **62**, 67-78.

Niederreither, K., Subbarayan, V., *Dollé*, P., and Chambon, P. (1999). Embryonic retinoic acid synthesis is essential for early mouse post- implantation development. *Nat. Genet.* **21**, 444-448.

Niederreither, K., Vermot, J., Messaddeq, N., Schuhbaur, B., Chambon, P., and *Dollé*, P. (2001). Embryonic retinoic acid synthesis is essential for heart morphogenesis in the mouse. *Development* **128**, 1019-1031.

O'Brien, T. X., Lee, K. J., and Chien, K. R. (1993). Positional specification of ventricular myosin light chain 2 expression in the primitive murine heart tube. *Proc. Natl. Acad. Sci. U S A* **90**, 5157-5161.

Piedra, M. E., Icardo, J. M., Albajar, M., Rodriguez-Rey, J. C., and Ros, M. A. (1998). Pitx2 participates in the late phase of the pathway controlling left- right asymmetry. *Cell* **94**, 319-324.

Rossant, J., Zirngibl, R., Cado, D., Shago,M., and Giguere, V. (1991). Expression of a retinoic acid response element-hsplacZ transgene defines specific domains of transcriptional activity during mouse embryogenesis. *Genes Dev.* **5**, 1333-1344.

Ruberte, E., *Dollé*, P., Chambon, P., and Morriss-Kay, G. (1991). Retinoic acid receptors and cellular retinoid binding proteins. II. Their differential pattern of transcription during early morphogenesis in mouse embryos. *Development* **111**, 45-60.

Ruberte, E., *Dollé*, P., Krust, A., Zelent, A., Morriss-Kay, G., and Chambon, P. (1990). Specific spatial and temporal distribution of retinoic acid receptor gamma transcripts during mouse embryogenesis. *Development* **108**, 213-222.

Ryan, A. K., Blumberg, B., Rodriguez-Esteban, C., Yonei-Tamura, S., Tamura, K., Tsukui, T., de la, P. J., Sabbagh, W., Greenwald, J., Choe, S., Norris, D. P., Robertson, E. J., Evans, R. M., Rosenfeld, M. G., and Izpisua Belmonte, J. C. (1998). Pitx2 determines left-right asymmetry of internal organs in vertebrates. *Nature* **394**, 545-551.

Saitou, M., Narumiya, S., and Kakizuka, A. (1994). Alteration of a single amino acid residue in retinoic acid receptor causes dominant-negative phenotype. *J. Biol. Chem.* **269**, 19101-19107.

Saitou, M., Sugai, S., Tanaka, T., Shimouchi, K., Fuchs, E., Narumiya, S., and Kakizuka, A. (1995). Inhibition of skin development by targeted expression of a dominant-negative retinoic acid receptor. *Nature* **374**, 159-162.

Semina, E. V., Reiter, R., Leysens, N. J., Alward, W. L., Small, K. W., Datson, N. A., Siegel-Bartelt, J., Bierke-Nelson, D., Bitoun, P., Zabel, B. U., Carey, J. C., and Murray, J.

C. (1996). Cloning and characterization of a novel bicoid-related homeobox transcription factor gene, RIEG, involved in Rieger syndrome. *Nat. Genet.* **14**, 392-399.

Shiratori, H., Sakuma, R., Watanabe, M., Hashiguchi, H., Mochida, K., Sakai, Y., Nishino, J., Saijoh, Y., Whitman, M., and Hamada, H. (2001). Two-step regulation of left-right asymmetric expression of pitx2: initiation by nodal signaling and maintenance by Nkx2. *Molec. Cell* **7**, 137-149.

Smith, S. M., and Dickman, E. D. (1997). New insights into retinoid signaling in cardiac development and physiology. *Trends Cardiovasc. Med.* **7**, 324-329.

Srivastava, D., Cserjesi, P., and Olson, E. N. (1995). A subclass of bHLH proteins required for cardiac morphogenesis. *Science* **270**, 1995-1999.

Sucov, H. M., Dyson, E., Gumeringer, C. L., Price, J., Chien, K. R., and Evans, R. M. (1994). RXR alpha mutant mice establish a genetic basis for vitamin A signaling in heart morphogenesis. *Genes Dev.* **8**, 1007-1018.

Tran, C. M. and Sucov, H. M. (1998). The RXRalpha gene functions in a non-cell-autonomous manner during mouse cardiac morphogenesis. *Development* **125**, 1951-1956.

Tsukui, T., Capdevila, J., Tamura, K., Ruiz-Lozano, P., Rodriguez-Esteban, C., Yonei-Tamura, S., Magallon, J., Chandraratna, R. A., Chien, K., Blumberg, B., Evans, R. M., and Belmonte, J. C. (1999). Multiple left-right asymmetry defects in Shh(-/-) mutant mice unveil a convergence of the shh and retinoic acid pathways in the control of Lefty-1. *Proc. Natl. Acad. Sci. U S A* **96**, 11376-11381.

Wasiak, S. and Lohnes, D. (1999). Retinoic acid affects left-right patterning. *Dev. Biol.* **215**, 332-342.

Wendling, O., Dennefeld, C., Chambon, P., and Mark, M. (2000). Retinoid signaling is essential for patterning the endoderm of the third and fourth pharyngeal arches. *Development* **127**, 1553-1562.

Wendling, O., Ghyselinck, N. B., Chambon, P., and Mark, M. (2001). Roles of retinoic acid receptors in early embryonic morphogenesis and hindbrain patterning. *Development* **128**, 2031-2038.

Wilkinson, D. G. (1992). Whole mount in situ hybridization of vertebrate embryos. In situ hybridization: A practical Approach. (D.G.Wilkinson, Ed.), pp. 75-83, Oxford University Press, New York.

Wilson, J. G. and Warkany, J. (1949). Aortic-arch and cardiac anomalies in the offspring of vitamin A deficient rats. *Am. J. Anat.* **85**, 113-155.

Wilson, J. G., Roth, C.B., and Warkany, J. (1953). An analysis of the syndrome of malformations induced by maternal vitamin A deficiency. Effects of restoration of vitamin A at various times during gestation. *Am. J Anat.* **92**, 189-217.

Wurst, W. and Joyner, A. L. (1993). Production of targeted embryonic stem cell clones. Gene targeting: A practical approach (A. L. Joyner, Ed.), pp. 33-61, IRL Press at Oxford University Press, England.

Yagi, T., Ikawa, Y., Yoshida, K., Yasuyo, S., Takeda, N., Mabuchi, I., Yamamoto, T., and Aizawa, S. (1990). Homologous recombination at c-fyn locus of mouse embryonic stem cells with use of diphtheria toxin A-fragment gene in negative selection. *Proc. Natl. Acad. Sci. U S A* **87**, 9918-9922.

Yamaguchi, M., Nakamoto, M., Honda, H., Nakagawa, T., Fujita, H., Nakamura, T., Hirai, H., Narumiya, S., and Kakizuka, A. (1998). Retardation of skeletal development and cervical abnormalities in transgenic mice expressing a dominant-negative retinoic acid receptor in chondrogenic cells. *Proc. Natl. Acad. Sci. U S A* **95**, 7491-7496.

Yoh, S. M., Chatterjee, V. K., and Privalsky, M. L. (1997). Thyroid hormone resistance syndrome manifests as an aberrant interaction between mutant T3 receptors and transcriptional corepressors. *Mol. Endocrinol.* **11**, 470-480.

Yoshioka, H., Meno, C., Koshiba, K., Sugihara, M., Itoh, H., Ishimaru, Y., Inoue, T., Ohuchi, H., Semina, E. V., Murray, J. C., Hamada, H., and Noji, S. (1998). Pitx2, a bicoid-type homeobox gene, is involved in a lefty-signaling pathway in determination of left-right asymmetry. *Cell* **94**, 299-305.

Zambrowicz, B. P., Imamoto, A., Fiering, S., Herzenberg, L. A., Kerr, W. G., and Soriano, P. (1997). Disruption of overlapping transcripts in the ROSA beta geo 26 gene trap strain leads to widespread expression of beta-galactosidase in mouse embryos and hematopoietic cells. *Proc. Natl. Acad. Sci. U S A* **94**, 3789-3794.

Zeller, R., Bloch, K. D., Williams, B. S., Arceci, R. J., and Seidman, C. E. (1987). Localized expression of the atrial natriuretic factor gene during cardiac embryogenesis. *Genes Dev.* **1**, 693-698.

Zile, M. H. (1998). Vitamin A and embryonic development: an overview. *J. Nutr.* **128**, 455S-458S.

Zile, M. H., Kostetskii, I., Yuan, S., Kostetskaia, E., St Amand, T. R., Chen, Y., and Jiang, W. (2000). Retinoid signaling is required to complete the vertebrate cardiac left/right asymmetry pathway. *Dev. Biol.* **223**, 323-338.

CHAPTER 5

GENERAL DISCUSSION

Retinoids have remarkable abilities to modulate and transform a plastic vertebrate bauplan in very specific ways. They can change the identities of segments along the antero-posterior axis, as well as influence patterning along the left-right axis. Retinoid signaling also plays a crucial role in the development of the posterior embryo, which generates the diverse lineages of the trunk and caudal region. Of concern to vertebrate biology is the near ubiquitous issue of redundancy among members of gene families afforded by their larger genomes. The RARs represent an excellent example of this principal; one that is challenging to address due to the pleiotropic nature of retinoid signaling. Furthermore, of particular importance is the dosage-dependence of biological processes to both aberrant retinoid levels and RAR gene loss. We have seen this for hindbrain development, vertebral patterning, and tail bud formation. Indeed, a major component of my doctoral dissertation has been the assessment of RARγ gene dose to the effects of exogenous retinoid signaling on vertebral patterning and tail bud development. The latter half of the work described herein has concerned itself with the question of RAR function during development. To study this issue, a gene replacement approach involving a potent RAR dominant negative was used to circumvent functional redundancy among the RARs specifically within the RARγ expression domain. These experiments shed new light on the function of RA signaling in vertebral patterning and caudal development, and reveal new roles for the RARs in cardiac morphogenesis.

5.1. Role Of RARγ In Transducing The Retinoid Signal During Vertebral Patterning

5.1.1. RARγ Can Pattern Cervical Vertebrae During The Late Window Of RA Sensitivity

Axial patterning is sensitive to exogenous retinoids during two distinct periods which roughly correspond to times that vertebral precursors are undergoing a transition from a mesenchymal to epithelial phenotype (Kessel and Gruss, 1990; Kessel, 1991). The first window of RA sensitivity corresponds to the ingression and establishment of the paraxial mesodermal lineage and its subsequent condensation to somites. It is during this period that *hox* genes become activated and somite identity is established. Excess retinoids during this early window perturbs vertebral patterning along with anteriorizations in *hox* gene expression. The later period of retinoid sensitivity, termed respecification, occurs when the somites split along their dorsal-ventral axis and revert to a mesenchymal state to give rise to the prevertebrae (or sclerotome). The effect of retinoids at this stage, however, do not noticeably change *hox* expression patterns or levels. It thus remains to be established how the retinoids influence vertebral patterning independently of *hox* gene regulation.

Both the presomitic mesoderm and prevertebrae express RARγ, and thus this gene can conceivably mediate the effects of retinoids during the two windows (Ruberte *et al.*, 1990). This was examined by challenging RARγ-null embryos with exogenous RA. While RARγ-null fetuses were markedly resistant to craniofacial malformations induced by early retinoid treatments, cervical vertebral defects were only mildly attenuated. In contrast, RA treatments at later times, particularly at E10.5, rescued RARγ-null defects. This rescue effect likely occurs by over-occupying the remaining RARs. As the prevertebrae also express RARα, this receptor could conceivably mediate this rescue effect on RARγ ablation (Ruberte *et al.*, 1990). Indeed, in unpublished observations, I noted a loss of RA-mediated rescue in RARα/RARγ double null mutants. Furthermore, RARβ has been shown to mediate the effects of excess RA on *hoxd4* induction (Folberg *et al.*, 1999b). Thus, the RARs function redundantly in the respecification of the vertebrae, consistent with their expression in the prevertebrae. The lack of RARγ also seriously compromised the ability of a late pulse of RA to transform the occipital and

exoccipital bones at the base of the skull, but not more posterior cervical vertebrae. These results argue that the respecification of the rostral-most vertebral identities requires intact RARγ function, and that this receptor normally functions during the late window.

5.1.2. Possible Targets Of RAR-Mediated Respecification

Paralog group 4 *hox* genes act synergistically to pattern the cervical vertebrae (Horan *et al.*, 1995a, 1995b), and the mutation of single group 4 genes gives rise to a similar vertebral phenotype to that of RAR null embryos (Lohnes *et al.*, 1993, 1994). Furthermore, the group 4 genes contain functional RAREs which establish their rostral expression boundaries and mediate their responsiveness to RA (Gould *et al.*, 1998; Morrison *et al.*, 1997; Packer *et al.*, 1998; Popperl and Featherstone, 1993). Thus, RAR ablation presumably affects vertebral patterning by delaying the activation and preventing the correct rostral setting of group 4 *hox* genes. This is consistent with the effect of retinoid signaling in the early period of vertebral specification. However, *hox* gene expression persists in the prevertebrae (Kessel and Gruss, 1990; Gaunt *et al.*, 1988, 1989) raising the issue of whether *hox* genes mediate retinoid function at subsequent stages of vertebral development, particularly during the respecification window.

This hypothesis is supported by Folberg and colleagues (1999a), who demonstrated that the loss of *hoxd4* from the RARγ-null background abolished the retinoid rescue of the C2 to C1 transformation. This suggests that *hoxd4* functions epistatically to RARγ to elicit vertebral defects caused by excess RA. Importantly, these results also suggest that the respecification of vertebral identities requires *hox* function. However, *hoxd4* expression is unaffected in RARγ null embryos, and is still efficiently induced by RA treatment at E10.5 in these mutants (Folberg *et al.*, 1999a). As later expression of paralogous group 4 members depends on promiscuous cross-regulatory relationships between one another (Gould *et al.*, 1997; Packer *et al.*, 1998), it remains possible that subtle effects of RARγ loss on group 4 genes may be diluted through this resilient autoregulatory network, leading to normal *hoxd4* levels in somite derivatives. According to this model, when retinoid signaling is impaired in addition to the loss of *hoxd4*, the strain on the cross-regulatory network should become manifested as decreased group 4 expression in RARγ/*hoxd4* double nulls. An important caveat to this theory is

that *hoxb4* expression is unaffected in RARγ/*hoxd4* double mutants (Folberg *et al.*, 1999a). However, expression was examined at E9.5, a full day before the respecification window and several days prior the appearance of prevertebrae. This time may also be too early to assay an effect on the group 4 cross-regulation, which likely functions to maintain established *hox* expression patterns in the descendants of somites.

A precedent for the importance of the timing in *hox* cross-regulation has been elegantly demonstrated by Packer and colleagues (1998). They observe that the expression of a transgenic reporter harboring *hoxa4* regulatory elements is reduced in *hoxa4*$^{-/-}$ embryos specifically between E10.5 and E12.5. Group 4 *hox* members also synergize extensively in the patterning of the cervical vertebrae (Horan *et al.*, 1995b). The absence of all three group 4 genes render the entire cervical region into a default C1 state, suggesting the importance of cross-regulation in vertebral patterning. Thus, it remains possible that group 4 expression is subtly downregulated in RARγ/*hoxd4* nulls during the respecification window, which then leads to obvious deficiencies in the maintenance of *hox* expression in the condensing prevertebral elements. This would have to be tested by assessing the expression of group 4 genes in RARγ/*hoxd4* double mutants within the prevertebrae at E12.5. Furthermore, to determine if the lack of RA rescue in RARγ/*hoxd4* double nulls is due to inadequate *hox* cross-regulation, *in situ* hybridization analyses of group 4 prevertebral expression in RARγ/*hoxd4* double nulls would have to be compared to RARγ$^{-/-}$ embryos following RA treatment. There should be clear differences between the RARγ and RARγ/*hoxd4* groups if *hox* genes do indeed mediate the rescue effect of exogenous RA.

It has been well established that retinoid signaling is required to initiate the expression of several distal *hox* genes in the anterior region of the embryo (see section 1.6.9.). However, due to the early loss of *hox* regulation associated with ablation of the RAREs, the role of these elements in the later maintenance and elaboration of group 4 *hox* expression remains to be addressed. Indeed, driving the expression of a dominant negative RAR within developing prevertebral chondrocytes efficiently induces vertebral defects concomitantly with a severe down-regulation of *hoxa4* expression in the prevertebrae at E12.5 (Yamaguchi *et al.*, 1998). Furthermore, as RARs and *hox* genes are co-expressed in prevertebrae at least until E12.5, then *hox* promoters presumably

remain accessible to RAR regulation at stages subsequent to the specification of somites. Thus, retinoid signaling may pattern vertebrae during the respecification window at least in part by regulating *hox* genes in the prevertebrae. This could be examined by using a cre-lox strategy to specifically excise RAREs of group 4 *hox* promoters at later times in development, particularly during sclerotome formation and differentiation (i.e., between E10.5-E12.5). A possible approach may involve the targeting of *loxP* sequences adjacent to the 3' RAREs of group 4 genes and mating the resulting mice to transgenic strains expressing Cre recombinase in the prevertebrae. A suitable promoter that directs expression specifically within the prevertebrae is the *collagen type II α1 chain* regulatory sequences used by Yamaguchi and colleagues (1998). Alternatively, one can use the hormone-inducible Cre system developed by Brocard and colleagues (1997) to specifically ablate *hox* RAREs within the condensing prevertebrae. The results from such experiments should demonstrate decisively whether the respecification of vertebrae by retinoid signaling is indeed *hox* gene dependent. In addition, to determine if vertebral patterning results from the differential proliferative effects of Hox proteins in condensing prevertebrae, one can utilize a similar *cre-lox* approach to efficiently excise entire paralogous *hox* groups within this tissue, and assay the effects on chondrogenesis and vertebral patterning. At present, such experiments have yet to be described, thus the elucidation of Hox and RAR function in late aspects of vertebral morphogenesis remains the province of future work.

RA signaling may also impact on *hox* function during the respecification window without necessarily altering *hox* expression. Particularly, RA may alter Hox protein binding preferences to their target promoters by regulating the expression of PBX family of Hox co-factors. PBX proteins constitute a divergent class of homeobox-containing factors belonging to the *extradenticle* family which impart binding site specificity to the Hox proteins (reviewed in Mann and Chan, 1996). At least one member of the PBX family, *meis2*, is regulated by retinoids (Oulad-Abdelghani *et al.,* 1997). There is also some evidence that RA is able to induce PBX proteins post-transcriptionally (Knoepfler and Kamps, 1997). Furthermore, both PBX and Meis1 are able to associate with a Hox protein, forming a complex that directs the binding of the Hox partner to its response element (Shamugam *et al.,* 1999). Interestingly, within these triple complexes, the Meis

partner does not contact the DNA, suggesting it functions to enhance or stabilize the binding of the Hox/PBX heterodimer to their cognate elements. Thus, RA may affect vertebral patterning during the late window by altering the composition of functional Hox/PBX/Meis complexes, which in turn renders their binding to target promoters less stable or less efficient. Alternatively, RA may induce the formation of specific PBX-Hox complexes which then dictate the binding specificity of Hox proteins to their target promoters. In support of this, RA treatment has been shown to induce ternary complex formation involving HoxB1, Pbx1, and either Meis1 or Prep1, a divergent member of the PBX family (Ferretti *et al.,* 2000).

RARs and *hox* genes could also synergize in separate, parallel pathways to elicit vertebral form. For example, RARs are particularly enriched in the condensing prevertebrae (Ruberte *et al.*, 1990), and aberrant retinoid signaling inhibits the proliferation of chondrocytes within developing limbs (reviewed in Underhill *et al.*, 2001). Thus, RARs could affect vertebral patterning in the late window by regulating the chondrogenesis of the vertebra. In support of this, the expression of a dominant negative RAR within condensing prevertebrae leads to the transformation and malformation of the cervical vertebrae not unlike those seen in RAR double null mutants, demonstrating that vertebral patterning can be easily perturbed well after their initial specification has occurred (Yamaguchi *et al.*, 1998). Possible targets of retinoid action in prevertebral condensations include *sox9* (Sekiya *et al.*, 2000), an important regulator of chondrogenesis, and TGFβ2 (Tsuiki *et al.*, 1999), a potent inhibitor of chondrocyte proliferation. BMPs are another group of TGFβ factors that regulate chondrogensis in response to retinoid signaling (Rodriguez-Leon *et al.,* 1999; Underhill *et al.,* 2001). Interestingly, a similar effect on chondrogenesis has been proposed to explain the action of *hox* genes in vertebral patterning (Duboule, 1995), and there is some evidence for the differential proliferative abilities of various *hox* genes in the bone forming mesenchyme of the limb buds (Goff and Tabin, 1997). Thus, in addition to requiring RAR activity for the initiation of expression, *hox* genes may further collaborate with retinoid signaling in the final realization of vertebral form by regulating chondrocyte proliferation. In this scenario *hox* genes and RARs control different, non-overlapping sets of target genes required for chondrogenesis.

5.2. The Role Of Retinoid Signaling In Caudal Development

5.2.1. Exogenous RA Inhibits Nascent Mesoderm Formation

Retinoids have the ability to alter the development of the caudal embryo depending on their dose and time of exposure (Griffith and Wiley, 1990; Kessel and Gruss, 1991; Kessel, 1992). In particular, excess RA at E8 in the mouse leads to severe defects in caudal development, including a complete dysgenesis of the posterior embryo; a condition referred to as caudal regression (Kapron-Bras and Trasler, 1988a; Tibbles and Wiley, 1988; Yasuda *et al.,* 1990). Exogenous RA also results in neural tube defects affecting both the anterior and posterior neuropores when administered prior to the closure of these regions (Kapron-Bras and Trasler, 1988a, 1988b; Kessel and Gruss, 1991; Moriss-Kay *et al.,* 1994; Sulik *et al.,* 1995; Tibbles and Wiley, 1988; Yasuda *et al.,* 1986, 1990). Likewise, the loss of retinoid signaling in RARα/RARγ double mutants leads to dramatic failures of neural tube closure in the anterior neuropore region (Lohnes *et al.,* 1994; Wendling *et al.,* 2001). Due to the complex histology of the caudal embryo during posterior neuropore closure stages, pharmacological studies could not agree if the primary effect following RA exposure lies within mesoderm or neuroepithelium (Griffith and Wiley, 1991; Kapron-Bras and Trasler, 1988a, Tibbles and Wiley, 1988; Yasuda *et al.,* 1990). The mutation of RARγ results in a resistance to retinoid-induced caudal regression (Lohnes *et al.,* 1993) and thus serves as an excellent model for the evaluation of the molecular targets of retinoid excess, and the determination of the primary tissues affected by acute RA exposure during caudal development.

The caudal embryo develops from similar morphogenetic processes as those governing gastrulation. Fate mapping studies in various vertebrates suggest that axial elongation derives largely from a continuation of the ingression movements of precursors initiated by the primitive streak (Catala *et al.*, 1995; Kanki and Ho, 1997; Tam, 1984). This is mediated by a complex blastema called the tail bud which replaces the streak as the major source of new mesoderm from E8.5 onwards (Tam *et al.*, 2000). Landmark studies from several laboratories demonstrate that a transcription factor, *brachyury*, is critically required for caudal mesoderm formation (Beddington *et al.*, 1992; Wilkinson *et*

al., 1990). Ectopic expression of this gene in amphibians is sufficient to promote excess mesoderm formation (Cunliffe and Smith, 1992). Furthermore, elegant chimeric analysis from Beddington's group refined a role for *brachyury* in driving morphogenetic movements required for mesoderm ingression through the streak (Wilson and Beddington, 1997; Wilson *et al.*, 1995). In its absence, mesodermal precursors accumulate in the streak and fail to become incorporated in the embryo, consequently leading to severe axial truncations resembling those caused by excess RA at E8.5. However, evidence linking retinoid signaling and *brachyury* function is surprisingly lacking. This was addressed by examining the effects of exogenous RA on the caudal development of wild type and RA-resistant RARγ-null embryos on the expression of *brachyury* and several other markers of early posterior tissues. RA was found to rapidly and reproducibly attenuate *brachyury* expression before any evidence for caudal dysmorphogenesis. This effect displayed a gene-dosage sensitivity to RARγ, consistent with the strong caudal expression of this receptor during tail bud formation stages (Ruberte *et al.*, 1990). Moreover, additional markers of caudal mesoderm, including *wnt3a,* and *cdx4* were also rapidly reduced following acute RA exposure. As neuroepithelial markers were unaffected by RA, these results demonstrated that newly forming mesoderm is the primary lesion in retinoid-induced caudal dysgenesis.

These results have for the first time established a regulatory relationship between *brachyury* and retinoid signaling. Whether *brachyury* is a direct target of RA is currently unsubstantiated by the available evidence and thus remains a matter of speculation. In this regard, our observations also suggest an early effect of excess RA on *wnt3a* expression. This gene is expressed in the nascent mesoderm from E7.5 onwards and is a faithful lineage marker for newly forming caudal mesoderm (Takada *et al.,* 1994). Interestingly, the loss of this gene, like that of *brachyury*, leads to axial truncations, consistent with the effects of excess RA on posterior development (Greco *et al.,* 1996; Takada *et al.,* 1994). Shum and colleagues (1999) observed a similar rapid down-regulation of *wnt3a* expression in response to a pulse of RA. Furthermore, *wnt3a* is responsive to exogenous retinoids throughout tail bud development, as we noted a retinoid-induced decrease in *wnt3a* transcripts during the initial formation of the tail bud

at E8.5, while Shum and colleagues observed an effect at E9.5, when the tail bud is well established.

Analysis of the proximal *brachyury* regulatory region in mice reveals the presence of several conserved binding elements for TCF/LEF factors, the transcriptional mediators of Wnt signaling (Arnold *et al.,* 2000; Yamaguchi *et al.,* 1999). This enhancer is sufficient to direct expression of a reporter in the primitive streak and nascent mesoderm, while axial mesodermal expression requires additional yet unidentified sequences (Clements *et al.,* 1996). These findings hint at a possible role for *wnt3a* regulation of *brachyury* expression in the mesoderm emerging from the streak, and later on in the tail bud. Indeed, the initiation of *brachyury* expression is independent of *wnt3a* function, as *brachyury* transcripts are found throughout the primitive streak in *wnt3a*$^{-/-}$ embryos during early somite stages (Yamaguchi *et al.,* 1999). This is consistent with the earlier appearance of *brachyury* transcripts in the primitive streak relative to *wnt3a* expression (Takada *et al.,* 1994; Wilkinson *et al.,* 1990). Subsequent *brachyury* expression in posterior mesoderm is abolished in *wnt3a* mutants, demonstrating a role for Wnt signaling in the maintenance of *brachyury* expression during the formation of the tail bud (Yamaguchi *et al.,* 1999).

Also, it is important to keep in mind the possibility of cross-regulatory loops when considering *brachyury* expression. For instance, the expression of *wnt3a* and *wnt5a* is reduced in the *brachyury* (or *T/T*) mutants during late gastrulation, suggesting a requirement of *brachyury* function in the expression of caudal *wnt* factors (Rashbass *et al.*, 1994; Yamaguchi *et al.,* 1999). It therefore appears that the TCF binding sites function to maintain *brachyury* expression in the developing tail bud, thereby establishing an cross-regulatory loop between *brachyury* and Wnt signaling in the formation of the caudal embryo. Furthermore, as RAREs have not been described in the *brachyury* promoter, retinoid regulation of *wnt3a* remains a tempting explanation for the acute effects of RA signaling on *brachyury* expression. Confirmation of this hypothesis requires a thorough analysis of the regulatory elements driving *wnt3a* expression.

Interestingly, RA has been shown to antagonize the activation of a Wnt responsive reporter containing LEF/TCF binding sites (Easwaran *et al.,* 1999). It appears that this inhibition of Wnt reporter activity by retinoids is mediated by the sequestration

of β-catenin by RARs. β-catenin is an intracellular mediator of Wnt signaling required for the full activation of LEF/TCF targets. Particularly, in response to Wnt signaling, β-catenin translocates to the nucleus, where it converts LEF/TCF factors from repressors to activators (reviewed in Wodarz and Nusse, 1998). Thus, a possible mechanism whereby RA signaling down-regulates *brachyury* involves competition with LEF/TCF for β-catenin binding, resulting in the inhibition of Wnt-mediated activation of *brachyury* expression. This then leads to a loss of *wnt3a* expression due to the feedback regulation of Wnts by Brachyury.

Several studies in amphibians point to the existence of cross-regulatory interactions between FGF signaling and *brachyury* expression (Casey *et al.*, 1998; Conlon *et al.*, 1996; Kim *et al.*, 1998; Latinkic *et al.*, 1997). These feedback loops appear to be mediated at the level of the *cis*-regulatory regions for both FGF and *brachyury*. FGF, along with a TGFβ factor, is able to activate the *brachyury* promoter in *Xenopus* embryos (Latinkic *et al.*, 1997), and *brachyury* itself regulates *eFGF* expression in frogs by binding to a conserved T-box factor element in the *eFGF* promoter (Casey *et al.*, 1998). Furthermore, the regulation of *brachyury* by FGF factors is supported by genetic studies in zebrafish (Griffin *et al.*, 1995, 1998), and the mutation of the FGF receptor gene (*fgfr1*) in the mouse leads to loss of morphogenetic activity of the streak along with aberrant mesodermal patterning and differentiation in the caudal embryo (Ciruna *et al.*, 1997; Deng *et al.*, 1994; Yamaguchi *et al.*, 1994). Despite these convincing observations, FGF signaling has not been implicated in the regulation of *brachyury* in the mouse. This is at odds with the apparent conservation of the FGF-*brachyury* cross-regulatory loop in other vertebrates. Perhaps redundancies in FGF signaling may partially explain the lack of a demonstrable connection between FGFs and *brachyury* in the mouse. However, if FGFs do indeed regulate *brachyury* at some level, an alluring model of how retinoid signaling can infringe upon *brachyury* regulation involves the competition for limiting transcriptional co-regulators, such as p300/CBP, which are used by both RARs and AP-1 factors, the transcriptional effectors of the FGF pathway (Goodman and Smolik, 2000). Alternatively, RA signaling may interfere with FGF signaling by inhibiting kinases acting downstream of Ras and upstream of AP-1, such as JNK (c-Jun N-terminal kinase). Several reports have indeed shown that RA signaling is able to inhibit JNK activity,

which in turn leads to the loss AP-1 function (Caelles *et al.,* 1997; Lee *et al.,* 1998, 1999). This further complicates an already dense picture of the possible avenues retinoid signaling may take to alter *brachyury* expression. Therefore, at present it remains difficult to distinguish at what level retinoids regulate *brachyury* expression: either directly *via* RAREs, or more likely, indirectly through the disruption of cross-regulatory networks involving *wnt3a* and/or FGF signaling.

5.2.2. RA Levels And The Differentiation Of Caudal Mesoderm

The distribution of endogenous retinoids in developing embryos offers important insights in the functioning of retinoid signaling during caudal development. HPLC studies (Horton and Maden, 1995; Maden et al., 1998), RARE reporter mice (Balkan *et al.*, 1992; Mendelsohn *et al.*, 1991; Rossant *et al.*, 1991) and tissue explant assays using retinoid sensitive reporter cells (e.g., Figure 3-5; Wagner et al, 1992) all demonstrate that the caudal region of E8.5 embryos is devoid of bioactive retinoids. Furthermore, our studies, and that of others (Fujii *et al.,* 1997) demonstrated that the posterior embryo expresses *p450RAI/cyp26A1*, a RA-catabolic enzyme, throughout tail bud development (e.g., Figure 3-7). This suggests that tail bud formation is particularly sensitive to aberrant retinoid levels and embryos employ Cyp26A1 to effectively render the posterior region free of RA. *Cyp26A1* is an RA-target gene (Fujii *et al.,* 1997; Loudig *et al.*, 2000; White *et al.,* 1996), and is thus involved in a substrate feedback loop whereby more RA enhances *cyp26A1* expression, which then leads to increased RA catabolism. Indeed, we showed that a short pulse of RA resulted in the saturation of the caudal embryo with this compound and led to a greater than 22-fold increase in *cyp26A1* expression. By 6 hours following the RA insult, most of the bioactive retinoids were cleared from the tail bud. However, by this point the lesion in tail bud formation had occurred as *brachyury* and *wnt3a* expression declined considerably 4 hours following treatment. Consistent with this, the mutation of *cyp26A1* results in an excess RA-like caudal regression syndrome concomitant with a reduction of *brachyury* and *wnt3a* expression and aberrant tail bud development (Abu-Abed *et al.*, 2001; Sakai *et al.,* 2001). Collectively, these results suggest that tail bud formation requires a strict exclusion of bioactive retinoids from the caudal region.

As the tail bud blastema is central to the formation and differentiation of caudal mesoderm, perhaps a fruitful line of inquiry lies in suggesting a more general role for retinoid signaling in the regulation of tissue differentiation in the posterior embryo. As an interesting corollary, excess RA can convert prospective paraxial mesoderm to a neuronal fate. Exogenous RA applied during tail bud formation stages results in the appearance of ectopic neural tube-like structures in the dysgenic caudal embryo, which are positive for a number of neuroepithelial markers (Shum *et al.,* 1999; Tibbles and Wiley, 1988; Yasuda *et al.,* 1990). Importantly, the loss of *wnt3a* also leads to ectopic neural tissues in the caudal embryo, in agreement with its down-regulation following acute RA exposure (Shum *et al.,* 1999; Yoshikawa *et al.,* 1997). This ectopic neuralization is restricted to tissues fated to develop into paraxial mesoderm. Furthermore, Yamaguchi and colleagues (1999) show that *brachyury* is reduced specifically within the prospective paraxial mesoderm of *wnt3a* mutants. While ectopic neuralization has not been observed for *brachyury* mutants, the mutation of a related gene, *tbx6*, whose transcripts co-localize with *brachyury* in the primitive streak, results in a complete neuralization of paraxial tissues (Chapman and Papaioannou, 1998). Strikingly, these mutants have three neural tubes, with the ectopic ones lying adjacent to the notochord and medial neural tube. Moreover, inhibiting *brachyury* function in *Xenopus* animal caps results in the formation of neural structures (Rao, 1994). These explants normally form mesoderm in response to forced expression of *brachyury*, suggesting that the inhibition of *brachyury* function is sufficient to promote neural fates in naïve tissues. Also, in the mouse, the loss of *brachyury* is associated with abnormal somite differentiation in addition to the general lack of caudal mesoderm (Conlon *et al.,* 1995; Rashbass *et al.,* 1994). Thus, the activities of Wnts and T-box genes are critical for the instruction of paraxial mesodermal fate in ingressing cells of the late primitive streak, and excess retinoids appear to antagonize this behavior in part *via* the down-regulation of *wnt3a*.

How then, is endogenous retinoid signaling related to normal mesodermal differentiation? Several different approaches reveal that endogenous retinoids are enriched in the trunk of the embryo and are absent in the posterior region (Fig. 1-2; Fig. 3-5; section 1-2). Moreover, it appears that the expression of *cyp26A1* within the caudal embryo ensures a lack of RA in ingressing mesoderm in the primitive streak remnant and

tail bud. This creates a RA-enriched region immediately rostral to a RA-deficient caudal embryo. As *brachyury* and *wnt3a* are expressed in ingressing mesoderm and are sensitive to RA, then retinoid signaling may normally promote paraxial mesoderm differentiation in part by down-regulating *brachyury* and *wnt3a* expression in naïve mesoderm. In this model, relatively undifferentiated paraxial mesoderm encounters RA diffusing from the posterior trunk and down-regulates the expression of *brachyury* to allow for the differentiation of this tissue into somites (Fig. 5-1).

Figure 5-1. Simplified model for the differentiation of paraxial mesoderm by RA during tail bud development.

Schematic representation of *brachyury* (blue) and *cyp26A1* (red) expression domains and RA distribution (green) in the E8.5 caudal embryo. The gradient of *brachyury* expression is depicted as increased dark shading towards the caudal embryo. *Cyp26A1* expression renders the caudal region devoid of bioactive retinoids and creates a sharp gradient of RA distribution in the rostral pre-somitic mesoderm. RA diffusing from the posterior trunk attenuates *brachyury* expression in the rostral-most paraxial mesoderm and allows for the condensation of somites. The hypothetical gradient of RA is indicated extending into the pre-somitic mesoderm from the caudal-most somitic region. Somites are indicated as gray ovals. Light gray oval with dotted lines indicates condensing somite. Abbreviations: no, notochord; psm, pre-somitic mesoderm; so, somites.

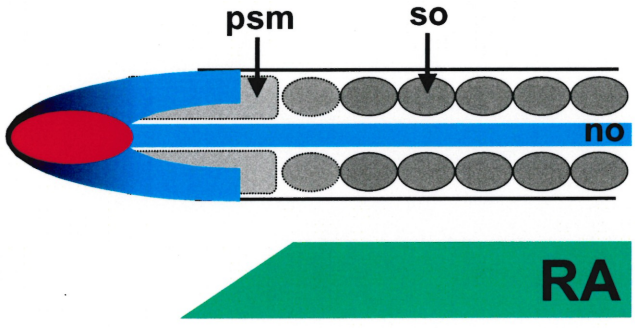

There is some precedence linking *brachyury* expression with the state of mesodermal differentiation. To begin with, *brachyury* is expressed in a graded fashion along the caudal embryo, with the highest levels occurring in the posterior-most, newly ingressed mesoderm (Kispert and Herrmann, 1994; Wilkinson *et al.,* 1990). This roughly correlates with the differentiation state of paraxial mesoderm along the axis, with more naïve tissues expressing higher amounts of *brachyury*. In addition, the ectopic expression of *brachyury* in the most rostral, and therefore more differentiated, compartment of the paraxial mesoderm prevents its differentiation into somites (Dubrulle *et al.*, 2001). As *brachyury* directs morphogenetic cell movements, the epithelialization of paraxial mesoderm may be incompatible with its expression. Thus, RA may normally promote this process by attenuating *brachyury* expression in the rostral-most pre-somitic mesoderm (Fig. 5-1).

Interestingly, there is evidence supporting a role for endogenous RA in mesoderm differentiation in the tail bud. The mutation of *raldh2* results in severe axial truncations and aberrant mesoderm formation, which occur to a similar extent to that seen with excess RA (Niederreither *et al.,* 1999). These embryos also completely lack RA production in the trunk, thus serving as an important test for the proposed mesoderm differentiation model. As discussed above, the activity of *brachyury* is critical for the formation of mesoderm, and its attenuation by excess RA is sufficient to account for the axial truncation evoke by such a treatment. Therefore, according to the model, aberrant regulation of *brachyury* should also be the underlying cause of the truncations observed in the *raldh2* null embryos. In a series of impressive rescue experiments, Wilson and Beddington (1997) show that the dosage of *brachyury* within the cells of the streak is crucial for their proper ingression in *T/T* embryos. Interestingly, chimeras generated from ES lines expressing higher that normal amounts of Brachyury protein display a deficiency of posterior mesoderm production and differentiation because of a premature exit from the streak. Thus, the over-expression as well as deficiency of *brachyury* can lead to the same outcome; namely the loss of caudal tissues. In light of this, the axial truncation observed in *raldh2* null embryos may reflect an over-expression of *brachyury* in the streak. Unfortunately, the expression of this gene was not assessed in *raldh2*$^{-/-}$ embryos,

thus the model suggested here remains a speculative interpretation of retinoid function in caudal development.

Driving the expression of a dominant negative RAR in the posterior region can also be used to investigate this hypothesis. An ideal dominant negative for this purpose is the ligand-binding deficient RARγE described in chapter 4, which presents a lesion in the RA signaling pathway downstream of ligand availability. The *brachyury* promoter can be used to effect a loss of RAR function particularly within the *brachyury*-positive nascent mesoderm in the posterior embryo (Clemens *et al.,* 1996). Therefore, if retinoid signaling does indeed permit somite differentiation by down-regulating genes involved in primitive streak and tail bud function, then blocking RAR function in the newly forming mesoderm should result in an expansion of *brachyury* and *wnt3a* expression within rostral paraxial mesoderm, and inhibit somite differentiation.

5.3. Assessing Novel Roles For Retinoid Signaling During Development

5.3.1. An Alternative Model For Retinoid Signaling Deficiency During Mouse Development

The mutation of retinoid receptors revealed a high degree of functional overlap between the different RARs during development. While any single RAR mutant displays minimal or no abnormalities, the double mutants harbor a variety of developmental defects resembling the fetal VAD syndrome (Tables 1-1 and 1-2; Lohnes *et al.,* 1994; Mendelsohn *et al.,* 1994). A problem with these mutational studies is that, due to the presence of a remaining RAR gene, the full impact of RAR signaling during development cannot be assessed. Further difficulties lie in the impracticality of generating triple RAR mutants as the double mutants are embryo lethal. Moreover, if triple RAR heterozygotes are fertile, the numbers of triple RAR mutants expected from such a cross would nonetheless be too low for any meaningful assessment during development. Another mammalian model of retinoid signaling deficiency which presents its own unique caveats is the *raldh2* null mouse line generated by Niederreither and colleagues (1999). These mutant mice display severe deficiencies in overall development and die at mid-gestation

(between E9.5 and E10.5). Thus, there are gaps in our understanding of retinoid signaling, particularly during later events in mammalian development.

In an attempt to address this, I have employed a gene replacement strategy to target a dominant negative RARγ (named RARγE) to the endogenous RARγ locus. This dominant negative cannot bind RA and is thus expected to block retinoid-dependent processes (Saitou *et al.,* 1994). Indeed, the expression of the RARα version of this dominant negative in transgenic mice potently inhibits skin development (Saitou *et al.,* 1995) and vertebral patterning (Yamaguchi *et al.,* 1998); both of which require normal retinoid signaling. By targeting this powerful dominant negative receptor to the RARγ locus, its expression becomes restricted spatially and temporally within the RARγ domain, and thus limits the lesion in retinoid signaling specifically in RARγ-positive tissues (Ruberte *et al.,* 1990).

An important test for the effectiveness and specificity of RARγE in interfering with retinoid-dependent processes is assessing its influence on the formation of the pharyngeal arches. A number of studies demonstrate the sensitivity of these structures to aberrant retinoid signaling (Dupé *et al.*, 1999; Wendling *et al.*, 2000, 2001). Chimeras generated from RARγE ES cells also displayed a defective pharyngeal arch development, consistent with a specific interference of RAR function within the RARγ expression domain. Particularly impressive was the fact that only a single copy of this dominant negative was sufficient to reproduce the pharyngeal arch phenotype displayed by RAR double mutants. This demonstrates the singular potency of RARγE and its usefulness as an alternative to generating compound RAR mutants. The present chimeric analysis also provides additional support for the role of RAR signaling in the foregut endoderm in pharyngeal arch development.

5.3.2. Possible Role For Retinoid Signaling In LPM During Cardiac Development

Another process that is dependent on retinoid signaling is the development of the myocardium. RXRα, and to a much lesser degree, RARαγ double null mutants display deficiencies in cardiomyocytes by E11.5 (Kastner *et al.,* 1994, 1997b; Sucov *et al.,* 1994). These losses seem to stem from a precocious differentiation of the myocardium.

Moreover, myocardial cell loss is seen as early as E9 in *raldh2*$^{-/-}$ (Niederreither *et al.*, 2001), establishing a genetic basis for vitamin A signaling in mammalian heart development. Interestingly, chimeras generated from RARγE knock-in ES cells also display a severe myocardial deficiency, apparent as early as E9.5. However, as RARγ expression has not been described within the developing myocardium (Ruberte *et al.*, 1990), the myocardial loss in the RARγE chimeras was unlikely to result from an inhibition of retinoid signaling in the heart. Alternatively, the myocardium may indeed express RARγ, but only at extremely low levels that escape detection by *in situ* hybridization. In this scenario, the cardiomyocyte loss in RARγE chimeras could be due to aberrant retinoid signaling within the cardiac lineages.

Another possible explanation of the reduced myocardium in RARγE chimeras is that it results from a block in RAR function within the late LPM and its derivatives. There are several observations in favor of this hypothesis. To begin with, the developing LPM expresses RARγ from E8.25 onwards (Ruberte *et al.*, 1990), and plays an instructive role in cardiac looping morphogenesis, as well as continually supplying presumptive cardiomyocytes to the developing heart even following cardiac looping (Challice and Viragh, 1973; Manasek *et al.*, 1972; Stalsberg, 1969; reviewed in Harvey, 1998). Recent work in the chick demonstrates that myocardium is generated specifically from splanchnic mesoderm-derived mesenchymal cells at the extremities of the cardiac tube (Waldo *et al.*, 2001; van der Hoff *et al.*, 2001). As this *de novo* cardiomyocyte production occurs well after the induction of the heart field from ingressing cranial mesoderm, it is referred to as the secondary heart field (Waldo *et al.*, 2001). Importantly, splanchnic mesoderm derives from the LPM and expresses high amounts of RARγ (Ruberte *et al.*, 1990), thus a possible explanation of the myocardial defects in RARγE chimeras involves an inhibition of retinoid signaling within the secondary heart field. Interestingly, Waldo and colleagues (2001) map the secondary heart field to the mesoderm underneath the foregut endoderm, which, as was discussed earlier, critically requires RAR function for proper pharyngeal arch development. As strong RARγE chimeras displayed defects in retinoid signaling within the foregut endoderm, it is possible that the underlying splanchnic mesoderm was also similarly affected,

presumably leading to reduced cardiomyocyte numbers. Furthermore, retinoid signaling in the foregut endoderm is implicated in normal avian heart morphogenesis, although this reflects a much earlier requirement for retinoids in heart tube formation (Ghatpande *et al.,* 2000). Thus, there is much circumstantial evidence suggesting that a block in retinoid signaling within the LPM-derived splanchnic mesoderm can lead to reduced myocardial numbers by affecting the secondary heart field.

Additional data suggesting that the myocardial loss in RARγE chimeras was not due to a deficiency in retinoid signaling within the heart proper was provided by the normal expression of several cardiac markers in the chimeras. Despite extensive RARγE contribution and obvious cardiac defects, chimeric hearts still expressed ANF, *mlc2v, tbx5,* and *eHand.* In support of this, *raldh2*$^{-/-}$ hearts also expressed many chamber-specific markers at levels comparable to wild type controls, despite having severe myocardial deficiencies (Niederreither *et al.,* 2001). Lastly, the removal of RXRα specifically within the heart failed to elicit myocardial deficiencies, indicating that the loss of myocardium in RXRα null mutants may represent a requirement for retinoid signaling in tissues outside the heart (Chen *et al.,* 1998; Tran and Sucov, 1998). Taken together, these results are consistent with a non-cell-autonomous function for RAR signaling in the heart, and instead suggest that the myocardial loss observed in RARγE chimeras may be principally due to a deficiency in cardiomyocyte precursors in non-cardiac tissues, such as the LPM-derived splanchnopleure.

5.3.3. Role For Retinoid Signaling In Late Cardiac Looping Morphogenesis

An interesting property of aberrant retinoid signaling is its ability to perturb not only A-P patterning, but the formation of the L-R axis as well. Studies in avians and rodents indicate that excess RA can randomize the direction of heart looping if administered immediately following gastrulation and prior to heart looping (Dickman and Smith, 1996; Smith *et al.,* 1997; Shenefelt, 1972; Thompson *et al.,* 1969; Yasui *et al.,* 1998). The lack of vitamin A during development also results in laterality reversals (Heine *et al.,* 1985; Kostetskii *et al.,* 1999; reviewed in Sinning, 1998; Smith and Dickman, 1997; Zile, 1998), which can be rescued by exogenous retinoids (Dersch and Zile, 1993; Kostetskii *et al.,* 1998). These *situs* defects are associated with either the randomization of the

expression of several left determinants, including *nodal, lefty2,* and *pitx2,* with RA excess (Chauzaud *et al.,* 1999; Smith *et al.,* 1997; Tsukui *et al.,* 1999; Wasiak and Lohnes, 1999), or their loss in the VAD quail embryos (Zile *et al.,* 2000). In light of this it was interesting to discover that the expression of RARγE within the RARγ domain resulted in abnormal heart looping and was associated with reduced Pitx2 expression on the left side of the chimeras. However, these defects rarely consisted of complete reversals of heart looping, but more commonly affected the final positioning of the cardiac chambers relative to the midline of the embryo. As the hearts initiated looping, the abnormal heart development in the chimeras likely reflected a block in late aspects of looping morphogenesis.

The left laterality determinants are expressed in the LPM adjacent to the heart and during pre-somite stages instruct the linear heart tube to loop, generating the leftward displaced heart (reviewed in Capdevila *et al.*, 2000). This tissue therefore plays a crucial role in L-R patterning. However, the available *in situ* data suggests RARγ expression in LPM occurs at stages following the initiation of cardiac looping (Ruberte *et al.*, 1990). Thus, the abnormal ventricular positioning seen in RARγE chimeras is consistent with the relatively late expression of RARγ, and thus presumably this dominant negative, with respect to heart looping.

A tempting explanation for the late cardiac looping defects in RARγE chimeras involves the inhibition of cardiac precursor accretion within the secondary heart field, as discussed earlier for myocardial development. The caudal region of the heart plays a dynamic role in the generation of heart mesoderm, and some evidence suggests that the formation of the heart loop is caused by the preferential overgrowth of material on the left side of the developing heart (Challice and Viragh, 1973; Manasek *et al.*, 1972; Stalsberg, 1969; reviewed in Harvey, 1998). Specifically, the dorsal wall of the heart is continuous with splanchnic mesoderm, which continually supplies cells that become definitive myocardium following cardiac looping (Manasek *et al.*, 1972; Waldo *et al.,* 2001; van der Hoff *et al.*, 2001). Furthermore, there is an increased proliferation rate of caudal cardiac progenitors on the left side of the posterior heart region, which has been suggested as a mechanism for generating heart asymmetry (Stalsberg, 1969; Harvey, 1998). It is this population of cells that expresses *pitx2* during cardiac development (Hjalt

et al., 2000; Campione *et al.*, 2001). *Pitx2* is also an excellent lineage marker for left cardiomyocytes throughout heart development (Campione *et al.*, 2001). Thus, affecting splanchnic mesoderm can presumably lead to myocardial deficiencies as well as looping anomalies.

The targeting of RARγE within the RARγ locus provided a direct test for the requirement of retinoid signaling in the LPM, and its derivatives such as the splanchnopleure, during later stages of heart development. Consistent with this notion, we have observed both cardiomyocyte loss and ventricular malpositioning defects in RARγE chimeras containing strong mutant cell contribution in the splanchnopleure. We have also shown that Pitx2 was reproducibly down-regulated in the left splanchnopleure populated by RARγE cells. The work detailed here therefore suggests that retinoid signaling was required by the LPM to support cardiomyocyte proliferation as well as to promote heart looping.

5.3.4. Transcriptional Targets Of Retinoid Signaling During Heart Looping

Excess RA results in a rapid induction of *nodal, lefty2,* and *pitx2* (Chauzaud *et al.,* 1999; Smith *et al.,* 1997; Tsukui *et al.,* 1999; Wasiak and Lohnes, 1999). As the mis-expression of these genes in various species is sufficient to randomize organ *situs* (section 1.7.4.; reviewed in Capdevila *et al.,* 2000), their bilateralization upon RA treatment is sufficient to account for the observed reversals in cardiac looping. The expression of these genes are also down-regulated by inhibiting retinoid signaling (Chauzaud *et al.,* 1999; Zile *et al.,* 2000; chapter 4), suggesting some of them may be transcriptional targets of the RARs. Indeed, the *nodal* promoter harbors a RARE within its minimal asymmetric enhancer (Adachi *et al.*, 1999; Norris and Robertson, 1999). Furthermore, *lefty2* and *pitx2* are direct targets of Nodal signaling, since they are induced by ectopic Nodal expression (reviewed in Capdevila *et al.,* 2000) and contain Nodal response element (FAST binding sequences) within their asymmetric enhancers (Saijoh *et al.,* 1999; Shiratori *et al.,* 2001). RAREs have not been described in the promoters of these genes, thus the effects of excess RA during pre-looping stages may be due to indirect induction of *lefty2* and *pitx2* in response to *nodal* activation. Assuming that RARγE was expressed at stages prior to the initiation of cardiac looping, then the aberrant looping morphogenesis seen in the

chimeras may have resulted from a down-regulation of *nodal* expression, as occurs in VAD quails (Zile *et al.,* 2000). This would account for the strong reduction in Pitx2 expression observed in the chimeras. However, an important caveat to this hypothesis is that looping morphogenesis initiated properly in almost all the chimeras examined. Furthermore, as discussed above, RARγ transcripts have thus far not been detected earlier than E8.25; that is, at stages immediately following the initiation of looping. These observations therefore suggest that Nodal function likely remained intact in the RARγE chimeras, but that the maintenance of *pitx2* expression following looping was compromised.

At stages subsequent to heart looping, *pitx2* expression remains distinctly left-sided in many organs, including the heart (Campione *et al.,* 2001; Hjalt *et al.,* 2000). This later asymmetric expression remains crucial for the instruction of organ *situs* (Liu *et al.,* 2001). *Nodal* transcripts in the LPM decline after 12-14 somites (Collignon *et al.,* 1996; Lowe *et al.,* 1996), when the heart is midway through its looping morphogenesis, thus additional factors are required for the maintenance of *pitx2* expression at later stages. Shiratori and colleagues (2001) ascribe the maintenance of *pitx2* expression to Nkx2-5 binding elements in the *pitx2* promoter. Indeed, several different NK2 homeodomain factor proteins are expressed in cardiac lineages and in various organs during development (Biben *et al.,* 1998; Harvey, 1996; Pabst *et al.,* 1997). Although RAREs are not found in the *pitx2* promoter, retinoid signaling may nevertheless indirectly impact on the maintenance of expression of this gene. This is supported by the loss of Pitx2 within the heart, stomach, and left body wall in affected RARγE chimeras. Our results also established, for the first time, the importance of normal retinoid signaling to direct later aspects of cardiac looping morphogenesis, such as the proper positioning of the ventricles with respect to the midline. These findings therefore showed the utility of using a gene replacement approach to restrict the expression of RARγE in order to circumvent functional redundancy among the RARs within specific tissues.

5.4. Perspectives And Future Directions

Retinoid signaling has diverse roles in the elaboration of animal design; from the patterning of the axial skeleton to the elaboration of asymmetric development along the left-right axis. Due to the complexities of vertebrate biology, not all the effects of retinoids are well understood, particularly at the molecular level. This thesis has attempted to address certain inadequacies in our knowledge of retinoid signaling during mammalian embryogenesis, with particular emphasis given to exploration of the timing of retinoid function and possible transcriptional targets of aberrant retinoid signaling.

One such outstanding issue involves determining during which developmental period RARγ functions to sculpt the unique characteristics of the cervical vertebrae. A surprising finding from this study is that RARs were able to influence vertebral form relatively late during development, at a period corresponding to the differentiation of the rostral-most somites to sclerotome, the antecedent of the vertebrae. Furthermore, the ability of retinoid signaling to influence vertebral patterning at this time occurs independently of alterations in *hox* gene expression patterns and is therefore thought of involving *hox*-gene independent processes. However, as this remains largely unresolved, a straightforward experiment would be the removal of the *hox* genes, or the RAREs within their promoters, specifically during the formation of the vertebrae. The experiments should help define if the RARs are truly able to influence vertebral form independent of the *hox* genes.

Retinoids also influence the development of the caudal embryo, and excess RA can completely ablate all tissues below the lumbar region. The complexity of the posterior development thwarted previous embryological work as to the nature of retinoid-induced caudal regression. The work presented here attempted to resolve this issue with the use of lineage-specific markers and suggested newly forming mesoderm as the primary target of retinoid excess leading to caudal truncations. The results described, for the first time, a relationship between *brachyury* expression and retinoid signaling in the posterior embryos leading to the truncation of the axis. As the regulation of this important morphogenetic gene is poorly understood, future work should characterize the basis of the RA-dependent down-regulation of *brachyury* expression. Research activity should not

only be directed towards an extensive analysis of *cis*-regulatory sequences directing *brachyury* expression, but should also include the promoters of known regulators of *brachury*, such as *wnt3a*. In addition, these observations provide a verifiable hypothesis regarding retinoid signaling and *brachyury* function in paraxial mesoderm differentiation.

A major difficultly in assessing the contribution of RARs to any given developmental process is the large degree of functional overlap between the three RAR genes. Due to this redundancy, the conclusions drawn from knock-out phenotypes of these genes remains incomplete. This was addressed by developing a novel model of retinoid signaling deficiency involving the restricted expression of a potent and specific dominant negative. Moreover, this approach permitted an assessment of RAR function during heart looping, and revealed a previously unsuspected role for retinoid signaling in late looping morphogenesis. Importantly, these studies suggest a role for the RARs in cardiac development *via* the maintenance of *pitx2* expression. As RAREs have not been detected in the *pitx2* promoter, future work should determine if the regulators of *pitx2* expression, namely NK2 factors, are themselves retinoid targets. This can be accomplished by a systematic examination of the effects of excess RA on the embryonic expression of NK2 genes, followed by a dissection of the *cis*-regulatory sequences of any of the genes that respond to RA. Furthermore, the results also offer a novel tool in the investigation of RAR function and can be used to reveal new roles for these receptors in various developmental processes.

In conclusion, vitamin A has proven itself to be indispensable for life and embryogenesis. Its derivatives, although simple in structure, have humbled us with their abilities to influence several key events in vertebrate ontogeny, including antero-posterior and left-right patterning. Due to their pleiotropic natures, it is with little doubt that surprising roles will continue to emerge from the study of the retinoids in the development of animal form.

REFERENCES

Abu-Abed, S.S., Beckett, B.R., Chiba, H., Chithalen, J.V., Jones, G., Metzger, D., Chambon, P., and Petkovich, M. (1998). Mouse P450RAI (CYP26) expression and retinoic acid-inducible retinoic acid metabolism in F9 cells are regulated by retinoic acid receptor γ and retinoid X receptor α. *J. Biol. Chem.* **273**: 2409-2415.

Abu-Abed, S., Dollé, P., Metzger, D., Beckett, B., Chambon, P., and Petkovich, M. (2001). The retinoic acid-metabolizing enzyme, CYP26A1, is essential for normal hindbrain patterning, vertebral identity, and development of posterior structures. *Genes Dev.* **15**: 226-240.

Adachi, H., Saijoh, Y., Mochida, K., Ohishi, S., Hashiguchi, H., Hirao, A., and Hamada, H. (1999). Determination of left/right asymmetric expression of *nodal* by a left side-specific enhancer similarity to a *lefty-2* enhancer. *Genes Dev.* **13**: 1589-1600.

Alexandre, D., Clarke, J.D.W., Oxtoby, E., Yan, Y.-L., Jowett, T., and Holder, N. (1996). Ectopic expression of *Hoxa-1* in the zebrafish alters the fate of the mandibular arch neural crest and phenocopies a retinoic acid-induced phenotype. *Development* **122**: 735-746.

Alland, L., Muhle, R., Hou Jr, H., Potes, J., Chin, L., Schreiber-Agus, N., and DePinho, R.A. (1997). Role for N-CoR and histone deacetylase in Sin3-mediated transcriptional repression. *Nature* **387**: 49-55.

Allenby, G., Bocquel, M.-T., Saunders, M., Kazmer, S., Speck, J., Rosenberger, M., Lovey, A., Kastner, P., Grippo, J.F., Chambon, P., and Levin, A.A. (1993). Retinoic acid receptors and retinoid X receptors: interactions with endogenous retinoic acids. *Proc. Natl. Acad. Sci. USA* **90**: 30-34.

Amaya, E., Musci, T., and Kirscher, M. (1991). Expression of a dominant negative mutant of the FGF receptor disrupts mesoderm formation in *Xenopus* embryos. *Cell* **66**: 257-270.

Ang, H.L., Deltour, L., Hayamizu, T.F., Zgombic-Knight, M., and Duester, G. (1996). Retinoic acid synthesis in mouse embryos during gastrulation and craniofacial development linked to class IV alcohol dehydrogenase gene expression. *J. Biol. Chem.* **271**: 9526-9534.

Ang, H.L., and Duester, G. (1999). Retinoic acid biosynthetic enzyme ALDH1 localizes in a subset of retinoid-dependent tissues during *Xenopus* development. *Dev. Dyn.* **215**: 264-272.

Aranda, A., and Pascual, A. (2001). Nuclear hormone receptors and gene expression. *Physiol. Rev.* **81**: 1269-1304.

Arnold, S.J., Stappert, J., Bauer, A., Kispert, A., Herrmann, B.G., and Kremler, R. (2000). *Brachyury* is a target gene of the Wnt/β-catenin signaling pathway. *Mech. Dev.* **91**: 249-258.

Aubin, J., Lemieux, M., Tremblay, M., Bérard, J., Jeannotte, L. (1997). Early postnatal lethality in *Hoxa-5* mutant mice is attributable to respiratory tract defects. *Dev. Biol.* **192**: 432-445.

Avantaggiato, V., Acampora, D., Tuorto, F., and Simone, A. (1996). Retinoic acid induces stage-specific repatterning of the rostral central nervous system. *Dev. Biol.* **175**: 347-357.

Ayer, D.E. (1999). Histine deacetylases: transcriptional repression with SINers and NuRDs. *Trends Cell Biol.* **9**: 193-198.

Balkan, W., Colbert, M., Bock, C., and Linney, E. (1992). Transgenic indicator mice for studying activated retinoic acid receptors during development. *Proc. Natl. Acad. Sci. USA.* **89**: 3347-3351.

Bannister, A.J., and Kouzarides, T. (1996). The CBP co-activator is a histone acetyltransferase. *Nature* **384**: 641-643.

Barettino, D., Vivanco-Ruiz, M.M., and Stunnenberg, H.G. (1994). Characterization of the ligand-dependent transactivation domain of thyroid hormone receptor. *EMBO J.* **13**: 3039-3049.

Barrow, J.R., Stadler, H.S., and Capecchi, M.R. (2000). Roles of *Hoxa1* and *Hoxa2* in patterning the early hindbrain of the mouse. *Development* **127**: 933-944.

Bastein, J., Adam-Sitah, S., Riedl, T., Egly, J.M., Chambon, P., and Rochette-Egly, C. (2000). TFIIH interacts with the retinoic acid receptor gamma and phosphorylates its AF-1-activating domain through cdk7. *J. Biol. Chem.* **275**: 21896-21904.

Beddington, R.S.P. (1994). Induction of a second neural axis by the mouse node. *Development* **120**:613-620.

Beddington, R.S., Rashbass, P. and Wilson, V. (1992). Brachyury-a gene affecting mouse gastrulation and early organogenesis. *Development (Suppl.)*: 157-165.

Beddington, R.S.P., and Robertson, E.J. (1998). Anterior patterning in mouse. *Trends Genet.* **14**: 277-284.

Beddington, R.S.P., and Robertson, E.J. (1999). Axis development and early asymmetry in mammals. *Cell* **96**: 195-209.

Biben, C., Schneider, A., Brand, T., and Arnold, H.H. (1997). Expression of NK-2 class gene *nkx2-6* in the foregut endoderm and heart. *Mech. Dev.* **73**: 125-127.

Blanco, J.C., Minucci, S., Lu, J., Yang, X.J., Walker, K.K., Chen, H., Evans, R.M., Nakatani, Y., and Ozato, K. (1998). The histone acetylase PCAF is a nuclear receptor coactivator. *Genes Dev.* **12**: 1638-1651.

Blumberg, B., Bolado, J., Jr., Moreno, T.A., Kinter, C., Evans, R.M., and Papalopulu, N. (1997). An essential role for retinoid signaling in anteroposterior neural patterning. *Development* **124**: 373-379.

Boettger, T., Wittler, L., and Kessel, M. (1998). FGF8 functions in the specification of the right body side in the chick. *Curr. Biol.* **9**: 277-280.

Boulet, A.M., and Capecchi, M.R. (1996). Targeted disruption of *Hoxc-4* causes esophageal defects and vertebral transformations. *Dev. Biol.* **177**: 232-249.

Bourguet, W., Ruff, M., Chambon, P., Gronemeyer, H., and Moras, D. (1995). Crystal structure of the ligand-binding domain of the human nuclear eceptor RXR-α. *Nature* **375**: 377-382.

Bouwmeester, T., Kim, S-H., Sasai, Y., Lu, B., and DeRobertis, E.M. (1996). Cerberus is a head inducing secreted factor expressed in the anterior endoderm of Spemann's organizer. *Nature* **382**: 595-601.

Brocard, J., Warot, X., Wendling, O., Messaddeq, N., Vonesch, J.L., Chambon, P., and Metzger, D. (1997). Spatio-temporally controlled site-specific somatic mutagenesis in the mouse. *Proc. Natl. Acad. Sci. USA* **94**: 14559-14563.

Brooke, N.M., Garcia-Fernàndez, J., and Holland, P.W.H. (1998). The ParaHox gene cluster is an evolutionary sister of the Hox gene cluster. *Nature* **392**: 920-922.

Caelles, C., Gonzalez-Sancho, J.M., and Munoz, A. (1997). Nuclear hormone receptor antagonism with AP-1 by inhibition of the JNK pathway. *Genes Dev.* **11**: 3351-3364.

Campione, M., Ros, M.A., Icardo, J.M., Piedra, E., Christoffels, V.M., Schweickert, A., Blum, M., Franco, D., and Moorman, A.F.M. (2001). *Pitx2* expression defines a left cardiac lineage of cells: evidence for atrial and ventricular molecular isomerism in the *iv/iv* mice. *Dev. Biol.* **231**: 252-264.

Campione, M., Steinbeisser, H., Schweickert, A., Deissler, K., van Bebber, F., Lowe, L.A., Nowotschin, S., Viebahn, C., Haffter, P., Kuehn, M. R., and Blum, M. (1999). The homeobox gene *Pitx2*: mediator of asymmetric left-right signaling in the vertebrate heart and gut looping. *Development* **126**: 1225-1234.

Capdevila, J., Vogan, K. J., Tabin, C. J., and Izpisua Belmonte, J. C. (2000). Mechanisms of left-right determination in vertebrates. *Cell* **101**, 9-21.

Carlson, B.M. (1996). "Patten's Foundation of Embryology.", 6th Ed. McGraw-Hill Inc., New York.

Casey, B., and Hackett, B.P. (2000). Left-right malformations in man and mouse. *Curr. Op. Genes. Dev.* **10**: 257-261.

Casey, E.S., O'Reilly, M-A.J., Conlon, F.L., and Smith, J.C. (1998). The T-box transcription factor regulates expression of *eFGF* through binding to a non-palindromic response element. *Development* **125**: 3887-3894.

Catala, M., Teillet, M.A., and LeDouarin, N.M. (1995). Organization and development of the tail bud analyzed with the quail-chick chimera system. *Mech. Dev.* **51**: 51-65.

Chakravarti, D., LaMorte, V.J., Nelson, M.C., Nakajima, T., Schulman, I.G., Juguilon, H., Montminy, M., and Evans, R. M. (1996). Role of CBP/P300 in nuclear receptor signaling. *Nature* **383**: 99-103.

Challice, C. E. and Viragh, S. (1973). The architectural development of the early mammalian heart. *Tissue Cell* **6**, 447-462.

Chambon, P. (1996). A decade of molecular biology of retinoic acid receptors *FASEB J.* **10**: 940-954.

Chang, H., Zwijsen, A., Vogel, H., Huylebroeck, D., and Matzuk, M.M. (2000). Smad5 is essential for left-right asymmetry in mice. *Dev. Biol.* **219**: 71-78.

Chapman, D.L., and Papaioannou, V.E. (1998). Three neural tubes in mouse embryos with mutations in the T-box gene *Tbx6*. *Nature* **391**: 695-697.

Charité, J., de Graaff, W., Shen, S., and Deschamps, J. (1994). Ectopic expression of *Hoxb-8* causes duplication of the ZPA in the forelimb and homeotic transformation of axial structures. *Cell* **78**: 589-601.

Chazaud, C., Chambon, P., and Dolle, P. (1999). Retinoic acid is required in the mouse embryo for left-right asymmetry determination and heart morphogenesis. *Development* **126**, 2589-2596.

Chen, D., and Evans, R.M. (1995). A transcriptional co-repressor that interacts with nuclear hormone receptors. *Nature* **377**: 454-457.

Chen, H., Lin, R.J., Schiltz, R.L., Chakravarti, D., Nash, A., Nagy, L., Privalsky, M.L., Nakatani, Y., and Evans, R.M. (1997). Nuclear receptor coactivator ACTR is a novel histone acetyltransferase and forms a multimeric activation complex with P/CAF and CBP/p300. *Cell* **90**: 569-580.

Chen, H., Lin, R.J, Xie, W., Wilpitz, H., and Evans, R.M. (1999). Regulation of hormone-induced histone hyperacetylation and gene activation via acetylation of an acetylase. *Cell* **98**: 675-686.

Chen, Y.P., Dong, D., Kostetskii, I., and Zile M.H. (1996). Hensen's node from vitamin A-deficient quail embryo induces chick limb bud duplication and retains is normal asymmetric expression of *sonic hedgehog (shh). Dev. Biol.* **173**: 256-264.

Chen, Y.P., Huang, L., Russo, A.F., and Solursh, M. (1992). Retinoic acid is enriched in Hensen's node and is developmentally regulated in the early chicken embryo. *Proc. Natl. Acad. Sci. USA* **89**: 10056-10059.

Chen, Y.P., Huang, L., and Solursh, M. (1994). A concentration gradient of retinoids in the early *Xenopus laevis* embryo. *Dev. Biol.* **161**: 70-76.

Chisaka, O., and Capecchi, M. (1991). Regionally restricted developmental defects resulting from targeted disruption of the mouse homeobox gene *hox1.5. Nature* **350**: 473-479.

Chiba, H., Clifford, J., Metzger, D., and Chambon, P. (1997). Distinct retinoid X receptor-retinoic acid receptor heterodimers are differentially involved in the control of expression of retinoid target genes in F9 embryonal carcinoma cells. *Mol. Cell Biol.* **17**: 3013-3020.

Cho, K.W.Y., and DeRobertis, E.M. (1990). Differential activation of *Xenopus* homeobox genes by mesoderm-inducing growth factors and retinoic acid. *Genes Dev.* **4**: 1910-1916.

Ciruna, B.G., Schwartz, L., Harpal, K., Yamaguchi, T.P., and Rossant, J. (1997). Chimeric analysis of *fibroblast growth factor receptor-1* (*Fgfr1*) function: a role for FGFR1 in morphogenetic movement through the primitive streak. *Development* **124**: 2829-2841.

Clements, D., Taylor, H.C., Herrmann, B.G. and Stott, D. (1996). Distinct regulatory control of the brachyury gene in axial and non-axial mesoderm suggests separation of mesoderm lineages early in mouse gastrulation. *Mech. Dev.* **56**, 139-149.

Collingnon, J., Varlet, I., and Robertson, E.J. (1996). Relationship between asymmetric *nodal* expression and the direction of embryonic turning. *Nature* **381**: 155-158.

Collins, M.D., and Mao, G.E. (1999). Teratology of retinoids. *Annu. Rev. Pharmacol. Toxicol.* **39**: 399-430.

Condie, B.G., and Capecchi, M.R. (1993). Mice homozygous for a targeted disruption of *Hoxd-3 (Hox-4.1)* exhibit anterior transformations of the first and second cervical vertebrae, the atlas and axis. *Development* **119**: 579-595.

Condie, B.G., and Capecchi, M.R. (1994). Mice with targeted disruptions in the paralogous genes hoxa-3 and hoxd-3 reveal synergistic interactions. *Nature* **370**: 304-307.

Conlon, F.L., Lyon, K.M., Takaesu, N., Barth, K.S., Kispert, A., Herrmann, B., and Robertson, E.J. (1994). A prinmary requirement for nodal in the formation and maintenance of the primitive streak in the mouse. *Development* **120**: 1919-1928.

Conlon, F.L., Sedgwick, S.G., Weston, K.M., and Smith, J.C. (1996). Inhibition of Xbra transcription activation causes defects in mesodermal patterning and reveals autoregulation of Xbra in dorsal mesoderm. *Development* **122**: 2427-2435.

Conlon, R.A. (1995). Retinoic acid and pattern formation in vertebrates. *Trends Genet.* **11**: 314-319.

Conlon, R.A., and Rossant, J. (1992). Exogenous retinoic acid rapidly induces anterior ectopic expression of murine *Hox-2* genes in vivo. *Development* **116**: 357-368.

Cordes, S.P. (2001). Molecular genetics of cranial nerve development in mouse. *Nat. Rev. Neurosci.* **2**: 611-623.

Cox, W.G., and Hemmati-Brivanlou, A. (1995). Caudalization of neural fate by tissue recombination and bFGF. *Development* **121**: 4349-4358.

Crossely, P.H., and Martin, G.R. (1995). The mouse Fgf8 gene encodes a family of polypeptides and is expressed in regions that direct outgrowth and patterning in the developing embryo. *Development* **121**: 439-451.

Cunliffe, V. and Smith, J.C. (1992). Ectopic mesoderm formation in xenopus embryos caused by widespread expression of a brachyury homologue. *Nature* **358**, 427-430.

Danielian, P.S., White, R., Lees, J.A., and Parker, M.G. (1992). Identification of a conserved region required for hormone dependent transcriptional activation by steroid hormone receptors. *EMBO J.* **11**: 1025-1033.

Delmotte, M.H., Tahayato, A., Formstecher, P., and Lefebvre, P. (1999). Serine 157, a retinoic acid receptor alpha residue phosphorylated by protein kinase C in vitro, is involved in RXR-RARalpha heterodimerization and transcriptional activity. *J. Biol. Chem.* **274**: 38225-38231.

Deltour, L., Foglio, M.H., and Duester, G. (1999a). Metabolic deficiencies in alcohol dehydrogenase *Adh1*, *Adh3*, and *Adh4* null mutant mice: Overlapping roles of *Adh1* and

Adh4 in ethanol clearance and metabolism of retinol to retinoic acid. *J. Biol. Chem.* **274**: 16796-16801.

Deltour, L., Foglio, M.H., and Duester, G. (1999b). Impaired retinol utilization in *Adh4* alcohol dehydrogenase mutant mice. *Dev. Genet.* **25**: 1-10.

Deng, C.X., Wynshaw-Boris, A., Shen, M.M., Daugherty, C., Ornitz, D.M., and Leder, P. (1994). Murine FGFR-1 is required for early postimplantation growth and axial organization. *Genes Dev.* **8**: 3045-3057.

DeRobertis, E.M., Larrain, J., Oelgeschlager, M., and Wessely, O. (2000). The establishment of Spemann's organizer and patterning of the vertebrate embryo. *Nat. Rev. Gen.* **1**: 171-181.

de Roos, K., Sonneveld, E., Compaan, B., ten Berge, D., Durston, A.J., and van der Saag, P.T. (1999). Expression of retinoic acid 4-hydroxylase (CYP26) during mouse and Xenopus laevis embryogenesis. *Mech. Dev.* **82**: 205-211.

Dersch, H., and Zile, M.H. (1993). Induction of normal cardiovascular development in the vitamin A-deprived quail embryo by natural retinoids. *Dev. Biol.* **160**: 424-433.

Deschamps, J., van den Akker, E., Forlani, S., de Graff, W., Oosterveen, T., Roelen, B., and Roelfsema, J. (1999). Initiation, establishment, and maintenance of *Hox* gene expression patterns in the mouse. *Int. J. Dev. Biol.* **43**: 635-650.

de The, H., Vivanco-Ruiz, M.M., Tiollais, P., Stunnenberg, H., and Dejean, A. (1990). Identification of a retinoic acid responsive element in the retinoic acid receptor beta gene. *Nature* **343:** 177-180.

Dickman, E. D. and Smith, S. M. (1996). Selective regulation of cardiomyocyte gene expression and cardiac morphogenesis by retinoic acid. *Dev. Dyn.* **206**, 39-48.

Dickman, E.D., Thaller, C., and Smith, S.M. (1997). Temporally-regulated retinoic acid depletion produces specific neural crest, ocular and nervous system defects. *Development* **124**: 3111-3121.

Dillworth, F.J., Fromental-Ramain, C., Remboutsika, E., Renecke, A., and Chambon, P. (1999). Ligand-dependent activation of transcription *in vitro* by retinoic acid receptor α/ retinoid X receptor α heterodimers that mimics transactivation by retinoids *in vivo*. *Proc. Natl. Acad. Sci. USA* **96**: 1995-2000.

Ding, J., Yang, L., Yan, Y.L., Chen, A., Desai, N., Wynshaw-Boris, A., and Shen, M.M. (1998). Crypto is required for correct orientation of the anterior-posterior axis in the mouse embryo. *Nature* **395**: 702-707.

Dollé, P., Fraulob, V., Kastner, P., and Chambon, P. (1994). Developmental expression of murine retinoid x receptor (RXR) genes. *Mech. Dev.* **45**: 91-104.

Dollé, P., Ruberte, E., Kastner, P., Petkovich, M., Stoner, C.M., Gudas, L.J., Chambon, P. (1989). Differential expression of the genes encoding the retinoic acid receptors α, β, γ and CRABP in the developing limbs of the mouse. *Nature* **342**: 702-705.

Dollé, P., Ruberte, E., Leroy, P., Morriss-Kay, G.M., and Chambon, P. (1990). Retinoic acid receptors and cellular retinoid binding proteins. I. A systematic study of their differential pattern of transcription during mouse organogenesis. *Development* **110:** 1133-1151.

Duboule, D. (1995). Vertebrate Hox genes and proliferation: an alternative pathway to homeosis? *Curr. Op. Genes. Dev.* **5**: 525-528.

Duboule, D., and Dollé, P. (1989). The structural and functional organization of the murine *HOX* gene family resembles that of *Drospohila* homeotic genes. *EMBO J.* **8**: 1497-1505.

Dubrulle, J., McGrew, M.J., and Pourquié, O. (2001). FGF signaling controls somite boundary position and regulates segmentation clock control of spatiotemporal *Hox* gene activation. *Cell* **106**: 219-232.

Duester, G. (2000). Families of retinoid dehydrogenases regulating vitamin A function: Production of visual pigment and retinoic acid. *Eur. J. Biochem.* **267**: 4315-4324.

Dupé, V., Davenne, M., Brocard, J., Dollé, P., Mark, M., Dierich, A., Chambon, P., and Rijli, F.M. (1997). In vivo functional analysis of the *Hoxa1* 3' retinoic acid response element (3' RARE). *Development* **124**: 399-410.

Dupé, V., Ghyselinck, N.B., Wendling, O., Chambon, P., and Mark, M. (1999). Key roles of retinoic acid receptors alpha and beta in the patterning of the caudal hindbrain, pharyngeal arches and otocyst in the mouse. *Development* **126**: 5051-5059.

Dupé, V., and Lumsden, A. (2001). Hindbrain patterning involves graded responses to retinoic acid signaling. *Development* **128**: 2199-2208.

Durand, B., Sauders, M., Gaudon ,C., Roy, B., Losson, R., and Chambon, P. (1994). Activation function 2 (AF-2) of retinoic acid receptor and 9-*cis* retinoic acid receptor: presence of a conserved autonomous constitutive acting domain and influence of the nature of the response element on AF-2 activity. *EMBO J.* **13**: 5370-5382.

Durston, A.J., Timmermans, J.P.M., Hage, W.J.,Hendriks, H.F.J., de Vries, N.J., Heidiveld, M., and Nieuwkoop, P.D. (1989). Retinoic acid causes an anteroposterior transformation in the developing central nervous system. *Nature* **340**: 140-144.

Easwaran, V., Pishvaian, M., Salimuddin, and Byers, S. (1999). Cross-regulation of β-catenin-LEF/TCF and retinoid signaling pathways. *Curr. Biol.* **9**: 1415-1418.

Echelard, Y., Epstein, D.J., St-Jacques, B., Shen, L., Mohler, J., McMahon, J.A., and McMahon, A.P. (1993). Sonic hedgehog, a member of a family of putative signaling molecules, is implicated in the regulation of CNS polarity. *Cell* **75**: 1417-1430.

Ericson, J., Briscoe, J., Rashbass, P., van Heyningen, V., and Jessel, T.M. (1997). Graded sonic hedgehog signaling and the specification of cell fate in the ventral neural tube. *Cold Spring Harb. Symp. Quant. Biol.* **62**: 451-466.

Fawcett, D., Pasceri, P., Fraser, R., Colbert, M., Rossant, J., and Giguère, V. (1995). Postaxial polydactyly in forelimbs of CRABP-II mutant mice. *Development* **121**: 671-679

Feldman, B., Poueymirou, W., Papaioannou, V.E., DeChiara, T.M., and Goldfarb, M. (1995). Requirement of FGF-4 for postimplantation mouse development. *Science* **267**: 246-249.

Feng, W., Ribeiro, R.C., Wagner, R.L., Nguyen, H., Apriletti, J.W., Fletterick, R.J., Baxter, J.D., Kushner, P.J., and West, B.L. (1998). Hormone-dependent coactivator binding to a hydrophobic cleft on nuclear receptors. *Science* **280**: 1747-1749.

Ferretti, E., Marshall, H., Pöpperl, H., Maconochie, M., Krumlauf, R., and Blasi, F. (2000). Segmental expression of *hoxb2* in r4 requires two separate sites that integrate cooperative interactions between Prep1, Pbx and Hox proteins. *Development (Suppl.)* **127**: 155-166.

Fiorella, P., and Napoli, J. (1991). Expression of cellular retinoic acid binding protein (CRABP) in Escherichia coli: Characterization and evidence that holo-CRABP is a substrate in retinoic acid-metabolism. *J. Biol. Chem.* **266**: 16572-16579.

Fiorella, P., and Napoli, J. (1994). Microsomal retinoic acid metabolism: effects of cellular retinoic acid-binding protein (type I) and C18-hydroxylation as an initial step. *J. Biol. Chem.* **269**: 10538-10544.

Fiorella, P.D., Giguère, V., and Napoli, J.L. (1993). Expression of cellular retinoic acid binding protein (type II) in *Escherichia coli*: characterization and comparison to cellular retinoic acid binding protein (type I). *J. Biol. Chem.* **268**: 21545-21552.

Folberg, A., Nagy Kovács, E.N., and Featherstone, M.S. (1997). Characterization and retinoic acid responsiveness of the murine *Hoxd4* transcription unit. *J. Biol. Chem.* **272**: 29151-29157.

Folberg, A., Nagy Kovács, E.N., Huang, H., Houle, M., Lohnes, D., and Featherstone, M.S. (1999a). *Hoxd4* and *RARγ* □interact synergistically in the specification of the cervical vertebrae. *Mech. Dev.* **89**: 65-74.

Folberg, A., Nagy Kovács, E.N., Luo, J., Giguère, V., and Featherstone, M.S. (1999b) *RARβ* mediates the response of *Hoxd4* and *Hoxb4* to exogenous retinoic acid. *Dev. Dyn.* **215**: 96-107.

Folkers, G.E., van der Leede, B.-jM., van der Saag, P.T. (1993). The retinoic acid receptor-β2 contains two separable cell-specific transactivation domains, at the N-terminus and in the ligand-binding domain. *Mol. Endocrinol.* **7**: 616-627.

Fondell, J.D., Ge, H., and Roeder, R.G. (1996). Ligand induction of a transcriptionally active thyroid hormone receptor coactivator complex. *Proc. Natl. Acad. Sci. USA* **93**: 8329-8333.

Forman, B.M., Yange, C.R., Au, M., Casanova, J., Ghysdael, J., Samuels, H.H. (1989). A domain containing leucine-zipper-like motifs mediate novel in vivo interactions between the thyroid hormone and retinoic acid receptors. *Mol. Endocrinol.* **3**: 1610-1626.

Frasch, M., Chen, X., and Lufkin, T. (1995). Evolutionary-conserved enhancers direct region-specific expression of the murine Hoxa1 and Hoxa2 loci in both mice and Drosophila. *Development* **121**: 957-974.

Freedman, L.P. (1999). Increasing the complexity of coactivation in nuclear receptor signaling. *Cell* **97**: 5-8.

Fry, C.J., and Peterson, C.L. (2001). Chromatin remodeling enzymes: who's on first? *Curr. Biol.* **11**: R185-R197.

Fujii, H., Sato, T., Kaneko, S., Gotoh, O., Fujii-Kuriyama, Y., Osawa, K., Kato, S., and Hamada, H. (1997). Metabolic inactivation of retinoic acid by a novel P450 differentially expressed in developing mouse embryos. *EMBO J.* **16**: 4163-4173.

Gage, P.J., Hoonkyo, S., and Camper, S. (1999). Dosage requirement of Pitx2 for development of multiple organs. *Development* **126**: 4643-4651.

Gaio, U., Schweickert, A., Fischer, A., Garratt, A.N., Muller, T., Ozcelik, C., Lankes, W., Strehle, M., Britsch, S., Blum, M., and Birchmeier, C. (1999). A role of the cryptic gene in the correct establishment of the left-right axis. *Curr. Biol.* **9**: 1339-1342.

Gale, E., Zile, M., Maden, M. (1999). Hindbrain respecification in the retinoid-deficient quail. *Mech. Dev.* **89**: 43-54.

Gaunt, S.J., Sharpe, P.T., and Duboule, D. (1988). Spatially restricted domains of homeo-gene transcripts in mouse embryos: relation to a segmented body plan. *Development (Suppl.)* **104**: 169-179.

Gaunt, S.J., Krumlauf, R., and Doboule, D. (1989). Mouse homeo-genes within a sunfamily, Hox1.4, -2.6, and –5.1, display similar antero-posterior domains of expression in the embryo, but show stage- and tissue-dependent differences in their regulation. *Development* **107**: 131-141.

Gavalas, A., and Krumlauf, R. (2000). Retinoid signaling and hindbrain patterning. *Curr. Opin. Gene. Dev.* **10**: 380-386.

Gavalas, A., Studer, M., Lumsden, A., Rijii, F., Krumlauf, R., and Chambon, P. (1998). *Hoxa1* and *Hoxb1* synergize in patterning the hindbrain, cranial nerves and second pharyngeal arch. *Development* **125**: 1123-1136.

Gavalas, A., Trainor, P., Ariza-McNaughton, L., and Krumlauf, R. (2001). Synergy between *Hoxa1* and *Hoxb1*: the relationship between arch patterning and the generation of cranial neural crest. *Development* **128**: 3017-3027.

Ghatpande, S., Ghatpande, A., Zile, M., and Evans, T. (2000). Anterior endoderm is sufficient to rescue foregut apoptosis and heart tube morphogenesis in an embryo lacking retinoic acid. *Dev. Biol.* **219**: 59-70.

Ghyselinck, N.B., Dupé, V., Dierich, A., Messaddeq, N., Garnier, J.M., Rochette-Egly, C., Chambon, P., and Mark, M. (1997). Role of the retinoic acid receptor beta (RARβ) during mouse development. *Int. J. Dev. Biol.* **41**: 425-447.

Ghyselinck, N.B., Bavik, C., Sapin, V., Mark, M., Bonnier, D., Hindelang, C., Dierich, A., Nilsson, C.B., Hakansson, H., Sauvant, P., Azais-Braesco, V., Frasson, M., Picaud, S., and Chambon, P. (1999). Cellular retinol-binding protein I is essential for vitamin A homeostasis. *EMBO J* **18**: 4903-4914.

Giguère, V., Ong, E.S., Segui, P., and Evans, R.M. (1987). Identification of a receptor for the morphogen retinoic acid. *Nature* **330**: 624-629.

Gilbert, S.F. (1994). "Developmental Biology", 4th Ed. Sinauer Associates, Inc., Sunderland, Massachusettes.

Glass, C.K., Rose, D.W., and Rossenfeld, M.G. (1997). Nuclear receptor coactivators. *Curr. Op. Cell Biol.* **9**: 222-232.

Glass, C.K., and Rosenfeld, M.G. (2000). The coregulator exchange in transcriptional functions of nuclear receptors. *Genes Dev.* **14**: 121-141.

Glinka, A., Wu, W., Delius, H., Monaghan, A.P., Blumenstock, C., and Niehrs, C. (1998). Dickkopf-1 is a member of a new family of secreted proteins and functions in head induction. *Nature* **391**: 357-362.

Godsave, S.F., Koster, C.H., Getahun, A., Mathu, M., Hooiveld, M., van der Wees, J., Hendricks, J., and Durston, A.J. (1998). Graded retinoid responses in the developing hinbrain. *Dev. Dyn.* **213**: 39-49.

Goff, D.J., and Tabin, C.J. (1997). Analysis of Hoxd-13 and Hoxd-11 misexpression in chick limb buds reveals that Hox genes affect both bone condensation and growth. *Development* **124**: 627-636.

Golding, J.P., Trainor, P., Krumlauf, R., and Gassmann, M. (2000). Defects in pathfinding by cranial neural crest cells in mice lacking the neuregulin receptor ErbB4. *Nat. Cell Biol.* **2**: 103-109.

Goodman, R.H., and Smolik, S. (2000) CBP/p300 in cell growth, transformation, and development. *Genes Dev.* **14**: 1553-1577.

Gorry, P., Lufkin, T., Dierich, A., Rochette-Egly, C., Décimo, D., Dollé, P., Mark, M., Durand, B., and Chambon, P. (1994). The cellular retinoic acid binding protein I (CRABPI). is dispensable. *Proc. Natl. Acad. Sci. USA* **90**: 932-936.

Gould, A. (1997). Functions of the polycomb group and trithorax group related genes. *Curr. Op. Genes. Dev.* **7**: 488-494.

Gould, A., Itasaki, N., and Krumlauf, R. (1998). Initiation of rhombomeric *Hoxb4* expression requires induction by somites and a retinoid pathway. *Neuron* **21**: 39-51.

Gould, A., Morrison, A., Sproat, G., White, R.A.H., and Krumlauf, R. (1997). Positive cross-regulation and enhancer sharing: two mechanisms for specifying overlapping *Hox* expression patterns. *Genes Dev.* **11**: 900-913.

Gottesman, M.E., Quandro, L., and Blaner, W.S. (2001). Studies of vitamin A metabolism in mouse model systems. *BioEssays* **23**: 409-419.

Goumans, M.-J., and Mummery, C. (2000). Functional analysis of the TGFβ receptor/Smad pathway through gene ablation in mice. *Int. J. Dev. Biol.* **44**: 253-265.

Graham, A., Papalopulu, N., and Krumlauf, R. (1989). The murine and *Drosophila* homeobox clusters have common features of organization and expression. *Cell* **57**: 367-378.

Greco, T.L., Takada, S., Newhouse, M.M., McMahon, J.A., McMahon, A.P., and Camper, S.A. (1996). Analysis of the *vestigial tail* mutation demonstrates that *Wnt-3a* gene dosage regulates mouse axial development. *Genes. Dev.* **10**: 313-324.

Greer, J.M., Puetz, J., Thomas, KR., and Capecchi, M.R. (2000). Maintenance of functional equivalence during paralogous Hox gene evolution. *Nature* **403**: 661-665.

Griffin, K.J.P., Amacher, S.L., Kimmel, C.B., and Kimelman, D. (1998). Molecular identification of *spadetail*: regulation of zebrafish trunk and tail mesoderm formation by T-box genes. *Development* **125**: 3379-3388.

Griffin, K., Patient, R., and Holder, N. (1995). Analysis of FGF function in normal and *no tail* zebrafish embryos reveals separate mechanisms for formation of the trunk and tail. *Development* **121**: 2983-2994.

Griffith, C.M., and Wiley, M.J. (1991). Effects of retinoic acid on chick tail bud development. *Teratology* **43**: 217-224.

Gritsman, K., Zhang, J., Cheng, S., Heckscher, E., Talbot, W.S., and Schier, A.F. (1999). The EGF-CFC protein one-eye pinhead is essential for nodal signaling. *Cell* **97**: 121-132.

Grondona, J.M., Kastner, P., Gansmuller, A., Décimo, D., and Chambon, P. (1996). Retinal dysplasia and degeneration in *RARβ2/RARγ2* compound mutant mice. *Development* **122**: 2173-2188.

Gu, W., Malik, S., Ito, M., Yuan, C-X., Fondell, J.D., Zhang, X., Martinez, E., Qin, J., and Roeder, R.G. (1999). A novel human SRB/MED-containing cofactor complex, SMCC, involved in transcription regulation. *Mol. Cell* **3**: 97-108.

Gustafson, A.-L., Dencker, L., and Eriksson, U. (1993). Non-overlapping expression of CRBPI and CRABPI during pattern formation of limbs and craniofacial structures in the early mouse embryo. *Development* **117**: 451-460.

Harvey, R.P. (1996). Nk-2 homeobox gene and heart development. *Dev. Biol.* **178**: 203-216.

Harvey, R.P. (1998). Cardiac looping-an uneasy deal with laterality. *Semin. Cell Dev. Biol.* **9**: 101-108.

Haselbeck, R.J., Hoffmann, I., and Duester, G. (1999). Distinct functions for *Aldh1* and *Raldh2* in the control of ligand production for embryonic retinoid signaling pathways. *Dev. Genet.* **25**: 353-364.

Haub, O., and Goldfarb, M. (1991). Expression of fibroblast growth factor-5 gene in the mouse embryo. *Development* **112**: 397-406.

Hebert, J.M., Boyle, M., and Martin, G.R. (1991). mRNA localization studies suggest that murine FGF-5 plays a role in gastrulation. *Development* **112**: 407-415.

Heery, D.M., Kalkhoven, E., Hoare, S., and Parker, M.G. (1997). A signature motif in transcription co-activators mediates binding to nuclear receptors. *Nature* **387**: 733-736.

Heine, U. I., Roberts, A. B., Munoz, E. F., Roche, N. S., and Sporn, M. B. (1985). Effects of retinoid deficiency on the development of the heart and vascular system of the quail embryo. *Virchows Arch. B Cell Pathol. Incl. Mol. Pathol.* **50**, 135-152.

Heinzel, Y., Lavinsky, R.M., Mullen, T.M., Soderstrom, M., Laherty, C.D., Torchia, J., Yang, Y.M., Brard, G., Ngo, S.D., Davie, J.R., Seto, E., Eisenman, R.N., Rose, D.W., Glass, C.K., and Rosenfeld, M.G. (1997). A complex containing N-CoR, mSin3 and histone deacetylase mediates transcriptional repression. *Nature* **387**: 43-48.

Hendrickx, A.G., Silverman, S., Pellegrini, M., and Steffek, A.J. (1980). Teratological and radiocephalometric analysis of craniofacial malformations induced with retinoic acid in rhesus monkeys (*Macaca mulatta*). *Teratology* **22**: 13-22.

Herrmann, B.G., Labeit, S., Poustka, A., King, T.R., and Lehrach, H. (1990). Cloning of the *T* gene required in mesoderm formation in the mouse. *Nature* **343**: 617-622.

Herrmann, B.G. (1991). Expression pattern of the Brachyury gene in whole mount Twis/Twis mutant embryos. *Development* **113**: 913-917.

Heyman, R.A., Mangelsdorf, D.J., Dyck, J.A.., Stein, R.B., Eichele, G., Evans, R.M., and Thaller, C. (1992). 9-*cis* retinoic acid is a high affinity ligand for the retinoid X receptor. *Cell* **68**: 397-406.

Heyer, J., Escalante-Alcalde, D., Lia, M., Boettinger, E., Edelmann, W., Stewart, C.L., and Kucherlapati, R. (1999). Postgastrulation Smad2-deficient embryos show defects in embryo turning and anterior morphogenesis. *Proc. Natl. Acad. Sci. USA.* **96**: 12595-12600.

Hjalt, T. A., Semina, E. V., Amendt, B. A., and Murray, J. C. (2000). The Pitx2 protein in mouse development. *Dev. Dyn.* **218**, 195-200.

Hofmann, C., and Eichele, G. (1994). Retinoids in development. In *The Retinoids: Biology, Chemistry, and Medicine* (Sporn, M.B., Roberts, A.B., and Goodman, D.S., eds), 2nd Ed. Raven Press, New York.

Hogan, B., Beddington, R., Constantini, F., and Lacy, E. (1994). "Manipulating the Mouse Embryo. A Laboratory Manual.", 2nd Ed. Cold Spring Harbor Laboratory Press, New York.

Hogan, B., Thaller, C., and Eichele, G. (1992). Evidence that Hensen's node is a site of retinoic acid synthesis. *Nature* **359**: 237-241.

Hollemann, T., Chen, Y., Grunz, H., and Pieler, T. (1998). Regionalized metabolic activity establishes boundaries of retinoid signaling. *EMBO J.* **17**: 7361-7372.

Holowacz, T., and Sokol, S. (1999). FGF is required for posterior neural patterning but not neural induction. *Dev. Biol.* **205**: 296-308.

Horan, G.S., Wu, K., Wolgemuth, D.J., and Behringer, R.R. (1994). Homeotic transformation of cervical vertebrae in *Hoxa4* mutant mice. *Proc. Natl. Acad. Sci. USA* **91**: 12644-12648.

Horan, G.S.B., Nagy Kovács, E., Behringer, R.R., and Featherstone, M.S. (1995a). Mutations in paralogous Hox genes result in overlapping hometoic transformations of the axial skeleton: evidence for unique and redundant function. *Dev. Biol.* **169**: 359-372.

Horan, G.S., Ramirez-Solis, R., Featherstone, M.S., Wolgemuth, D.J., Bradley, A., Behringer, R.R. (1995b). Compound mutants for the paralogous *Hoxa-4*, *Hoxb-4*, and *Hoxd-4* genes show more complete homeotic transformations and a dose-dependent increase in the number of vertebrae transformed. *Genes Dev.* **9**: 1667-1677.

Hörlein, A.J., Naar, A.M., Heinzel, T., Torchia, J., Gloss, B., Kurokawa, R., Ryan, A., Kamei, Y., Soderstrom, M., Glass, C.K., and et al., (1995). Ligand-independent repression by the thyroid hormone receptor mediated by a nuclear receptor co-repressor. *Nature* **377**: 397-404.

Horton, C., Maden, M. (1995). Endogenous distribution of retinoids during normal development and teratogenesis in the mouse embryo. *Dev. Dyn.* **202**: 312-323.

Hu, X., and Lazar, M.A. (1999). The CoRNR motif controls the recruitment of corepressors by nuclear hormone receptors. *Nature* **402**: 93-96.

Huang, E.Y., Zhang, J., Miska, E.A., Guenther, M.G., Kouzarides, T., and Lazar, M.A. (2000). Nuclear receptor corepressors partner with class II histone deacetylases in a Sin3-independent repression pathway. *Genes Dev* **14**: 45-54.

Isaac, A., Sargent, M.G., and Cooke, J. (1997). Control of vertebrate left-right asymmetry by a snail-related zinc finger gene. *Science* **275**: 1301-1304.

Isaacs, H., Tannahill, D., and Slack, J. (1992). Expression of a novel FGF in the *Xenopus* embryo: a new candidate inducing factor for mesoderm formation and antero-posterior patterning. *Development* **114**: 711-720.

Izraeli, S., Lowe, L.A., Bertness, V.L., Good, D.J., Dorward, D.W., Kirsch, I.R., and Kuehn, M.R. (1999). The SIL gene is required for mouse embryonic axial development and left-right specification. *Nature* **399**: 691-694.

Jegalian, B.G., and DeRobertis, E.M. (1992). Homeotic transformations in the mouse induced by overexpression of a human *hox3.3* transgene. *Cell* **71**: 901-910.

Jouve, C., Palmeirim, I., Henrique, D., Beckers, J., Gossler, A., Ish-Horowicz, D., and Pourquié, O. (2000). Notch signaling is required for cyclicexpression of the hairy-like gene *HES1* in the presomitic mesoderm. *Development* **127**: 1421-1429.

Kamei, Y., Xu, L., Heinzel, T., Torchia, J., Kurokawa, R., Gloss, B., Lin, S.-C., Heyman, R.A., Rose, D.W., Glass, C.K., and Rosenfeld, M.G. (1996). A CBP integrator complex mediates transcriptional activation and AP-1 inhibition by nuclear receptors. *Cell* **85**: 403-414.

Kanki, J.P., and Ho, R.K. (1997). The development of the posterior body in zebrafish. *Development* **124**: 881-893.

Kapron-Bras, C.M. and Trasler, D.G. (1988a). Histological comparison of the effects of the splotch gene and retinoic acid on the closure of the mouse neural tube. *Teratology* **37**, 389-399.

Kapron-Bras, C.M. and Trasler, D.G. (1988b). Interaction between the splotch mutation and retinoic acid in mouse neural tube defects in vitro. *Teratology* **38**, 165-173.

Kao, H.Y., Downes, M., Ordentlich, P., and Evans, R.M. (2000). Isolation of a novel histone deacetylase reveals that class I and class II deacetylases promote SMRT-mediated repression. *Genes Dev.* **14**: 55-66.

Kastner, P., Grondona, J., Mark, M., Gansmuller, A., LeMeur, M., Decimo, D., Vonesch, J.L., Dolle, P., and Chambon, P. (1994). Genetic analysis of RXRα developmental function: convergence of RXR and RAR signaling pathways in heart and eye morphogenesis. *Cell* **78**: 987-1003.

Kastner, P., Mark, M., and Chambon, P. (1995). Nonsteroid nuclear receptors: what are the genetic studies telling us about their role in real life? *Cell* **83**: 859-869.

Kastner, P., Mark, M., Leid, M., Gansmuller, A., Chin, W., Grondona, J.M., Décimo, D., Krezel, W., Dierich, A., and Chambon, P. (1996). Abnormal spermatogenesis in RXRβ mutant mice. *Genes Dev.* **10**: 80-92.

Kastner, P., Mark, M., Ghyselinck, N., Krezel, W., Dupe, V., Grondona, J.M., and Chambon, P. (1997a). Genetic evidence that the retinoid signal is transduced by heterodimeric RXR/RAR functional units during mouse development. *Development* **124**: 313-326.

Kastner, P., Messaddeq, N., Mark, M., Wendling, O., Grondona, J.M., Ward, S., Ghyselinck, N., and Chambon, P. (1997b). Vitamin A deficiency and mutations of RXRα, RXRβ, and RARα lead to early differentiation of embryonic ventricular cardiomyocytes. *Development* **124**: 4749-4758.

Kaufman, S. and Bard, J.B.L. (1999). "The Anatomical Basis of Mouse Development". Academic Press, San Diego.

Kengaku, M., and Okamoto, H. (1995). bFGF as a possible morphogen for the anteroposterior axis of the central nervous system in *Xenopus*. *Development* **121**: 3121-3130.

Kessel, M. (1992). Respecification of vertebral identities by retinoic acid. *Development* **115**: 487-501.

Kessel, M., Balling, R., and Gruss, P. (1990). Variations of cervical vertebrae after expression of a *Hox1.1* (*A7*) transgene in mice. *Cell* **61**: 301-308.

Kessel, M. and Gruss, P. (1990). Murine developmental control genes. *Science* **249**: 374-379.

Kessel, M. and Gruss, P. (1991). Homeotic transformations of murine vertebrae and concomitant alteration of *Hox* codes induced by retinoic acid. *Cell* **67**: 89-104.

Kim, J., Lin, J.J., Xu, R.H. and Kung, H.F. (1998). Mesoderm induction by heterodimeric AP-1 (c-jun and c-fos) and its involvement in mesoderm formation through the embryonic fibroblast growth factor/xbra autocatalytic loop during the early development of xenopus embryos. *J. Biol. Chem.***273**, 1542-1550.

Kispert, A. and Herrmann, B.G. (1994). Immunohistochemical analysis of the brachyury protein in wild-type and mutant mouse embryos. *Dev. Biol.* **161**, 179-193.

Kitamura, K., Miura, H., Miyagawa-Tomita, S., Yanazawa, M., Katoh-Fukui, Y., Suzuki, R., Ohuchi, H., Suehiro, A., Motegi, Y., Nakahara, Y., Kondo, S., and Yokoyama, M. (1999). Mouse Pitx2 deficiency leads to anomalies of the ventral body wall, heart, extra- and petiocular mesoderm and right pulmonary isomerism. *Development* **126**, 5749-5758.

Kmita, M., van der Hoeven, F., Zákány, J., Krumlauf, R., and Duboule, D. (2000). Mechanisms of *Hox* gene colinearity: transposition of the anterior *Hoxb1* gene into the posterior *HoxD* complex. *Genes Dev.* **14**: 198-211.

Knittel, T., Kessel, M., Kim, M.H., and Gruss, P. (1995). A conserved enhancer of the human and murine *Hoxa7* gene specifies the anterior boundaries of expression during embryonal development. *Development* **121**: 1077-1088.

Knoepfler, P.S., and Kamps, M.P. (1997). The Pbx family of proteins is strongly upregulated by a post-transcriptional mechanism during retinoic acid-induced differentiation of P19 embryonal carcinoma cell. *Mech. Dev.* **63**: 5-14.

Kolm, P.J., Apekin, V., and Sive, H. (1997). *Xenopus* hindbrain patterning requires retinoid signaling. *Dev. Biol.* **192**: 1-16.

Kolm, P.J., and Sive, H. (1995). Regulation of the *Xenopus* labial homeodomain genes, HoxA1 and HoxD1: activation by retinoids and peptide growth factors. *Dev. Biol.* **167**: 34-49.

Kondo, T., and Duboule, D. (1999). Breaking colinearity in the mouse *HoxD* complex. *Cell* **97**: 407-417.

Korzus, E., Torchia, J., Rose, D.W., Xu, L., Kurokawa, R., McInerney, E.M., Mullen, T.M., Glass, C.K., and Rosenfeld, M.G. (1998). Transcription factor-specific requirements for coactivators and their acetyltransferase functions. *Science* **279**: 703-707.

Kostetskii, I., Jiang, Y., Kostetskaia, E., Yuan, S., Evans, T., and Zile, M. (1999). Retinoid signaling required for normal heart development regulates GATA- 4 in a pathway distinct from cardiomyocyte differentiation. *Dev. Biol.* **206**, 206-218.

Kostetskii, I., Yuan, S. Y., Kostetskaia, E., Linask, K. K., Blanchet, S., Seleiro, E., Michaille, J. J., Brickell, P., and Zile, M. (1998). Initial retinoid requirement for early avian development coincides with retinoid receptor coexpression in the precardiac fields and induction of normal cardiovascular development. *Dev. Dyn.* **213**, 188-198.

Kostic, D., and Capecchi, M. (1994). Targeted disruptions of the murine *Hoxa-4* and *Hoxa-6* genes result in homeotic transformations of components of the vertebral column. *Mech. Dev.* **46**: 231-247.

Krezel, W., Dupé, V., Mark, M., Dierich, A., Kastner, P., and Chambon, P. (1996). RXRγ null mice are apparently normal and compound RXRα$^{+/-}$/RXRβ$^{-/-}$/RXRγ$^{-/-}$ mutant mice are viable. *Proc. Natl. Acad. Sci. USA* **93**: 9010-9014.

Krumlauf, R. (1994). *Hox* genes in vertebrate development. *Cell* **78**: 191-201.

Kurokawa, R., DiRenzo, J., Boehm, M., Sugarman, J., Gloss, B., Rosenfeld, M.G., Heyman, R.A., and Glass, C.K. (1994). Regulation of retinoid signaling by receptor polarity and allosteric control of ligand binding. *Nature* **371**: 528-531.

Kurokawa, R., Söderström, M., Hörlein, A.J., Halachmi, S., Brown, M., Rosenfeld, M.G., and Glass, C.H. (1995). Polarity-specific activities of retinoic acid receptors determined by a co-repressor. *Nature* **377**: 451-454.

Kurokawa, R., Yu, V.C., Näär, A., Kyakumoto, S., Han, Z., Silverman, S., Rosenfeld, M.G., and Glass, C.K. (1993). Differential orientations of the DNA-binding domain and carboxy-terminal dimerization interface regulate binding site selection by nuclear receptor heterodimers. *Genes Dev.* **7**: 1423-1435.

Latinkic, B.V., Umbhauer, M., Neal, K.A., Lerchner, W., Smith, J.C. and Cunliffe, V. (1997). The *Xenopus brachyury* promoter is activated by fgf and low concentrations of activin and suppressed by high concentrations of activin and by paired-type homeodomain proteins. *Genes Dev.***11**, 3265-3276.

Lamb, T.M., and Harland, R.M. (1995). Fibroblast growth factor is a direct neural inducer, which combined with noggin generates anterior-posterior neural patterning. *Development* **121**: 3627-3636.

Lampron, C., Rochette-Egly, C., Gorry, P., Dollé, P., Mark, M., Lufkin, T., LeMeur, M., and Chambon, P. (1995). Mice deficient in cellular retinoic acid binding protein II (CRABPII). or in both CRABPI and CRABPII are essentially normal. *Development* **121**: 539-548.

Langston, A.W., and Gudas, L.J. (1992). Identification of a retinoic acid responsive enhancer 3' of the murine homeobox gene Hox1.6. *Mech. Dev.* **38**: 217-227.

Lawrence, P.A. (2001). Morphogens: how big is the big picture. *Nature Cell Biol.* **3**: E151-E154.

Lawson, K.A., Meneses, J.J., and Pedersen, R.A. (1991). Clonal analysis of epiblast fate during germ layer formation in the mouse embryo. *Development* **113**: 891-911.

Lee, H.-Y., Sueoka, N., Hong, W.-K., Mangelsdorf, D.J., Claret, F.X., and Kurie, J.M. (1999). All-*trans*-retinoic acid inhibits jun N-terminal kinase by increasing dual-specific phosphatase activity. *Mol. Cell Biol.* **19**: 1973-1980.

Lee, H.-Y., Walsh, G.L., Dawson, M., Hong, W.K., and Kurie, J.M. (1998). All-*trans*-retinoic acid inhibits jun N-terminal kinase dependent signaling pathways. *J. Biol. Chem.* **273**: 7066-7071.

Lee, J.W., Ryan, F., Swaffield, J.C., Johnston, S.A., and Moore, D.D. (1995). Interaction of thyroid-hormone receptor with a conserved transcriptional mediator. *Nature* **374**: 91-94.

Leid, M., Kastner, P., Lyons, R., Nakshatri, H., Saunders, M., Zacharewski, T., Chen, J.Y., Staub, A., Garnier, J.M., Mader, S., and Chambon, P. (1992). Purification, cloning and RXR identity of the HeLa cell factor with which RAR or TR heterodimerizes bind target sequences efficiently. *Cell* **68**: 377-395.

Levin, M., Johnson, R.L., Stern, C.D., Kuehn, M., and Tabin, C. (1995). A molecular pathway determining left-right asymmetry in chick embryogenesis. *Cell* **82**: 803-814.

Levin, M., Pagan, S., Roberts, D.J., Cooke, J., Kuehn, M.R., and Tabin, C.J. (1997). Left/right patterning signals and the independent regulation of different aspects of situs in the chick embryo. *Dev. Biol.* **189**: 27-67.

Li, E., Sucov, H.M., Lee, K.F., Evans, R.M., and Jaenisch, R. (1993). Normal development and growth of mice carrying a targeted disruption of the α1 retinoic acid receptor gene. *Proc. Natl. Acad. Sci. USA* **90**: 1590-1594.

Lin, C. R., Kioussi, C., O'Connell, S., Briata, P., Szeto, D., Liu, F., Izpisua-Belmonte, J. C., and Rosenfeld, M. G. (1999). Pitx2 regulates lung asymmetry, cardiac positioning and pituitary and tooth morphogenesis. *Nature* **401**, 279-282.

Liu, C., Liu, W., Lu, M. F., Brown, N. A., and Martin, J. F. (2001). Regulation of left-right asymmetry by thresholds of Pitx2c activity. *Development* **128**, 2039-2048.

Logan, M., Pagan-Westphal, S. M., Smith, D. M., Paganessi, L., and Tabin, C. J. (1998). The transcription factor Pitx2 mediates situs-specific morphogenesis in response to left-right asymmetric signals. *Cell* **94**, 307-317.

Lohnes, D., Dierich, A., Ghyselinck, N., Kastner, P., Lampron, C., LeMeur, M., Lufkin, T., Mendelsohn, C., Nakshatri, H., and Chambon, P. (1992). Retinoid receptors and binding proteins. *J. Cell Sci.* Suppl. **16**: 69-76.

Lohnes, D., Kastner, P., Dierich, A., Mark, M., LeMeur, M., and Chambon, P. (1993). Function of retinoic acid receptor γ in the mouse. *Cell* **73**: 643-658.

Lohnes, D., Mark, M., Mendelsohn, C., Dolle, P., Dierich, A., Gorry, P., Gansmuller, A., and Chambon, P. (1994). Function of the retinoic acid receptors (RARs) during development (I). Craniofacial and skeletal abnormalities in RAR double mutants. *Development* **120**: 2723-2748.

Lohr, J.L., Danos, M.C., and Yost, J.H. (1997). Left-right asymmetry of a nodal-related gene is regulated by dorsoanterior midline structures during *Xenopus* development. *Development* **124**: 1467-1472.

Loudig, O., Babichuk, C., White, J., Abu-Abed, S., Mueller, C., and Petkovich, M. (2000). Cytochrome P450RAI (CYP26). promoter: a distinct composite retinoic acid response element underlies the complex regulation of retinoic acid metabolism. *Mol. Endocrinol.* **14**: 1483-1497.

Lowe, L.A., Supp, D.M., Sampath, K., Yokoyama, T., Wright, C.V.E., Potter, S.S., Overbeek, P., and Kuehn, M.R. (1996). Conserved left-right of nodal expression and alterations in murine *situs inversus*. *Nature* **381**: 158-161.

Lowe, L.A., Yamada, S., and Kuehn, M.R. (2001). Genetic dissection of *nodal* function in patterning the mouse embryo. *Development* **128**: 1831-1843.

Lu, M. F., Pressman, C., Dyer, R., Johnson, R. L., and Martin, J. F. (1999). Function of Rieger syndrome gene in left-right asymmetry and craniofacial development. *Nature* **401**, 276-278.

Lufkin, T., Lohnes, D., Mark, M., Dierich, A., Gorry, P., Gaub, M.P., LeMeur, M., and Chambon, P. (1993). High postnatal lethality and testis degeneration in retinoic acid receptor α □mutant mice. *Proc. Natl. Acad. Sci. USA* **90**: 7225-7229.

Lufkin, T., Mark, M., Hart, C.P., Dollé, P., LeMeur, M., and Chambon, P. (1992). Homeotic transformations of the occipital bones of the skull by ectopic expression of a homeobox gene. *Nature* **359**: 835-841.

Luo, J., Pasceri, P., Conlon, R.A., Rossant, J., and Giguère, V. (1995). Mice lacking all isoforms of retinoic acid receptor β develop normally and are susceptible to the teratogenic effects of retinoic acid. *Mech. Dev.* **53**: 61-71.

McCaffery, P., and Dräger, U.C. (1994). Hot spots of retinoic acid synthesis in the developing spinal cord. *Proc. Natl. Acad. Sci. USA.* **91**: 7194-7197.

MacLean, G., Abu-Abed, S., Dollé, P., Tahayato, A., Chambon, P., and Petkovich, M. (2001). Cloning of a novel retinoic-acid metabolizing cytochrome P450, *Cyp26B1*, and comparative expression analysis with *Cyp26A1* during early murine development. *Mech. Dev.* **107**: 195-201.

Maconochie, M.K., Nonchev, S., Studer, M., Chan, S.K., Popperl, H., Sham, M.H., Mann, R.S., and Krumlauf, R. (1997). Cross-regulation in the mouse Hoxb complex: the expression of Hoxb2 in rhombomere 4 is regulated by Hoxb1. *Genes Dev.* **18**: 1885-1895.

Maden, M., Gale, E., Kostetskii, I., and Zile, M. (1996). Vitamin A-deficient quail embryos have half a hindbrain and other neural defects. *Curr. Biol.* **6**: 417-426.

Maden, M., Graham, A., Zile, M., and Gale, E. (2000). Abnormalities of somite development in the absence of retinoic acid. *Int. J. Dev. Biol.* **44**: 151-159.

Maden, M., Sonneveld, E., van der Saag, P.T., and Gale, E. (1998). The distribution of endogenous retinoic acid in the chick embryo: implications for developmental mechanisms. *Development* **125**: 4133-4144.

Mader, S., Chen, J-Y., Chen, Z., White, J., Chambon, P., and Gronemeyer, H. (1993a). The patterns of binding of RAR, RXR, and TR homodimers and heterodimers to direct repeats are dictated by the binding specificities of the DNA binding domains. *EMBO J.* **12**: 5029-5041.

Mader, S., Leroy, P., Chen, J-Y., and Chambon, P. (1993b). Multiple parameters control the selectivity of nuclear receptors for their response elements: selectivity and promiscuity in response element recognition by retinoic acid receptors and retinoid x receptors. *J. Biol. Chem.* **268**: 591-600.

Majumder, K., and Overbeek, P.A. (1999). Left-right asymmetry and cardiac looping. In "Heart Development", R.P. Harvey and N. Rosenthal, Eds. Academic Press, San Diego. Pp 391-402.

Manasek, F.J., Burnside, M.B., and Waterman, R.E. (1972). Myocardial cell shape as a mechanism of embryonic heart looping. *Dev. Biol.* **29**: 349-371.

Mangelsdorf, D.J., Borgmeyer, U., Heyman, R.A., Zhou, J.Y., Ong, E.S., Oro, A.E., Kakizuka, A., and Evens, R.M. (1992). Characterization of the three RXR genes that mediate the action of 9-*cis* retinoic acid. *Genes Dev.* **6**: 329-344.

Mangelsdorf, D.J., and Evans, R.M. (1995). The RXR heterodimers and orphan receptors. *Cell* **83**: 841-850.

Mangelsdorf, D.J., Ong, E.S., Dyck, J.A., and Evans, R.M. (1990). Nuclear receptor that identifies a novel retinoic acid response pathway. *Nature* **345**: 224-229.

Mangelsdorf, D.J., Thummel, C., Beato, M., Herrlich, P., Schütz, G., Umesono, K., Blumberg, B., Kastner, P., Mark, M., Chambon, P., and Evans, R.M. (1995). The nuclear receptor superfamily: the second decade. *Cell* **83**: 835-839.

Mangelsdorf, D.J., Umesono, K., and Evans, R.M. (1994). The retinoid receptors. In *The Retinoids: Biology, Chemistry, and Medicine* (Sporn, M.B., Roberst, A.B., and Goodman, D.S., eds), 2nd Ed.. Raven Press, New York.

Mangelsdorf, D.J., Umesono, K., Kliewer, S.A., Borgmeyer, U., Ong, E.S., and Evans, R.M. (1991). A direct repeat in the cellular retinol-binding protein type II gene confers differential regulation by RXR and RAR. *Cell* **66**: 555-561.

Manley, N.R., and Capecchi, M.R. (1997). Hox group 3 paralogous genes act synergistically in the formation of somitic and neural crest-derived structures. *Dev. Biol.* **192**: 274-288.

Mann, R.S., and Chan, S.K. (1996). Extra specificity from extradenticle: the partnership between HOX and PBX/EXD homeodomain proteins. *Trends Genet.* **12**: 258-262.

Manner, J. (2000). Cardiac looping in the chick embryo: a morphological review with special reference to terminological and biomechanical aspects of the looping process. *Anat. Rec.* **259**, 248-262.

Manzanares, M., Bel-Vialar, S., Ariza-McNaughton, L., Ferretti, E., Marshall, H., Maconochie, M.M., Blasi, F., and Krumlauf, R. (2001). Independent regulation and maintenance phases of *Hoxa3* expression in the vertebrate hindbrain involve auto- and cross-regulatory mechanisms. *Development* **128**: 3595-3607.

Marmorstein, R. (2001). Protein modules that manipulate histone tails for chromatin regulation. *Nat. Rev. Mol. Cell Biol.* **2**: 422-432.

Marshall, H., Nonchev, S., Sham, M.H., Muchamore, I., Lumsden A., and Krumlauf, R. (1992). Retinoic acid alters hindbrain *Hox* code and induces transformation of rhombomeres 2/3 into a 4/5 identity. *Nature* **370**: 567-571.

Marshall, H., Studer, M., Pöpperl, H., Aparicio, S., Kuroiwa, A., Brenner, S., and Krumlauf, R. (1994). A conserved retinoic acid response element required for early expression of the homeobox gene *Hoxb1*. *Nature* **370**: 567-571.

Marszalek, J.R., Ruiz-Lozano, P., Roberts, E., Chien, K., and Goldstein, L.S.B. (1999). *Situs inversus* and embryonic ciliary morphogenesis defects in mouse mutants lacking the KIF3A subunit of kinesin II. *Proc. Natl. Acad. Sci. USA* **96**: 5043-5048.

Marvin, M.J., DiRocco, G., Gardiner, A., Bush, S.M., and Lassar, A.B. (2001). Inhibition of Wnt activity induces heart formation from posterior mesoderm. *Genes Dev.* **15**: 316-327.

McMahon, A.P. (2000). More surprises in the hedgehog signaling pathway. *Cell* **100**: 185-188.

McCaffery, P., Wagner, E., O'Neil, J., Petkovich, M., and Dräger, U.C. (1999). Dorsal and ventral retinal terrirories defined by retinoic acid synthesis, break-down and nuclear receptor expression. *Mech. Dev.* **82**: 119-130.

McGinnis, W., and Krumlauf, R. (1992). Homeobox genes and axial patterning. *Cell* **68**: 283-302.

Means, A.L., and Gudas, L.J. (1995). The roles of retinoids in vertebrate development *Ann. Rev. Biochem.* **64**: 201-233.

Mendelsohn, C., Batourina, E., Fung, S., Gilbert, T., and Dodd, J. (1999). Stromal cells mediate retinoid-dependent functions essential for renal development. *Development* **126**: 1139-1148.

Mendelsohn, C., Lohnes, D., Decimo, D., Lufkin, T., LeMeur, M., Chambon, P., and Mark, M. (1994a). Function of the retinoic acid receptors (RARs) during development. (II). Multiple abnormalities at various stages of organogenesis in RAR double mutants. *Development* **120**: 2749-2771.

Mendelsohn, C., Mark, M., Dolle, P., Dierich, A., Gaub, M.-P., Krust, A., Lampron, C., and Chambon, P. (1994b). Retinoic acid receptor β2 (RARβ2) null mutant mice appear normal. *Dev. Biol.* **166**: 246-258.

Mendelsohn, C., Ruberte, E., LeMeur, M., Morriss-Kay, G., and Chambon, P. (1991). Developmental analysis of the retinoic acid-inducible RAR-β2 promoter in transgenic animals. *Development* **113**: 723-734.

Meno, C., Gritsman, K., Ohishi, S., Ohfuji, Y., Heckscher, E., Mochida, K., Shimono, A., Konodoh, H., Talbot, W.S., Robertson, E.J., Schier, A.F., and Hamada, H. (1999). Mouse lefty2 and zebrafish antivin are feedback inhibitors of nodal signaling during vertebrate gastrulation. *Mol. Cell.* **4**: 297-298.

Meno,C., Ito, Y., Saijoh, Y., Matsuda, Y., Tashiro, K., Kuhara, S., and Hamada, H. (1997). Two closely-related left-right asymmetrically expressed genes, lefty-1 and lefty-2: their distinct expression domains, chromosomal linkage and direct neuralizing activity in *Xenopus* embryos. *Genes Cells* **2**: 513-524.

Meno, C., Saijoh, Y., Fujii, H., Ikeda, M., Yokoyama, T., Yokoyama, M., Toyoda, Y., and Hamada, H. (1996). Left-right asymmetric expression of the TGFβ-family member *lefty* in mouse embryos. *Nature* **381**: 151-155.

Meno, C., Shimono, A., Saijoh, Y., Yashiro, K., Mochida, K., Sachiko, O., Noji, S., Kondoh, H., and Hamada, H. (1998). *Lefty-1* is required forleft-right determination as a regulator of *lefty-2* and *nodal. Cell* **94**: 287-297.

Meyer, B.I., and Gruss, P. (1993) Mouse Cdx-1 expression during gastrulation. *Development* **117**: 191-203.

Meyers, E.N., and Martin, G.R. (1999). Differences in left-right axis pathways in mouse and chick: functions of FGF8 and SHH. *Science* **285**: 403-406.

Minucci, S., Leid, M., Toyama, R., Saint-Jeannet, J-P., Peterson, V.J., Horn, V., Ishmael, J.E., Bhattacharyya, N., Dey, A., Dawid, I.B., and Ozato, K. (1997). Retinoid x receptor (RXR) within the RXR-Retinoic Acid Receptor binds its ligand and enhances retinoid-dependent gene expression. *Mol. Cell. Biol.* **17**: 644-655.

Miura, S., Miyagawa, S., Morishima, M., Ando, M., and Takao, A. (1990). Retinoic acid-induced visceroatrial heterotaxy syndrome in rat embryos. In "Developmental cardiology: morphogenesis and function", D.B. Clark and A. Takao, Eds. Futura, Mount Kisco, New York. Pp 467-484.

Mochizuki, T., Saijoh, Y., Tsuchiya, K., Shirayoshi, Y., Takai, S., Taya, C., Yonekawa, H., Yamada, H., Yamada, K., Nihei, H., Nakatsuji, N., Overbeek, P.A., Hamada, H., and Yokoyama, T. (1998). Cloning of *inv,* a gene that controls left/right asymmetry and kidney development. *Nature* **395**: 177-181.

Moroni, M.C., Vigano, M.A., Mavilio, F. (1993). Regulation of the human HOXD4 gene by retinoids. *Mech. Dev.* **44**: 139-154.

Morrison, A., Moroni, C.M., Ariza-McNaughton, L., Krumlauf, R., and Mavillio, F. (1996). In vitro and transgenic analysis of a human HOXD4 retinoid-responsive enhancer. *Development* **122**: 1895-1907.

Morrison, A., Ariza-McNaughton, L., Gould, A., Featherstone, M., and Krumlauf, R. (1997). HOXD4 and regulation of the group 4 paralog genes. *Development* **124**: 3135-3146.

Morriss-Kay, G. (1993). Retinoic acid and craniofacial development: molecules and morphogenesis. *Bioessays* **15**: 9-15.

Morriss-Kay, G., Ward, S. and Sokolova, N. (1994). The role of retinoids in normal development and retinoid-induced malformations. *Arch. Toxicol.* (Supp) **16**:112-117.

Morriss-Kay, G.M., Murphy, P., Hill, R.E., and Davidson, D.R. (1991). Effects of retinoic acid excess on expression of Hox2.9 and Krox-20 and on morphological segmentation in the hindbrain of mouse embryos. *EMBO J.* **10**: 2985-2995.

Moss, J.B., Xavier-Neto, J., Shapiro, M.D., Nayeem, S.M., McCaffery, P., Drager, U.C., and Rosenthal, N. (1998). Dynamic patterns of retinoic acid synthesis and response in the developing mammalian heart. *Dev. Biol.* **199**: 55-71.

Nagpal, S., Frinat, S., Nakshatri, H., and Chambon, P. (1993). RARs and RXRs: evidence for two autonomous transactivation functions (AF-1 and AF-2) and heterodimerization *in vivo*. *EMBO J.* **12**: 2349-2360.

Nagpal, S., Saunders, M., Kastner, P., Durand, B., Nakshatri, H., and Chambon, P. (1992). Promoter context- and response element-dependent specificity of the transcriptional activation and modulating functions of retinoic acid receptors. *Cell* **70**: 1007-1019.

Nagy, L., Kao, H.Y., Chakravarti, D., Lin, R.J., Hassig, C.A., Ayer, D.E., Schreiber, S.L., and Evans, R.M. (1997). Nuclear receptor repression mediated by a complex containing SMRT, mSin3A, and histone deacetylase. *Cell* **89**: 373-380.

Napoli, J.L. (1999). Interactions of retinoid binding proteins and enzymes in retinoid metabolism. *Biochim. Biophys. Acta* **1440**: 139-162.

Napoli, J.L. (2000). A gene knockout corroborates the integral function of cellular retinol-binding protein in retinoid metabolism. *Nutr. Rev.* **58**: 230-241.

Niederreither, K., McCaffery, P., Dräger, U.C., Chambon, P., and Dollé, P. (1997). Restricted expression and retinoic acid-induced downregulation of the retinaldehyde dehydrogenase type 2 (RALDH-2) gene during mouse development. *Mech. Dev.* **62**: 67-78.

Niederreither, K., Subbarayan, V., Dollé, P., and Chambon, P. (1999). Embryonic retinoic acid synthesis is essential for early mouse post-implantation development. *Nature Genet.* **21**: 444-448.

Niederreither, K., Vermot, J., Schuhbaur, B., Chambon, P., and Dollé, P. (2000). Retinoic acid synthesis and hindbrain patterning in the mouse embryo. *Development* **127**: 75-85.

Niederreither, K., Vermot, J., Messaddeq, N., Schuhbaur, B., Chambon, P., and Dolle, P. (2001). Embryonic retinoic acid synthesis is essential for heart morphogenesis in the mouse. *Development* **128**, 1019-1031.

Nieuwkoop, P.D. (1952). Activation and organization of the central nervous system in amphibians. Part I: induction and activation. *J. Exp. Zool.* **120**: 1-31.

Nieuwkoop, P.D., and Nigtevecht, G.V. (1954). Neural induction and transformation in explants of competent ectoderm under the influence of fragments of anterior notochord in Urodeles. *J. Embryol. Exp. Morph.* **2**: 175-193.

Niswander, L., and Martin, G.R. (1992). Fgf-4 expression during gastrulation, myogenesis, limb and tooth development in the mouse. *Development* **114**: 755-768.

Nonaka, S., Tanaka, Y., Okada, Y., Takeda, S.,Harada, A., Kanai, Y., Kido, M., and Hirokawa, N. (1998). Randomization of left-right asymmetry due to loss of nodal cilia generating leftward flow of extraembryonic fluid in mice lacking KIF3A motor protein. *Cell* **95**: 829-837.

Nonchev, S., Manconochie, M., Gould, A., Morrison, A., and Krumlauf, R. (1997). Cross-regulatory interactions between hox genes and the control of segmental expression in the vertebrate central nervous system. *Cold Spring Harb. Symp. Quant. Biol.* **62**: 313-323.

Norris, D.P., and Robertson, E.J. (1999). Asymmetric and node-specific *nodal* expression patterns are controlled by two distinct *cis*-acting regulatory elements. *Genes Dev.* **13**: 1575-1588.

Noy, N. (2000). Retinoid-binding proteins: mediators of retinoid action. *Biochem. J.* **348**: 481-495.

Ogryzko, V.V., Kotani, T., Zhang, X., Schiltz, R.L., Howard, T., Yang, X-J., Howard, B.H., Qin, J., and Nakatani, Y. (1998). Histone-like TAFs within the PCAF histone acetylase complex. *Cell* **94**: 35-44.

Ogryzko, V.V., Schlitz, R.L., Russanova, V., Howard, B.H., and Nakatani, Y. (1996). The transcriptional coactivators p300 and CBP are histone acetyltransferases. *Cell* **87**: 953-959.

Ogura, T., and Evans, R.M. (1995). A retinoic acid-triggered cascade of *HOXB1* gene activation. *Proc. Natl. Acad. Sci. USA* **92**: 387-391.

Oh, S.P., and Li, E. (1997). The signaling pathway mediated by the type IIB activin receptor controls axial patterning and lateral asymmetry in the mouse. *Genes. Dev.* **11**: 1812-1826.

Okada, Y., Nonka, S., Saijoh, Y., Hamada, H., and Hirokawa, N. (1999). Abnormal nodal flow precedes situs inversus in *in* and *inv* mice. *Mol. Cell.* **4**: 459-468.

Ong, D.E., MacDonald, P.N., Gubitosi, A.M. (1988). Esterification of retinol in rat liver: possible participation by cellular retinol-binding protein and cellular retinol binding-protein II. *J. Biol. Chem.* **263**: 5789-5796.

Oro, A.E., McKeown, M., and Evans, R.M. (1990). Relationship between the product of the *Drosophila ultraspiracle* locus and the vertebrate retinoid x receptor. *Nature* **347**: 298-301.

Orr-Urtreger, A., Givol, D., Yayo, A., Yarden, Y., and Lonai, P. (1991). Developmental expression of two murine fibroblast growth factors, flg and bek. *Development* **113**: 1419-1434.

Oulad-Abdelghani, M., Chazaud, C., Bouillet, P., Mattei, M.G., Dollé, P., and Chambon, P. (1998). Stra13/lefty, a retinoic acid-inducible novel member of the transforming growth factor-beta superfamily. *Int. J. Dev. Biol.* **42**: 23-32.

Oulad-Abdelghani, M., Chazaud, C., Bouillet, P., Sapin, V., Chambon, P., and Dolle, P. (1997) *Meis2*, A novel mouse Pbx-related homeobox gene induced by retinoic acid during differentiation of P19 embryonal carcinoma cells. *Dev. Dyn.* **210**: 173-183.

Pabst, O., Schneider, A., Brand, T., and Arnold, H.H. (1997). The mouse *nkx2-3* homeodomain gene is expressed in gut mesenchyme during pre- and postnatal mouse development. *Dev. Dyn.* **209**: 29-35.

Packer, A.I., Crotty, D.A., Elwell, V.A., and Wolgemuth, D.J. (1998). Expression of the murine *Hoxa4* gene requires both autoregulation and a conserved retinoic acid response element. *Development* **125**: 1991-1998.

Pagan-Westphal, S.M., and Tabin, C.J. (1998). The transfer of left-right positional information during chick embryogenesis. *Cell* **93**: 25-35.

Palmeirim, I., Enrique, D., Ish-Horowicz, D., and Pourquié, O. (1997). Avian hairy gene expression identifies a molecular clock linked to vertebrate segmentation and somitogenesis. *Cell* **91**: 639-648.

Papalopulu, N., and Kintner, C. (1996). A posteriorising factor, retinoic acid, reveals that anteroposterior patterning controls the timing of neuronal differentiation in *Xenopus* neuroectoderm. *Development* **122**: 3409-3418.

Patel, K., Isaac, A., and Cooke, J. (1999). Nodal signaling and the roles of the transcription factors SnR and Pitx2 in vertebrate left-right asymmetry. *Curr. Biol.* **9**: 609-612.

Perez-Castro, A.V., Toth-Rogler, L.E., Wei, L., Nguyen-Huu, M.C. (1989). Spatial and temporal pattern of expression of the cellular retinoic acid-binding protein and the cellular retinol-binding protein during mouse embryogenesis. *Proc. Natl. Acad. Sci. USA* **86**: 8813-8817.

Perissi, V., Staszewski, L.M., McInerney, E.M., Kurokawa, R., Krones, A., Rose, D.W., Lambert, M.H., Milturn, M.V., Glass, C.K., and Rosenfeld, M.G. (1999). Molecular determinants of nuclear receptor-corepressor interaction. *Genes Dev.* **13**: 3198-3208.

Perlmann, T., Rangarajan, P.N., Umesono, K., and Evans, R.M. (1993). Determinants for selective RAR and TR recognition of direct repeat HREs. *Genes Dev.* **7**: 1411-1422.

Petkovich, M., Brand, N.J., Krust, A., and Chambon, P. (1987). A human retinoic acid receptor which belongs to the family of nuclear receptors. *Nature* **330**: 444-450.

Piedra, M. E., Icardo, J. M., Albajar, M., Rodriguez-Rey, J. C., and Ros, M. A. (1998). Pitx2 participates in the late phase of the pathway controlling left- right asymmetry. *Cell* **94**, 319-324.

Pollock, R.A., Jay, G., and Bieberich, C.J. (1992). Altering the boundaries of *hox3.1* expression: evidence for antipodal gene regulation. *Cell* **71**: 911-923.

Pöpperl, H., Bienz, M., Studer, M., Chan, S.K., Aparicio, S., Brenner, S., Mann, R.S., and Krumlauf, R. (1995). Segmental expression of Hoxb-1 is controlled by a highly conserved autoregulatory loop dependent upon exd/pbx. *Cell* **81**: 1031-1042.

Pöpperl, H., and Featherstone, M. (1992). An autoregulatory element of the murine Hox4.2 gene. *EMBO J.* **11**: 3673-3680.

Pöpperl, H., and Featherstone, M.S. (1993). Identification of a retinoic acid response element upstream of the murine Hox-4.2 gene. *Mol. Cell. Biol.* **13**: 257-265.

Pourquié, O. (2000). Segmentation of the paraxial mesoderm and vertebrate somitogenesis. *Curr. Top. Develop. Biol.* **47**: 81-105.

Pownall, M.E., Tucker, A.S., Slack, J.M.W., and Isaacs, H.V. (1996). *eFGF*, *Xcad3* and *Hox* genes form a molecular pathway that establishes the anteroposterior axis in *Xenopus*. *Development* **122**: 3881-3892.

Quadro, L., Blaner, W.S., Salchow, D.J., Vogel, S., Piantedosi, R., Gouras, P., Freeman, S., Cosma, M.P., Colantuoni, V., and Gottesman, M.E. (1999). Impaired retinal function and vitamin A availability in mice lacking retinol-binding protein. *EMBO J.* **18:** 4633-4644.

Rachez, C., Suldan, Z., Ward, J., Chang, C.P., Burakov, D., Erdjument-Bromage, H., Tempst, P., and Freedman, L.P. (1998). A novel protein complex that interacts with the vitamin D3 receptor in a ligand-dependent manner and enhances VDR transactivation in a cell-free system. *Genes Dev.* **12**: 1787-1800.

Ramírez-Solis, R., Zheng, H., Whiting, J., Krumlauf, R., and Bradley, A. (1993). Hoxb-4 (Hox2.6). mutant mice show homeotic transformation of a cervical vertebra and defects in the closure of the sternal rudiments. *Cell* **73**: 279-294.

Rancourt, D.E., Tsuzuki, T., and Capecchi, M.R. (1995). Genetic interaction between *hoxb-5* and *hoxb-6* is revealed by nonallelic noncomplementation. *Genes Dev.* **9**: 108-122.

Rao, Y. (1994). Conversion of a mesodermalizing molecule, the xenopus brachyury gene, into a neuralizing factor. *Genes Dev.* **8**, 939-947.

Rashbass, P., Wilson, V., Rosen, B. and Beddington, R.S. (1994). Alterations in gene expression during mesoderm formation and axial patterning in brachyury (t) embryos. *Int. J. Dev. Biol.* **38**, 35-44.

Rastinejad, F., Perlmann, T., Evans, R.M., and Sigler, P.B. (1995). Structural determinants of nuclear receptor assembly on DNA direct repeats. *Nature* **375**: 203-211.

Ray, W.J., Bain, G., Yao, M., and Gottlieb, D.I. (1997). CYP26, a novel mammalian cytochrome P-450, is incuded by retinoic acid and defines a new family. *J. Biol. Chem.* **272**: 18702-18708.

Rebagliati, M.R., Toyama, R., Fricke, C., Haffter, P., and Dawid, I.B. (1998). Zebrafish nodal-related genes are implicated in axial patterning and establishing left-right axis asymmetry. *Dev. Biol.* **199**: 261-272.

Redkar, A., Montgomery, M., and Litvin, J. (2001). Fate map of the early avian cardiac progenitor cells. *Development* **128**: 2269-2279.

Renaud, J-P., Rochel, N., Ruff, M., Vivat, V., Chambon, P., Gronemeyer, H., and Moras, D. (1995). Crystal structure of the RAR-γ ligand-binding domain bound to all-*trans* retinoic acid. *Nature* **378**: 681-689.

Riddle, R.D., Johnson, R.L., Laufer, E., and Tabin, C. (1993). Sonic hedgehog mediates the polarizing activity of the ZPA. *Cell* **75**: 1401-1416.

Rochette-Egly, C., Adam, S., Rossignol, M., Egly, J.M., and Chambon, P. (1997). Stimulation of RARα □activation function AF-1 through binding to the general transcription factor TFIIH and phosphorylation by CDK7. *Cell* **90**: 97-107.

Rodriguez-Esteban, C., Capdevila, J., Economides, A.N., Pascula, J., Ortiz, A., and Izpisua-Belmonte, J.C. (1999). The novel Cer-like protein Caronte mediates the establishment of embryonic left-right asymmetry. *Nature* **401**: 243-251.

Rodriguez-Leon, J., Merino, R., Macias, R., Ganan, Y., Santesteban, E., and Hurle, J.M. (1999). Retinoic acid regulates programmed cell death through BMP signaling. *Nat. Cell Biol.* **1**: 125-126.

Roelink, H. and Nusse, R. (1991). Expression of two members of the wnt family during mouse development--restricted temporal and spatial patterns in the developing neural tube. *Genes Dev.* **5**, 381-388.

Romert, A., Tuvendal, P., Simon, A., Dencker, L., and Eriksson, U. (1998). The identification ofa 9-cis retinol dehydrogenase in the mouse reveals a pathway for synthesis of 9-cis retinoic acid. *Proc. Natl. Acad. Sci. USA* **95**: 4404-4409.

Rosen, E.D., Beninghof, E.G., and Koenig, R.J. (1993). Dimerization interfaces of thyroid hormone, retinoic acid, vitamin D, and retinoid X receptors. *J. Biol. Chem.***268**: 11534-11541.

Ross, S.A., McCaffery, P.J., Drager, U.C., and De Luca, L.M. (2000). Retinoids in Embryonal Development. *Physiol. Rev.* **80**: 1021-54.

Rossant, J., Zirngibl, R., Cado, D., Shago, M., and Giguère, V. (1991). Expression of a retinoic acid response element-hsplacZ transgene defines specific domains of transcriptional activity during mouse embryogenesis. *Genes Dev.* **5**: 1333-1344.

Ruberte, E., Dolle, P., Chambon, P., and Morriss-Kay, G. (1991). Retinoic acid receptors and cellular retinoid binding proteins II. Their differential pattern of transcription during early morphogenesis in mouse embryos. *Development* **111**: 45-60.

Ruberte, E., Dolle, P., Krust, A., Zelent, A., Morriss-Kay, G., Chambon, P. (1990). Specific spatial and temporal distribution of retinoic acid receptor gamma transcripts during mouse embryogenesis. *Development* **108**: 213-222.

Ruberte, E., Friederich, V., Chambon, P., and Morris-Kay, G. (1993). Retinoic acid receptors and cellular retinoid binding proteins III. Their differential pattern of transcription during mouse nervous system development. *Development* **118**: 267-282.

Ruiz i Altaba, A., and Jessell, T. (1991a). Retinoic acid modifies the pattern of cell differentiation of the central nervous system of the neurula stage *Xenopus laevis* embryos. *Development* **112**: 945-958.

Ruiz i Altaba, A., and Jessell, T. (1991b). Retnoic acid modifies mesodermal patterning in early *Xenopus* embryos. *Genes Dev.* **5**: 175-187.

Ryan, A. K., Blumberg, B., Rodriguez-Esteban, C., Yonei-Tamura, S., Tamura, K., Tsukui, T., de la, P. J., Sabbagh, W., Greenwald, J., Choe, S., Norris, D. P., Robertson, E. J., Evans, R. M., Rosenfeld, M. G., and Izpisua Belmonte, J. C. (1998). Pitx2 determines left-right asymmetry of internal organs in vertebrates. *Nature* **394**, 545-551.

Sadler, T.W. (2000). " Langman's Medical Embryology.", 8th Ed. Lippincott, Williams, and Wilkins, Philadelphia.

Saegusa, H., Takahashi, N., Noguchi, S., and Suemori, H. (1996). Targeted disruption in the mouse *Hoxc-4* locus results in axial skeleton homeosis and malformation of the xiphoid process. *Dev. Biol.* **174**: 55-64.

Saijoh, Y., Adachi, H., Mochida, K., Ohishi, S., Hirao, A., and Hamada, H. (1999). Distinct transcriptional regulatory mechanisms underlie left-right asymmetric expression of *lefty-1* and *lefty-2*. *Genes Dev.* **13**; 259-269.

Saitou, M., Narumiya, S., and Kakizuka, A. (1994). Alteration of a single amino acid residue in retinoic acid receptor causes dominant-negative phenotype. *J. Biol. Chem.* **269**, 19101-19107.

Saitou, M., Sugai, S., Tanaka, T., Shimouchi, K., Fuchs, E., Narumiya, S., and Kakizuka, A. (1995). Inhibition of skin development by targeted expression of a dominant- negative retinoic acid receptor. *Nature* **374**, 159-162.

Sakai, Y., Meno, C., Fujii, H., Nishino, J., Shiratori, H., Yukio, S., Rossant, J., and Hamada, H. (2001). The retinoic acid-inactivating enzyme CYP26 is essential for establishing an uneven distribution of retinoic acid along the anterio-posterior axis within the mouse embryo. *Genes Dev.* **15**: 213-225.

Sampath, K., Cheng, A.M.S., Frisch, A., and Wright, C.V.E. (1997). Functional differences among *Xenopus* nodal-related genes in left-right axis determination. *Development* **124**: 3293-3302.

Sampath, K., Rubenstein, A.L., Cheng, A.M., Liang, J.O., Fekany, K., Solnica-Krezel, L., Korzh, V., Halpern, M.E., and Wright, C.V. (1998). Induction of the zebrafish ventral brain and floorplate requires Cyclops/nodal signaling. *Nature* **395**: 185-189.

Schlange, T., Schnipkoweit, I., Andrée, B., Ebert, A., Zile, M.H., Arnold, H.-H., and Brand, T. (2001). Chick CFC controls lefty1 expression in the embryonic midline and nodal expression in the lateral plate. *Dev. Biol.* **234**: 376-389.

Schneider, A., Mijalski, T., Sclange, T., Dai, W., Overbeek, P., Arnold, H.H., and Brand, T. (1999). The homeobox gene NKX3.2 is a target of left-right signaling and is expressed on opposite sides in chick and mouse embryos. *Curr. Biol.* **9**: 911-914.

Schneider, V.A., and Mercola, M. (2001). Wnt antagonism initiates cardiogenesis in *Xenopus laevis*. *Genes Dev.* **15**: 304-315.

Schultheiss, T.M., Burch, J.B.E., and Lassar, A.B. (1997). A role for bone morphogenetic proteins in the induction of cardiac myogenesis. *Genes Dev.* **11**: 451-462.

Schultheiss, T.M., and Lassar, A.B. (1999). Vertebrate heart induction. In "Heart Development", R.P. Harvey and N. Rosenthal, Eds. Academic Press, San Diego. Pp 52-62.

Schultheiss, T.M., Xydas, S., and Lassar, A.B. (1995). Induction of avian cardiac myogenesis by anterior endoderm. *Development* **121**: 4203-4214.

Schwabe, J.W.R., Chapman, L., Finch, J.T., and Rhodes, D. (1993). The crystal structure of the estrogen receptor DNA-binding domain bound to DNA: how receptors discriminate between their response elements. *Cell* **75**: 567-578.

Sefton, M., Sanchez, S., and Nieto, M.A. (1998). Conserved and divergent roles for the members of the Snail family of transcription factors in the chick and mouse embryo. *Development* **125**: 3111-3121.

Sekiya, I., Tsuji, K., Koopman, P., Watanabe, H., Yamada, Y., Shinomiya, K., Nifuji, A., and Noda, M. (2000). SOX9 enhances aggrecan gene promoter/enhancer activity and is up-regulated by retinoic acid in a cartilage-derived cell line, TC6. *J. Biol. Chem.* **275**: 10738-10744.

Semina, E. V., Reiter, R., Leysens, N. J., Alward, W. L., Small, K. W., Datson, N. A., Siegel-Bartelt, J., Bierke-Nelson, D., Bitoun, P., Zabel, B. U., Carey, J. C., and Murray, J. C. (1996). Cloning and characterization of a novel bicoid-related homeobox transcription factor gene, RIEG, involved in Rieger syndrome. *Nat. Genet.* **14**, 392-399.

Shamugam, K., Green, N.C., Rambaldi, I., Sargovi, H.U., and Featherstone, M.S. (1999) PBX and MEIS as non-DNA-binding proteins in trimeric complexes with HOX proteins. *Mol. Cell. Biol.* **19**: 7577-7588.

Sharpe, C.R. (1991). Retinoic acid can mimic endogenous signals involved in transformation of the *Xenopus* nervous system. *Neuron* **7**: 239-247.

Shen, W.F., Rozenfeld, S., Kwong, A., Köm Ves, L.G., Lawrence, H.J., and Largman, C. (1999) HoxA9 forms triple complexes with PBX2 and MEIS1 in myeloid cells. *Mol. Cell. Biol.* **19**: 3051-3061.

Shenefelt, R.E. (1972). Morphogenesis of malformations in hamsters caused by retinoic acid: relation to dose and stage at treatment. *Teratology* **5**: 103-118.

Shiratori, H., Sakuma, R., Wantanabe, M., Hashiguchi, H., Mochida, K., Sakai, Y., Nishino, J., Saijoh, Y., Whitman, M., and Hamada, H. (2001). Two-step regulation of left-right asymmetric expression of *Pitx2*: initiation by nodal signaling and maintenance by Nkx2. *Mol. Cell.* **7**: 137-149.

Shum, A.S.W., Poon L.L.M., Tang, W.W.T., Koide, T., Chan, B.W.H., Leung, Y.-C.G., Shiroishi, T., and Copp, A.J. (1999). Retinoic acid induces down-regulation of *Wnt-3a*, apoptosis and diversion of tail bud cells to a neural fate in the mouse embryo. *Mech. Dev.* **84**: 17-30.

Simeone, A., Acampora, D., Arcioni, L., Andrews, P.W., Boncinelli, E., and Mavilio, F. (1990). Sequential activation of HOX2 homeobox genes by retinoic acid in human embryonal carcinoma cells. *Nature* **346**: 763-766.

Simeone, A., Acampora, D., Nigro, V., Faiella, A., D'Esposito, M., Stornaiuolo, A., Mavilio, F., and Boncinelli, E. (1991). Differential regulation by retinoic acid of the homeobox genes of the four HOX loci in human embryonal carcinoma cells. *Mech. Dev.* **33**: 215-227.

Sinning, A.R. (1998). Role of vitamin A in the formation of congenital heart defects. *Anat. Rec. (New Anat.)* **253**: 147-153.

Simeone, A., Avantaggiato, V., Moroni, M.C., Mavilio, F., Arra, C., Cotelli, F., Nigro, V., and Acampora, D. (1995). Retinoic acid induces stage-specific antero-posterior transformation of the rostral central nervous system. *Mech. Dev.* **51**: 83-98.

Sive, H.L., and Cheng, P.F. (1991). Retinoic acid perturbs the expression of *Xhox.lab* genes and alters mesoderm determination in *Xenopus laevis*. *Genes Dev.* **5**: 1321-1332.

Sive, H.L., Draper, B.W., Harland, R.M., and Weintraub, H. (1990). Identification of a retinoic acid-sensitive period during primary axis formation in *Xenopus laevis*. *Genes Dev.* **4**: 932-942.

Smith, S. M., and Dickman, E.D. (1997). New insights into retinoid signaling in cardiac development and physiology. *Trends Cardiovasc. Med.* **7**, 324-329.

Smith, S.M., Dickman, E.D., Thompson, R.P., Sinning, A.P., Wunsch, A.M., and Markwald, R.R. (1997). Retinoic acid directs cardiac laterality and the expression of early markers of precardiac asymmetry. *Dev. Biol.* **182**: 162-171.

Song, J. and Slack, J. (1996). XFGF9: A new fibroblast growth factor from *Xenopus* embryos *Dev. Dyn.* **206**: 427-436.

Spencer, T.E., Jenster, G., Burcin, M.M., Allis, C.D., Zhou, J., Mizzen, C.A., McKenna, N.J., Onate, S.A., Tsai, S.Y., and O'Malley, B.W. (1997). Steroid receptor coactivator-1 is a histone acetyltransferase. *Nature* **389**: 194-198.

Stalsberg, H. (1969). The origin of heart asymmetry: Right and left contributions to the early chick embryo heart. *Dev. Biol.* **19**: 109-127.

Stern, C.D. (2001). Initial patterning of the central nervous system: How many organizers? *Nat. Rev. Neurosci.* **2**: 92-98.

Studer, M., Gavalas, A., Marshall, H., Ariza-McNaughton, L., Rijli, F.M., Chambon, P., and Krumlauf, R. (1998). Genetic interactions between *Hoxa1* and *Hoxb1* reveal new roles in regulation of early hindbrain patterning. *Development* **125**: 1025-1036.

Studer, M., Lumsden, A., Ariza-McNaughton, L., Bradley, A., and Krumlauf, R. (1996). Altered segmental identity and abnormal migration of motor neurons in mice lacking *Hoxb-1*. *Nature* **384**: 630-634.

Studer, M., Pöpperl, H., Marshall, H., Kuroiwa, A., and Krumlauf, R. (1994). Role of a conserved retinoic acid response element in rhombomere restriction of Hoxb1. *Science* **265**: 1728-1732.

Subbarayan, V., Kastner, P., Mark, M., Dierich, A., Gorry, P., and Chambon, P. (1997). Limited specificity and large overlap of the functions of the mouse RARγ1 and RARγ2 isoforms. *Mech. Dev.* **66**: 131-142.

Sucov, H.M., Dyson, E., Gumeringer, C.L., Price, J., Chein, K.R., and Evans, R.M. (1994). RXRα mutant mice establish a genetic basis for vitamin A signaling in heart morphogenesis. *Genes. Dev.* **8**: 1007-1018.

Sucov, H.M., Izisua-Belmonte, J.C., Ganan, Y., and Evans, R. (1995). Mouse embryos lacking RXRα are resistant to retinoic-acid-induced limb defects. *Development* **121**: 3997-4003.

Sucov, H.M., Murakami, K.K., Evans, R.M. (1990). Characterization of an autoregulated response element in the mouse retinoic acid receptor type beta gene. *Proc. Natl. Acad. Sci. USA* **87**: 5392-5396.

Sulik, K.K., Dehart, D.B., Rogers, J.M., and Chernoff, N. (1995). Teratogenicity of low doses of all-*trans* retinoic acid in presomite mouse embryos. *Teratology* **51**: 398-403.

Supp, D.M., Witte, D.P., Potter, S.S., and Brueckner, M. (1997). Mutation of an axonemal dynein affects left-right asymmetry in inversus viscerum mice. *Nature* **389**: 963-966.

Swindell, E.C., Thaller, C., Sockanathan, S., Petkovich, M., Jessell, T.M., Eichele, G. (1999). Complementary domains of retinoic acid production and degradation in the early chick embryo. *Dev Biol* **216**: 282-296.

Tabata, T. (2001). Genetics of morphogen gradients. *Nat. Rev. Genet.* **2**: 620-630.

Taira, M., Saint-Jeannet, J-P., and Dawid, I.B. (1997). Role of the *Xlim-1* and *Xbra* genes in anteroposterior patterning of neural tissue by the head and trunk organizer. *Proc. Natl. Acad. Sci. USA* **94**: 895-900.

Tada, M., O'Reilly, M.-A.J., and Smith, J.C. (1997). Analysis of competence and of *Brachyury* autoinduction by use of hormone-inducible *Xbra*. *Development* **124**: 2225-2234.

Tada, M., and Smith, J.C. (2000). *Xwnt11* is a target of *Xenopus* Brachyury: regulation of gastrulation movements via Dishevelled, but not through the canonical Wnt pathway. *Development* **127**: 2227-2238.

Takada, S., Stark, K.L., Shea, M.J., Vassileva, G., and McMahon, J.A. (1994). Wnt-3a regulates somite and tailbud formation in the mouse embryo. *Genes. Dev.* **8**: 174-189.

Takeda, S., Yonekawa, Y., Tanaka, Y., Okada, Y., Nonaka, S., and Hirokawa, N. (1999). Left-right asymmetry and kinesin superfamily protein KIF3A: new inights in determination of laterality and mesoderm induction by *kif3A*$^{-/-}$ mice analysis. *J. Cell Biol.* **145**: 825-836.

Tam, P.P.L. (1984). The histogenic capacity of tissues in the caudal end of the embryonic axos of the mouse. *J. Embryol. Exp. Morph.* **82**: 253-266.

Tam, P.P.L. (1986). A study on the pattern of prospective somites in the presomitic mesoderm of mouse embryos. *J. Embryol. Exp. Morph.* **92**: 269-285.

Tam, P.P.L., and Behringer, R.R. (1997). Mouse gastrulation: the formation of the mammalian body plan. *Mech. Dev.* **68**: 3-25.

Tam, P.P.L., Goldman, D., Camus, A., and Schoenwolf, G.C. (2000). Early events of somitogenesis in higher vertebrates: allocation of precursor cells during gastrulation and the organization of a meristic pattern in the paraxial mesoderm. *Curr. Top. Develop. Biol.* **47**: 1-32.

Tam, P.P.L., Parameswaran, M., Kinder, S.J., and Weinberger, R.P. (1997). The allocation of epiblast cells to the embryonic heart and other mesodermal lineages: the role of ingression and tissues movement during gastrulation. *Development* **124**: 1631-1642.

Tam, P.P.L., and Schoenwolf, G.C. (1999). Cardiac fate maps: lineage allocation, morphogenetic movement, and cell commitment. In "Heart Development", R.P. Harvey and N. Rosenthal, Eds. Academic Press, San Diego. Pp 3-18.

Tam, P.P.L., and Steiner, K.A. (1999). Anterior patterning by synergistic activity of the early gastrula organizer and the anterior germ layer tissues of the mouse embryo. *Development* **126**: 5171-5179.

Tam, P.P.L. and Tan, S.-S. (1992). The somitogenetic potential of cells in the primitive streak and the tailbud of organogenesis-stage mouse embryo. *Development* **115**: 703-715.

Taneja, R., Rochette-Egly, C., Plassat, J.L., Penna, L., Gaub, M.P., and Chambon, P. (1997). Phosphorylation of activation functions AF-1 and Af-2 of RAR alpha and RAR gamma is indispensable for differentiation of F9 cells upon retinoic acid and camp treatment. *EMBO J.* **16**: 6452-6465.

Thomas, P., and Beddington, R. (1996). Anterior primitive endoderm may be responsible for patterning the anterior neural plate in the mouse embryo. *Curr. Biol.* **6**: 1487-1496.

Thompson, J.N., Howell, J. McC., Pitt, G.A.J., and McLaughlin, C.I. (1969). The biological activity of retinoic acid in the domestic fowl and the effects of vitamin A deficiency on the chick embryo. *Br. J. Nutr.* **23**: 471-490.

Tibbles, L., and Wiley, M.J. (1988). A comparative study of the effects of retinoic acid given during the critical period for inducing spina bifida in mice and hamsters. *Teratology* **37**: 113-125.

Torchia, J., Rose, D.W., Inostroza, J., Kamei, Y., Westin, S., Glass, C.K., and Rosenfeld, M.G. (1998). The transcriptional co-activator p/CIP binds CBP and mediates nuclear-receptor function. *Nature* **387**: 677-683.

Trainor, P., and Krumlauf, R. (2000). Plasticity in mouse neural crest reveals a new patterning role for cranial mesoderm. *Nat. Cell Biol.* **2**: 96-102.

Tsuda, T., Philp, N., Zile, M.H., and Linask. K.K. (1996). Left-right asymmetric localization of flectin in the extracellular matrix during heart looping. *Dev. Biol.* **173**: 39-50.

Tsuiki, H., and Kishi, K. (1999). Retinoid-induced limb defects II: involvement of TGF-beta 2 in retinoid-induced inhibition of limb bud development. *Rep. Toxicol.* **13**: 113-122.

Tsukui, T., Capdevila, J., Tamura, K., Ruiz-Lozano, P., Rodriguez-Esteban, C., Yonei-Tamura, S., Magallon, J., Chandraratna, R. A., Chien, K., Blumberg, B., Evans, R. M., and Belmonte, J. C. (1999). Multiple left-right asymmetry defects in Shh(-/-) mutant mice unveil a convergence of the shh and retinoic acid pathways in the control of Lefty-1. *Proc. Natl. Acad. Sci. U S A* **96**, 11376-11381.

Tzahor, E., and Lassar, A.B. (2001). Wnt signals from the neural tube block ectopic cardiogenesis. *Genes Dev.* **15**: 255-260.

Underhill, T.M., Sampaio, A.V., and Weston, A.D. (2001). Retinoid signaling and skeletal development. *Novartis Found. Symp.* **232**: 171-185.

van den Hoff, M.J.B., Kruithof, B.P.T., Moorman, A.F.M., Markwald, R.R., and Wessels, A. (2001). Formation of myocardium after the initial development of the linear heart tube. *Dev. Biol.* (in press). Published in the world wide web on November 1, 2001, (www.idealibrary.com).

van der Hoeven, F., Zákány, J., and Duboule, D. (1996). Gene transpositions in the *HoxD* complex reveal a hierarchy of regulatory controls. *Cell* **85**: 1025-1035.

van der Wees, J., Schilthuis, J.G., Koster, C.H., Diesveld-Schipper, H., Folkers, G.E., van der Saag, P.T., Dawson, M.I., Shudo, K., van der Burg, B., and Durston, A.J. (1998). Inhibition of retinoic acid receptor-mediated signalling alters positional identity in the developing hindbrain. *Development* **125**: 545-556.

Van Maldergem, L., Jauniaux, E., and Gillerot, Y. (1992). Morphological features of a case of retinoic acid embryopathy. *Prenatal Diag.* **12**: 699-701.

Verbout, A.J. (1985). The development of the vertebral column. *Adv. Anat. Embryol. Cell Biol.* **90**: 1-122.

Vesque, C., Maconochie, M., Nonchev, S., Ariza-McNaughton, L., Kuroiwa, A., Charnay, P., and Krumlauf, R. (1996). Hoxb-2 transcriptional activation in rhombomeres 3 and 5 requires an evolutionarily conserved cis-acting element in addition to the krox-20 binding site. *EMBO J.* **15**: 71-88.

Voegel, J.J., Heine, M.J.S., Tini, M., Vivat, V., Chambon, P., and Gronemeyer, H. (1998). The coactivator TIF2 contains three nuclear receptor-binding motifs and mediates transactivation through CBP binding-dependent and –independent pathways. *EMBO J.* **17**: 507-519.

Vonesch, J.L., Nakshatri, H., Philippe, M., Chambon, P., and Dollé, P. (1994). Stage and tissue-specific expression of the alcohol dehydrogenase 1 (Adh-1) gene during mouse development. *Dev. Dyn.* **199**: 199-213.

Wagner, M., Han, B., and Jessell, T.M. (1992). Regional differences in retinoid release from embryonic neural tissue detected by an in vitro reporter assay. *Development* **116**: 55-66.

Waldo, K.L., Kumiski, D.H., Wallis, K.T., Stadt, H.A., Hutsun, M.R., Platt, D.H., and Kirby, M.L. (2001). Conotruncal myocardium arises from a secondary heart field. *Development* **128**: 3179-3188.

Wasiak, S. and Lohnes, D. (1999). Retinoic acid affects left-right patterning. *Dev. Biol.* **215**, 332-342.

Webster, N.J., Green, S., Jin, J.R., and Chambon, P. (1988). The hormone-binding domains of the estrogen and glucocorticoid receptors contain an inducible transcription activation function. *Cell* **54**: 199-207.

Wendling, O., Dennefeld, C., Chambon, P., and Mark, M. (2000). Retinoid signaling is essential for patterning the endoderm of the third and fourth pharyngeal arches. *Development* **127**, 1553-1562.

Wendling, O., Ghyselinck, N.B., Chambon, P., and Mark, M. (2001). Roles of retinoic acid receptors in early embryonic morphogenesis and hindbrain patterning. *Development* **128**: 2031-2038.

White, J.A., Guo, Y.-D., Baetz, K., Beckett-Jones, B., Bonasoro, J., Hsu, K.E., Dilworth, F.J., Jones, G., and Petkovich, M. (1996). Identification of the retinoic acid-inducible all-trans-retinoic acid 4-hydroxylase. *J. Biol. Chem.* **272**: 18538-18541.

White, J.A., Beckett-Jones, B., Guo, Y.-D., Dilworth, J., Bonasoro, J., Jones, G., and Petkovich, M. (1997). cDNA cloning of human retinoic acid-metabolizing enzyme (hP450RAI) identifies a novel family of cytochromes P450 (CYP26). *J. Biol. Chem.* **271**: 29922-29927.

White, J.A., Ramshaw, H., Taimi, M., Stangle, W., Zhang, A., Everingham, S., Creighton, S., Tam, S.-P., Jones, G., and Petkovich, M. (2000a). Identification of the human cytochrome P450, P450RAI-2, which is predominantly expressed in the adult cerebellum and is responsible for all-*trans*-retinoic acid metabolism. *Proc. Natl. Acad. Sci. USA* **97**: 6403-6408.

White, J.C., Highland, M., Kaiser, M., Clagett-Dame, M. (2000b). Vitamin A-deficiency results in the dose-dependent acquisition of anterior character and shortening of the caudal hindbrain of the rat embryo. *Dev. Biol.* **220**: 263-284.

Wilkinson, D.G., Bhatt, S. and Herrmann, B.G. (1990). Expression pattern of the mouse t gene and its role in mesoderm formation. *Nature* 343, 657-659.

Wilkinson, D.G., Peters, G., Dickson, C., and McMahon, A.P. (1988). Expression of the FGF-related proto-oncogene int-2 during gastrulation and neurulation in the mouse. *EMBO J.* **7**: 691-695.

Wilson, J.C., Roth, C.B., and Warkany, J. (1953). An analysis of the syndrome of maternal vitamin A deficiency. Effects of restoration of vitamin A at various times during gestation. *Am. J. Anat.* **92**: 189-217.

Wilson, J.G., and Warkany, J. (1948). Malformations in the genitourinary tract induced by maternal vitamin A deficiency in the rat. *Am. J. Anat.* **83**: 357-407.

Wilson, J.G., and Warkany, J. (1949). Aortic-arch and cardiac abnormalities on the offspring of vitamin A deficient rats. *Am. J. Anat.* **85**: 113-155.

Wilson, P.A., and Hemmati-Brivanlou, A. (1997). Vertebrate neural induction: inucers, inhibitors, and a new synthesis. *Neuron* **18**: 699-710.

Wilson, V. and Beddington, R. (1997). Expression of t protein in the primitive streak is necessary and sufficient for posterior mesoderm movement and somite differentiation. *Dev. Biol.* **192**, 45-58.

Wilson, V., Manson, L., Skarnes, W.C., and Beddington, R.S.P. (1995). The *T* gene is necessary for normal mesodermal morphogenetic cell movements during gastrulation. *Development* **121**: 877-886.

Wodarz, A., and Nusse, R. (1998). Mechanisms of Wnt signaling in development. *Annu. Rev. Cell Dev. Biol.* **14**: 59-88.

Wolbach, S.B., and Howe, P.R. (1925). Tissue changes following deprivation of fat-soluble A vitamin. *J. Exp. Med.* **42**: 753-777.

Wood, H., Pall, G., and Morriss-Kay, G. (1994). Exposure to retinoic acid before or after the onset of somitogenesis reveals separate effects on rhombomeric segmentation and 3' HoxB gene expression domains. *Development* **120**: 2279-2285.

Wurst, J-M., Bourguet, W., Renaud, J-P., Vivat, V., Chambon, P., Moras, D., and Gronemeyer, H. (1996). A canonical structure for the ligand-binding domain of nuclear receptors. *Nat. Struct. Biol.* **3**: 87-94.

Yamada, T. (1994). Caudalization by the amphibian organizer: *brachyury*, convergent extension and retinoic acid. *Development* **120**: 3051-3062.

Yamaguchi, M., Nakamoto, M., Honda, H., Nakagawa, T., Fujita, H., Nakamura, T., Hirai, H., Narumiya, S., and Kakizuka, A. (1998). Retardation of skeletal development and cervical abnormalities in transgenic mice expressing a dominant-negative retinoic acid receptor in chondrogenic cells. *Proc. Natl. Acad. Sci. U S A* **95**, 7491-7496.

Yamaguchi, T.P., Harpal, K., Henkemeyer, M., and Rossant, J. (1994). fgfr-1 is required for embryonic growth and mesodermal patterning during mouse gastrulation. *Genes Dev.* **8**: 3032-3044.

Yamaguchi, T.P., Takada, S., Yoshikawa, Y., Wu, N., and McMahon, A.P. (1999). T (Brachyury) is a direct target of Wnt3a during paraxial mesoderm specification. *Genes. Dev.* **13**: 3185-3190.

Yan, Y.T., Gritsman, K., Ding, J., Burdine, R.D., Corrales, J.D., Price, S.M., Talbot, W.S., Schier, A.F., and Shen, M.M. (1999). Conserved requirement for EGF-CFC genes in vertebrate left-right axis formation. *Genes Dev.* **13**: 2527-2537.

Yao, T.P., Ku, G., Zhou, N., Scully, R., and Livingston, D.M. (1996). The nuclear hormone recepto coactivator SRC-1 is a specific target of p300. *Proc. Natl. Acad. Sci. USA* **93**: 10626-10631.

Yoshikawa, Y., Fujimori, T., McMahon, A.P., and Takada, S. (1997). Evidence that absence of Wnt-3a signaling promotes neuralization instead of paraxial mesoderm development in the mouse. *Dev. Biol.* **183**: 234-242.

Yasuda, Y., Konishi, H., Kihara, T. and Tanimura, T. (1990). Discontinuity of primary and secondary neural tube in spina bifida induced by retinoic acid in mice. *Teratology* **41**, 257-274.

Yasuda, Y., Okamoto, M., Konishi, H., Matsuo, T., Kihara, T., and Tanimura, T. (1986). Developmental anomalies induced by all-trans retinoic acid in fetal mice: I. Macroscopic findings. *Teratology* **34**: 37-49.

Yasui, H., Morishima, M., Nakazawa, M., and Aikawa, E. (1998). Anomalous looping, atrioventricular cushion dysplasia, and unilateral ventricular hypoplasia in the mouse embryos with right isomerm induced by retinoic acid. *Anat. Rec.* **250**: 210-219.

Yokouchi, Y., Vogan, K.J., Pearse, R.V., II, and Tabin, C.J. (1999). Antagonist signaling by Caronte, a novel Cerberus-related gene, establishes left-right asymmetric gene expression. *Cell* **98**; 573-583.

Yokoyama, T., Copeland, N.G., Jenkins, N.A., Nontgomery, C.A., Elder, F.F., and Overbeek, P.A. (1993). Reversal of left-right asymmetry: a situs inversus mutation. *Science* **260**: 679-682.

Yu, V.C., Delsert, C., Anderson, B., Holloway, J.M., Devary, O.V., Näär, A.M., Kim, S.Y., Boutin, J-M., Glass, C.K., Rosenfeld, M.G. (1991). RXRβ: a coregulator that enhances binding of retinoic acid, thyroid hormone, and vitamin D receptors to their cognate response elements. *Cell* **67**: 1251-1266.

Yuan, C.X., Ito, M., Fondell, J.D., Fu, Z.Y., and Roeder, R.G. (1998). The TRAP220 component of a thyroid hormone receptor-associated protein (TRAP) coactivator complex interacts directly with nuclear receptors in a ligand-dependent fashion. *Proc. Natl. Acad. Sci. USA*. **95**: 7939-7944.

Zakany, J., Kmita, M., Alarcon, P., de la Pompa J.-L., and Duboule (2001). Localized and transient transcription of *Hox* genes suggests a link between patterning and the segmentation clock. *Cell* **106**: 207-217.

Zechel, C., Shen, X.-Q., Chambon, P., and Gronemeyer, H. (1994a). Dimerization interfaces formed between the DNA binding domains determine the cooperative binding of RXR/RAR and RXR/TR heterodimers to DR5 and DR4 elements. *EMBO J.* **13**: 1414-1425.

Zechel, C., Shen, X.-Q., Chen, J.-Y., Chen, Z.-P., Chambon, P., and Gronemeyer, H. (1994b). The dimerization interfaces formed between the DNA binding domains of RXR, RAR and TR determine the binding specificity and polarity of the full-length receptors to direct repeats. *EMBO J.* **13**: 1425-1433.

Zelent, A., Mendelsohn, C., Kastner, P., Garnier, J.M., Ruffenach, F., Leroy, P., and Chambon, P. (1991). Differentially expressed isoforms of the mouse retinoic acid receptor β are generated by the usage of two promoters and alternative slpicing. *EMBO J.* **10**: 71-81.

Zhang, H., and Bradley, A. (1996). Mice deficient for BMP2 are nonviable and have defects in amnion/chorion and cardiac development. *Development* **122**: 2977-2986.

Zhang, F., Pöpperl, H., Morrison, A., Kovàcs, E.N., Prideaux, V., Schwartz, L., Krumlauf, R., Rossant, J., and Featherstone, M.S. (1997). Elements both 5' and 3' to the murine Hoxd4 gene establish anterior borders of expression in mesoderm and neuroectoderm. *Mech. Dev.* **67**: 49-58.

Zhang, F., Kovács, E.N., and Featherstone, M.S. (2000). Murine *Hoxd4* expression in the CNS requires multiple elements including a retinoic acid response element. *Mech. Dev.* **96**: 79-89.

Zhang, M., Kim, H.-J., Marshall, H., Gendron-Maguire, M., Lucas, D.A., Baron, A., Gudas, L.J., Gridley, T., Krumlauf, R., and Grippo, J.F. (1994). Ectopic *Hoxa-1* induces rhombomere transformation in mouse hindbrain. *Development* **120**: 2431-2442.

Zhang, X.-K., Lehmann, J., Hoffmann, B., Dawson, M, Cameron, J., Graupner, G., Hermann, T., Tran, P., and Pfahl, M. (1992). Homodimer formation of retinoid X receptor induced by 9-*cis* retinoic acid. *Nature* **358**: 587-591.

Zhang, X.M., Ranalho-Santos, M., and McMahon, A.P. (2001). *Smoothened* mutants reveal redundant roles for Shh and Ihh signaling including regulation of L/R asymmetry by the mouse node. *Cell* **105**: 781-792.

Zhao, D., McCaffery, P., Ivins, K.J., Neve, R.L., Hogan, P., Chin, W.W., and Drager, U.C. (1996). Molecular identification of a mojor retinoic acid synthesizing enzyme, a retinaldehyde dehydrogenase. *Eur. J. Biochem.* **15**: 15-22.

Zhu, L., Marvin, M.J., Gardiner, A., Lassar, A.B., Mercola, M., Stern, C.D., and Levin, M. (1999). *Cerberus* regulates left-right asymmetry of the embryonic head and heart. *Curr. Biol.* **9**; 931-938.

Zile, M.H. (1998). Vitamin A and embryonic development: an overview. *J. Nutr.* **128**: 455S-458S.

Zile, M.H. (2001). Function of vitamin A in vertebrate embryonic development. *J. Nutr.* **131**: 705-708.

Zile, M. H., Kostetskii, I., Yuan, S., Kostetskaia, E., St Amand, T. R., Chen, Y., and Jiang, W. (2000). Retinoid signaling is required to complete the vertebrate cardiac left/right asymmetry pathway. *Dev. Biol.* **223**, 323-338.

APPENDIX I

Staging of the Early Mouse Embryo

Embryonic Day (E)	Stage
6.0	Pre-streak egg cylinder
6.5	Early primitive streak (gastrulation)
7.0	Mid-primitive streak
7.25	Early neurulation, cardiac crescent formation
7.5	Late primitive streak, early head fold
8.0	Late head fold, early somitogenesis, linear heart tube
8.25	Early heart looping
8.5	Anterior neuropore closure, pharyngeal arch formation, somitogenesis, primitive streak remnant, heart looping
9.5	Posterior neuropore closure, tail bud formation, advanced somitogenesis

Data obtained from Kaufman and Bard (1999) and Fishman and Chien (1997).